Univerzita Karlova v Praze, Přírodovědecká fakulta
Charles University in Prague, Faculty of Science

Doktorský studijní program: Parazitologie
Ph.D. study program: Parasitology

Mrg. Jan Pyrih

Kofaktory obsahující železo u anaerobního parazita *Giardia intestinalis*

Iron containing cofactors in anaerobic parasite *Giardia intestinalis*

Disertační práce/ Ph.D. Thesis

Thesis supervisor : prof. RNDr. Jan Tachezy, Ph.D.

Prague 2015

Declaration of the author

I declare that I elaborated the PhD thesis independently. I also proclaim that the literary sources were cited properly and neither this work nor the substantial part of it have been used to reach the same or any other academic degree.

Prohlašuji, že jsem závěrečnou práci zpracoval samostatně a že jsem uvedl všechny použité informační zdroje a literaturu. Tato práce ani její podstatná část nebyla předložena k získání jiného nebo stejného akademického titulu.

.....

Mgr. Jan Pyrih

Declaration of the thesis supervisor

Data presented in this thesis resulted from team collaboration at the Laboratory of biochemical and molecular parasitology and during projects with our partners. I declare that the involvement of Mgr. Jan Pyrih in this work was substantial and that he contributed significantly to obtain the results.

.....

prof. RNDr. Jan Tachezy, PhD.

Thesis supervisor

Acknowledgements

Many thanks to my supervisor Jan Tachezy and to all lab fellows for the support and help during all those years.

Table of Contents:

Abstract

Iron is an essential element in nearly all organisms. It is present mainly as a component of iron sulfur (FeS) clusters or as a heme iron. These cofactors enable proteins to transfer electrons or diatomic gasses, signal sensing and enzyme catalysis. Numerous FeS and heme depending proteins are involved in photosynthesis and respiratory chain pathways, which are well described processes. However, there is still much to learn about more recently discovered pathways such as formation of FeS clusters in various cell compartments and about roles of novel FeS or heme proteins. Particularly, only limited information is available about how FeS clusters are assembled or how heme is used in anaerobic protists, in which cytochrome-dependent respiration and photosynthesis does not occur. We decided to focus on iron cofactors in anaerobic parasite *Giardia intestinalis*. This organism undergone dramatic reductive evolution that resulted in formation of one of the smallest eukaryotic genome and the most reduced form of mitochondria, the mitosome. We characterized some components of mitochondrial (ISC) and cytoplasmic (CIA) FeS assembly machineries. We have detected ISC components in mitosome by proteomic analysis. Furthermore we investigated the presence and subcellular localization of CIA proteins in *Giardia*. In the *Giardia* genome, we identified only some components of CIA machinery including Nbp35, Nar1, Cia1, Cia2 and two genes with similarity to Tah18. Moreover, we found that some CIA proteins display dual cytoplasmic/ mitosomal localization, which may facilitate the connection between ISC and CIA machineries.

Known set of *Giardia* hemoproteins is limited to a single flavohemoglobin and four cytochrome b_5 proteins. We showed that *Giardia* cytochromes b_5 (gCYTb_5) belong to yet uncharacterized group of proteins (cytb_5 type II). They lack typical C-terminal transmembrane domain and possess specific amino acid motif around essentials heme binding histidines. Moreover, we found, that cytb_5 type II are ubiquitously present in eukaryotes in contrary to typical cytochromes b_5 (type I), which are present only in aerobic eukaryotic cells. We showed that gCYTb_5 paralogues are all present in *Giardia* cytosol and we proved that recombinant gCYTb_5 proteins bind heme *in vitro*. Additionally, we demonstrated that *Giardia* can import extracellular heme and incorporate it into the cytoplasmic gCYTb_5-IV. Previously it was believed that anaerobic protists live entirely without heme. Therefore, our experiments demonstrated for the first time that heme is present and utilized by anaerobic protist *Giardia intestinalis* and most likely by other anaerobes possessing cytb_5.

Abstrakt

Železo je nepostradatelným prvkem téměř pro všechny organismy. Nejčastěji je v buňce přítomné jako součást železitosirných (FeS) klastrů a hemu. Díky těmto kofaktorům mají proteiny schopnost katalyzovat enzymatickou reakci, přenášet elektrony a plyny a nebo detekovat signál. Mnoho FeS a hemových proteinů se účastní dobře prostudovaných drah, jako je fotosyntéza nebo dýchací řetězec. Nicméně o syntéze FeS klastrů v různých buněčných kompartmentech nebo o roli nově objevených FeS nebo hemo-proteinů se stále mnoho informací neví. Velmi málo je známo především o tom, jak jsou u anaerobně žijících protistů FeS klastry formovány nebo jak je využíván hem. V těchto organismech se totiž dráhy dýchacího řetězce či fotosyntézy nevyskytují. Rozhodli jsme se proto zaměřit na železo obsahující kofaktory u anaerobního parazita *Giardia intestinalis*. Tento organismus prošel dramatickou reduktivní evolucí, jejímž výsledkem je vznik jednoho z nejmenších eukaryotických genomů a nejvíce redukované formy mitochondrie - mitosomu. Charakterizovali jsme některé komponenty mitochondriální (ISC) a cytoplasmatické (CIA) FeS klastrovací dráhy. Pomocí proteomické analýzy jsme nejprve detekovali komponenty dráhy ISC v mitosomu. Poté jsme analyzovali přítomnost a buněčnou lokalizaci CIA proteinů. V genomu *G. intestinalis* jsme identifikovali pouze některé komponenty dráhy CIA (Nbp35, Nar1, Cia1, Cia2 a dva geny podobné Tah18). Pro některé z nich jsme navíc ukázali, že mají duální cytoplasmaticko-mitosomální lokalizaci. Tyto proteiny by mohly umožňovat spojení ISC a CIA dráhy.

Mezi známé hemo-proteiny u *G. intestinalis* patří pouze flavohemoglobin a čtyři cytochromy b_5. Ukázali jsme, že cytochromy b_5 v *G. intestinalis* (gCYTb_5) patří do prozatím necharakterizované skupiny proteinů (cytb_5 typ II). Nemají typickou transmembránovou doménu na C-konci a obsahují specifickou aminokyselinovou sekvenci v okolí esenciálních histidinů, které váží hem. Navíc jsme zjistili, že cytochromy b_5 typu II jsou u eukaryot všudypřítomné na rozdíl od typických cytochromů b_5 (typ I), které se vyskytují pouze v aerobních eukaryotických buňkách. Ukázali jsme, že jsou všechny paralogy gCytb_5 proteinů přítomné v cytoplasmě *G. intestinalis* a že rekombinantní gCytb_5 proteiny váží hem *in vitro*. Navíc jsme ještě prokázali, že je *G. intestinalis* schopná importovat hem z extracelulárního prostředí a zabudovávat ho do cytoplasmatického gCYTb_5–IV. Dříve se předpokládalo, že anaerobní prvoci žijí zcela bez hemu. Naše experimenty poprvé prokázaly, že je hem přítomen a využíván anaerobním protistem *Giardia intestinalis* a pravděpodobně i dalšími anaeroby majícími cytb_5 proteiny.

1. Introduction

Iron is a transition metal, which is able to form cation with an incomplete set of electrons in d orbital. Iron is present in nature mainly in two oxidative states, Fe^{2+} and Fe^{3+}. The most common way how to incorporate iron within the protein is as a part of more complicated inorganic structures called cofactors. These cofactors enables proteins to transfer diatomic gasses as well as electrons in various metabolic pathways. Moreover, they are involved in signal sensing and in a wide scale of chemical catalysis. Therefore, iron is an essential element in vast majority of living organisms.

However, intracellular iron is also toxic due to its ability to catalyze the formation of free radicals. Therefore, the iron uptake and storage is tightly regulated process (1). In higher concentrations iron is stored in its insoluble form (Fe^{3+}) in proteins such as ferritin.

Although organisms living in anaerobic conditions have reduced well-known iron-dependent pathways such as mitochondrial respiratory chain, they require iron for FeS cluster containing proteins (FeS-proteins) involved in anaerobic energy metabolism and for their multiplication. Various reduced types of anaerobic mitochondria are unified by conservation of Iron-sulfur (FeS) clusters (ISC) assembly pathway (2). In the most reduced forms of mitochondria, such as mitosomes of *Giardia intestinalis*, FeS cluster assembly is the only pathway identified so far (3). The essentiality of ISC machinery is most likely the reason for keeping the organelle during the reductive evolution.

Iron sulfur clusters are cofactors containing iron ions bridged by sulfide ions in variable oxidation states. The importance of iron sulfur proteins has been recently underlined by discoveries of FeS proteins involved in DNA metabolism and ribosome biogenesis (4-6).

Another ubiquitous iron cofactor is heme, an iron coordinating porphyrin. Heme proteins are involved in electron transport, diatomic gasses carriage and oxidative stress defense. Heme synthesis pathway is highly conserved, and it is essential in most organisms (7,8), although it can be bypassed by heme import from external environment (9,10). Heme dependent pathways are highly reduced in anaerobes, for example no intracellular hemoproteins have been identified in *Entamoeba histolytica* (11) and the only gene for flavohemoglobin and three genes for cytochrome b_5 like proteins with unknown cellular function were identified in *G. intestinalis* (12).

1.1. Iron acquisition, metabolism and homeostasis

Iron is mostly present in Fe^{3+} form in the environment, however, within the proteins it is present usually in Fe^{2+} state. There are several ways how to acquire iron from the environment. In *Arabidopsis thaliana* inducible ferric reductase reduces Fe^{3+} in the soil. Released Fe^{2+} is then transported across the plasma membrane by IRT1 transporter (13). In maize or rice chelating strategy is used (14). Siderophores with the ability to bind Fe^{3+} are synthesized in the cytoplasm of maize and released to the environment. Then siderophores with loaded iron are transported into the cell via YS1 transporter (15).

In yeast *Saccharomyces cerevisiae*, similarly to *Arabidopsis*, reductive mechanism includes Fre1 and Fre2 ferric reductases (16). After reduction, copper ferroxidase (Fet3) together with Ftr1 permease perform oxidation of Fe^{2+} to Fe^{3+} and transport of iron into the cell. In non-reductive iron uptake of yeast, siderophores (etc. ferrioxamine B, ferrichrome) with bound Fe^{3+} are transported by Sit1 and Arn1/2 transporters (17). In procyclic forms of *Trypanosoma brucei* it was shown that reduced iron is taken from ferric complexes via reductive mechanism and then it is incorporated to the mitochondrial complexes (18). Similarly, under low iron availability, expression of ferric reductase LFR1 and ferrous translocase LHR1 are upregulated in *Leishmania* (19).

Usual sources of iron in bacteria are siderophores, heme or transferrin. Specific pathways for uptake include an outer membrane receptor and an inner membrane ATP-binding cassette (ABC) transporter (20). In Gram-negative bacteria, various periplasmic binding proteins are involved in order to transport Fe^{3+} between both membranes (21).

Iron is essential and important element for survival and virulence of parasites (22). In mammals, extracellular iron is transferred in specialized proteins and free iron is essentially unavailable. Therefore parasites developed specific mechanisms for iron acquisition from host iron-binding proteins such as tranferrin, lactoferrin, ferritin or heme. Extracellular iron protein transferrin is specifically recognized by unique transferrin receptor on the surface of the flagellar pocket in *Trypanosoma brucei* cells (23). Lactoferrin is likely source of iron for *Trichomonas vaginalis*, *Tritrichomonas foetus* or *Entamoeba histolytica* (24-26). In human, liver ferritin contains 50% of iron corporal reserves. Ferritin specifically binds to *Entamoeba* surface and its internalization through clathrin-coated vesicles was observed *in vitro* (27). Therefore, it is possible that liver ferritin is an important source of iron during hepatic abscess stage of *Entamoeba* infection. Several cysteine peptidases are considered as a virulence

factors during infection of opportunistic parasite *Acanthamoeba castellanii*, as its ability to degrade lactoferrin, transferin, hemoglobine and ferritin was described *in vitro* (28).

Within the cell, iron is usually stored in multimeric ferritin in form of Fe^{3+}. Ferritin consist of light and heavy chain subunits in vertebrates, whereas in plants and bacteria whole complex is formed only by a single protein similar to heavy chain subunit (29). Ferritins are cytoplasmic, however, in some organisms, they are localized in mitochondria or in plastid (30), where they are likely involved in iron homeostasis (31). The amount of ferritin within the cell is tightly regulated. mRNA for ferritin possesses IRE (iron responsible element) in 5' UTR. In human cells with low level of intarcellular iron, IRE site is blocked by iron responsive proteins IRP1/IRP2 that inhibit ferritin translation (32). IREs are present also in 3' UTR of mRNA for transferrin receptor. Binding of IRPs in 3'UTR of the mRNA prevent nuclease digestion and prolong translation (33). Interestingly, gene for ferritin is usually absent in protists (34).

In yeast, where genes for ferritin are absent in the genome, other mechanisms for iron homeostasis likely occur. Recently, cytosolic FeS cluster binding glutaredoxin complex Grx3/Grx4, Fra1 and Fra2 proteins were identified as iron sensors (35) (Figure 1). Upon signal, transcriptional factor Aft1 regulates expression of genes involved in iron import such as Fet3 and Frt1. Excessive iron is stored and transported in vacuole via CCC1 vacuolar importer (36). Tyw1 protein in yeast is FeS protein involved in modified tRNA synthesis. However, it was suggested that under iron overload this protein serves as an iron storage protein on the surface of the endoplasmic reticulum (37). In *Giardia*, the mechanism of iron sensing and regulation is yet unknown. Genes for ferritin, ferric reductase or genes involved in iron sensing have not been identified in the *Giardia* genome, thus far (38).

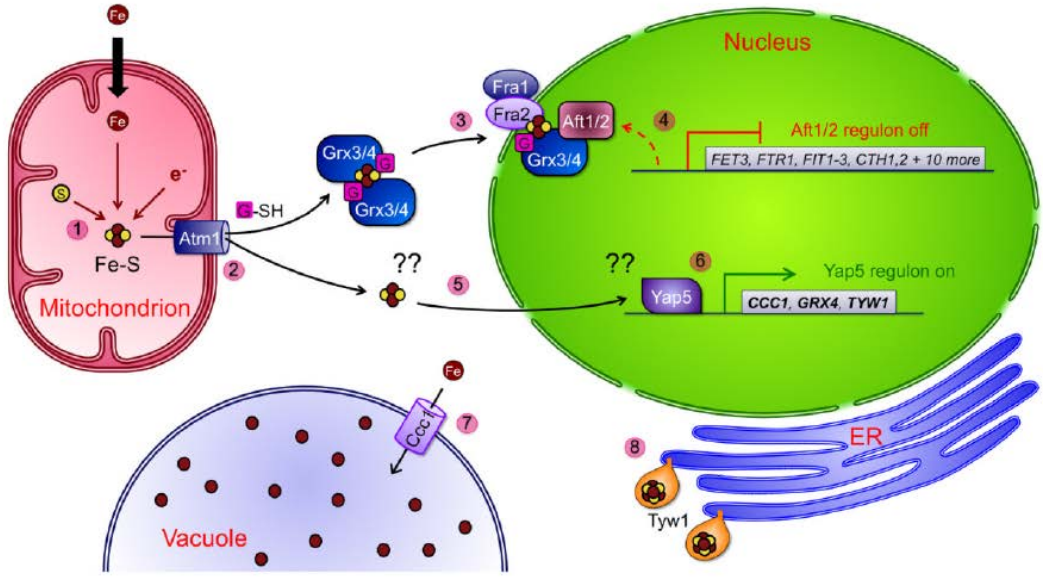

Figure 1. Current understanding of iron sensing and regulation in yeast. 1) FeS clusters are assembled in mitochondria. 2) Unknown substrate generated by ISC machinery is exported via Atm1 transporter. For this step glutathione is required. 3) Grx3 and Grx4, which form GSH-ligated FeS bridged heterocomplexes are proposed to relay signal to Fra1, Fra2 and Aft1 proteins. 4) Aft1 dissociates from DNA upon interaction with Grx3/4; transcription is stopped. 5) and 6) yet unknown ISC dependent signal is used for controlling of CCC1, Grx4 and Tyw1 genes. 7) CCC1 stimulates iron import in the vacuole. 8) Tyw1 protein serves as a iron storage protein on the surface of endoplasmic reticulum. Figure according to (1).

1.2. FeS clusters

Iron sulfur clusters are cofactors containing iron bridged by sulfide in several defined structures. The most common are [2Fe-2S] rhomb and [4Fe-4S] cubane clusters. The former cluster is formed by two iron cations with two bridging sulfides, the later consist of four tetrahedrally situated iron atoms bridged by four sulfide ligands. Both are usually coordinated by four sulfite ions from cysteinyl ligands of the protein. There are also highly complicated cluster structures, such as FeMoco (Fe_7MoS_9C) cluster in nitrogenase or H-cluster in hydrogenase. Interestingly, in Rieske protein, one of the [2Fe-2S] cluster is coordinated by two histidine and two cysteine residues, which results in increased redox potential of the cluster (39). Majority of clusters mediate transfer of electrons. However, also catalytic function of clusters was demonstrated. [4Fe-4S] cluster in aconitase reacts directly with the

substrate and serves as Lewic acid in conversion of citrate to isocitrate (40). FeS clusters can generate radicals in S-adenosylmethionine dependent enzymes or serves as a sulfur donor in lipoic acid or biotin synthesis (41). Additionally, FeS clusters are labile when exposed to oxygen. This behavior is important for the function of several redox sensing proteins in bacteria (42).

1.3. FeS proteins and their function

Proteins with FeS cluster cofactor are present in vast majority of organisms. For example, approximately 100 FeS proteins are known from *Arabidopsis thaliana* (43) and similar amount from yeast (44). The unique feature of FeS proteins is their ability to cover a wide range of reduction potentials (–700 mV to 400 mV) (45). Consequently, they belong among the most common electron carriers in nature. FeS proteins are involved in processes such as DNA metabolism, respiration, photosynthesis, hormone biosynthesis and cell growth. Especially DNA metabolism is significantly impaired in cell lines where proteins from FeS clusters synthesis pathways were depleted or their expression was lowered using various reverse genetic techniques. FeS cofactors are present in variety of DNA-maintaining proteins such as Rad3, helicases, endonucleases, primases, DNA polymerase or DNA glycosylases (5,43,44). In aerobic organisms, FeS clusters play crucial role in proteins of respiratory chain (Complex I, II, III) (46). FeS dependent proteins such as aconitase and succinate dehydrogenase are components of the tricarboxylic acid cycle and therefore important for energy generation and aminoacid metabolism (47). In plastid bearing organisms, mutations in proteins of SUF pathway (responsible for FeS assembly in plastid) result in defective photosynthesis (48,49). Particularly clusters on photosystem I are affected. Interestingly, lethal phenotype for several genes of SUF pathway cannot be rescued with sucrose (product of photosynthesis). Therefore, some other essential pathways such as leucine, thiamine and isoprenoid biosynthesis in plastid are likely affected as well. Moreover, the activities of cytosolic hormone synthesis proteins such as aldehyde oxidase are decreased in ISC pathway mutants (50). FeS enzymes such as isopropylmalate isomerase, glutamate synthase or sulfite reductase are required for amino acid synthesis.

In anaerobes, especially energy metabolism and DNA maintenance are considered as essential FeS dependent pathways. Interestingly, gene for ferredoxin 1, which is likely involved in FeS cluster synthesis in *Trichomonas vaginalis* was deleted with no obvious

phenotype (51), However, the function of this gene was likely substituted by other ferredoxins (51). Up to date no other component of FeS cluster synthesis pathway has been targeted by reverse genetic approach in any other anaerobe.

1.4. Subcellular distribution of FeS cluster assembly pathways in eukaryotes

Iron sulfur cluster assembly pathway (ISC) and Sulfur activation pathway (SUF) are present in most prokaryotes. The genes are organized as an operone (52). In *Escherichia coli*, both pathways are functioning simultaneously. However, SUF pathway is preferred in oxidative stress conditions (53). Although these pathways vary in the number of genes, they are analogically organized. They both possess cysteine desulfurase, electron donor oxidoreductase and FeS scaffold proteins. Another FeS cluster synthesis machinery - NIF pathway, was discovered in nitrogen fixing bacteria in which facilitates synthesis of the cluster in nitrogenase (52,54).

In eukaryotes, FeS cluster containing proteins are distributed in several subcellular compartments (Figure 2). Biogenesis of mitochondrial FeS proteins is dependent on activity of ISC pathway. The ISC pathway likely originated from α-proteobacterial ancestor of mitochondria (55). Analogically, FeS proteins in chloroplast are maturated via SUF pathway originated from cyanobacterial ancestor of chloroplast (56). Cytosolic FeS cluster assembly machinery (CIA) is the only pathway unique for eukaryotes. It is ubiquitously present in cytoplasm. In contrast to ISC and SUF pathway, CIA machinery lacks cysteine desulfurase. CIA machinery is therefore dependent on export of yet uncharacterized, most likely sulfur compound from mitochondria (6,57). Eukaryotes use CIA pathway for assembly and delivery of clusters to proteins that are present in cytosol or targeted to nucleus.

Interestingly, there are several exceptions from this common scheme. For example, ISC pathway is replaced by NIF pathway in hydrogenosome of amoeba *Mastigamoeba balamuthi* (58) and likely by SUF pathway in mitochondria of *Pygsuia biforma* (59). Moreover, it is possible that in mitosomes of *Entamoeba histolytica*, there is no FeS cluster synthesis pathway as there are no components for ISC machinery (60). The presence of NIF components in these organelles was suggested (61), but not confirmed in subsequent studies (58,62).

CIA machinery is ubiquitous in cytoplasm of all eukaryotes. Nevertheless, some components of SUF system in case of *Blastocystis hominis* and NIF system in *Mastigamoeba*

balamuthi and *Entamoeba histolytica* were identified to be additionally present in cytoplasm (58,63). Interestingly, some components including cysteine desulfurase (IscS), IscU, Nfu and Isd11 from ISC system in mammals were detected also in cytoplasmic or nuclear fraction (64-66). For human cytoplasmic IscS it was proposed to act in molybdenum cofactor synthesis (67). In yeast, IscS protein is partially localized in nucleus (68), where it is likely involved in thiolation of tRNA as in bacteria cells (69). Similar suggestion was proposed for *Trypanosoma brucei* (70). In this parasite, IscS and iscU proteins were identified in mitochondria and also in nuclei. Moreover, in Isd11 and IscU knockdown cell lines, decrease in tRNA thiolation was observed (70,71).

In plants and yeast it has been demonstrated, that mitochondrial ISC pathway is essential for FeS cluster assembly in cytoplasm and nucleus via interaction with CIA pathway. However, molecular basis of ISC and CIA pathway interaction is yet unknown. By reverse genetics techniques it has been demonstrated that protein Erv1 (Mitochondrial FAD-linked sulfhydryl oxidase) from intermembrane space of mitochondria, ATM1 (ABC transporter in inner mitochondrial membrane) and glutathione are involved in this connection (6,57,72,73). Recently, it has been shown that glutathione as a cofactor is bound to ATM1 protein in yeast (74). Significance of Erv1 for mitochondrial export machinery has recently been questioned (75). Decreased enzymatic activities for cytoplasmic FeS proteins were observed only in a single Erv1 mutant strain. However, in further detailed screening of this mutant strain mutation in another gene (glutathione cysteine ligase) was discovered. Therefore likely the observed phenotype was caused by glutathione depletion (75).

When ATM1 gene in plants and yeast was deleted, cytosolic FeS cluster biogenesis was strongly affected. What is the exported substrate for CIA is still unclear though. In yeast, iron accumulation in mitochondria of ATM1 mutant was observed, which could mean that compound exported via ATM1 contains iron. However, this phenomenon was rather caused by ATM1 dependent iron sensing mechanism (Figure 1) (76,77). Moreover, in plant ATM1 mutants there is no iron accumulation in mitochondria (57). Therefore, the current view is that the enigmatic compound exported from mitochondria is not preassembled FeS cluster, but rather the unknown form of sulfur compound.

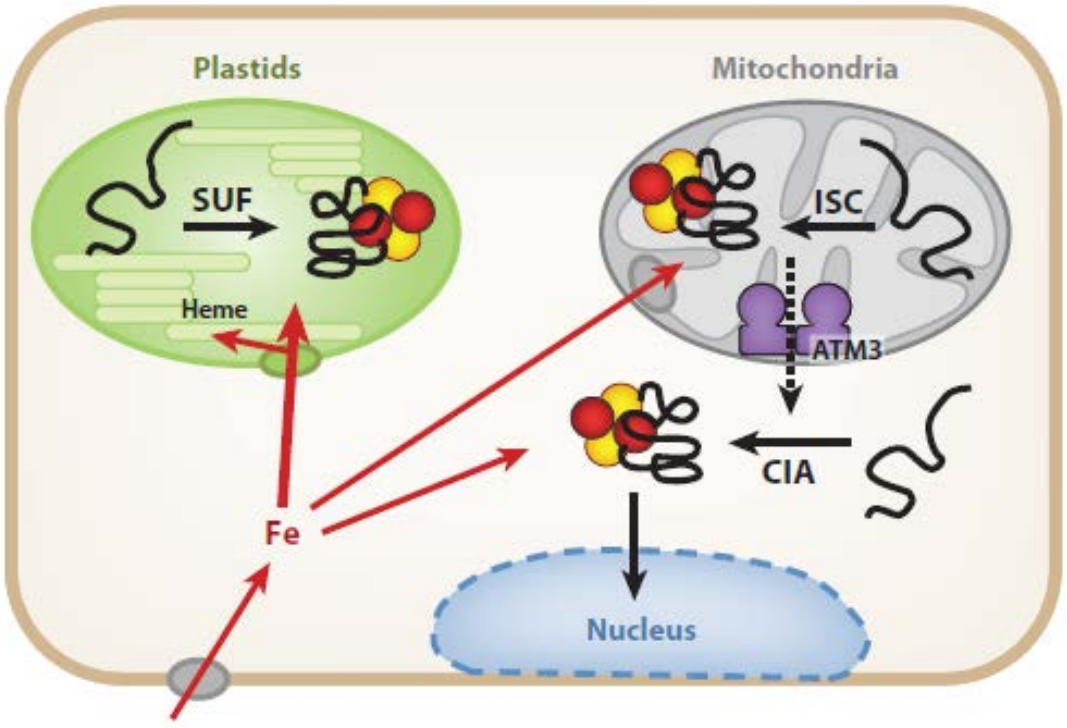

Figure 2. Compartmentalization of Iron cofactor synthesis in *Arabidopsis thaliana*. SUF pathway is involved in FeS cluster assembly in plastid. ISC pathway maturates FeS proteins in mitochondria and is involved in unknown sulfur compound export, which is essential for CIA function in cytoplasm and maturation of nuclear FeS proteins. Figure according to (77).

1.4.1. Iron sulfur cluster assembly pathway (ISC)

In the first step, sulfur in form of persulfite is donated from L-cystein to scaffold protein IscU via cystein desulfurase (IscS) (78). During this step, IscS-IscU complex linked by disulfide bridge is assembled (79). In addition, Isd11 protein form transient subcomplex with IscS and it is necessary for IscS protein stability (80,81). In bacteria, it was proposed that IscU undergo a conformational change from disorganized to structured form upon interaction with IscS. [2Fe-2S] cluster is then assembled on folded IscU protein (82). In this step, S^0 is reduced to S^{2-}, which requires electrons from ferredoxin and mitochondrial ferredoxin reductase. Ferredoxin reductase is NADPH dependent flavin adenine dinucleotide (FAD) containing protein (83). Frataxin, protein ubiquitously present in mitochondria of eukaryotes is an iron donor candidate for ISC pathway (84,85). However, its direct involvement in this process was never experimentally confirmed. Interestingly, this protein was observed to interact with ferrochelatase in yeast (86), therefore it might also play role in heme

biosynthesis. Recent studies suggested that frataxin is involved in the initial step of FeS cluster assembly during IscU-IscS complex formation (85,87).

Transient FeS cluster in IscU is then destabilized by interaction with chaperon system comprising of the mtHsp70 (Ssq1 in yeast), Grx5, cochaperon Jac1 and nucleotide exchange factor GrpE (88,89). Likely, mtHsp70 facilitate FeS cluster transfer via formation of complex with Grx5 (88). The destabilized [2Fe-2S] cluster is either directly incorporated into apoprotein or transiently transferred to FeS transfer proteins Nfu, A-type ISC proteins (IscA1 and 2), BolA3, Ind1 and Iba57 (90,91). These proteins are involved in insertion of more complex [4Fe-4S] clusters into specific mitochondrial apoproteins. Iba57, IscA1 and IscA2 likely participate directly in the formation of [4Fe-4S] cluster (92,93). However, the mechanism is currently unknown (94). In absence of these components, [4Fe-4S] cluster on aconitase is not assembled (95). Additionally, the cluster insertion into Complex I was described to P-loop NTPase Ind1 protein (46). In fibroblasts where mutant forms of Nfu and BolA3 proteins were expressed, enzyme activities for respiratory complexes were affected in contrary to unchanged activities of mitochondrial aconitase (90).

In green algae and various anaerobic eukaryotes or bacteria, hydrogenase maturases HydD, HydG and HydE are usually present (96,97). These are necessary for formation of H-cluster in hydrogenase (98).

1.4.2. Nitrogen fixation system (NIF)

NIF system was originally characterized in nitrogen fixing bacteria *Azotobacter* (99). It is specialized in the synthesis of complicated iron-molybdenum cofactor (FeMo-co) in nitrogenase. NifS as a cysteine desulfurase and NifU as scaffold protein serve in the initial step of FeMo-co synthesis (100). In this step, FeS clusters (most likely [2Fe-2S] and [4Fe-4S]) are assembled. Then FeS cluster is modified in complicated S-adenosyl methionine dependent machinery composed of core NifB, NifEN and NifH proteins. Resulting FeMo-co is then inserted into apo-dinitrogenase (NifDK) (101).

Interestingly in bacteria, the NIF system has been identified also in non-nitrogen-fixing anaerobic bacteria *Helicobacter pylori*, in which the NifS and NifU components function in FeS cluster assembly, whereas the ISC and SUF machineries are absent (102). Moreover, it was demonstrated, that NifS and NifU genes from *E. histolytica* and *H. pylori* can restore cluster assembly activity in *Escherichia coli* where ISC an SUF systems are

deleted (103,104). However, this substitution was functional only under anaerobic conditions, which are characteristic for all organisms where genes from NIF system are present.

1.4.3. Cytosolic Iron sulfur assembly pathway (CIA)

The Cytosolic Iron/Sulfur cluster Assembly (CIA) pathway is ubiquitous in all eukaryotic cells and eight proteins in this pathway have been identified thus far (Tah18, Dre2, Nbp35, Cfd1, Nar1, Cia1, Cia2 and MMS19) (Figure 3).

Cytosolic P-loop NTPase Nbp35 and Cfd1 that are related to Ind1 form a scaffold heterotetrameric complex that coordinate transient [4Fe-4S] cluster (105). Nbp35 protein contains additional stable FeS cluster binding site on C-terminal part of the protein (106). It was proposed that cluster assembly on Nbp35 is nucleotide-dependent step (106). Transient cluster is transferred to various apoproteins with assistance of hydrogenase-like protein Nar1 and CIA targeting complex formed by Cia1, Cia2 and Mms19 protein (91). Glutaredoxin proteins (Grx3/Grx4) were reported to be essential for cluster synthesis via CIA pathway. These proteins are however involved in the control of iron homeostasis in cytoplasm and are not considered as CIA proteins (76).

Furthermore, diflavin oxidoreductase Tah18 and FeS protein Dre2 were identified as early acting CIA members. In their absence, FeS clusters on Nbp35 protein are not assembled (107,108). However, whether transient cluster (or both) on Nbp35 were specifically affected was not investigated. It was demonstrated, that FMN and FAD cofactors of Tah18 can maintain electron transfer from NADPH to Dre2 (107). Additionally, it was proposed, that these electrons are then transferred to Nbp35 protein. Nevertheless, the experimental evidence is missing. Several other functions unrelated to FeS synthesis, such as controlling of mitochondrial integrity and cellular death (109), involvement in synthesis of diferric-tyrosyl radical (Fe(III)2-Y•) cofactor of ribonuribonucleotide reductase (110) or nitric oxide synthesis (111) were suggested for Tah18 and Dre2 proteins in yeast. However, these alternative functions were not confirmed in further studies nor observed in any other organism up to date.

Interestingly, in plants, no gene for Cfd1 has been identified and Nbp35 possibly acts as a homodimer (112). Moreover, it was pointed out that in anaerobes, Tah18 and Dre2 proteins are not present (113). Therefore their involvement in CIA is likely connected to oxygen rich environment of aerobic living organism.

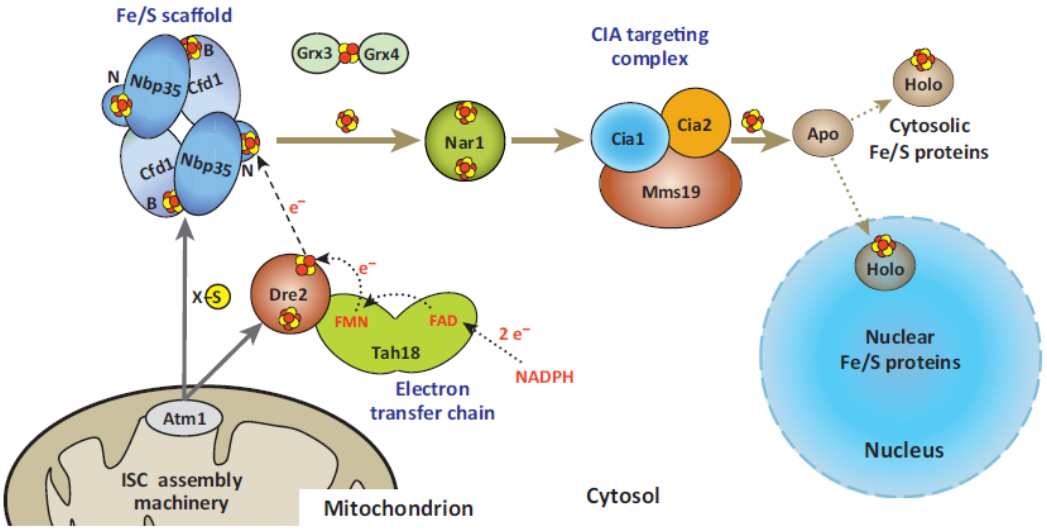

Figure 3. Model for the maturation of cytosolic and nuclear FeS proteins in yeast. Sulfur source X-S is exported from mitochondria by Atm1 transporter. Figure according to (44).

1.4.4. Sulfur mobilization pathway (SUF)

Cysteine desulfurase (Nfs2) in the plastid of *Arabidopsis thaliana* share homology to SufS from cyanobacteria (48). For proper desulfurase activity of Nfs2, SUFE1 protein is required. The protein complex that consists of SUFB, SUFC and SUFD subunits serves as a scaffold (114). The stoichiometry of the subunits in the scaffold is 1:2:1 (BC_2D). Flavin adenine domain of SufB is considered to be responsible for S^0 to S^{2-} reduction during cluster assembly process (115). SUFA, GRX14, GRX16 and three Nfu proteins (Nfu1, 2 and 3) are used as FeS carrier proteins. Interestingly, knockout mutants for Nfu2, SUFA, and both glutaredoxin related proteins (GRX16 and 14) are viable, suggesting redundancy of these individual proteins (reviewed in (116). In contrary, P-loop NTPase protein HCF101 (High chlorophyll fluorescence protein 101) is essential and specifically required for [4Fe-4S] cluster assembly in photosystem I (49).

Interestingly, HCF101 from plastid, Ind1 from mitochondria and nbp35 in cytoplasm are close homologues and thus they represent the only group of proteins present in all three major eukaryotic FeS cluster assembly pathways.

Iron donor for cluster assembly in plastid is unknown. Triple mutant in three major iron storage ferritin proteins did not result in decrease FeS protein activities in chloroplast (30).

Plasmodium falciparum harbors the plastid derived organelle called apicoplast. This organelle was acquired via secondary or tertiary endosymbiosis from red algae (117). Although apicoplast does not function in photosynthesis, it is involved in various processes such as fatty acid synthesis, lipoate synthesis, tRNA modification, and 2-C-methyl-D-erythritol 4-phosphate (MEP) isoprenoid biosynthesis (118). Core components of SUF pathway machinery (SufS, SufE, SufB and SufC) were identified in apicoplast. (119,120). They are essential for *Plasmodium* as was demonstrated by dominant negative approach (120). Interestingly, mutants are viable only when supplemented by IPP (isopentenyl pyrophosphate, intermediate in MEP biosynthesis), which implies the role of FeS clusters in isoprenoid synthesis (120).

1.5. FeS cluster assembly in *Giardia intestinalis*

Giardia intestinalis is an important unicellular human parasite of small intestine. It forms resistant cysts, which contaminate food and water. Beavers and other animals are important natural reservoirs of the human infective strains (mainly assemblage A and B) (121). *Giardia* possesses 8 flagella organized in 4 functional groups and attachment disk to adhere to the surface of the intestine. *Giardia* has undergone dramatic reductive evolution likely driven by its parasitic and anaerobic lifestyle. It contains the most reduced form of mitochondria - mitosomes (3). In mitosomes, DNA and nearly all typical mitochondrial pathways were lost. Only two pathways are conserved so far, ISC machinery and protein import pathway. Attempts to identify proteins involved in protein import pathway revealed very limited set of proteins (122). Mitosomal reduction could be exemplified by homologue of mitochondrial processing peptidase (MPP), the enzyme involved in cleavage of leader presequences of imported proteins (123). While in other eukaryotes this enzyme consists of two subunits α and β, in *Giardia* MPP function is maintained only by catalytically active β subunit (123).

As *Giardia* is anaerobe, many usual roles for FeS cluster containing proteins are not needed and corresponding genes are not present in the genome. However, FeS clusters are required for proteins of energy metabolism such as pyruvate ferredoxin reductase (PFO), ferredoxins, hydrogenase, or in enzymes involved in DNA metabolism. *Giardia* therefore needs ISC and CIA FeS cluster assembly pathways to maturate these proteins.

1.5.1. ISC pathway in *Giardia*

IscS was the first ISC component identified in *Giardia* genome (124). Later, IscU, IscS and [2Fe-2S] ferredoxin were localized in mitosomes of *G. intestinalis* (3,125). Episomal expression of tagged version of these proteins and polyclonal antibodies enabled to visualize the organelle under fluorescence microscope (3,125). Moreover, these proteins were used to demonstrate that mitosome share common mode of mitochondrial protein targeting (125). Other typical ISC genes were identified when the genomic data were completed (38). *Giardia* possesses genes for Nfu, IscA, mHSP70, Jac1, Grx5 and GrpE (38). Grx5 protein from mitosome was characterized (126). It possesses N terminal extension necessary for mitosomal targeting and is capable to bind FeS cluster.

Ind1 as well as its target protein mitochondrial respiratory Complex I are absent in genomic data. Interestingly, Iba57 for which direct function in [4Fe-4S] cluster formation was suggested is also not present (94). Other proteins involved in [4Fe-4S] cluster formation and delivery such as IscA and Nfu are present. Therefore likely [4Fe-4S] clusters are assembled in mitosome in the absence of Iba57. Interestingly, genes for ferredoxin reductase, frataxin and Isd11 proteins are also absent. These genes are essential in other organisms and it is unknown how *Giardia* supplements their function. Pyruvate: ferredoxin oxidoreductase with an ability to reduce ferredoxin is present in the genome, however it is localized in cytoplasm (127).

1.5.2. CIA pathway

In *Giardia*, Nar1, Cia1 and Cia2 genes were identified. Interestingly, three paralogues for Nbp35 are present within the genomic sequence (Nbp-1, Nbp-2 and Nbp-3). MMS19, Dre2 and usual cellular partner of Nbp35 protein (Cfd-1) are absent (128).

Additionally, two genes with similarity to Tah18 protein were identified. However, in phylogenetic reconstructions, they do not cluster with Tah18 proteins in other eukaryotes (128). These proteins rather share common origin with pyruvate NADP+ oxidoreductase (PNO).

1.6. FeS cluster assembly in other anaerobic protists

1.6.1. *Trichomonas vaginalis*

Trichomonas vaginalis, a close relative of *Giardia*, is an anaerobic sexually transmitted parasite of human. It possesses anaerobic type of mitochondria lacking DNA - hydrogenosomes. Hydrogenosomes contribute to energy metabolism through substrate-level phosphorylation (129). Amino acid metabolism is another role suggested for hydrogenosome, as hydrogenosomal aminotransferases and H and L proteins of glycine cleavage system (GCS) were identified. However, other two proteins of GCS (T and P) are absent therefore the function of H and L proteins is unclear (130).

Similarly to other mitochondria derived organelles, hydrogenosomes are involved in FeS cluster assembly. Hydrogenosomal localization of ISC components was confirmed for IscU, IscS, ferredoxin, frataxin and mitochondrial mtHsp70 (125,131,132). Other ISC proteins in hydrogenosome were found by proteomic analysis (IscA2, Jac1, GrpE, Isd11, Nfu1-4) (133-135). Hydrogenase maturases HydF, HydG and HydE are present to form H cluster of hydrogenases (96). Interestingly, neither genomic nor proteomic data revealed presence of Grx5. It is possible that the function of Grx5 is substituted by another FeS carrier protein as likely occur in viable knockouts of Grx14 and Grx16 in plastid of *Arabidopsis* (77). Ind1 proteins are present and likely serve for FeS cluster assembly on remnants of complex I.

Ferredoxin is reduced by hydrogenosomal pyruvate:ferredoxin oxidoreductase (PFO) whereas ferredoxin reductase is not present (136).

CIA machinery comprise of Nbp35, Cfd1, Nar1, Cia1, and Cia2 proteins whereas genes for Tah18, Dre2 and MMS19 are absent (128). Components of mitochondrial export machinery, Atm1, Erv1 and glutathione are absent in trichomonads as well, thus connection between ISC and CIA pathways is unknown.

In the genome of *Trichomonas vaginalis*, vast majority of genes are present as multiple paralogues, including genes for ISC and CIA pathways. Only two proteins are present as a single gene (IscU from ISC and Cia2 from CIA pathway). For example there are six genes for mitochondrial Hsp70 or seven genes for ferredoxin. Interestingly, expression of only three ferredoxin genes (Fdx3, 6 and 7) is upregulated together with components of ISC pathway, when iron source is restricted in the environment (134). Those ferredoxins therefore likely function in ISC pathway as electron donors. Interestingly, proteomic analysis revealed

that most of the ISC and CIA gene paralogues are simultaneously expressed and coregulated in response to iron (134).

1.6.2. *Entamoeba histolytica*

Intestinal human parasite *Entamoeba histolytica* causes amoebic dysentery. It is transmitted in form of cyst in contaminated food or water. *Entamoeba* contains reduced mitochondria, mitosome, which harbors sulfate activation pathway (60). This pathway is involved in the conversion of anorganic sulfate into biologically active form (137). Apart from DNA and energy metabolism, mitosomes also lack ISC pathway. Instead, ISC system is replaced by NIF system, likely acquired from bacteria.

There is a controversy about possible dual localization of NIF proteins. Maralikova et al. partially localized both NifU and NifS proteins in cytoplasm and mitosomes (61). It was estimated, that NifS and NifU are 10x more concentrated within the mitosomes than in cytoplasm. However in other analysis, both NifU and NifS genes were found to be present exclusively in cytoplasm of *Entamoeba* (58,62). Moreover, the presence of NifU and NifS within the mitosome was not confirmed by proteomic analysis (60,62).

Apart from NIF system, CIA machinery is present within the cytoplasm of *Entamoeba histolytica*. Genome of *E. histolytica* contains Nbp35, Cfd1, Nar1, Cia1, Cia2 and MMS19 protein (128). Nbp35 and Cfd1 were shown to interact with each other by *in vitro* and *in vivo* studies (138). CIA pathway is devoid of Tah18 and Dre2 protein as well as components of mitochondrial export system (Erv1 and ATM1) (139). The coordination of NIF and CIA pathways in cytosol is an attractive field of future investigations.

1.6.3. *Mastigamoeba balamuthi*

Mastigamoeba balamuthi is a free living relative of *E. histolytica*. Like *Entamoeba*, *M. balamuthi* lives under anaerobic conditions, e.g. in anaerobic layer of small wells and pools. *M. balamuthi* possesses reduced form of mitochondria (hydrogenosome) that lack genome and likely harbours sulfate activation pathway (140). In contrary to mitosomes of *E. histolytica*, hydrogenosomes of *Mastigamoeba* are involved in energy metabolism.

NIF system is present partially in the hydrogenosome and partially in the cytoplasm. Interestingly, dual localization of NIF pathway is maintained by two independent NifS and NifU gene sets (58). One NifU and NifS set lacks and other possesses N-terminal targeting

sequences. Predicted localization of all four NIF genes was confirmed experimentally (58). CIA machinery share common features with *Entamoeba*. Genes for Nbp35, Cfd1, Nar1, Cia1, Cia2 and MMS19 are present while genes for Tah18, Dre2, Erv1 and Atm1 are missing (58).

1.6.4. *Blastocystis hominis*

Blastocystis hominis is an unicellular stramenopile living in anaerobic environment of gastrointestinal tract of human. It has anaerobic mitochondria with the genome and capacity to maintain electrochemical proton gradient across mitochondrial membrane. Clusters are assembled through ISC system in mitochondria and CIA in cytoplasm.

Nbp35, Nar1 and Tah18-like proteins were identified in cytoplasm of *Blastocystis* using immunoelectron microscopy and heterologous expression in yeast (63). Moreover, genes for Cia1, Cia2 and MMS19 proteins are present in *Blastocystis* genome, however, the localization of these proteins has not been investigated (63). Genes for Cfd1 and Dre2 proteins are absent.

In addition to CIA, fused SufB and SufC genes (SufCB) from SUF system were identified in cytoplasm of *Blastocystis* (63). Under oxidative stress conditions, the expression of SufCB protein is upregulated. Therefore, it is likely that this gene is involved in cluster assembly under stress condition such as SUF system in bacteria.

1.6.5. *Pygsuia biforma*

The breviate *Pygsuia biforma* is a free-living anaerobic amoeboid flagellate living in hypoxic marine sediments (141). Recently, RNA-seq-based reconstruction of the mitochondrial proteome of *Pygsuia biforma* was reported (142). One hundred twenty-two proteins were predicted to localize in its anaerobic mitochondria. Some components of ISC machinery such as mHsp70, GrpE, Nfu1 and Ind1 were identified. Interestingly, genes for both IscU and IscS are absent in the dataset. Authors claimed that the lack of reads for IscS and IscU homologues in *Pygsuia* transcriptome most likely represents genuine absence of the genes as high depth of Illumina sequencing coverage was obtained for another ISC genes, *nfu1* and *ind1*.

Additionally, two genes for SUFCB fusion proteins have been found. Mitochondrial localization of one SUFBC (mSUFCB) was predicted by *in silico* analysis and then confirmed

using heterologous expression of the protein in yeast and immunostaining in *Pygsuia*. Authors therefore suggested that functional fusion of ISC and SUF pathway occurred in *Pygsuia*, where the function of IscU and IscS homologues is most likely replaced by mSUFCB protein (142). However, in predicted mitochondrial proteome of *Pygsuia* no protein with cysteine desulfurase activity was identified. For SUFB and SUFC proteins in plants or for mSUFCB protein in *Pygsuia*, cysteine desulfurase activity was never demonstrated. In another breviate *Breviata anathema*, gene for IscU and partial sequence for *iscs* have been identified (142). Thus, as no complete genomic sequence is available for *Pygsuia* it is possible that IscS and IscU homologues are yet to be discovered. Concerning CIA machinery, genes for Nbp35, Cfd1, Cia1, Cia2 and Nar1 proteins were found, whereas genes for Tah18 and Dre2 are absent in the dataset.

1.7. Heme

Heme is a flat shaped cofactor, where iron is coordinated in tetrapyrrole ring (porphyrin) with four nitrogens as ligands. Heme is bound to a protein chain via one or two axial ligands which complete the octahedral coordination around the iron ion and via residues that interact with porphyrin structure (143). In the electron carriers, the protein provides two axial ligands (typically histidine or methionine), which ensure a low-spin state of the iron ion and low reorganization energy of the site (144). If one axial ligand site is unoccupied, iron can bind water in hydroxylation reactions catalyzed by cytochrome p450 or carry diatomic gasses as hemoglobin (145). Several types of heme were identified, differing in additional functional group ligands. Most common type of heme is heme *b*, other important types include heme *a* and heme *c* with additional functional groups on carbohydrate backbone. Heme is bound in various enzymes and serves for chemical catalysis and electron transfer. Based on its type and protein structure it can operate with redox potential from –400 mV (Cyt c3) to +400 mV (Cyt b_{559}) (146). In cytochromes, most common binding sites represent two axial histidines. In siroheme proteins (sulfite reductase, nitrate reductase) the cysteine ligand bridge iron in heme to [4Fe-4S] cluster (147).

1.8. Heme synthesis, metabolism and homeostasis

To fulfill their heme requirements, a vast majority of organisms possess a heme biosynthetic pathway that converts δ-aminolevulinic acid (ALA) to heme in seven

consecutive steps, which are conserved in all domains of life (Figure 4) (148). Briefly, eight molecules of ALA are converted into urogen in three consecutive enzymatic steps (porphobilinogen synthase, porphobilinogen deaminase, urogen synthase) (149). The intermediate uroporphyrinogen III (urogen) represents the common precursor for all tetrapyrroles and is therefore an important branchpoint of the pathway. Then protoporphyrin IX is synthesized from urogen via coprogen and protogen intermediates (uroporphyrinogen decarboxylase; coproporphyrinogen oxidase; protoporphyrinogen oxidase) (150). Finally, the insertion of ferrous iron into protoporphyrin IX by ferrochelatase creates heme (151).

Archaea and most bacteria synthesize ALA from glutamate (C5 pathway), while α-proteobacteria do it by condensation of succinyl-CoA with glycine (C4 pathway) (152). Endosymbiotic events influenced formation of heme synthesis pathways in eukaryotes. In heterotrophs, C4 pathway is mosaic of pathway from mitochondrial α-proteobacterial predecessor and pre-eukaryotic host (153). It is partially localized in cytoplasm and mitochondria (Figure 4). In phototrophs, C5 pathway of cyanobacterial origin is usually localized in plastid and was acquired by primary or secondary endosymbiosis (153). Interestingly, in Apicomplexan parasites and Chromerids, which undergone secondary or tertiary plastid endosymbiosis (154), mixture of both C4 and C5 pathways is present and is localized both in mitochondria and plastid (148).

Coproporphyrinogen III oxidase and protoporphyrinogen IX oxidase of heme biosynthetic pathway (Figure 4) are oxygen-dependent proteins. These enzymes can be substituted using oxygen independent analogous proteins (coproporphyrinogen III dehydrogenase, oxygen-independent protoporphyrinogen IX oxidase) under anaerobiosis (155). Novel pathway of heme synthesis was recently described in *Archea* and several bacterial species (156). It include genes involved in urogen formation that are present also typical heme synthesis pathway. However, other “nir like” proteins that share homology to proteins involved in heme d_1 biosynthesis in denitrifying bacteria are involved (156). Some "nir like" proteins are similar to *S*-adenosyl-L-methionine-dependent uroporphyrinogen III methyltransferase (SUMT), an enzyme involved in formation of heme d_1 precursor (precorrin-2) from urogen (157).

Interestingly, several organisms bypassed their heme requirement by importing heme from external environment. *Caenorhabditis elegans* and *Bodo saltans* acquire heme from ingested bacteria cells. Parasites such as *Trypanosoma brucei* or blood sucking ticks can obtain heme from their hosts (10,158).

Heme homeostasis is tightly regulated process. Expression of the initial enzyme of heme synthesis (ALA synthase) is repressed by hemin (Fe^{3+} oxidation product of heme) (159). Free heme is degraded by heme oxygenase, which converts heme to biliverdin (160). To avoid toxic effect of free heme, heme oxygenase expression is rapidly induced after oxidative stress exposure (161). However, whole intracellular networks that mediate heme homeostasis in eukaryotes remain poorly understood (162). Hap1 protein (heme activator protein) in *S. cerevisiae* plays important role in heme dependent transcriptional activation of genes involved in respiration and oxidative damage control (163,164). Recently, novel proteins involved in heme homeostasis were described in *C. elegans* (165). For example, multidrug resistance protein 5 (Mrp5) likely acts as a heme exporter in *C. elegans* (166). Transcriptional regulator HrtR senses and binds a heme molecule in order to regulate the expression of the proteins involved in heme import in lactic acid bacteria *Lactococcus lactis* (167). However, how heme homeostasis is maintained in anaerobic parasites is unknown.

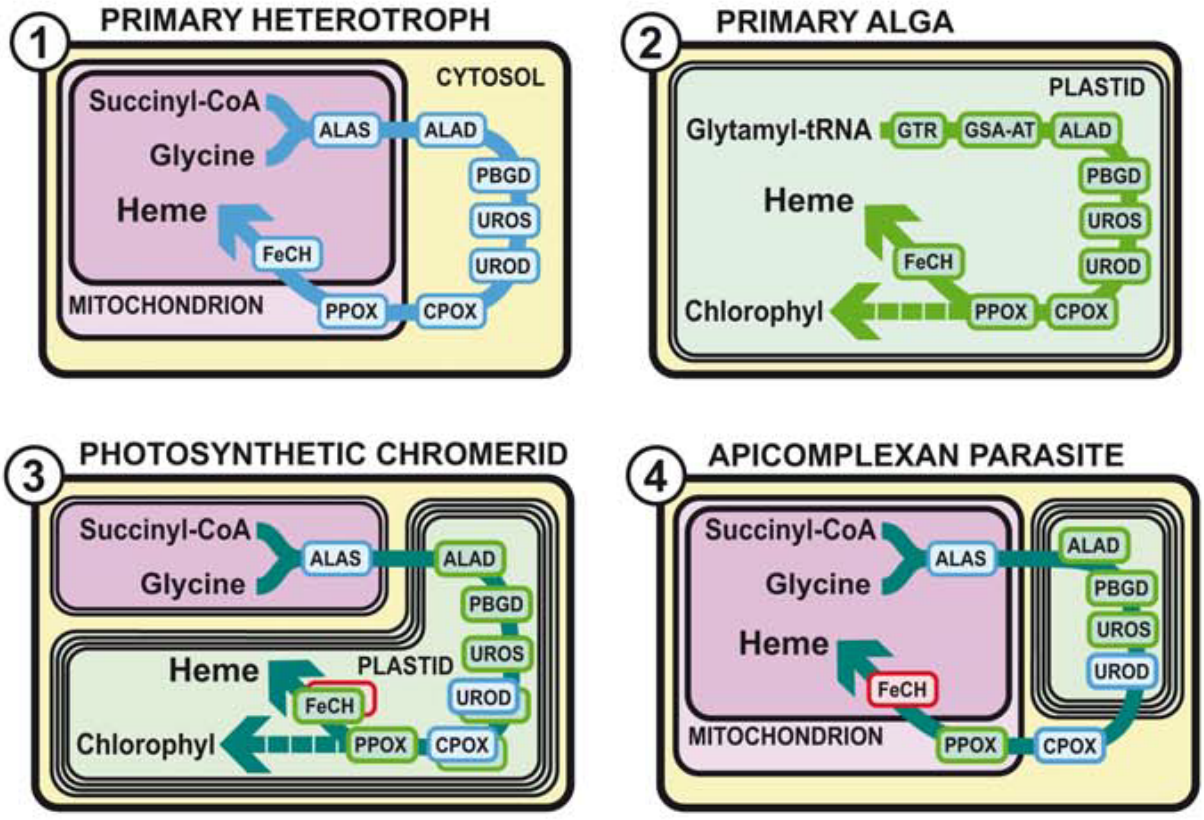

Figure 4. Distribution of heme pathway synthesis in mitochondria, plastid and cytoplasm in Eukaryotes.

Localization of heme synthesis enzymes in eukaryotes. In picture no 1. typical distribution of heme synthesis enzymes in heterotrophs such as *S. cerevisiae* or human is highlighted. Plastidal C5 pathway (no. 2) is present in most phototrophs, whereas in Chromerids and Apicomplexan parasites (no 3. and 4.) heme synthesis pathway share both mitochondrial and plastidal features. ALAS, ALA-synthase; GTR, glutamyl-tRNA reductase; GSA-AT, glutamate 1-semialdehyde aminotransferase; ALAD, ALA-dehydratase; PBGD, porphobilinogen deaminase; UROS, uroporphyrinogen synthase; UROD, uroporphyrinogen decarboxylase; CPOX, coproporphyrinogen oxidase; PPOX, protoporphyrinogen oxidase; FeCH, ferrochelatase. Figure according to (148).

1.9. Heme proteins and their function

Heme proteins play an important role mainly in chemical catalysis, electron transfer and diatomic gas transfer. Several types of cytochromes are part of respiratory chain complexes. Lanosterol 14alfa-demethylase and c-22 sterol desaturase (both members of cytochrome p450 family) are involved in sterol synthesis. Heme peroxidases, flavohemoglobin or catalases are involved in oxidative/nitrosative stress defense (168). Additionally, the number of new signal transduction heme containing proteins such as adenylate/guanylate cyclase is uprising (169). Cytochrome b_5 (cytb_5) proteins are small C-tail anchored proteins with many suggested oxidoreductase based functions (170). Cytb_5 is a model protein for posttranslational targeting of C-tail anchored proteins (171). The charge and length of transmembrane domain likely determine the localization of the protein either in the outer mitochondrial membrane or in the membrane of endoplasmic reticulum (171). During fatty acid desaturation on the surface of endoplasmic reticulum, electrons transferred from reduced cytb_5 are necessary (172). Cytb_5 is also essential for monooxygenase reaction catalysed by cytochrome p450 (170). The outer mitochondrial cytb_5 is highly expressed in rat testis and likely functions in 17α-hydroxyprogesterone synthesis (173). Additionally, cytb_5 domains are integrated to more complex proteins with various catalytic functions (fatty acid desaturases, hydroxylases or sulfite oxidases).

Many of the previously mentioned hemoproteins are essential (7,174). Interestingly, aerobic protist *Phytomonas serpens* was observed to growth without heme (175). It lacks heme synthesis pathway, and possess alternative systems in which heme is normally involved. For example, cytb_5 domain in Δ9-fatty acid desaturase, which is ubiquitously present in excavates, was lost in *P. serpens* (175). Respiratory chain in *P. serpens* lack complex III and

IV and serves in reoxidizing NADH produced during glycolysis (176). Interestingly, complex II is present and still active in *P. serpens* grown without heme, although the protein possesses typical heme binding motifs on SDH4 subunit (175). Unique ability to adapt for life without heme was further demonstrated on lanosterol 14α-demethylase. This enzyme produces ergosterol when *P. serpens* is cultured under heme-rich conditions. However, when heme amount is limiting, lanosterol instead of ergosterol is incorporated into the cellular membrane of *P. serpens* (175). Surprisingly, genome of *P. serpens* encodes other putative heme binding proteins. For example 19 genes for cytb_5-like proteins are present. It is possible, that they are used under heme- rich conditions as lanosterol 14α-demethylase or they are essential in yet unknown natural conditions.

1.10. Heme binding proteins in *Giardia intestinalis*

Heme is a key and usually an essential cofactor for aerobic eukaryotes, whereas anaerobic organisms were believed to live without heme. However, recent analysis of genomes of several anaerobic protists including *G. intestinalis* revealed presence of some putative heme-binding proteins (148). *G. intestinalis* lacks all enzymes of heme synthetic pathway. However, its genome contains genes for flavohemoglobin and cytb_5 proteins (12,177). Interestingly, the latter protein is conserved in most anaerobic protists except *E. histolytica* and *Blastocystis hominis* (148).

1.10.1. Flavohemoglobin

Giardia encodes a single gene for flavohemoglobin. This protein is usually present in various bacteria and fungi. It was demonstrated that this gene was likely acquired by lateral gene transfer (178). Flavohemoglobins usually possess nitric oxide dioxygenase activity, which protects cells against NO-mediated damage. The ability to bind heme and flavin adenine dinucleotide cofactor was confirmed for recombinant *Giardia* flavohemoglobin *in vitro* (177). Moreover it was shown that this protein displays similar biochemical behavior to other known flavohemoglobins. It possesses NADH and NADPH oxidase activity and it catalyzes NO breakdown (179).

1.10.2. Cytochrome b_5

Three genes for *Giardia* cytb_5 (gCYTb_5 I-III) were identified in the genome of *Giardia*. The ability to bind heme *in vitro* was demonstrated for gCYTb_5-I (12). Interestingly, when compared to previously characterized cytb_5 proteins in yeast and mammals, proteins from *Giardia* display unusually low redox potentials and lack typical C-terminal transmembrane domain. Typical cytb_5 are short proteins (around 10-15 kDa). Interestingly gCYTb_5 proteins possess N- and C-terminal charged extensions (12).

1.11. Heme binding proteins in other anaerobic protists

Trichomonas vaginalis possesses 5 genes coding for cytb_5-like proteins (148). Similarly to *Giardia*, they all lack transmembrane domain. Additionally, the presence of adenylate/guanylate cyclase (PAS domain) protein was suggested (148). PAS domain is found in various signal transduction proteins where heme is serving as a signal sensor (180). In contrary to *Giardia*, *T. vaginalis* lacks flavohemoglobin. The presence of heme within the cells was not studied. However, it was suggested that AP65 (malic enzyme) possibly mediate adherence of *T. vaginalis* to vaginal epithelial cells in heme-dependent manner (181). The mechanism is unclear though. It was shown that AP65 together with another adhesin (AP51) are likely able to bind heme or hemoglobin (182).

Entamoeba histolytica expresses two extracellular heme scavenging proteins EhHmbp26 and EhHmbp45 (183,184). They possibly serve as a hemophores with high affinity for heme and they probably cooperate with putative heme or iron importing pathway. However, no target heme-binding protein has been identified in this parasite so far (148). Thus, the involvement of these proteins in iron acquisition is more favorable scenario.

Blastocystis is the second eukaryote known to lack cytb_5 proteins. Interestingly, heme binding subunit of succinate dehydrogenase and putative DNA-binding HLH protein with PAS domain were identified in genomic data of this protist (148). In *Encephalitozoon* only cytb_5s are present whereas in *Cryptosporidium* in addition to cytb_5s, two putative PAS domain containing proteins are present (148).

1.12. Other iron containing proteins

Various proteins are able to bind iron in non-heme, non-FeS cluster form. Bacterial flavodiiron proteins (FDPs) are able to bind diiron center with histidine and carboxylate

residues as ligands (185). These proteins are believed to function as an oxygen or nitric oxide reductases to provide protection against oxidative/nitrosative stresses. Interestingly, FDPs were identified in the genome of *Trichomonas vaginalis*, *Giardia intestinalis*, *Entamoeba histolytica* and *Spironucleus salmonicida* (186,187). Likely, FDP genes in these protists were acquired by lateral gene transfer (187).

In *T. vaginalis*, one of four FDP homologues has been investigated in some detail. This protein is targeted to hydrogenomes of *T. vaginalis*, where it likely functions as an oxygen reductase but is unable to utilize nitric oxide as a substrate (188). *Giardia* FDP homologue lacks mitosomal targeting presequence. Therefore it is likely cytoplasmic. Similarly to *T. vaginalis*, *Giardia* FDP has high O_2-reductase activity, but very low NO-reductase activity (189). Therefore, *Giardia* FDP is likely involved in cellular defense against oxygen.

Ribonucleotid reductase (RNR) is an essential protein of DNA metabolism ubiquitous in all eukaryotes. It catalyzes the formation of deoxyribonucleotides from ribonucleotides. The protein contains diferric iron center. Each iron ion is coordinated by five oxygen and one nitrogen ligands and both iron ions are bridged by glutamate side chain and O^{2-} ion (190). Interestingly, gene coding for RNR is missing in the genome of *Giardia intestinalis* (38,191). *Giardia* therefore depends on the salvage of exogenous purine deoxynucleosides (191).

2. Aims

- To characterize cytochromes b_5 proteins and their ability to bind heme *in vitro* and in *G. intestinalis*
- To test the presence of heme in *G. intestinalis*
- To characterize Tah18-like oxidoreductases from *G. intestinalis*
- To investigate the composition of ISC and CIA pathways and cellular localization of their components

3. List of publications and author contribution

- Martincova E., Voleman L., Pyrih J., Zarsky V., Vondrackova P., Kolisko M., Tachezy J., Dolezal P. **Probing the biology of *Giardia intestinalis* mitosomes using**

in vivo enzymatic tagging. Molecular and Cellular Biology. 2015 Jun;35(16):2864-74.

- Together with Eva Martincová: precipitation of Pam18 interacting proteins, analysis of proteomic data and precipitation protocol development. Individually: construction of the vector for cytosolic BirA expression in *Giardia*.

- Pyrih J., Harant K., Martincova E., Sutak R., Lesuisse E., Hrdy I., Tachezy J. ***Giardia intestinalis*** **incorporates heme into cytosolic cytochrome b_5.** Eukaryot Cell. 2014 Feb;13(2):231-9.

    - Development of technique for detection low heme concentration in *Giardia* cytoplasm using HPLC; sample preparation for low temperature spectroscopy; cloning of majority of constructs; isolation and spectroscopic measurement of activities of recombinant enzymes expressed in bacteria; detection and localization of proteins using immunofluorescence techniques and cell fractionation; phylogenetic analysis of cytochromes b_5 and *in silico* analysis of cytochrome b_5 type II subgroup, manuscript preparation.

- Jedelský P.L., Doležal P., Rada P., Pyrih J., Šmíd O., Hrdý I., Šedinová M., Marcinčiková M., Voleman L.,Perry A.J., Beltrán N.C.,Lithgow T., Tachezy J. **The minimal proteome in the reduced mitochondrion of the parasitic protist *Giardia intestinalis*.** PLoS One. 2011 Feb 24;6(2):e17285.

    - Localization of GiOR proteins using immunofluorescence microscopy and cellular fractionation; measurement of the ability of these proteins to transfer electrons from NADPH to various electron acceptors. Cloning constructs for GiOR related experiments.

Unpublished data

- Pyrih J., Martincová E., Kolisko M., Stojanovová D., Somsuvro B., Lukeš J., Roger A., Tachezy J. **Iron Sulphur cluster assembly in cytoplasm of anaerobic living protist *G. intestinalis*.** Manuscript in preparation.

    - Crosslinking and precipitacion of GiOR-1 and Cia2 interacting proteins; immunofluorescence and cell fractionation; phylogenetic analysis of Tah18 domain containing proteins; production and purification of polyclonal antibodies in rats; cloning of majority of constructs, manuscript preparation

4. Summary

- **Novel type of cytochrome b_5 in *Giardia* and other eukaryotes**

We identified new gCYTb_5 paralogue in *Giardia* genome named gCYTb_5-IV that is divergent from known gCYTb_5 proteins (192). It possesses N terminal domain (about 100 amino acid residues) with unknown homology. Another new giardial cytb5-like protein that we identified is GiTax. This proteins appears to be an ortholog of the *T. brucei* axonemal protein TAX-2, which is important for flagellar function (193). This protein lack heme iron-coordinating histidine ligands and therefore likely does not bind heme (192).

We demonstarted that native recombinant gCYTb_5-IV as well as gCYTb_5 II and III proteins are able to bind heme *in vitro* (192) as was previously showed for gCYTb-I (177). Moreover, we demonstrated that gCYTb_5-IV is able to bind heme within the cell of *Giardia intestinalis*. Furthermore, we showed *in vitro* that heme binding ability is drastically lowered when first axial heme-binding histidine in gCYTb_5-IV is mutated to leucine. The same effect was observed in living *Giardia* cells, when mutated protein was overexpressed (192).

Transmembrane domain (TM) is responsible for targeting of cytb_5 on the surface of mitochondria or endoplasmic reticulum in mammals, yeast or plants (194). Interestingly, our bioinformatic analysis revealed that all gCYTb_5 proteins lack TM domain. Hence, we investigated the localization of these cytb_5 proteins in *Giardia*. In order to detect gCYTb_5 in the cell, we fused gCYTb_5-I-IV with hemagglutinin-tag. Based on immunofluorescence microscopy and analysis of subcellular fractions, all four gCYTb_5 appeared to be cytosolic proteins, which is consistent with the lack of transmembrane domain.

Analysis of primary structure and phylogeny comparing set of 102 cytb_5 protein sequences across all eukaryotic supergroups revealed the existence of three subgroups of cytb_5 proteins (named type I, II, III). Type I cytb_5 group consists of already characterized cytb_5 from mitochondria or endoplasmic reticulum. The first axial histidine within the HPGG motif of type I cytb_5s is surrounded by acidic residues, whereas the second histidine is part of conserved GHS motif. *Giardia* gCYTb_5 proteins belong to type II. This group is characterized by lack of C-terminal transmembrane domain and possess modified heme binding site. In type II cytb_5 proteins, first axial histidine is not surrounded by acidic residues and the second one is part of the H-X-WV(N/S) motif.

Importantly, cytb_5 type II represent a novel group of cytb_5 proteins that are ubiquitous in both aerobes and anaerobes (192). However, the function of type II cytb_5 is unknown and it has not been studied so far. Apart from type I and II cytb_5, we defined type III cytb_5 that is present in fungi (192).

- **Heme utilization in *Giardia***

Our data demonstrated, that *Giardia* is able to import extracellular heme and incorporate it in the cytoplasmic cytb_5 (192). This is the first report when heme was identified within the anaerobic cell. Moreover, our data suggested that *Giardia* somehow maintains heme homeostasis. Overexpression of heme binding protein (gCYTb_5-IV) in cytoplasm resulted in increased cellular heme content. Moreover, heme loading on cytoplasmic cytb_5 was dependent on concentration of heme in culture media. We can speculate that overexpression of CYTb_5-IV results in increased demands for cellular heme, which may provide a signal to increase the import of heme from the environment. However, how heme homeostasis is maintained in *Giardia* is unclear. Searches in the genome of *Giardia* failed to identify any candidates for proteins involved in regulation of heme homeostasis.

It would be interesting to investigate the essentiality of heme within the *Giardia* and other anaerobes. However, no define heme-free media is currently available to address this question.

- **Characterization of Tah18-like oxidoreductases from *G. intestinalis***

Giardia possesses two genes coding for proteins with similarity to Tah18 (GiOR-1 and 2) (195). GiOR proteins in *Giardia* together with Tah18 and cytochrome p450 reductase homologues are of similar length and contain $NADP^+$ binding site together with FMN and

FAD redox centers (CPR domain; derived from cytochrome p450 reductase like domain) (107,195). Moreover, CPR domain is integrated in methionine synthase, sulfite reductase, nitric oxide synthase and Pyruvate:NADP+ oxidoreductase. Recently, gene phylogeny was used for identification of Tah18 homologues in various eukaryotes (128). In this analysis, Giardia GiOR proteins clustered together with Pyruvate: NADP+ oxidoreductase homologues. However, the statistical support was rather low (128).

In our phylogenetic anaysis we used additional CPR domains from proteins encoded in genomes of other metamonads. Our data revealed, that Tah18 and GiORs have different evolutional origin (Pyrih, unpublished data). GiORs clustered together with CPR domain of CPR-hydrogenase fusion proteins, which are present in closely related metamonads, whereas Tah18 homologues formed distinct branch. In GiOR-1 and GiOR-2, hydrogenase domain was likely secondarily lost, as the fusion protein is present in ancestral metamonads such as *Trimastix* or *Carpediemonas*. Considering the absence of Dre2 which forms electron donor complex with Tah18 in all metamonad lineage, it is likely that GiOR proteins possess different function than Tah18. Similarly, CIA pathway of close relative metamonad *Spironucleus salmonicida* apparently functions without Tah18 protein as genes for CRP domain containing proteins are absent in the genome (186).

We hypothesized that diflavin reductase GiOR-1 in *Giardia* might be an oxidoreductase of cytb_5. We prepared the GiOR-1 recombinant protein in native form and confirmed its ability to bind FMN and FAD cofactors. The native protein was able to reduce gCYTb_5s, when NADPH was added as an electron donor to the reaction mixture (192). However, further detailed studies of GiOR-1 revealed that GiOR-1 protein is exclusively localized inside of mitosomes (Pyrih, unpublished results), while gCYTb_5s are cytoplasmic and their presence in the mitosome was not observed. Moreover, co-precipitation of GiOR-1 and interacting proteins has not revealed any gCYTb_5 (Pyrih, unpublished data). Therefore it is likely that GiOR-1 is not a physiological oxidoreductase of gCYTb_5 *in vivo*. Similar artificial reactivity of Tah18 domain containing proteins with cytochromes was already reported (196).

GiOR-2 protein was previously observed to be associated with unknown vesicles (195). However, whether the protein exists also in cytoplasm was not tested. It is a close homolog of GiOR-1 that possess FMN, FAD and NADPH binding sites. Therefore it is possible that GiOR-2 may function as gCYTb_5 oxidoreductase.

No homologue of ferredoxin reductase, that is usually involved in ISC pathway, is present in genomic data of all sequenced *Giardia* strains. GiOR-1 protein identified in

Giardia mitosomes is diflavin oxidoreductase with ability to transfer electron from NADPH to artificial acceptors such as dichlorophenolindophenol, methyl viologen, and cytb_5 (195). Interestingly, oxidoreductases of cluster assembly machineries (Arh1 in ISC pathway and SufB in SUF pathway) contain FAD binding domain and NADH or NADPH oxidoreductase activity. Moreover, most of proteins co-precipitated with GiOR-1 belong to ISC pathway (Pyrih, unpublished data). Therefore, it is possible that GiOR-1 serves as the reductase of mitosomal ferredoxin (GiFdx) *in vivo*. Nevertheless, we failed to confirm this hypothesis. GiOR-1 protein prepared and isolated from bacteria was unable to reduce recombinant GiFdx (195).

- **ISC pathway in *Giardia***

In 2011, we published the first proteome of *Giardia* mitosome. Mitosomal fractions were obtained via differential ultracentrifugation in optiprep gradient (195). As separation of pure mitosomal fraction not appeared to be feasible, we used quantitative mass spectrometry for localization of organelle proteins. Two subcellular fractions with different content of mitosomes and contaminating organelles were compared. Proteins with the same ratio as marker mitosomal proteins were selected. Therefore, from total 638 identified proteins, 139 putative mitosomal proteins were filtered. The presence of key ISC proteins (IscU, IscS, ferredoxin, Grx5, Nfu, IscA, mHsp70 and GrpE) in mitosomes was detected and confirmed by epitope tagging and overexpression in *Giardia*. Interestingly, no other mitochondrial pathway apart from protein import pathway was identified, although the presence of some proteins (e.g. GiOR-1, GL50803_9296) with unknown function was confirmed to localize in mitosome (195).

Recently, another approach was used to explore mitosomal proteome (197). Reporter mitosomal proteins were subcloned with biotin acceptor peptide and expressed together with biotin ligase. Proteins of interest were then biotynilated *in vivo*. The protein was subsequently crosslinked with its putative protein partners and whole complex was purified by streptavidin coupled to Dyna-Beads. As beads can be washed up to 2% SDS (sodium dodecyl sulfate) without release of the target protein, highly pure complexes of cross-linked proteins were obtained and analyzed by mass spectrometry. For example, only 14 proteins were co-precipitated with GiOR-1. From those, first 9 hits were already known mitosomal proteins (Pyrih, unpublished data). At least 10 novel proteins with no clear homology to known

eukaryotic proteins were co-precipitated with components of mitosomal protein import machinery (for example GL50803_3491, GL50803_9696, GL50803_27910). The presence of these proteins in mitosome was subsequently confirmed by episomal expression of tagged proteins (197). Some proteins such as GL50803_3491, GL50803_9296 were identified in previous proteomic analysis (195).

Altogether, these proteomic datasets provide useful tool for reconstruction of ISC mitosomal pathway. Interestingly, some ISC proteins that are conserved and essential in other eukaryotes are missing in *Giardia* (e.g frataxin, ferredoxin reductase and Isd11, Iba57). In addition to ISC pathway, proteins from mitochondrial protein import machinery were identified together with several proteins with unknown homologues. It is possible, that some of those unknown proteins (for example GL50803_3491, GL50803_9696, GiOR-1) might be functional homologs of frataxin, ferredoxin reductase or Isd11 proteins. For protein (GL50803_27910) close sequence homology to rhodanese was observed. As rhodanese-like proteins are usually involved in sulfur metabolism (198), involvement of this protein in ISC pathway is possible. Interestingly, the presence of Jac1 was not found in any proteomic data, although gene for Jac1 is encoded in the genome and tagged Jac1 expressed in Giardia was observed in mitosomes (195).

Giardia possesses minimalistic genomic sequence with just few introns and is known to possess simplified machinery for DNA replication, transcription, RNA processing, and most metabolic pathways (38). We were able to show that some proteins without homology to other eukaryotic proteins are present within the mitosome of *Giardia*. Therefore our data suggest that during the evolution of mitosome, loss of some mitochondrial genes and pathways happened simultaneously with invention of new *Giardia* specific proteins (197).

- **Characterization of CIA machinery**

Searches for homologues of CIA pathway in *Giardia* genome database revealed genes for Nbp35, Nar1, Cia1, and Cia2. CIA machinery in *G. intestinalis* is apparently devoid of MMS19, Cdf1, Tah18 (see discussion above), and Dre2 proteins. The absence of MMS19 is not surprising as the enzyme is missing in various members of *Stramenophila*, *Apicomplexa*, *Viridiplantae* or *Microsporidia* (128). Moreover, MMS19 protein is the only protein involved in CIA machinery in plants which is not essential (199). Missing gene for Cfd1 could be explained by possible substitution with Nbp35 that is encoded in *Giardia* by three paralogous genes. Similar situation occurs in plants, where Cfd1 is not present and Nbp35 acts as a

homodimer (112). Interestingly, genes for Cfd1 were identified in other metamonads, *T. vaginalis*, *Carpediemonas membranifera* and *Chilomastix cuspidata*, suggesting secondary loss of Cfd1 in *Giardia* and *Spironucleus salmonicida* (Pyrih, unpublished data). The Absence of Tah18 and Dre2 gene is consistent with lack of these genes in other anaerobes (200). However, how clusters in anaerobes are assembled in the absence of this essential electron donor complex is unclear.

To investigate cellular localization of CIA proteins, corresponding genes were subcloned for epitope tagged protein expression in *Giardia* or specific antibodies were raised against them. Proteins were visualized using fluorescence microscopy and subcellular fractionation. While all CIA components share expected cytoplasmic distribution, several proteins displayed additional mitosomal distribution. In combination with co-precipitation techniques, two Nbp35 paralogues were identified on the surface of the mitosome. Localization of Cia2 protein is however more complicated. Based on protein protection assay, the protein is localized into intermembrane space or mitosomal matrix (Pyrih, unpublished data). Based on co-precipitation experiments, Cia2 protein is situated near to outer mitosomal membrane (Pyrih, unpublished data), as nearly all proteins co-precipitated with Cia2 were previously co-precipitated also with Tom40 and GiMOMP35 proteins (197). Both Tom40 and GiMOMP35 are integral outer mitosomal proteins facing both to cytosol and intermembrane space of the mitochondria (122,197). Combining these two observations we concluded that Cia2 is likely present in intermembrane space of the mitosome (Pyrih, unpublished data).

It is unknown whether ISC pathway in mitosome and CIA pathway in cytoplasm are connected, as Atm1 and Erv1 genes are absent (38). Therefore, it is possible that both pathways act independently. However, no cysteine desulfurase (possible sulfur donor for CIA) was identified in cytoplasm of *Giardia*. Moreover, Nbp35 proteins, which are initial CIA proteins were identified on the surface of the mitosome. Additionally, no essential FeS protein candidate apart from ISC pathway members itself was identified within the mitosome of *Giardia*. Therefore, it seems likely that mitosomal ISC pathway is connected with CIA for FeS cluster assembly in cytoplasm.

We can speculate that Cia2 protein in IMS space might be involved in ISC-CIA connection. It was described, that Cia2 protein in yeast possesses reactive cysteine with unknown function (201). Based on the sequence, the same is true for *Giardia* homologue. Therefore, it is possible that this reactive cysteine is somehow involved in transfer of sulfur compound in intermembrane space of the mitosome.

Further research needs to be done to understand the possible interaction between ISC and CIA machineries in *Giardia*.

5. List of alternative protein names

In this work	Full name	Bacteria	Yeast	Human	Plants
IscU	Iron-sulfur cluster scaffold homolog	IscU	Isu1	IscU	Isu1
IscS	Cysteine desulfurase	IscS	Nfs1	IscS	Nfs1
Ferredoxin	Ferredoxin, adrenodoxin	Fdx	Yah1	ADX1	Fd
Ferredoxin reductase	Ferredoxin reductase, adrenodoxin red	FNR	Arh1	ADXR, FDXR	FNR
Frataxin	Frataxin	CyaY	Yfh1	FXN	FH-1
mtHsp70	Mitochondrial heat shock protein 70 kDa	HSCA	Ssq1 (not orthologue)	mtHsp70	HSCA
Jac1	HSCB iron sulfur cluster co-chaperone	HSCB	Jac1	HSCB	HSCB
GrpE	Nucleotide exchange factor GrpE	GrpE	Mge1	Mge1	GrpE
Ind1	Iron-sulfur protein IND1	-	Ind1 (Yarrowia)	Nubpl	IndH
ATM1	ATP-binding casette transporter subfamily B member 7	-	ATM1	ABCB7	ATM3
Dre2	Cytokine induced poptosis inhibitor 1, anamorsin	-	Dre2	Ciapin1	Dre2
Tah18	NADPH Dependent Diflavin Oxidoreductase 1	-	Tah18	NDOR1	ATR3
Nbp35	Nucleotide binding protein 1	-	Nbp35	Nubp1	Nbp35
Cfd1	Nucleotide binding protein 2	-	Cfd1	Nubp2	-
Nar1	Nuclear prelamin A	-	Nar1	IOP1/NARF	Nar1
Cia1	Cytosolic iron-sulfur protein assembly I	-	Cia1	IOP1	Cia1
Cia2	Cytosolic iron-sulfur protein assembly II	-	Cia2	Mip18	AE7
MMS19	MMS19 Nucleotide Excision Repair Homolog	-	Met18	MMS19	Met18

6. References

1. **Outten, C. E. and A. N. Albetel**. 2013. Iron sensing and regulation in *Saccharomyces cerevisiae*: Ironing out the mechanistic details. Current Opinion in Microbiology **16**:662-668.

2. **Makiuchi, T. and T. Nozaki**. 2014. Highly divergent mitochondrion-related organelles in anaerobic parasitic protozoa. Biochimie **100C**:3-17.

3. **Tovar, J., G. Leon-Avila, L. B. Sanchez, R. Sutak, J. Tachezy, M. van der Giezen, M. Hernandez, M. Muller, and J. M. Lucocq**. 2003. Mitochondrial remnant organelles of *Giardia* function in iron-sulphur protein maturation. Nature **426**:172-176.

4. **Stehling, O., A. A. Vashisht, J. Mascarenhas, Z. O. Jonsson, T. Sharma, D. J. A. Netz, A. J. Pierik, J. A. Wohlschlegel, and R. Lill**. 2012. MMS19 assembles Iron-Sulfur proteins required for DNA metabolism and genomic integrity. Science **337**:195-199.

5. **Luo, D. X., D. G. Bernard, J. Balk, H. Hai, and X. F. Cui**. 2012. The DUF59 family gene AE7 acts in the cytosolic Iron-Sulfur cluster assembly pathway to maintain nuclear genome integrity in *Arabidopsis*. Plant Cell **24**:4135-4148.

6. **Kispal, G., P. Csere, C. Prohl, and R. Lill**. 1999. The mitochondrial proteins Atm1p and Nfs1p are essential for biogenesis of cytosolic Fe/S proteins. Embo Journal **18**:3981-3989.

7. **Ke, H. J., P. A. Sigala, K. Miura, J. M. Morrisey, M. W. Mather, J. R. Crowley, J. P. Henderson, D. E. Goldberg, C. A. Long, and A. B. Vaidya**. 2014. The heme biosynthesis pathway is essential for *Plasmodium falciparum* development in mosquito stage but not in blood stages. Journal of Biological Chemistry **289**:34827-34837.

8. **Awa, Y., N. Iwai, T. Ueda, K. Suzuki, S. Asano, J. Yamagishi, K. Nagai, and M. Wachi**. 2005. Isolation of a new antibiotic, alaremycin, structurally related to 5-

aminolevulinic acid from *Streptomyces sp* A012304. Bioscience Biotechnology and Biochemistry **69**:1721-1725.

9. **Rao, A. U., L. K. Carta, E. Lesuisse, and I. Hamza**. 2005. Lack of heme synthesis in a free-living eukaryote. Proceedings of the National Academy of Sciences of the United States of America **102**:4270-4275.

10. **Lara, F. A., U. Lins, G. H. Bechara, and P. L. Oliveira**. 2005. Tracing heme in a living cell: hemoglobin degradation and heme traffic in digest cells of the cattle tick *Boophilus microplus*. Journal of Experimental Biology **208**:3093-3101.

11. **Hernandez-Cuevas, N. A., C. Weber, C. C. Hon, and N. Guillen**. 2014. Gene expression profiling in *Entamoeba histolytica* identifies key components in iron uptake and metabolism. Plos One **9**.

12. **Alam, S., J. Yee, M. Couture, S. J. Takayama, W. H. Tseng, A. G. Mauk, and S. Rafferty**. 2012. Cytochrome b(5) from *Giardia lamblia*. Metallomics **4**:1255-1261.

13. **Brumbarova, T., P. Bauer, and R. Ivanov**. 2015. Molecular mechanisms governing *Arabidopsis* iron uptake. Trends in Plant Science **20**:124-133.

14. **Romheld, V.** 1987. Different strategies for iron acquisition in higher plants. Physiologia Plantarum **70**:231-234.

15. **Grotz, N. and M. L. Guerinot**. 2006. Molecular aspects of Cu, Fe and Zn homeostasis in plants. Biochimica et Biophysica Acta-Molecular Cell Research **1763**:595-608.

16. **Desilva, D. M., C. C. Askwith, D. Eide, and J. Kaplan**. 1995. The Fet3 gene-product required for high-affinity iron transport in yeast is a cell-surface Ferroxidase. Journal of Biological Chemistry **270**:1098-1101.

17. **Haas, H.** 2003. Molecular genetics of fungal siderophore biosynthesis and uptake: the role of siderophores in iron uptake and storage. Applied Microbiology and Biotechnology **62**:316-330.

18. **Mach, J., J. Tachezy, and R. Sutak**. 2013. Efficient iron uptake via a reductive mechanism in procyclic *Trypanosoma brucei*. Journal of Parasitology **99**:363-364.

19. **Flannery, A. R., R. L. Renberg, and N. W. Andrews**. 2013. Pathways of iron acquisition and utilization in *Leishmania*. Current Opinion in Microbiology **16**:716-721.

20. **Saha, R., N. Saha, R. S. Donofrio, and L. L. Bestervelt**. 2013. Microbial siderophores: a mini review. Journal of Basic Microbiology **53**:303-317.

21. **Krewulak, K. D. and H. J. Vogel**. 2008. Structural biology of bacterial iron uptake. Biochimica et Biophysica Acta-Biomembranes **1778**:1781-1804.

22. **Sutak, R., E. Lesuisse, J. Tachezy, and D. R. Richardson**. 2008. Crusade for iron: iron uptake in unicellular eukaryotes and its significance for virulence. Trends in Microbiology **16**:261-268.

23. **Bitter, W., H. Gerrits, R. Kieft, and P. Borst**. 1998. The role of transferrin-receptor variation in the host range of *Trypanosoma brucei*. Nature **391**:499-502.

24. **Leon-Sicairos, N., M. Reyes-Lopez, A. Canizalez-Roman, R. M. Bermudez-Cruz, J. Serrano-Luna, R. Arroyo, and M. de la Garza**. 2005. Human hololactoferrin: endocytosis and use as an iron source by the parasite *Entamoeba histolytica*. Microbiology-Sgm **151**:3859-3871.

25. **Tachezy, J., J. Kulda, I. Bahnikova, P. Suchan, J. Razga, and J. Schrevel**. 1996. *Tritrichomonas foetus*: Iron acquisition from lactoferrin and transferrin. Experimental Parasitology **83**:216-228.

26. **Lehker, M. W. and J. F. Alderete**. 1992. Iron regulates growth of *Trichomonas vaginalis* and the expression of immunogenic trichomonad proteins. Molecular Microbiology **6**:123-132.

27. **Lopez-Soto, F., N. Leon-Sicairos, M. Reyes-Lopez, J. Serrano-Luna, C. Ordaz-Pichardo, C. Pina-Vazquez, G. Ortiz-Estrada, and M. de la Garza**. 2009. Use and endocytosis of iron-containing proteins by *Entamoeba histolytica* trophozoites. Infection Genetics and Evolution **9**:1038-1050.

28. **Ramirez-Rico, G., M. Martinez-Castillo, M. de la Garza, M. Shibayama, and J. Serrano-Luna**. 2015. *Acanthamoeba castellanii* proteases are capable of degrading

iron binding proteins as a possible mechanism of pathogenicity. Journal of Eukaryotic Microbiology **62**:614-622.

29. **Theil, E. C.** 1987. Ferritin - structure, gene regulation, and cellular function in animals, plants, and microorganisms. Annual Review of Biochemistry **56**:289-315.

30. **Ravet, K., B. Touraine, J. Boucherez, J. F. Briat, F. Gaymard, and F. Cellier**. 2009. Ferritins control interaction between iron homeostasis and oxidative stress in *Arabidopsis*. Plant Journal **57**:400-412.

31. **Drysdale, J., P. Arosio, R. Invernizzi, M. Cazzola, A. Volz, B. Corsi, G. Biasiotto, and S. Levi**. 2002. Mitochondrial ferritin: A new player in iron metabolism. Blood Cells Molecules and Diseases **29**:376-383.

32. **Pantopoulos, K.** 2004. Iron metabolism and the IRIE/IRP regulatory system - An update. Redox-Active Metals in Neurological Disorders **1012**:1-13.

33. **Casey, J. L., M. W. Hentze, D. M. Koeller, S. W. Caughman, T. A. Rouault, R. D. Klausner, and J. B. Harford**. 1988. Iron responsive elements - regulatory RNA sequences that control messenger RNA levels and translation. Science **240**:924-928.

34. **Suchan, P., D. Vyoral, J. Petrak, R. Sut'ak, D. Rasoloson, E. Nohynkova, P. Dolezal, and J. Tachezy**. 2003. Incorporation of iron into *Tritrichomonas foetus* cell compartments reveals ferredoxin as a major iron-binding protein in hydrogenosomes. Microbiology-Sgm **149**:1911-1921.

35. **Kumanovics, A., O. S. Chen, L. T. Li, D. Bagley, E. M. Adkins, H. L. Lin, N. N. Dingra, C. E. Outten, G. Keller, D. Winge, D. M. Ward, and J. Kaplan**. 2008. Identification of FRA1 and FRA2 as genes involved in regulating the yeast iron regulon in response to decreased mitochondrial iron-sulfur cluster synthesis. Journal of Biological Chemistry **283**:10276-10286.

36. **Li, L. T., O. S. Chen, D. M. Ward, and J. Kaplan**. 2001. CCC1 is a transporter that mediates vacuolar iron storage in yeast. Journal of Biological Chemistry **276**:29515-29519.

37. **Li, L. T., X. Jia, D. M. Ward, and J. Kaplan**. 2011. Yap5 protein regulated transcription of the TYW1 gene protects yeast from high iron toxicity. Journal of Biological Chemistry **286**:38488-38497.

38. **Morrison, H. G., A. G. McArthur, F. D. Gillin, S. B. Aley, R. D. Adam, G. J. Olsen, A. A. Best, W. Z. Cande, F. Chen, M. J. Cipriano, B. J. Davids, S. C. Dawson, H. G. Elmendorf, A. B. Hehl, M. E. Holder, S. M. Huse, U. U. Kim, E. Lasek-Nesselquist, G. Manning, A. Nigam, J. E. J. Nixon, D. Palm, N. E. Passamaneck, A. Prabhu, C. I. Reich, D. S. Reiner, J. Samuelson, S. G. Svard, and M. L. Sogin**. 2007. Genomic minimalism in the early diverging intestinal parasite *Giardia lamblia*. Science **317**:1921-1926.

39. **Zu, Y. B., M. M. J. Couture, D. R. J. Kolling, A. R. Crofts, L. D. Eltis, J. A. Fee, and J. Hirst**. 2003. Reduction potentials of Rieske clusters: Importance of the coupling between oxidation state and histidine protonation state. Biochemistry **42**:12400-12408.

40. **Emptage, M. H., T. A. Kent, M. C. Kennedy, H. Beinert, and E. Munck**. 1983. Mossbauer and electron-paramagnetic-res studies of activated Aconitase - development of a localized valence state at a subsite of the [4Fe-4S] cluster on binding of Citrate. Proceedings of the National Academy of Sciences of the United States of America-Biological Sciences **80**:4674-4678.

41. **Wang, S. C. and P. A. Frey**. 2007. S-adenosylmethionine as an oxidant: the radical SAM superfamily. Trends in Biochemical Sciences **32**:101-110.

42. **Fleischhacker, A. S. and P. J. Kiley**. 2011. Iron-containing transcription factors and their roles as sensors. Current Opinion in Chemical Biology **15**:335-341.

43. **Balk, J. and M. Pilon**. 2011. Ancient and essential: the assembly of iron-sulfur clusters in plants. Trends in Plant Science **16**:218-226.

44. **Netz, D. J. A., J. Mascarenhas, O. Stehling, A. J. Pierik, and R. Lill**. 2014. Maturation of cytosolic and nuclear iron-sulfur proteins. Trends in Cell Biology **24**:303-312.

45. **Beinert, H.** 2000. Iron-sulfur proteins: ancient structures, still full of surprises. Journal of Biological Inorganic Chemistry **5**:2-15.

46. **Bych, K., S. Kerscher, D. J. A. Netz, A. J. Pierik, K. Zwicker, M. A. Huynen, R. Lill, U. Brandt, and J. Balk**. 2008. The iron-sulphur protein Ind1 is required for effective complex I assembly. Embo Journal **27**:1736-1746.

47. **Xu, X. M., H. Lin, M. Latijnhouwers, and S. G. Moller**. 2009. Dual localized AtHscB involved in Iron Sulfur protein biogenesis in *Arabidopsis*. Plos One **4**.

48. **Van Hoewyk, D., S. E. Abdel-Ghany, C. M. Cohu, S. K. Herbert, P. Kugrens, M. Pilon, and E. A. H. Pilon-Smits**. 2007. Chloroplast iron-sulfur cluster protein maturation requires the essential cysteine desulfurase CpNifS. Proceedings of the National Academy of Sciences of the United States of America **104**:5686-5691.

49. **Lezhneva, L., K. Amann, and J. Meurer**. 2004. The universally conserved HCF101 protein is involved in assembly of [4Fe-4S]-cluster-containing complexes in *Arabidopsis thaliana* chloroplasts. Plant Journal **37**:174-185.

50. **Teschner, J., N. Lachmann, J. Schulze, M. Geisler, K. Selbach, J. Santamaria-Araujo, J. Balk, R. R. Mendel, and F. Bittner**. 2010. A novel role for *Arabidopsis* mitochondrial ABC transporter ATM3 in Molybdenum cofactor biosynthesis. Plant Cell **22**:468-480.

51. **Land, K. M., M. G. Delgadillo-Correa, J. Tachezy, S. Vanacova, C. L. Hsieh, R. Sutak, and P. J. Johnson**. 2004. Targeted gene replacement of a ferredoxin gene in *Trichomonas vaginalis* does not lead to metronidazole resistance. Molecular Microbiology **51**:115-122.

52. **Roche, B., L. Aussel, B. Ezraty, P. Mandin, B. Py, and F. Barras**. 2013. Iron/sulfur proteins biogenesis in prokaryotes: Formation, regulation and diversity. Biochimica et Biophysica Acta-Bioenergetics **1827**:455-469.

53. **Dai, Y. Y. and F. W. Outten**. 2012. The *E. coli* SufS-SufE sulfur transfer system is more resistant to oxidative stress than IscS-IscU. Febs Letters **586**:4016-4022.

54. **Fu, W. G., R. F. Jack, T. V. Morgan, D. R. Dean, and M. K. Johnson**. 1994. Nifu gene-product from *Azotobacter vinelandii* is a homodimer that contains 2 Identical [2Fe-2S] clusters. Biochemistry **33**:13455-13463.

55. **Richards, T. A. and M. van der Giezen**. 2006. Evolution of the Isd11-IscS complex reveals a single alpha-proteobacterial endosymbiosis for all eukaryotes. Molecular Biology and Evolution **23**:1341-1344.

56. **Balk, J. and S. Lobreaux**. 2005. Biogenesis of iron-sulfur proteins in plants. Trends in Plant Science **10**:324-331.

57. **Bernard, D. G., Y. F. Cheng, Y. D. Zhao, and J. Balk**. 2009. An allelic mutant series of ATM3 reveals its key role in the biogenesis of cytosolic Iron-Sulfur proteins in *Arabidopsis*. Plant Physiology **151**:590-602.

58. **Nyvltova, E., R. Sutak, K. Harant, M. Sedinova, I. Hrdy, J. Paces, C. Vlcek, and J. Tachezy**. 2013. NIF-type iron-sulfur cluster assembly system is duplicated and distributed in the mitochondria and cytosol of *Mastigamoeba balamuthi*. Proceedings of the National Academy of Sciences of the United States of America **110**:7371-7376.

59. **Stairs, C. W., L. Eme, M. W. Brown, C. Mutsaers, E. Susko, G. Dellaire, D. M. Soanes, M. van der Giezen, and A. J. Roger**. 2014. A SUF Fe-S Cluster Biogenesis System in the Mitochondrion-Related Organelles of the Anaerobic Protist Pygsuia. Current Biology **24**:1176-1186.

60. **Mi-ichi, F., M. Abu Yousuf, K. Nakada-Tsukui, and T. Nozaki**. 2009. Mitosomes in *Entamoeba histolytica* contain a sulfate activation pathway. Proceedings of the National Academy of Sciences of the United States of America **106**:21731-21736.

61. **Maralikova, B., V. Ali, K. Nakada-Tsukui, T. Nozaki, M. van der Giezen, K. Henze, and J. Tovar**. 2010. Bacterial-type oxygen detoxification and iron-sulfur cluster assembly in amoebal relict mitochondria. Cellular Microbiology **12**:331-342.

62. **Dolezal, P., M. J. Dagley, M. Kono, P. Wolynec, V. A. Likic, J. H. Foo, M. Sedinova, J. Tachezy, A. Bachmann, I. Bruchhaus, and T. Lithgow**. 2010. The essentials of protein import in the degenerate mitochondrion of *Entamoeba histolytica*. Plos Pathogens **6**.

63. **Tsaousis, A. D., S. O. de Choudens, E. Gentekaki, S. J. Long, D. Gaston, A. Stechmann, D. Vinella, B. Py, M. Fontecave, F. Barras, J. Lukes, and A. J. Roger**. 2012. Evolution of Fe/S cluster biogenesis in the anaerobic parasite Blastocystis. Proceedings of the National Academy of Sciences of the United States of America **109**:10426-10431.

64. **Tong, W. H., G. N. L. Jameson, B. H. Huynh, and T. A. Rouault**. 2003. Subcellular compartmentalization of human Nfu, an iron-sulfur cluster scaffold protein, and its ability to assemble a [4Fe-4S] cluster. Proceedings of the National Academy of Sciences of the United States of America **100**:9762-9767.

65. **Land, T. and T. A. Rouault**. 1998. Targeting of a human iron-sulfur cluster assembly enzyme, nifs, to different subcellular compartments is regulated through alternative AUG utilization. Molecular Cell **2**:807-815.

66. **Tong, W. H. and T. Rouault**. 2000. Distinct iron-sulfur cluster assembly complexes exist in the cytosol and mitochondria of human cells. Embo Journal **19**:5692-5700.

67. **Marelja, Z., W. Stocklein, M. Nimtz, and S. Leimkuhler**. 2008. A novel role for human Nfs1 in the cytoplasm - Nfs1 acts as a sulfur donor for MOCS3, a protein involved in molybdenum cofactor biosynthesis. Journal of Biological Chemistry **283**:25178-25185.

68. **Nakai, Y., M. Nakai, H. Hayashi, and H. Kagamiyama**. 2001. Nuclear localization of yeast Nfs1p is required for cell survival. Journal of Biological Chemistry **276**:8314-8320.

69. **Kambampati, R. and C. T. Lauhon**. 1999. IscS is a sulfurtransferase for the in vitro biosynthesis of 4-thiouridine in *Escherichia coli* tRNA. Biochemistry **38**:16561-16568.

70. **Kovarova, J., E. Horakova, P. Changmai, M. Vancova, and J. Lukes**. 2014. Mitochondrial and nucleolar localization of cysteine desulfurase Nfs and the scaffold protein Isu in *Trypanosoma brucei*. Eukaryotic Cell **13**:353-362.

71. **Paris, Z., P. Changmai, M. A. T. Rubio, A. Zikova, K. D. Stuart, J. D. Alfonzo, and J. Lukes**. 2010. The Fe/S cluster assembly protein Isd11 is essential for tRNA thiolation in *Trypanosoma brucei*. Journal of Biological Chemistry **285**:22394-22402.

72. **Sipos, K., H. Lange, Z. Fekete, P. Ullmann, R. Lill, and G. Kispal**. 2002. Maturation of cytosolic iron-sulfur proteins requires glutathione. Journal of Biological Chemistry **277**:26944-26949.

73. **Lange, H., T. Lisowsky, J. Gerber, U. Muhlenhoff, G. Kispal, and R. Lill**. 2001. An essential function of the mitochondrial sulfhydryl oxidase Erv1p/ALR in the maturation of cytosolic Fe/S proteins. Embo Reports **2**:715-720.

74. **Srinivasan, V., A. J. Pierik, and R. Lill**. 2014. Crystal structures of nucleotide-free and glutathione-bound mitochondrial ABC transporter Atm1. Science **343**:1137-1140.

75. **Ozer, H. K., A. C. Dlouhy, J. D. Thornton, J. Hu, Y. Liu, J. J. Barycki, J. Balk, and C. E. Outten**. 2015. Cytosolic Fe-S Cluster Protein Maturation and Iron Regulation Are Independent of the Mitochondrial Erv1/Mia40 Import System. J.Biol.Chem.

76. **Li, H. R., D. T. Mapolelo, N. N. Dingra, S. G. Naik, N. S. Lees, B. M. Hoffman, P. J. Riggs-Gelasco, B. H. Huynh, M. K. Johnson, and C. E. Outten**. 2009. The yeast iron regulatory proteins Grx3/4 and Fra2 form heterodimeric complexes containing a [2Fe-2S] cluster with cysteinyl and histidyl ligation. Biochemistry **48**:9569-9581.

77. **Balk, J. and T. A. Schaedler**. 2014. Iron Cofactor Assembly in Plants. Annual Review of Plant Biology, Vol 65 **65**:125-+.

78. **Raulfs, E. C., I. P. O'Carroll, P. C. Dos Santos, M. C. Unciuleac, and D. R. Dean**. 2008. In vivo iron-sulfur cluster formation. Proceedings of the National Academy of Sciences of the United States of America **105**:8591-8596.

79. **Kato, S., H. Mihara, T. Kurihara, Y. Takahashi, U. Tokumoto, T. Yoshimura, and N. Esaki**. 2002. Cys-328 of IscS and Cys-63 of IscU are the sites of disulfide bridge formation in a covalently bound IscS/IscU complex: Implications for the mechanism of iron-sulfur cluster assembly. Proceedings of the National Academy of Sciences of the United States of America **99**:5948-5952.

80. **Saha, P. P., S. Srivastava, S. K. P. Kumar, D. Sinha, and P. D'Silva**. 2015. Mapping key residues of ISD11 critical for NFS1-ISD11 subcomplex stability: Implications in the development of mitochondrial disorder, COXPD19. J.Biol.Chem.

81. **Adam, A. C., C. Bornhovd, H. Prokisch, W. Neupert, and K. Hell**. 2006. The Nfs1 interacting protein Isd11 has an essential role in Fe/S cluster biogenesis in mitochondria. Embo Journal **25**:174-183.

82. **Markley, J. L., J. H. Kim, Z. Q. Dai, J. R. Bothe, K. Cai, R. O. Frederick, and M. Tonelli**. 2013. Metamorphic protein IscU alternates conformations in the course of its role as the scaffold protein for iron-sulfur cluster biosynthesis and delivery. Febs Letters **587**:1172-1179.

83. **Manzella, L., M. H. Barros, and F. G. Nobrega**. 1998. ARH1 of *Saccharomyces cerevisiae*: A new essential gene that codes for a protein homologous to the human adrenodoxin reductase. Yeast **14**:839-846.

84. **Schagerlof, U., H. Elmlund, O. Gakh, G. Nordlund, H. Hebert, M. Lindahl, G. Isaya, and S. Al-Karadaghi**. 2008. Structural basis of the iron storage function of frataxin from single-particle reconstruction of the iron-loaded oligomer. Biochemistry **47**:4948-4954.

85. **Gerber, J., K. Neumann, C. Prohl, U. Muhlenhoff, and R. Lill**. 2004. The yeast scaffold proteins Isu1p and Isu2p are required inside mitochondria for maturation of cytosolic Fe/S proteins. Molecular and Cellular Biology **24**:4848-4857.

86. **He, Y. N., S. L. Alam, S. V. Proteasa, Y. Zhang, E. Lesuisse, A. Dancis, and T. L. Stemmler**. 2004. Yeast frataxin solution structure, iron binding, and ferrochelatase interaction. Biochemistry **43**:16254-16262.

87. **Yan, R., P. V. Konarev, C. Iannuzzi, S. Adinolfi, B. Roche, G. Kelly, L. Simon, S. R. Martin, B. Py, F. Barras, D. I. Svergun, and A. Pastore**. 2013. Ferredoxin competes with bacterial frataxin in binding to the desulfurase IscS. Journal of Biological Chemistry **288**:24777-24787.

88. **Uzarska, M. A., R. Dutkiewicz, S. A. Freibert, R. Lill, and U. Muehlenhoff**. 2013. The mitochondrial Hsp70 chaperone Ssq1 facilitates Fe/S cluster transfer from Isu1 to Grx5 by complex formation. Molecular Biology of the Cell **24**:1830-1841.

89. **Dekker, P. J. T. and N. Pfanner**. 1997. Role of mitochondrial GrpE and phosphate in the ATPase cycle of matrix Hsp70. Journal of Molecular Biology **270**:321-327.

90. **Cameron, J. M., A. Janer, V. Levandovskiy, N. MacKay, T. A. Rouault, W. H. Tong, I. Ogilvie, E. A. Shoubridge, and B. H. Robinson**. 2011. Mutations in Iron-Sulfur Cluster scaffold genes NFU1 and BOLA3 cause a fatal deficiency of multiple respiratory chain and 2-Oxoacid dehydrogenase enzymes. American Journal of Human Genetics **89**:486-495.

91. **Lill, R.** 2009. Function and biogenesis of iron-sulphur proteins. Nature **460**:831-838.

92. **Muhlenhoff, U., N. Richter, O. Pines, A. J. Pierik, and R. Lill**. 2011. Specialized function of yeast Isa1 and Isa2 proteins in the maturation of mitochondrial [4Fe-4S] proteins. Journal of Biological Chemistry **286**:41205-41216.

93. **Sheftel, A. D., C. Wilbrecht, O. Stehling, B. Niggemeyer, H. P. Elsasser, U. Muhlenhoff, and R. Lill**. 2012. The human mitochondrial ISCA1, ISCA2, and IBA57 proteins are required for [4Fe-4S] protein maturation. Molecular Biology of the Cell **23**:1157-1166.

94. **Stehling, O. and R. Lill**. 2013. The role of mitochondria in cellular iron sulfur protein biogenesis: mechanisms, connected processes, and diseases. Cold Spring Harbor Perspectives in Biology **5**.

95. **Gelling, C., I. W. Dawes, N. Richhardt, R. Lill, and U. Muhlenhoff**. 2008. Mitochondrial Iba57p is required for Fe/S cluster formation on aconitase and activation of radical SAM enzymes. Molecular and Cellular Biology **28**:1851-1861.

96. **Putz, S., P. Dolezal, G. Gelius-Dietrich, L. Bohacova, J. Tachezy, and K. Henze**. 2006. Fe-hydrogenase maturases in the hydrogenosomes of *Trichomonas vaginalis*. Eukaryotic Cell **5**:579-586.

97. **Vignais, P. M., B. Billoud, and J. Meyer**. 2001. Classification and phylogeny of hydrogenases. Fems Microbiology Reviews **25**:455-501.

98. **Posewitz, M. C., P. W. King, S. L. Smolinski, L. P. Zhang, M. Seibert, and M. L. Ghirardi**. 2004. Discovery of two novel radical S-adenosylmethionine proteins required for the assembly of an active [Fe] hydrogenase. Journal of Biological Chemistry **279**:25711-25720.

99. **Jacobson, M. R., K. E. Brigle, L. T. Bennett, R. A. Setterquist, M. S. Wilson, V. L. Cash, J. Beynon, W. E. Newton, and D. R. Dean**. 1989. Physical and genetic map of the major Nif gene cluster from *Azotobacter vinelandii*. Journal of Bacteriology **171**:1017-1027.

100. **Dos Santos, P. C., D. R. Dean, Y. L. Hu, and M. W. Ribbe**. 2004. Formation and insertion of the nitrogenase iron-molybdenum cofactor. Chemical Reviews **104**:1159-1173.

101. **Curatti, L., J. A. Hernandez, R. Y. Igarashi, B. Soboh, D. Zhao, and L. M. Rubio**. 2007. In vitro synthesis of the iron-molybdenum cofactor of nitrogenase from iron, sulfur, molybdenum, and homocitrate using purified proteins. Proceedings of the National Academy of Sciences of the United States of America **104**:17626-17631.

102. **Olson, J. W., J. N. Agar, M. K. Johnson, and R. J. Maier**. 2000. Characterization of the NifU and NifS Fe-S cluster formation proteins essential for viability in *Helicobacter pylori*. Biochemistry **39**:16213-16219.

103. **Ali, V., Y. Shigeta, U. Tokumoto, Y. Takahashi, and T. Nozaki**. 2004. An intestinal parasitic protist, *Entamoeba histolytica*, possesses a non-redundant nitrogen fixation-like system for iron-sulfur cluster assembly under anaerobic conditions. Journal of Biological Chemistry **279**:16863-16874.

104. **Tokumoto, U., S. Kitamura, K. Fukuyama, and Y. Takahashi**. 2004. Interchangeability and distinct properties of bacterial Fe-S cluster assembly systems: Functional replacement of the isc and suf operons in *Escherichia coli* with the nifSU-like operon from *Helicobacter pylori*. Journal of Biochemistry **136**:199-209.

105. **Netz, D. J. A., A. J. Pierik, M. Stuempfig, U. Muhlenhoff, and R. Lill**. 2007. The Cfd1-Nbp35 complex acts as a scaffold for iron-sulfur protein assembly in the yeast cytosol. Nature Chemical Biology **3**:278-286.

106. **Netz, D. J. A., A. J. Pierik, M. Stumpfig, E. Bill, A. K. Sharma, L. J. Pallesen, W. E. Walden, and R. Lill**. 2012. A bridging [4Fe-4S] cluster and nucleotide binding are essential for function of the Cfd1-Nbp35 complex as a scaffold in Iron-Sulfur protein maturation. Journal of Biological Chemistry **287**:12365-12378.

107. **Netz, D. J. A., M. Stumpfig, C. Dore, U. Muhlenhoff, A. J. Pierik, and R. Lill**. 2010. Tah18 transfers electrons to Dre2 in cytosolic iron-sulfur protein biogenesis. Nature Chemical Biology **6**:758-765.

108. **Bernard, D. G., D. J. A. Netz, T. J. Lagny, A. J. Pierik, and J. Balk**. 2013. Requirements of the cytosolic iron-sulfur cluster assembly pathway in *Arabidopsis*. Philosophical Transactions of the Royal Society B-Biological Sciences **368**.

109. **Vernis, L., C. Facca, E. Delagoutte, N. Soler, R. Chanet, B. Guiard, G. Faye, and G. Baldacci**. 2009. A newly identified essential complex, Dre2-Tah18, controls mitochondria integrity and cell death after oxidative stress in yeast. Plos One **4**.

110. **Zhang, Y., H. R. Li, C. G. Zhang, X. X. An, L. L. Liu, J. Stubbe, and M. X. Huang**. 2014. Conserved electron donor complex Dre2-Tah18 is required for ribonucleotide reductase metallocofactor assembly and DNA synthesis. Proceedings of the National Academy of Sciences of the United States of America **111**:E1695-E1704.

111. **Nishimura, A., N. Kawahara, and H. Takagi**. 2013. The flavoprotein Tah18-dependent NO synthesis confers high-temperature stress tolerance on yeast cells. Biochemical and Biophysical Research Communications **430**:137-143.

112. **Bych, K., D. J. A. Netz, G. Vigani, E. Bill, R. Lill, A. J. Pierik, and J. Balk**. 2008. The essential cytosolic Iron-Sulfur protein Nbp35 acts without Cfd1 partner in the Green lineage. Journal of Biological Chemistry **283**:35797-35804.

113. **Basu, S., J. C. Leonard, N. Desai, D. A. I. Mavridou, K. H. Tang, A. D. Goddard, M. L. Ginger, J. Lukes, and J. W. A. Allen**. 2013. Divergence of Erv1-Associated

Mitochondrial Import and Export Pathways in Trypanosomes and Anaerobic Protists. Eukaryotic Cell **12**:343-355.

114. **Outten, F. W., M. J. Wood, F. M. Munoz, and G. Storz**. 2003. The SufE protein and the SufBCD complex enhance SufS cysteine desulfurase activity as part of a sulfur transfer pathway for fe-s cluster assembly in *Escherichia coli*. Journal of Biological Chemistry **278**:45713-45719.

115. **Wollers, S., G. Layer, R. Garcia-Serres, L. Signor, M. Clemancey, J. M. Latour, M. Fontecave, and S. O. de Choudens**. 2010. Iron-sulfur (Fe-S) cluster assembly: the SufBCD complex is a new type of Fe-S scaffold with a flavin redox cofactor. Journal of Biological Chemistry **285**:23329-23339.

116. **Couturier, J., B. Touraine, J. F. Briat, F. Gaymard, and N. Rouhier**. 2013. The iron-sulfur cluster assembly machineries in plants: current knowledge and open questions. Frontiers in Plant Science **4**.

117. **Williamson, D. H., M. J. Gardner, P. Preiser, D. J. Moore, K. Rangachari, and R. J. M. Wilson**. 1994. The evolutionary origin of the 35 Kb circular DNA of *Plasmodium falciparum* - new evidence supports a possible rhodophyte ancestry. Molecular & General Genetics **243**:249-252.

118. **Ralph, S. A., G. G. van Dooren, R. F. Waller, M. J. Crawford, M. J. Fraunholz, B. J. Foth, C. J. Tonkin, D. S. Roos, and G. I. McFadden**. 2004. Metabolic maps and functions of the *Plasmodium falciparum* apicoplast. Nature Reviews Microbiology **2**:203-216.

119. **Kumar, B., S. Chaubey, P. Shah, A. Tanveer, M. Charan, M. I. Siddiqi, and S. Habib**. 2011. Interaction between sulphur mobilisation proteins SufB and SufC: Evidence for an iron-sulphur cluster biogenesis pathway in the apicoplast of *Plasmodium falciparum*. International Journal for Parasitology **41**:991-999.

120. **Gisselberg, J. E., T. A. Dellibovi-Ragheb, K. A. Matthews, G. Bosch, and S. T. Prigge**. 2013. The Suf iron sulfur cluster synthesis pathway is required for apicoplast maintenance in malaria parasites. Plos Pathogens **9**.

121. **Caccio, S. M. and U. Ryan**. 2008. Molecular epidemiology of giardiasis. Molecular and Biochemical Parasitology **160**:75-80.

122. **Dagley, M. J., P. Dolezal, V. A. Likic, O. Smid, A. W. Purcell, S. K. Buchanan, J. Tachezy, and T. Lithgow**. 2009. The protein import channel in the outer mitosomal membrane of *Giardia intestinalis*. Molecular Biology and Evolution **26**:1941-1947.

123. **Smid, O., A. Matuskova, S. R. Harris, T. Kucera, M. Novotny, L. Horvathova, I. Hrdy, E. Kutejova, R. P. Hirt, T. M. Embley, J. Janata, and J. Tachezy**. 2008. Reductive evolution of the Mitochondrial Processing Peptidases of the unicellular parasites *Trichomonas vaginalis* and *Giardia intestinalis*. Plos Pathogens **4**.

124. **Tachezy, J., L. B. Sanchez, and M. Muller**. 2001. Mitochondrial type iron-sulfur cluster assembly in the amitochondriate eukaryotes *Trichomonas vaginalis* and *Giardia intestinalis*, as indicated by the phylogeny of IscS. Molecular Biology and Evolution **18**:1919-1928.

125. **Dolezal, P., O. Smid, P. Rada, Z. Zubacova, D. Bursac, R. Sutak, J. Nebesarova, T. Lithgow, and J. Tachezy**. 2005. *Giardia* mitosomes and trichomonad hydrogenosomes share a common mode of protein targeting. Proceedings of the National Academy of Sciences of the United States of America **102**:10924-10929.

126. **Rada, P., O. Smid, R. Sutak, P. Dolezal, J. Pyrih, V. Zarsky, J. J. Montagne, I. Hrdy, J. M. Camadro, and J. Tachezy**. 2009. The monothiol single-domain glutaredoxin is conserved in the highly reduced mitochondria of *Giardia intestinalis*. Eukaryotic Cell **8**:1584-1591.

127. **Emelyanov, V. V. and A. V. Goldberg**. 2011. Fermentation enzymes of *Giardia intestinalis*, pyruvate:ferredoxin oxidoreductase and hydrogenase, do not localize to its mitosomes. Microbiology-Sgm **157**:1602-1611.

128. **Tsaousis, A. D., E. Gentekaki, L. Eme, D. Gaston, and A. J. Roger**. 2014. Evolution of the cytosolic Iron-Sulfur cluster assembly machinery in Blastocystis species and other microbial eukaryotes. Eukaryotic Cell **13**:143-153.

129. Hrdy, I., .Tachezy, J., and Muller M. Metabolism of Trichomonad hydrogenosomes In: Tachezy J, editor. Hydrogenosomes and mitosomes: mitochondria of anaerobic eukaryotes. New York: Springer , 113-145. 2008.

130. **Carlton, J. M., R. P. Hirt, J. C. Silva, A. L. Delcher, M. Schatz, Q. Zhao, J. R. Wortman, S. L. Bidwell, U. C. M. Alsmark, S. Besteiro, T. Sicheritz-Ponten, C. J. Noel, J. B. Dacks, P. G. Foster, C. Simillion, Y. Van de Peer, D. Miranda-Saavedra, G. J. Barton, G. D. Westrop, S. Muller, D. Dessi, P. L. Fiori, Q. H. Ren, I. Paulsen, H. B. Zhang, F. D. Bastida-Corcuera, A. Simoes-Barbosa, M. T. Brown, R. D. Hayes, M. Mukherjee, C. Y. Okumura, R. Schneider, A. J. Smith, S. Vanacova, M. Villalvazo, B. J. Haas, M. Pertea, T. V. Feldblyum, T. R. Utterback, C. L. Shu, K. Osoegawa, P. J. de Jong, I. Hrdy, L. Horvathova, Z. Zubacova, P. Dolezal, S. B. Malik, J. M. Logsdon, K. Henze, A. Gupta, C. C. Wang, R. L. Dunne, J. A. Upcroft, P. Upcroft, O. White, S. L. Salzberg, P. Tang, C. H. Chiu, Y. S. Lee, T. M. Embley, G. H. Coombs, J. C. Mottram, J. Tachezy, C. M. Fraser-Liggett, and P. J. Johnson**. 2007. Draft genome sequence of the sexually transmitted pathogen *Trichomonas vaginalis*. Science **315**:207-212.

131. **Sutak, R., P. Dolezal, H. L. Fiumera, I. Hrdy, A. Dancis, M. Delgadillo-Correa, P. J. Johnson, M. Muller, and J. Tachezy**. 2004. Mitochondrial-type assembly of FeS centers in the hydrogenosomes of the amitochondriate eukaryote *Trichomonas vaginalis*. Proceedings of the National Academy of Sciences of the United States of America **101**:10368-10373.

132. **Dolezal, P., A. Dancis, E. Lesuisse, R. Sutak, I. Hrdy, T. M. Embley, and J. Tachezy**. 2007. Frataxin, a conserved mitochondrial protein, in the hydrogenosome of *Trichomonas vaginalis*. Eukaryotic Cell **6**:1431-1438.

133. **Rada, P., P. Dolezal, P. L. Jedelsky, D. Bursac, A. J. Perry, M. Sedinova, K. Smiskova, M. Novotny, N. C. Beltran, I. Hrdy, T. Lithgow, and J. Tachezy**. 2011. The core components of organelle biogenesis and membrane transport in the hydrogenosomes of *Trichomonas vaginalis*. Plos One **6**.

134. **Beltran, N. C., L. Horvathova, P. L. Jedelsky, M. Sedinova, P. Rada, M. Marcincikova, I. Hrdy, and J. Tachezy**. 2013. Iron-induced changes in the proteome of *Trichomonas vaginalis* hydrogenosomes. Plos One **8**.

135. **Schneider, R. E., M. T. Brown, A. M. Shiflett, S. D. Dyall, R. D. Hayes, Y. M. Xie, J. A. Loo, and P. J. Johnson**. 2011. The *Trichomonas vaginalis* hydrogenosome proteome is highly reduced relative to mitochondria, yet complex compared with mitosomes. International Journal for Parasitology **41**:1421-1434.

136. **Gorrell, T. E., N. Yarlett, and M. Muller**. 1984. Isolation and characterization of *Trichomonas vaginalis* ferredoxin. Carlsberg Research Communications **49**:259-268.

137. **Mi-ichi, F., T. Makiuchi, A. Furukawa, D. Sato, and T. Nozaki**. 2011. Sulfate activation in mitosomes plays an important role in the proliferation of *Entamoeba histolytica*. Plos Neglected Tropical Diseases **5**.

138. **Anwar, S., M. R. Dikhit, K. P. Singh, R. K. Kar, A. Zaidi, G. C. Sahoo, A. K. Roy, T. Nozaki, P. Das, and V. Ali**. 2014. Interaction between Nbp35 and Cfd1 proteins of cytosolic Fe-S cluster assembly reveals a stable complex formation in *Entamoeba histolytica*. Plos One **9**.

139. **Loftus, B., I. Anderson, R. Davies, U. C. M. Alsmark, J. Samuelson, P. Amedeo, P. Roncaglia, M. Berriman, R. P. Hirt, B. J. Mann, T. Nozaki, B. Suh, M. Pop, M. Duchene, J. Ackers, E. Tannich, M. Leippe, M. Hofer, I. Bruchhaus, U. Willhoeft, A. Bhattacharya, T. Chillingworth, C. Churcher, Z. Hance, B. Harris, D. Harris, K. Jagels, S. Moule, K. Mungall, D. Ormond, R. Squares, S. Whitehead, M. A. Quail, E. Rabbinowitsch, H. Norbertczak, C. Price, Z. Wang, N. Guillen, C. Gilchrist, S. E. Stroup, S. Bhattacharya, A. Lohia, P. G. Foster, T. Sicheritz-Ponten, C. Weber, U. Singh, C. Mukherjee, N. M. El-Sayed, W. A. Petri, C. G. Clark, T. M. Embley, B. Barrell, C. M. Fraser, and N. Hall**. 2005. The genome of the protist parasite *Entamoeba histolytica*. Nature **433**:865-868.

140. **Nyvltova, E., C. W. Stairs, I. Hrdy, J. Ridl, J. Mach, J. Paces, A. J. Roger, and J. Tachezy**. 2015. Lateral gene transfer and gene duplication played a key role in the evolution of *Mastigamoeba balamuthi* hydrogenosomes. Molecular Biology and Evolution **32**:1039-1055.

141. **Brown, M. W., S. C. Sharpe, J. D. Silberman, A. A. Heiss, B. F. Lang, A. G. B. Simpson, and A. J. Roger**. 2013. Phylogenomics demonstrates that breviate flagellates are related to opisthokonts and apusomonads. Proceedings of the Royal Society B-Biological Sciences **280**.

142. **Stairs, C. W., L. Eme, M. W. Brown, C. Mutsaers, E. Susko, G. Dellaire, D. M. Soanes, M. van der Giezen, and A. J. Roger**. 2014. A SUF Fe-S cluster biogenesis system in the mitochondrion-related organelles of the anaerobic protist Pygsuia. Current Biology **24**:1176-1186.

143. **Rydberg, P., E. Sigfridsson, and U. Ryde**. 2004. On the role of the axial ligand in heme proteins: a theoretical study. Journal of Biological Inorganic Chemistry **9**:203-223.

144. **Sigfridsson, E., M. H. M. Olsson, and U. Ryde**. 2001. Comparison of the inner-sphere reorganization energies of cytochromes, iron-sulfur clusters, and blue copper proteins. Journal of Physical Chemistry B **105**:5546-5552.

145. **Ortiz de Montellano and P**. 2010. Hydrocarbon hydroxylation by Cytochrome P450 enzymes. Chemical Reviews **110**:932-948.

146. **Shifman, J. M., B. R. Gibney, R. E. Sharp, and P. L. Dutton**. 2000. Heme redox potential control in de novo designed four-alpha-helix bundle proteins. Biochemistry **39**:14813-14821.

147. **Mcree, D. E., D. C. Richardson, J. S. Richardson, and L. M. Siegel**. 1986. The heme and Fe4S4 cluster in the crystallographic structure of *Escherichia coli* Sulfite Reductase. Journal of Biological Chemistry **261**:277-281.

148. **Koreny, L., M. Obornik, and J. Lukes**. 2013. Make it, take it, or leave it: heme metabolism of parasites. Plos Pathogens **9**.

149. **Shoolinginjordan, P. M.** 1995. Porphobilinogen deaminase and uroporphyrinogen-III synthase - structure, molecular biology, and mechanism. Journal of Bioenergetics and Biomembranes **27**:181-195.

150. **Dailey, H. A.** 2002. Terminal steps of haem biosynthesis. Biochemical Society Transactions **30**:590-595.

151. **Dailey, H. A., T. A. Dailey, C. K. Wu, A. E. Medlock, K. F. Wang, J. P. Rose, and B. C. Wang**. 2000. Ferrochelatase at the millennium: structures, mechanisms and [2Fe-2S] clusters. Cellular and Molecular Life Sciences **57**:1909-1926.

152. **Panek, H. and M. R. O'Brian**. 2002. A whole genome view of prokaryotic haem biosynthesis. Microbiology-Sgm **148**:2273-2282.

153. **Koreny, L., R. Sobotka, J. Janouskovec, P. J. Keeling, and M. Obornik**. 2011. Tetrapyrrole synthesis of photosynthetic chromerids is likely homologous to the unusual pathway of apicomplexan parasites. Plant Cell **23**:3454-3462.

154. **Petersen, J., A. K. Ludewig, V. Michael, B. Bunk, M. Jarek, D. Baurain, and H. Brinkmann**. 2014. *Chromera velia*, endosymbioses and the Rhodoplex hypothesis-plastid evolution in Cryptophytes, Alveolates, Stramenopiles, and Haptophytes (CASH Lineages). Genome Biology and Evolution **6**:666-684.

155. **Layer, G., J. Reichelt, D. Jahn, and D. W. Heinz**. 2010. Structure and function of enzymes in heme biosynthesis. Protein Science **19**:1137-1161.

156. **Storbeck, S., S. Rolfes, E. Raux-Deery, M. J. Warren, D. Jahn, and G. Layer**. 2010. A novel pathway for the biosynthesis of heme in Archaea: Genome-based bioinformatic predictions and experimental evidence. Archaea-An International Microbiological Journal.

157. **Lobo, S. A. L., A. Brindley, M. J. Warren, and L. M. Saraiva**. 2009. Functional characterization of the early steps of tetrapyrrole biosynthesis and modification in *Desulfovibrio vulgaris* Hildenborough. Biochemical Journal **420**:317-325.

158. **Koreny, L., J. Lukes, and M. Obornik**. 2010. Evolution of the haem synthetic pathway in kinetoplastid flagellates: An essential pathway that is not essential after all? International Journal for Parasitology **40**:149-156.

159. **Sedman, R. M. and T. R. Tephly**. 1980. Cardiac - Aminolevulinic Acid Synthetase-Activity - Effects of Fasting, Cobaltous Chloride and Hemin. Biochemical Pharmacology **29**:795-800.

160. **Kikuchi, G., T. Yoshida, and M. Noguchi**. 2005. Heme oxygenase and heme degradation. Biochemical and Biophysical Research Communications **338**:558-567.

161. **Choi, A. M. K. and J. Alam**. 1996. Heme oxygenase-1: Function, regulation, and implication of a novel stress-inducible protein in oxidant-induced lung injury. American Journal of Respiratory Cell and Molecular Biology **15**:9-19.

162. **Hamza, I.** 2006. Intracellular trafficking of porphyrins. Acs Chemical Biology **1**:627-629.

163. **Pfeifer, K., K. S. Kim, S. Kogan, and L. Guarente**. 1989. Functional dissection and sequence of yeast Hap1 activator. Cell **56**:291-301.

164. **Hon, T., H. C. Lee, Z. Z. Hu, V. R. Iyer, and L. Zhang**. 2005. The heme activator protein Hap1 represses transcription by a heme-independent mechanism in *Saccharomyces cerevisiae*. Genetics **169**:1343-1352.

165. **Severance, S., A. Rajagopal, A. U. Rao, G. C. Cerqueira, M. Mitreva, N. M. El-Sayed, M. Krause, and I. Hamza**. 2010. Genome wide analysis reveals novel genes essential for heme homeostasis in *Caenorhabditis elegans*. Plos Genetics **6**.

166. **Korolnek, T., J. B. Zhang, S. Beardsley, G. L. Scheffer, and I. Hamza**. 2014. Control of metazoan heme homeostasis by a conserved multidrug resistance protein. Cell Metabolism **19**:1008-1019.

167. **Sawai, H., M. Yamanaka, H. Sugimoto, Y. Shiro, and S. Aono**. 2012. Structural basis for the transcriptional regulation of heme homeostasis in *Lactococcus lactis*. Journal of Biological Chemistry **287**:30755-30768.

168. **Poole, R. K. and M. N. Hughes**. 2000. New functions for the ancient globin family: bacterial responses to nitric oxide and nitrosative stress. Molecular Microbiology **36**:775-783.

169. **Gunn, A., E. R. Derbyshire, M. A. Marletta, and R. D. Britt**. 2012. Conformationally distinct five-coordinate Heme-NO complexes of soluble Guanylate cyclase elucidated by multifrequency Electron Paramagnetic Resonance (EPR). Biochemistry **51**:8384-8390.

170. **Schenkman, J. B. and I. Jansson**. 2003. The many roles of cytochrome b(5). Pharmacology & Therapeutics **97**:139-152.

171. **Borgese, N., I. Gazzoni, M. Barberi, S. Colombo, and E. Pedrazzini**. 2001. Targeting of a tail-anchored protein to endoplasmic reticulum and mitochondrial outer membrane by independent but competing pathways. Molecular Biology of the Cell **12**:2482-2496.

172. **Uttaro, A. D.** 2006. Biosynthesis of polyunsaturated fatty acids in lower eukaryotes. Iubmb Life **58**:563-571.

173. **Ogishima, T., J. Y. Kinoshita, F. Mitani, M. Suematsu, and A. Ito**. 2003. Identification of outer mitochondrial membrane cytochrome b(5) as a modulator for androgen synthesis in Leydig cells. Journal of Biological Chemistry **278**:21204-21211.

174. **Wu, B., J. Novelli, J. Foster, R. Vaisvila, L. Conway, J. Ingram, M. Ganatra, A. U. Rao, I. Hamza, and B. Slatko**. 2009. The heme biosynthetic pathway of the obligate Wolbachia endosymbiont of *Brugia malayi* as a potential anti-filarial drug target. Plos Neglected Tropical Diseases **3**.

175. **Koreny, L., R. Sobotka, J. Kovarova, A. Gnipova, P. Flegontov, A. Horvath, M. Obornik, F. J. Ayala, and J. Lukes**. 2012. Aerobic kinetoplastid flagellate Phytomonas does not require heme for viability. Proceedings of the National Academy of Sciences of the United States of America **109**:3808-3813.

176. **Chaumont, F., A. N. Schanck, J. J. Blum, and F. R. Opperdoes**. 1994. Aerobic and anaerobic glucose metabolism of *Phytomonas* sp. isolated from *Euphorbia characias*. Molecular and Biochemical Parasitology **67**:321-331.

177. **Rafferty, S., B. Luu, R. E. March, and J. Yee**. 2010. *Giardia lamblia* encodes a functional flavohemoglobin. Biochemical and Biophysical Research Communications **399**:347-351.

178. **Andersson, J. O., A. M. Sjogren, L. A. M. Davis, T. M. Embley, and A. J. Roger**. 2003. Phylogenetic analyses of diplomonad genes reveal frequent lateral gene transfers affecting eukaryotes. Current Biology **13**:94-104.

179. **Mastronicola, D., F. Testa, E. Forte, E. Bordi, L. P. Pucillo, P. Sarti, and A. Giuffre**. 2010. Flavohemoglobin and nitric oxide detoxification in the human protozoan parasite *Giardia intestinalis*. Biochemical and Biophysical Research Communications **399**:654-658.

180. **Gilles-Gonzalez, M. A. and G. Gonzalez**. 2004. Signal transduction by heme-containing PAS-domain proteins. Journal of Applied Physiology **96**:774-783.

181. **Alderete, J. F., J. Nguyen, V. Mundodi, and M. W. Lehker**. 2004. Heme-iron increases levels of AP65-mediated adherence by *Trichomonas vaginalis*. Microbial Pathogenesis **36**:263-271.

182. **Ardalan, S., B. C. Lee, and G. E. Garber**. 2009. *Trichomonas vaginalis*: The adhesins AP51 and AP65 bind heme and hemoglobin. Experimental Parasitology **121**:300-306.

183. **Cruz-Castaneda, A. and J. Olivares-Trejo**. 2008. Ehhmbp45 is a novel hemoglobin-binding protein identified in *Entamoeba histolytica*. Febs Letters **582**:2806-2810.

184. **Cruz-Castaneda, A., J. Hernandez-Sanchez, and J. J. Olivares-Trejo**. 2009. Cloning and identification of a gene coding for a 26-kDa hemoglobin-binding protein from *Entamoeba histolytica*. Biochimie **91**:383-389.

185. **Vicente, J. B., M. A. Carrondo, M. Teixeira, and C. Frazao**. 2008. Structural studies on flavodiiron proteins. Globins and Other Nitric Oxide-Reactive Proteins, Part B **437**:3-19.

186. **Xu, F. F., J. Jerlstrom-Hultqvist, E. Einarsson, A. Astvaldsson, S. G. Svard, and J. O. Andersson**. 2014. The genome of *Spironucleus salmonicida* highlights a fish pathogen adapted to fluctuating environments. Plos Genetics **10**.

187. **Andersson, J. O., R. P. Hirt, P. G. Foster, and A. J. Roger**. 2006. Evolution of four gene families with patchy phylogenetic distributions: influx of genes into protist genomes. Bmc Evolutionary Biology **6**.

188. **Smutna, T., V. L. Goncalves, L. M. Saraiva, J. Tachezy, M. Teixeira, and I. Hrdy**. 2009. Flavodiiron protein from *Trichomonas vaginalis* hydrogenosomes: the terminal oxygen reductase. Eukaryotic Cell **8**:47-55.

189. **Di Matteo, A., F. M. Scandurra, F. Testa, E. Forte, P. Sarti, M. Brunori, and A. Giuffre**. 2008. The O-2-scavenging flavodiiron protein in the human parasite *Giardia intestinalis*. Journal of Biological Chemistry **283**:4061-4068.

190. **Logan, D. T., X. D. Su, A. Aberg, K. Regnstrom, J. Hajdu, H. Eklund, and P. Nordlund**. 1996. Crystal structure of reduced protein R2 of ribonucleotide reductase: The structural basis for oxygen activation at a dinuclear iron site. Structure **4**:1053-1064.

191. **Baum, K. F., R. L. Berens, J. J. Marr, J. A. Harrington, and T. Spector**. 1989. Purine deoxynucleoside salvage in *Giardia lamblia*. Journal of Biological Chemistry **264**:21087-21090.

192. **Pyrih, J., K. Harant, E. Martincova, R. Sutak, E. Lesuisse, I. Hrdy, and J. Tachezy**. 2014. *Giardia intestinalis* incorporates heme into cytosolic cytochrome b(5). Eukaryotic Cell **13**:231-239.

193. **Farr, H. and K. Gull**. 2009. Functional studies of an evolutionarily conserved, cytochrome *b*5 domain protein reveal a specific role in axonemal organisation and the general phenomenon of post-division axonemal growth in Trypanosomes. Cell Motility and the Cytoskeleton **66**:24-35.

194. **Mitoma, J. Y. and A. Ito**. 1992. The carboxy-terminal 10-amino acid residues of cytochrome-b5 are necessary for its targeting to the endoplasmic reticulum. Embo Journal **11**:4197-4203.

195. **Jedelsky, P. L., P. Dolezal, P. Rada, J. Pyrih, O. Smid, I. Hrdy, M. Sedinova, M. Marcincikova, L. Voleman, A. J. Perry, N. C. Beltran, T. Lithgow, and J. Tachezy**. 2011. The minimal proteome in the reduced mitochondrion of the parasitic protist *Giardia intestinalis*. PLoS.One. **6**:e17285.

196. **Olteanu, H. and R. Banerjee**. 2003. Redundancy in the pathway for redox regulation of mammalian methionine synthase - Reductive activation by the dual flavoprotein, novel reductase 1. Journal of Biological Chemistry **278**:38310-38314.

197. **Martincova, E., L. Voleman, J. Pyrih, V. Zarsky, P. Vondrackova, M. Kolisko, J. Tachezy, and P. Dolezal**. 2015. Probing the biology of *Giardia intestinalis* mitosomes using in vivo enzymatic tagging. Molecular and Cellular Biology **35**:2864-2874.

198. **Ramirez, P., H. Toledo, N. Guiliani, and C. A. Jerez**. 2002. An exported rhodanese-like protein is induced during growth of *Acidithiobacillus ferrooxidans* in metal sulfides and different sulfur compounds. Applied and Environmental Microbiology **68**:1837-1845.

199. **Han, Y. F., H. W. Huang, L. Li, T. Cai, S. Chen, and X. J. He**. 2015. The cytosolic Iron-Sulfur cluster assembly protein MMS19 regulates transcriptional gene silencing, DNA repair, and flowering time in *Arabidopsis*. Plos One **10**.

200. **Basu, S., J. C. Leonard, N. Desai, D. A. I. Mavridou, K. H. Tang, A. D. Goddard, M. L. Ginger, J. Lukes, and J. W. A. Allen**. 2013. Divergence of Erv1-associated mitochondrial import and export pathways in Trypanosomes and anaerobic protists. Eukaryotic Cell **12**:343-355.

201. **Weerapana, E., C. Wang, G. M. Simon, F. Richter, S. Khare, M. B. D. Dillon, D. A. Bachovchin, K. Mowen, D. Baker, and B. F. Cravatt**. 2010. Quantitative reactivity profiling predicts functional cysteines in proteomes. Nature **468**:790-U79.

MCB
Journals.ASM.org

Probing the Biology of *Giardia intestinalis* Mitosomes Using *In Vivo* Enzymatic Tagging

Eva Martincová,[a] Luboš Voleman,[a] Jan Pyrih,[a] Vojtěch Žárský,[a] Pavlína Vondráčková,[a] Martin Kolísko,[b] Jan Tachezy,[a] Pavel Doležal[a]

Department of Parasitology, Faculty of Science, Charles University in Prague, Prague, Czech Republic[a]; Centre for Microbial Diversity and Evolution, Department of Botany, University of British Columbia, Vancouver, BC, Canada[b]

Giardia intestinalis **parasites contain mitosomes, one of the simplest mitochondrion-related organelles. Strategies to identify the functions of mitosomes have been limited mainly to homology detection, which is not suitable for identifying species-specific proteins and their functions. An *in vivo* enzymatic tagging technique based on the *Escherichia coli* biotin ligase (BirA) has been introduced to *G. intestinalis*; this method allows for the compartment-specific biotinylation of a protein of interest. Known proteins involved in the mitosomal protein import were *in vivo* tagged, cross-linked, and used to copurify complexes from the outer and inner mitosomal membranes in a single step. New proteins were then identified by mass spectrometry. This approach enabled the identification of highly diverged mitosomal Tim44 (*Gi*Tim44), the first known component of the mitosomal inner membrane translocase (TIM). In addition, our subsequent bioinformatics searches returned novel diverged Tim44 paralogs, which mediate the translation and mitosomal insertion of mitochondrially encoded proteins in other eukaryotes. However, most of the identified proteins are specific to *G. intestinalis* and even absent from the related diplomonad parasite *Spironucleus salmonicida*, thus reflecting the unique character of the mitosomal metabolism. The *in vivo* enzymatic tagging also showed that proteins enter the mitosome posttranslationally in an unfolded state and without vesicular transport.**

Giardia intestinalis causes intestinal infection in diverse vertebrate species, including humans, where it causes the disease giardiasis (1). In addition to its medical and veterinary importance, *Giardia* is an interesting unicellular eukaryote (protist) from cell biology and evolutionary perspectives (2).

The binucleated *Giardia* trophozoite is equipped with eight flagella and an adhesive disc, which mediates attachment to its host's intestine. The interior of the cell is dominated by an endoplasmic reticulum (ER) network (3) and lysosome-like peripheral vacuoles that mediate the uptake and digestion of nutrients (4). There are also Golgi body-like encystation vesicles that distribute the cyst wall material to the cell surface during encystation of the parasite (5).

The mitosomes of *Giardia* are highly adapted forms of mitochondria and are approximately 100 nm in size. These organelles are surrounded by two membranes, but unlike mitochondria, they do not contain DNA. The mitosomal proteome is currently limited to 21 proteins, which primarily participate in iron-sulfur cluster biosynthesis and protein import and folding (6–8). The identification of mitosomal proteins has been accomplished mostly using bioinformatics techniques, such as phylogenetics (9, 10) and hidden Markov model (HMM)-based searches (6, 11), that detect homologous proteins. Thus, in contrast to hydrogenosomes and mitochondria, in which 20 to 50% of proteins have no assigned function (12–14), the vast majority of mitosomal proteins have known functions and orthologs in the mitochondria of other eukaryotes. Attempts to identify the mitosomal proteome using cell fractionation techniques have been largely stymied by the abundance of the ER and cytoskeletal structures in the cell (7). Analogous studies of the proteomes of encystation vesicles and peripheral vacuoles of *Giardia* using sophisticated organelle purification procedures have demonstrated the limits of direct organelle isolation approaches (15). As a result, several essential aspects of the mitosome, such as the nature of the translocase of the inner membrane (TIM) complex or the protein composition of the outer mitosomal membrane, remain unknown.

Here, we addressed the difficulty of the biochemical characterization of giardial mitosomes by employing an *in vivo* enzymatic tagging approach. The highly specific purification of biotinylated mitosomal proteins led to the identification of divergent *Gi*Tim44, the first component of the mitosomal TIM complex. In addition, over 10 novel mitosomal proteins from the mitosomal matrix and the outer mitosomal membrane were also identified, increasing the known mitosomal proteome by one-half. Most of these proteins reflect the unique and unpredictable character of giardial mitosome biology. Moreover, the compartment-specific protein tagging allowed us to identify the mode of mitosomal protein transport.

MATERIALS AND METHODS

Cell culture and fractionation. Trophozoites of *G. intestinalis* strain WB (ATCC 30957) were grown in TY-S-33 medium (16) supplemented with 10% heat-inactivated bovine serum (PAA Laboratories), 0.1% bovine bile, and antibiotics. Cells expressing the dihydrofolate reductase (DHFR)

Received 8 May 2015 **Returned for modification** 18 May 2015
Accepted 3 June 2015

Accepted manuscript posted online 8 June 2015

Citation Martincová E, Voleman L, Pyrih J, Žárský V, Vondráčková P, Kolísko M, Tachezy J, Doležal P. 2015. Probing the biology of *Giardia intestinalis* mitosomes using *in vivo* enzymatic tagging. Mol Cell Biol 35:2864–2874. doi:10.1128/MCB.00448-15.

Address correspondence to Pavel Doležal, pavel.dolezal@natur.cuni.cz.

Supplemental material for this article may be found at http://dx.doi.org/10.1128/MCB.00448-15.

doi:10.1128/MCB.00448-15

fusion protein were grown in medium supplemented with 100 μM pyrimethamine (PM).

Preparation of cell fractions. The cells were harvested by centrifugation at 1,000 × *g* at 4°C for 10 min in ice-cold phosphate-buffered saline (PBS), washed once in SM buffer (250 mM sucrose, 20 mM MOPS [morpholinepropanesulfonic acid], pH 7.4), and resuspended in SM buffer with protease inhibitors (cOmplete, EDTA-free; Roche). Cells were disrupted on ice by sonication with 1-s pulses and an amplitude of 40 for 1 min (Bioblock Scientific Vibra-Cell 72405). The lysate was then centrifuged at 2,750 × *g* for 10 min. The centrifugation step was repeated until the pellet containing unbroken cells, nuclei, and the cytoskeleton was no longer visible. The clear supernatant was centrifuged at 180,000 × *g* at 4°C for 30 min. The resulting high-speed supernatant represented the cytosolic fraction; the high-speed pellet (HSP) containing the mitosomes was resuspended in SM buffer containing protease inhibitors.

Fluorescence microscopy. *G. intestinalis* trophozoites were fixed and immunolabeled as previously described (17). Mitosomal *Gi*Tom40 was detected with a specific polyclonal antibody raised in rabbits (18), and the hemagglutinin epitope (HA tag) was recognized by a rat monoclonal antibody (Roche). The primary antibodies were detected by a donkey Alexa Fluor 594 (red)-conjugated anti-rabbit antibody and Alexa Fluor 594 (red)- or Alexa Fluor 488 (green)-conjugated anti-rat antibodies (Life Technologies), respectively. Alexa Fluor 488 (green)-conjugated streptavidin (Life Technologies) was used to detect biotinylation. Slides were mounted with Vectashield containing DAPI (4′,6-diamidino-2-phenylindole; Vector Laboratories). The slides were imaged with an Olympus Cell-R, IX81 microscope system, and the images were processed using ImageJ 1.41e software (NIH).

Cloning and transfection. The pTG vector was used for *Escherichia coli* biotin ligase (BirA) cloning and protein expression (17). The gene encoding BirA (WP_023308552) was amplified from pET21a-BirA (19). Table S1 in the supplemental material lists all the primers used in this study. To coexpress proteins with BirA, biotin acceptor peptide (BAP) was introduced into the pONDRA vector (6) using a reverse primer for *Gi*Pam18-BAP. This vector carrying the C-terminal BAP was used for the subsequent cloning of the other genes. All *Giardia* genes were amplified from genomic DNA. Mouse DHFR was amplified from pARL2-GDG (20) (kindly provided by Jude Przyborski, Philipps University Marburg). *G. intestinalis* transfection was performed as previously described (6). Briefly, 300 μl of *G. intestinalis* trophozoites (3.3×10^7 cells/ml) was electroporated with a Bio-Rad Gene Pulser using an exponential protocol (U = 350 V; C = 1,000 μF; R = 750 Ω). The transfected cells were grown in medium supplemented with antibiotics (57 μg/ml puromycin and 600 μg/ml G418).

Cross-linking, protein isolation, and mass spectrometry (MS). *G. intestinalis* cells were grown in standard medium supplemented with 50 μM biotin for 24 h prior to harvesting. The cells were harvested and fractionated as described above. The HSP (40 mg) was used for the cross-linking and protein isolation. The pellet was resuspended in PBS (pH 7.4) supplemented with protease inhibitors (Roche) at a final protein concentration of 1.5 mg/ml. Then, a 25 μM concentration of the cross-linker DSP (dithiobis [succinimidyl propionate]; Thermo Scientific) was added, followed by 1 h of incubation on ice. After the incubation, Tris (pH 8) was added at a final concentration of 50 mM, and the sample was incubated at room temperature for 15 min. The sample was centrifuged at 30,000 × *g* for 10 min at 4°C, and the resulting pellet was resuspended in boiling buffer (50 mM Tris, 1 mM EDTA, 1% SDS, pH 7.4) supplemented with protease inhibitors at a final protein concentration of 1.5 mg/ml. The sample was incubated at 80°C for 10 min and was centrifuged at 30,000 × *g* for 10 min at room temperature. The resulting supernatant was diluted 1:10 in incubation buffer (50 mM Tris, 150 mM NaCl, 5 mM EDTA, 1% Triton X-100, pH 7.4) supplemented with protease inhibitors. Then, 200 μl of streptavidin-coupled magnetic beads (Dynabeads MyOne Streptavidin C1; Invitrogen) was washed 3 times with incubation buffer, mixed with the sample, and incubated overnight at 4°C with gentle rotation. The beads were then subjected to the following washes: 3 times for 5 min each in incubation buffer supplemented with 0.1% SDS, once for 5 min in boiling buffer, once for 5 min in washing buffer (60 mM Tris, 2% SDS, 10% glycerol), and twice for 5 min each in incubation buffer supplemented with 0.1% SDS. Finally, proteins were eluted from the beads in SDS-PAGE sample buffer supplemented with 20 mM biotin for 5 min at 95°C.

The samples were analyzed by Western blotting using streptavidin-conjugated Alexa Fluor 488 and were visualized using a Molecular Imager FX imager (Bio-Rad). The eluate was resolved by SDS-PAGE and stained with Coomassie brilliant blue. The gel was cut, destained, trypsin digested, and analyzed on a mass spectrometer.

Mass spectrometry and MS/MS analyses. Spectra were acquired using a (4800 Plus MALDI-TOF/TOF) analyzer (Applied Biosystems/MDS Sciex) equipped with an Nd:YAG laser (355 nm) with a firing rate of 200 Hz. The tandem mass spectrometry (MS/MS) analyses were performed as previously described (21).

Protease protection assay. To determine whether proteins were embedded in the outer mitosomal membrane, 150 μg of the HSP fraction in SM buffer supplemented with protease inhibitors was incubated with 200 μg/ml trypsin for 10 min at 37°C. The control sample also contained 0.1% Triton X-100 to completely digest the proteins of the solubilized organelles. The samples were separated by SDS-PAGE and blotted onto a nitrocellulose membrane, and proteins were detected with antibodies.

To determine whether proteins were in the mitosomal matrix, 1 mg of the HSP fraction was resuspended in 400 μl of either hypotonic buffer (1 mM EDTA, 10 mM MOPS, pH 7.2), isotonic buffer (hypotonic buffer supplemented with 250 mM sucrose), or NaCl buffer (500 mM NaCl, 10 mM Tris, pH 7.4). Pellets were resuspended by gentle pipetting or by sonication with 1-s pulses and amplitude of 60 for 2 times 1 min (Bioblock Scientific Vibra Cell 72405). Subsequently, 100 μl of each sample was treated with a different concentration of proteinase K (PK) and incubated on ice for 20 min. The reaction was stopped by the addition of 2 μl of 1 mM phenylmethanesulfonyl fluoride (PMSF), and the mixture was incubated on ice for 10 min. For the protein precipitation, 20 μl of 100% trichloroacetic acid (TCA) was added, and the samples were incubated on ice for 30 min. The samples were then centrifuged at 30,000 × *g* at 4°C for 30 min. The resulting pellets were washed in acetone and centrifuged at 30,000 × *g* at 4°C for 30 min, air dried, and resuspended in SDS-PAGE sample buffer.

Electron microscopy. For transmission electron microscopy (TEM) studies, *G. intestinalis* cell pellets were fixed for 24 h in 2.5% glutaraldehyde in 0.1 M cacodylate buffer (pH 7.2) and were postfixed in 2% OsO_4 in the same buffer. The fixed samples were dehydrated by passage through an ascending ethanol and acetone series and were embedded in an Araldite-Poly/Bed 812 mixture. Thin sections were cut on a Reichert-Jung Ultracut E ultramicrotome and were stained using uranyl acetate and lead citrate. The sections were examined and photographed with a JEOL JEM-1011 electron microscope. Fine-structure measurements were performed with a Veleta camera and iTEM 5.1 software (Olympus Soft Imaging Solution GmbH).

Bioinformatic analyses. To identify the copurified proteins, their amino acid sequences were analyzed by BLASTP against the NCBI nr database using the following algorithms: HHpred at http://toolkit.tuebingen.mpg.de/hhpred# (22); HMMER3 at http://hmmer.janelia.org/ (23); and I-TASSER at http://zhanglab.ccmb.med.umich.edu/I-TASSER/ (24). The subcellular localization and topology of the proteins were predicted using TargetP at http://www.cbs.dtu.dk/services/ (25) and Phobius at http://phobius.sbc.su.se (26), respectively.

RESULTS

***In vivo* enzymatic tagging in *Giardia intestinalis*.** To gain insights into the composition of protein import pathways and other processes in giardial mitosomes, we took a direct biochemical ap-

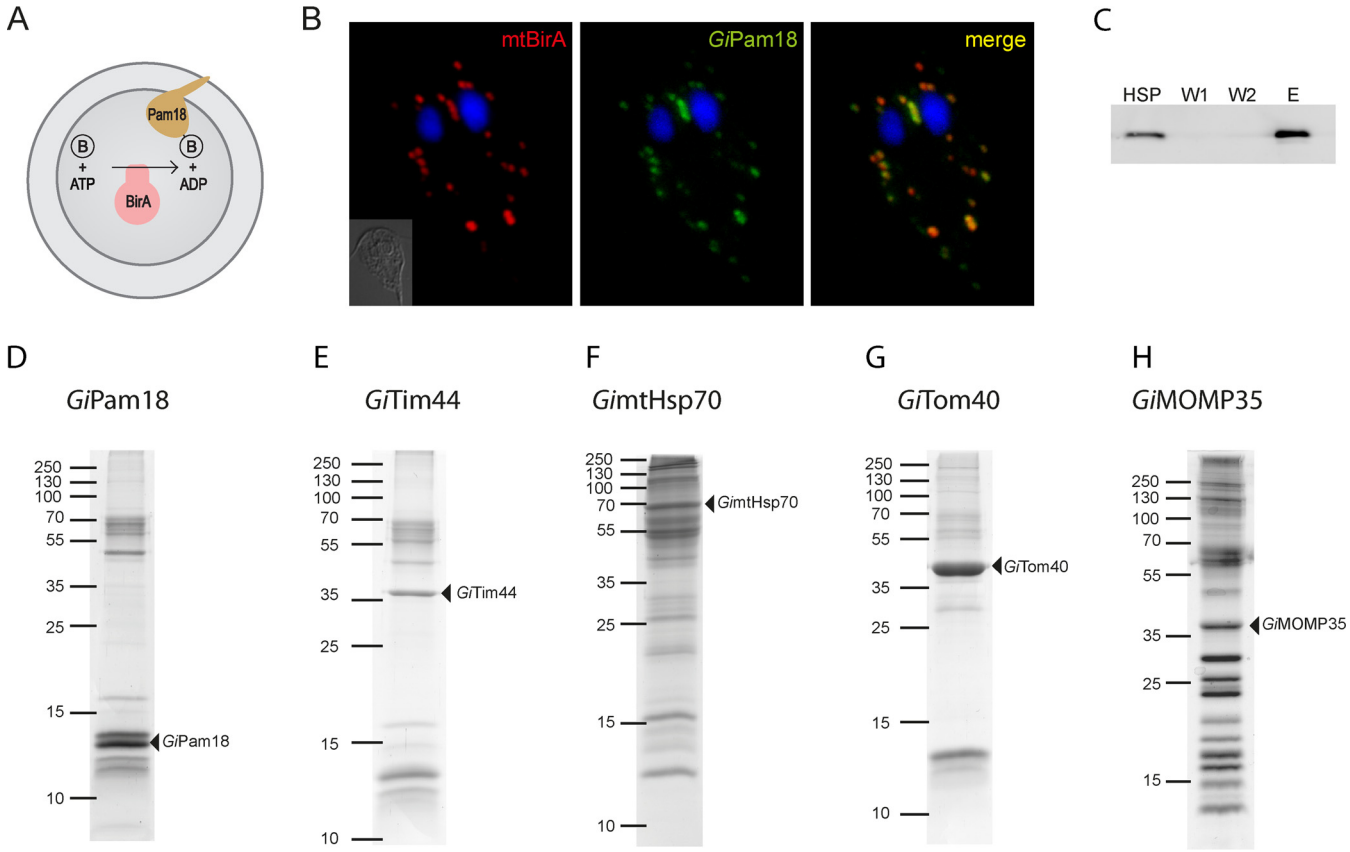

FIG 1 *Gi*Pam18 is biotinylated within mitosomes. (A) Schematic representation of mitosome-specific *in vivo* enzymatic tagging. *E. coli* biotin ligase (BirA) specifically biotinylates the biotin acceptor peptide when present in the same compartment. B, biotin. (B) BAP-tagged *Gi*Pam18 was successfully biotinylated by mtBirA. Cells were stained with an anti-HA tag antibody (red) and streptavidin-conjugated Alexa Fluor 488 (green) to detect mtBirA. Nuclei were stained with DAPI (blue). (C) Example of the purification steps (*Gi*Pam18) as analyzed on the Western blot by Alexa Fluor Fluor 488-streptavidin conjugate. (D to H) Protein profiles of the particular eluates from the streptavidin-coupled magnetic beads resolved by SDS-PAGE. The triangles indicate the proteins carrying the BAP tag.

proach involving highly specific protein pulldown assays followed by mass spectrometry analyses. To this end, an *in vivo* enzymatic tagging technique based on the biotin-avidin interaction was introduced into *Giardia*. This tagging relies on the highly specific *E. coli* biotin ligase (BirA), which uses one ATP molecule to catalyze the covalent attachment of biotin to the side chain of lysine within a biotin acceptor peptide (BAP) (27). A chimeric construct composed of *E. coli* BirA preceded by the N-terminal region of mitosomal *Gi*Mge1 and followed by a double HA tag was expressed in *Giardia*. The resulting strain contained mitosomally localized BirA (mtBirA). This construct was cotransformed with a second plasmid carrying a gene encoding mitosomal *Gi*Pam18 with the C-terminal BAP (Fig. 1A). Detection using a fluorescent streptavidin conjugate revealed the specific biotinylation of BAP (Fig. 1B). *Gi*Pam18-BAP-specific biotinylation was confirmed by Western blotting of a *Giardia* trophozoite lysate, which produced a single band of approximately 13 kDa, which corresponded to *Gi*Pam18-BAP. These results demonstrated that BirA remained active when delivered to *Giardia* mitosomes and that no nonspecific biotinylation was detected. Moreover, the use of mitosomal ATP during the biotinylation of the BAP had no apparent effects on mitosomal morphology, mitosomal distribution, or parasite growth.

Search for the TIM components. *Gi*Pam18-BAP was further used to identify putative components of the mitosomal TIM complex. As a part of the PAM complex at the inner mitochondrial membrane, Pam18 interacts with the translocation channel via Tim44 (28). HSPs, which were enriched for mitosomes, were obtained from *Giardia* trophozoites expressing mtBirA and *Gi*Pam18-BAP. The purification of the biotinylated proteins was initially performed under native conditions; however, the resulting eluates contained numerous contaminating proteins (data not shown). Thus, chemical cross-linking and denaturation conditions were used instead. The HSP was treated with a low concentration of the membrane-permeable reversible cross-linker DSP, which is commonly used to identify interacting proteins in various cellular compartments, including mitochondria (29, 30).

Upon cross-linking, the detergent-solubilized samples were passed over streptavidin-coupled magnetic beads, and the resulting protein fractions were analyzed via SDS-PAGE and Western blotting (Fig. 1C and D). The samples were then trypsin cleaved and analyzed by mass spectrometry. Analogous purification experiments were performed in parallel using HSPs isolated from wild-type *Giardia* cells and from *Giardia* cells expressing mtBirA only. These two samples were used as negative controls for the mass spectrometry protein identification. After the results of the negative controls were subtracted, the identified proteins were ordered according to their Mascot score. Although none of the

known mitosomal proteins were present in the negative controls, these proteins were abundant among the hits derived from the *Gi*Pam18-BAP samples. The high specificity of the purification procedures suggests that *Gi*Pam18-interacting partners were present among the top identified proteins. The remainder of the refined data set largely represented proteins of unknown function, and their amino acid sequences were analyzed using homology and topology detection software.

Mitosomes contain highly diverged Tim44. Of the proteins that copurified with *Gi*Pam18-BAP, GL50803_14845 had the highest Mascot score of the unknown proteins (see Fig. S3 in the supplemental material). Although pairwise sequence analyses of GL50803_14845 showed no obvious homology to known protein families, profile-sequence comparisons conducted with HHpred showed clear homology to Tim44, a key component of the TIM complex (Fig. 2A). The mitosomal localization of GL50803_14845, here referred to as *Gi*Tim44, was confirmed by its episomal expression in *Giardia* (Fig. 2B). Further comparisons with mitochondrial and hydrogenosomal Tim44 proteins revealed that *Gi*Tim44 is one of the most divergent Tim44 orthologs identified and that it consists of the C-terminal domain of Tim44, which has been suggested to interact with mitochondrial lipids. However, *Gi*Tim44 lacks recognizable N-terminal domain of Tim44 (Fig. 2C), which binds the import motor molecule mtHsp70 and the core subunit of the protein-conducting channel, Tim23 (31, 32).

The homology model of the C-terminal domain of *Gi*Tim44 indicated that this protein was capable of forming a conserved Tim44 structure containing a hydrophobic cavity, indicating its possible attachment to the mitosomal membrane (Fig. 2F). To test whether mitosomal *Gi*Tim44 interacts with its putative mitochondrial partner, *Gi*mtHsp70, *Giardia* trophozoites coexpressing mtBirA and *Gi*Tim44-BAP were generated. Following chemical cross-linking and purification, the proteins that copurified with *Gi*Tim44-BAP were analyzed by mass spectrometry. Similar to what was seen in the initial experiment, the purified sample was highly enriched for known mitosomal proteins (see Fig. S3 in the supplemental material). The five most highly enriched identified proteins included mitosomal *Gi*mtHsp70 and its nucleotide exchange factor, *Gi*Mge1, which strongly supports the hypothesis that Tim44 and Hsp70 interact within mitosomes.

Distant Tim44 orthologs in eukaryotes. The discovery of a divergent Tim44 in *Giardia* led us to search for other Tim44 orthologs in eukaryotes. Using Tim44-specific HMMs, we identified Tim44 orthologs in two free-living metamonads, *Carpediemonas membranifera* and *Ergobibamus cyprinoides*. However, no Tim44 orthologs were identified in the fish parasite *Spironucleus salmonicida* or in the group Euglenozoa, which includes medically important trypanosomes and leishmania.

Surprisingly, the HMMs identified two mitochondrial proteins, MRLP45 and Mba1, as belonging to the Tim44 protein family (Fig. 2C and D). Whereas MRLP45 is a subunit of the mitochondrial ribosome (33), Mba1 serves as a mitochondrial ribosome receptor during the membrane insertion of mitochondrially translated proteins (34). Their distribution in eukaryotes suggests that both proteins represent independent paralogs of Tim44 that are specialized for mitochondrial protein translation (Fig. 2D).

Search for the translocase of the TOM components. To identify outer mitosomal membrane components, *Gi*Tom40-BAP was coexpressed with the cytosolic version of BirA (cytBirA). As a result, mitosome-specific biotinylation was observed (see Fig. S1 in the supplemental material). Employing the same strategy as the one used for *Gi*Pam18 and *Gi*Tim44, the proteins obtained by *Gi*Tom40-BAP purification were identified using mass spectrometry. The proteins obtained from wild-type *Giardia* cells and *Giardia* cells expressing cytBirA only were subtracted from the data set.

Because *Gi*Tom40 is the only known outer mitosomal membrane protein, the specificity of the purification procedure could not be determined. Nevertheless, the absence of mitosomal matrix proteins among the most significant hits (see Fig. S3 in the supplemental material) indicated that a distinct subset of mitosomal proteins was obtained. However, the previously identified mitosomal protein GL50803_14939 was found among the hits (7) (see Fig. S3 in the supplemental material). According to transmembrane topology predictors, GL50803_14939 contains two transmembrane domains in its N-terminal region. To determine whether the protein is embedded in the outer or inner mitosomal membrane, an HSP isolated from *Giardia* expressing C-terminally HA-tagged GL50803_14939 was subjected to a protease protection assay. Similar to *Gi*Tom40, GL50803_14939 was sensitive to protease activity even without the addition of detergent, which suggests that GL50803_14939 is inserted into the outer membrane (Fig. 3A). Taken together, these data suggest that GL50803_14939, here referred to as mitosomal outer membrane protein 35 (*Gi*MOMP35), is anchored by two N-terminal transmembrane domains in the outer mitosomal membrane and that its C-terminal domain is in the cytosol. Whether the transmembrane domains of *Gi*MOMP35 are also responsible for its mitosomal targeting was tested by analyzing the expression of an N-terminally truncated version of the protein. Indeed, the removal of the transmembrane domains resulted in the cytosolic localization of the truncated *Gi*MOMP35 (see Fig. S2A in the supplemental material).

The function of the exposed soluble domain could not be predicted using bioinformatic analyses, which revealed no significant similarity of the domain to any known protein families. To examine the function of *Gi*MOMP35, we attempted to overexpress the full-length protein using a strong promoter (ornithine carbamoyltransferase) (35). However, a stable *Giardia* line could not be established after numerous attempts, indicating that the overexpression of *Gi*MOMP35 was lethal. Milder *Gi*MOMP35 overexpression (using the 5′ untranslated region [5′UTR] of glutamate dehydrogenase as a promoter) allowed a stable line of *Giardia* transformants to be established and inspected for mitosome-related defects. Approximately one half of the cells retained typical mitosomal distribution and morphology (Fig. 3B), whereas the other half exhibited dramatic membrane protrusions and aggregation (Fig. 3C to E).

Further analyses indicated that *Gi*Tom40 colocalized with these elongated structures (Fig. 3C). However, these structures were largely devoid of the mitosomal protein GL50803_9296, which localized to the mitosomal matrix (see Fig. S2B in the supplemental material). When examined with a transmission electron microscope, the structures were observed as tightly packed multimembrane complexes (Fig. 3F). These data suggest that the membrane protrusions corresponded to the enlarged and aggregated outer mitosomal membrane. In contrast, the overexpression of *Gi*MOMP35 did not result in an ER-related phenotype, as illus-

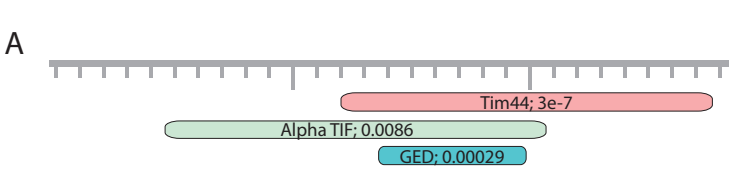

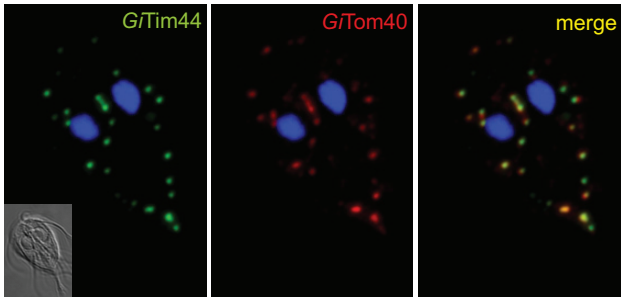

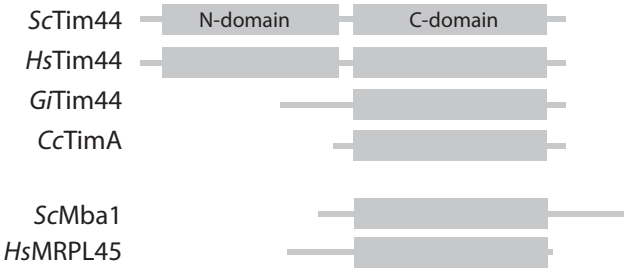

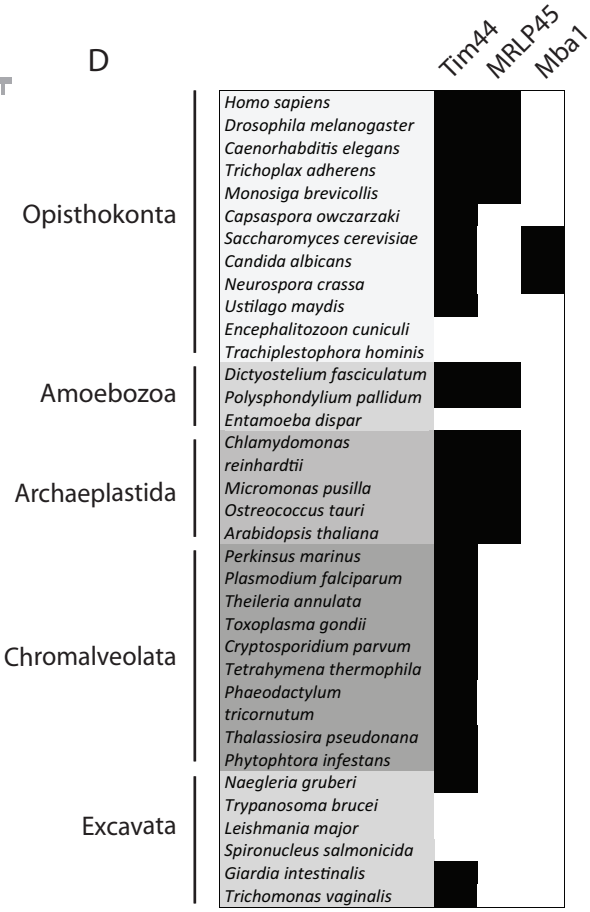

E

```
G.intestinalis      119 ---------- -----LALDF RRLR-SLLPS FDLPHFTENY GIDTLVAILG GYLNIFNTYN PQSYPRQTIA YLLDNCTSKL QKQ-LLEGIQ EKIRKDVDTH FRLHHIRGVK CTGLDLH---  219
C.membranifera      133 -------SQW GKGTELGINV GLVS-AWIP- ---------- --QFVAQIM- ---------- -EAYFMNDVA TLRECCADGA LSI-LLQGLK EQRDKHLSVQ GSTYRIGTTD LARVGG---D  216
E.cyprinoides       135 -----MACDL IGRDTQAAVA AARA-HFDRD FDLHQLQDSA A-AITGELM- ---------- -DAFFAGDVE TVAGLTAEVP RRL-LLDAMR QFLNARIEVT GWTYWAGEPA LRSADVSE-E  234
B.naejangsanensis   56 ---------- --DPALTAAI AGLK-ARDPN FDPHRFLEGA RQAY-ETIV- ---------- -GAYAKGDRE ALRPLLLDKV MGS-FEAGIA AREARGDIES AELVHPPRAD LELATAE--G  147
H.sapiens           281 DKVTDLLGGL FSKTEMSEVL TELL-RVDPA FDKDRFLKQC ENDIIPNVLL ---------- -EAMISGELD ILKDWQYEAT YSQ-LAHPIQ QAKALGLQFH SRILDIDNVD LAMGKMM--E  384
S.cerevisiae        259 NKV----GGF FAETESSRVY SQFK-LMDPT FSNESFTRHL REYIVPEILL ---------- -EAYVKGDVK VLKKWFSEAP FNV-YAAQQK IFKEQDVYAD GRILDIRGVE IVSAKLLAPQ  360
A.thaliana          301 --IQDMNEKF LKETDSASTY KELR-SRDPS FSLPDEAAEI EEVIKF-VLL ---------- -NAYSEGDVE TLKKYCSKEV IER-CTAERT AVQTHGVLFD NKLLHISEVS VSVTKMM--G  402
N.gruberi           348 EDIPDTEADI SSTSENALAM GAFK-KRDPR FDLDLLLVTM ETLTIPEIM- ---------- -SAYFNDDAH TLKKFVSESC YRQVFFPRIQ EFVHTKIKYD AKILHVEDVM LYTTRYD--A  452
P.falciparum        302 -------GKL FGETELAAAL REMK-MIDKN FKLSELMYLF EYVISKHIV- ---------- -ESYLIGDEF TLRLHCGSSA FNS-LNASIT LKKKKVFLD TNVLIYKNHF LKGAQRME-E  400
T.vaginalis         156 NASSVVVSKL TQPSKEQLVQ MSIQ-MYYPT FTISEFKQWI EKSFLPVLL- ---------- -ERYLRGNIK QLEELTSQQV AKE-RQLAVV QFLSNRLIIR TKLLSITDVD IMGFDFT--N  259
D.fasciculatum      362 GTIAGFVGGY TSSPALTKFY FDYRDLIMPG FFFNKFLPIA KSKFIPEFL- ---------- -EIVFANDVD GLEDFCGETL HKM-LSGIIA ANEAGHKVFD GKIVKIDTLD FMGINES--E  466

G.intestinalis      219 ---SMELHFT AILTGAYAVT NRS---GQTV NGGYNKSRD- -YLVDYSYRY YNGK------ ---------- WLLSALKMSI LSISAKPTYF Y 286
C.membranifera      217 DRPTLTVNET --LSHFFRVN LPR---GHCL HGS-KKGRDY TYTATISPEK GQWVDLTEGD AKEEVR---- WMLTDIHAET VDYVANKEE- - 295
E.cyprinoides       235 GVESFEFAVT --LSQLYAAT RAGEHGPELL HGSLRRGTDF EYVFKLRPAG EPRAIVGRG- -NQGPTR--- WIVSALLAPT LDATLEPRGA T 318
B.naejangsanensis   148 DRALAKVREL --AEVRGSLT PSG---GETV TEE----RRT AEIWTFERRL G--------- -TSDPN---- WALARVEPAA A--------- - 205
H.sapiens           385 QGFVLTITFQ --AQLVMVVR NPK---GEVV EGDPDKYLRM LYVWAIGRGQ DEL------- -NPYAA---- WRLLDISASS TEQIL----- - 452
S.cerevisiae        361 DIEVLVVGCR --AQEINLYR KKKT--GEIA AGDEANILMS SYAMVFIRDP EQIDD----- -DETEG---- WKILEFVRGG SRQFT----- - 431
A.thaliana          403 DSPIITAKFQ --TQEIYCVR DEN---GEIQ EGGQDTIHTV YHEWAMQGVE T----TELGE DAIYPI---- WRLREMCRNG VQALI----- - 474
N.gruberi           453 GNPALVISCA --VQYIHCMK NEA---GEIV EGGPKDIRKE NQMWIIKQDE S--------- -QETDD---- WYVSEVSMLN ADAVK----I V 520
P.falciparum        401 SSPWFIFTFH --TQQINCLK NKN---DEII EGKIDDIREV VYTIALSEHP E--------- -PCKEGLLYP YIVREFAIIG NTPSW----- - 470
T.vaginalis         260 RMPSILVRCS --ADHTNEVI TMNS--GTIV EGGPQDICHT DFIVVLTIDA S--------- -KQTPR---- WIASELRPDS TSNRI----- - 326
D.fasciculatum      467 NREETYFSFL VVVHHTYCIR LYQ---FEIV EGGDHEIIKT QMIVHMSVDT D--------- -LNEFG---- WCVSKLDVHP SESIY----- L 535
```

F

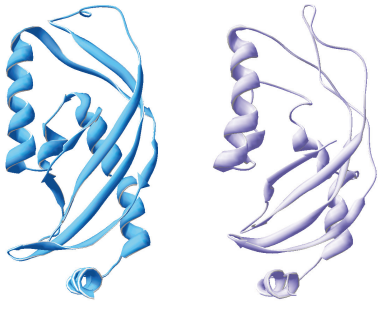

ScTim44 GiTim44

trated by the lack of colocalization between the ER and the enlarged mitosomes (Fig. 3E).

As an alternate means of investigating the function of *Gi*MOMP35, the cross-linked BAP-tagged protein was purified and subjected to mass spectrometry. As expected, *Gi*Tom40 was included in the significant hits; however, the obtained data set contained no clear indication of the function of *Gi*MOMP35 (see Fig. S3 in the supplemental material).

Newly identified mitosomal proteins. In addition to *Gi*Tim44 and *Gi*MOMP35, a number of other proteins of unknown function were identified from the pulldown experiments. The proteins that coprecipitated with BAP-tagged mitosomal Hsp70 (*Gi*mtHsp70) were added to the data sets derived from the *Gi*Pam18, *Gi*Tim44, *Gi*Tom40, and *Gi*MOP35 coimmunoprecipitations, and the data were analyzed together (Fig. 1D to H). *Gi*mtHsp70 is thought to be a central component of mitosomal metabolism and to participate in protein import and iron-sulfur cluster assembly.

Seventeen proteins (see Table S2 in the supplemental material) were subcloned into *Giardia* expression vectors to verify their mitosomal localization. These proteins were selected according to three criteria: (i) the protein copurified with more than one target molecule, (ii) the identification of the protein was highly significant, or (iii) homology predictors showed an affiliation with a particular protein family. Using this approach, mitosomal localization was confirmed for 13 of the proteins, including 3 with dual localization (Fig. 4). The localization of one protein (GL50803_92741) could not be confirmed because no viable transformants were obtained after three independent transfections. Particular attention was paid to GL50803_27910 and GL50803_16424. The first represents an ortholog of rhodanese, a protein involved in various aspects of sulfur metabolism (36), including the repair of iron-sulfur clusters (37). The latter was the only protein identified in all the pulldown experiments performed in this study (see Fig. S3 in the supplemental material); i.e., GL50803_16424 coprecipitated with the outer membrane, the inner membrane, and the matrix proteins, which might indicate its complicated topology. Moreover, the episomal expression of GL50803_16424 often but not always resulted in the formation of enlarged structures at the mitosomal sites (Fig. 4). Strikingly, this protein appears to be a member of the myelodysplasia-myeloid leukemia factor 1-interacting protein (Mlf1IP) family, which has been considered exclusive to metazoans (38). For the remainder of the confirmed mitosomal proteins, no recognizable homology could be identified. Moreover, with the exception of GL50803_27910, GL50803_3491, and GL50803_16424, these proteins appear to lack orthologs, even in other metamonad species; thus, they currently represent *Giardia*-specific molecules (see Table S3 in the supplemental material).

Mode of mitosomal protein import. Compartment-specific biotinylation allows one to determine whether a given protein is transported into an organelle co- or posttranslationally. To this end, we generated a *Giardia* strain expressing a cytosolic version of BirA (cytBirA) (Fig. 5). The ability of cytBirA to biotinylate the BAP on a mitosomal protein indicates that the protein is transported posttranslationally. Indeed, the biotinylation of *Gi*Tim44-BAP was observed upon coexpression with cytBirA (Fig. 5A). Similarly, the use of compartment-specific biotinylation allowed us to assess whether the reported presence of a SNARE protein, Sec20, in the mitosomes (39) indicated the fusion of secretory vesicles with the mitosomal surface. However, because no biotinylation of the mitosomal proteins was observed when BirA was targeted to the ER (data not shown), the integration of mitosomes into the secretory pathway could not be confirmed. The posttranslational transport of mitosomal proteins raised the question of whether these proteins are required to retain their unfolded state during import. To address that question, a chimeric construct encoding mitosomal *Gi*Mge1, mouse dihydrofolate reductase (DHFR), and a C-terminal HA tag was expressed in *Giardia*. The DHFR domain is a classical experimental substrate used in protein translocation studies due to its ability to fold upon the addition of a folate analog (40). Usually, the use of folate analogs requires the experiment to be performed *in vitro* on isolated organelles due to the effect of these analogs to the endogenous enzyme (40). However, *Giardia* lacks DHFR and instead relies on the purine salvage pathway (41), which allows for the *in vivo* use of DHFR-containing constructs. The localization of the chimeric protein was examined in cells incubated with or without the folate analog pyrimethamine (PM). As expected, in the absence of the folate analog, the targeting information on *Gi*Mge1 mediated the efficient delivery of this protein to the mitosomes (Fig. 5B). In contrast, the addition of PM resulted in an entirely cytosolic localization (Fig. 5C). These results demonstrate that the protein must remain unfolded before and during its import into mitosomes.

DISCUSSION

The *Giardia* mitosome remains one of the least well characterized forms of mitochondria. This is especially true for its biogenesis pathways, which ensure that the organelle maintains its integrity and functions. The aim of this study was to identify new mitosomal proteins, which might have diverged from known proteins beyond the sensitivity of homology detection algorithms or have been replaced by lineage-specific components. Because mitosomes represent one of the smallest membrane-bound cellular compartments of eukaryotes (42), biochemical approaches using cell fractionation techniques are highly challenging (7). The *in vivo* enzymatic tagging approach utilizing *E. coli* BirA introduced in this study allows proteins of interest to be purified and their transport through cellular organelles and their subcompartments to be monitored.

First, two key proteins involved in mitosomal protein import, which reside in different mitosomal membranes, were used to

FIG 2 A Tim44 homolog is present in giardial mitosomes. (A) HHpred analysis of GL50803_14845 shows the presence of a Tim44 domain. (B) HA-tagged *Giardia* Tim44 (*Gi*Tim44) localizes to mitosomes. Green, anti-HA antibody; red, anti-*Gi*Tom40 antibody; blue, nuclei stained with DAPI. (C) Domain structure of Tim44 orthologs in eukaryotes and bacteria. *Sc*, *Saccharomyces cerevisiae*; *Hs*, *Homo sapiens*; *Gi*, *Giardia intestinalis*; *Cc*, *Caulobacter crescentus*. (D) Distribution of Tim44 paralogs in eukaryotes. (E) Protein sequence alignment of *Gi*Tim44 with the C-terminal domains of Tim44 orthologs from *Carpediemonas membranifera*, *Ergobibamus cyprinoides*, *Brevundimonas naejangsanensis*, *Homo sapiens*, *Saccharomyces cerevisiae*, *Arabidopsis thaliana*, *Naegleria gruberi*, *Plasmodium falciparum*, *Trichomonas vaginalis*, and *Dictyostelium discoideum*. The sequences were aligned using MAFFT at http://mafft.cbrc.jp/alignment/server/. The residues involved in forming a hydrophobic pocket are framed in red (57). (F) Model of the C-terminal domain of *Gi*Tim44 obtained by Swiss-Model (58) using human Tim44 as a template (48).

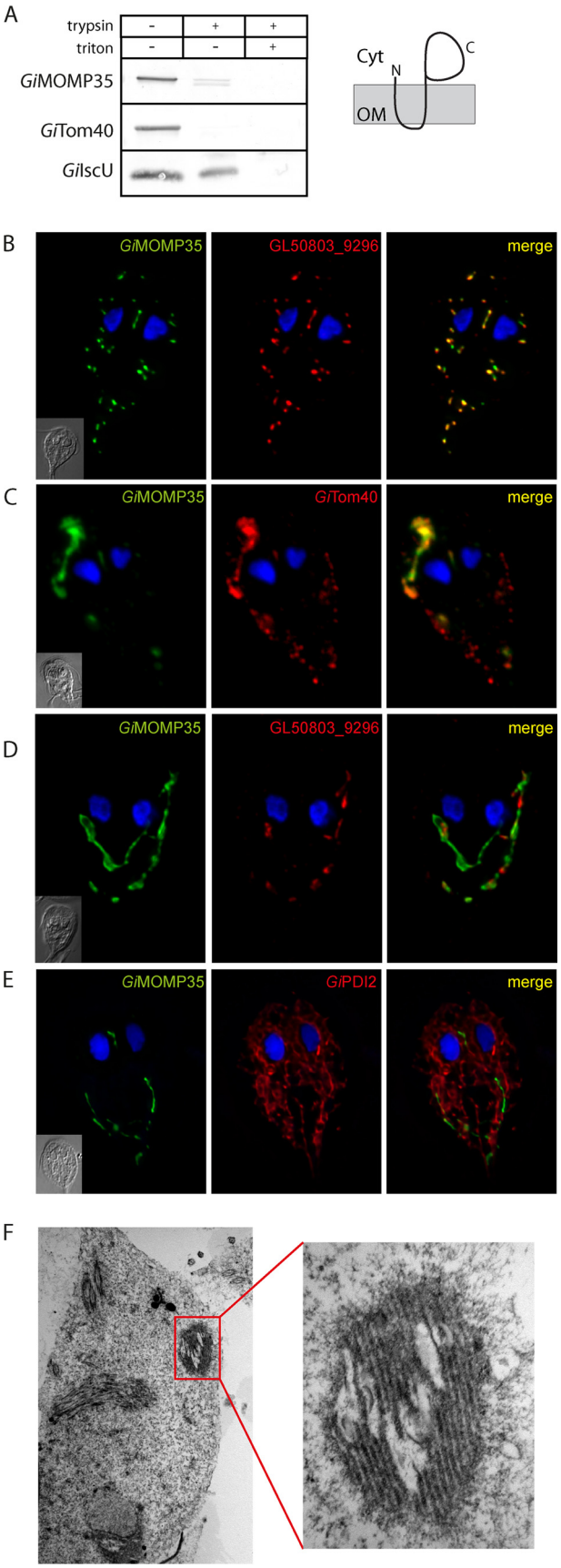

search for new mitosomal components. *Gi*Pam18 was the best available candidate to identify putative TIM components in mitosomes. The protein identified with this approach, *Gi*Tim44, represents one of the most diverged eukaryotic Tim44 proteins. The homology of *Gi*Tim44 is limited to the C-terminal membrane interaction domain, an arrangement reminiscent of the distant Tim44 ortholog found exclusively in alphaproteobacteria (43). However, despite the absence of the N-terminal domain, which has been shown to mediate an interaction with mtHsp70 (31), *Gi*mtHsp70 was found among the most significant proteins that copurified with *Gi*Tim44. This finding may indicate that the interaction between these proteins is conserved in mitosomes, although it is mediated by different amino acid residues. Unfortunately, no protein translocase candidate was found among the obtained data set, which lacked polytopic membrane proteins. This absence was likely due to the experimental conditions used, particularly the cross-linking chemistry and the preparation of samples for mass spectrometry (44). A customized procedure will be necessary to identify such proteins.

Using *Gi*Tim44 as a query, related sequences were found in metamonads such as *C. membranifera* and *E. cyprinoides*. Surprisingly, no Tim44 ortholog was identified in the recently published genome of the hydrogenosome-bearing fish parasite *S. salmonicida* (45). According to further HMM-based searches, Tim44 has been lost several times in the evolution of eukaryotes. Previous reports have shown that this protein is absent from Entamoeba (46) and microsporidian species (47), which also carry highly adapted mitosomes. Strikingly, the Tim44 protein is also missing from the entire group of kinetoplastida, which contain complex aerobic mitochondria. However, our Tim44-specific HMM identified additional new Tim44 paralogs in the mitochondria of opisthokonts, amoebozoa, and plants. Specifically, the mitochondrial proteins MRLP45 and Mba1 participate in mitochondrial translation and membrane protein insertion, respectively (33, 34). MRLP45 is a component of the large subunit of the mitoribosome, the structure of which was recently been resolved (33). The structure of MRLP45 clearly demonstrates its homology to the C-terminal domain of Tim44 (48). Although Mba1 is not a mitoribosome component, it binds the large subunit of the mitoribosome and cooperates with OxaI in the membrane insertion of mitochondrially translated proteins (34). Despite the differences in the molecular architecture of the complexes containing MRLP45 and Mba1, it is likely that these proteins perform analogous functions.

FIG 3 *Gi*MOMP35 is an outer mitosomal membrane protein. (A) Protease protection assay of high-speed pellets isolated from *Giardia* expressing HA-tagged *Gi*MOMP35. After incubation with trypsin, the samples were immunolabeled with antibodies against the HA tag, the outer membrane protein *Gi*Tom40, and the matrix protein *Gi*IscU. The sensitivity of *Gi*MOMP35 to the protease indicates its outer membrane localization. The drawing shows the suggested topology of *Gi*MOMP35. Cyt, cytosol; OM, outer mitosomal membrane. (B) Cells expressing HA-tagged *Gi*MOMP35 were stained with an anti-HA tag antibody (green) and an anti-GL50803_9296 antibody (red). Nuclei were stained with DAPI (blue). In addition to exhibiting typical mitosomal morphology (B), approximately 50% of the observed trophozoites contained elongated tubular structures (C to E). These structures colocalized with *Gi*Tom40 (red) (C); however, only a small fraction exhibited costaining for GL50803_9296 (red) (D). The structures were devoid of the ER marker *Gi*PDI2 (red) (E). These data indicate that the elongated tubular structures represent an enlarged outer mitosomal membrane. Under transmission electron microscopy, the structures appeared as organized membrane layers (F).

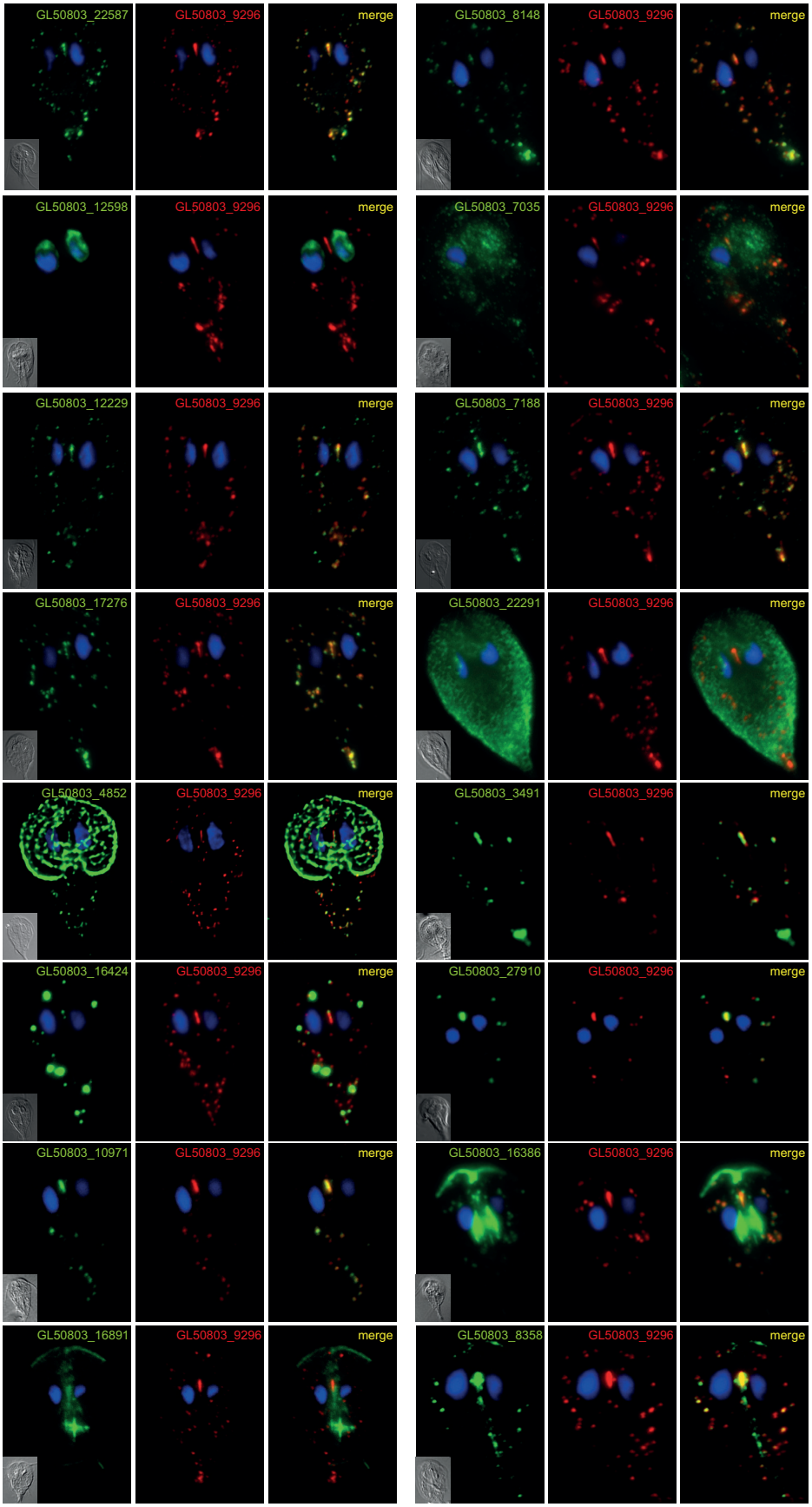

FIG 4 Localization of putative mitosomal proteins. Selected HA-tagged proteins were expressed in *Giardia*, and their cellular localization was determined using immunofluorescence microscopy. The cells were stained with anti-HA tag (green) and anti-GL50803_9296 (red) antibodies. Nuclei were stained with DAPI (blue).

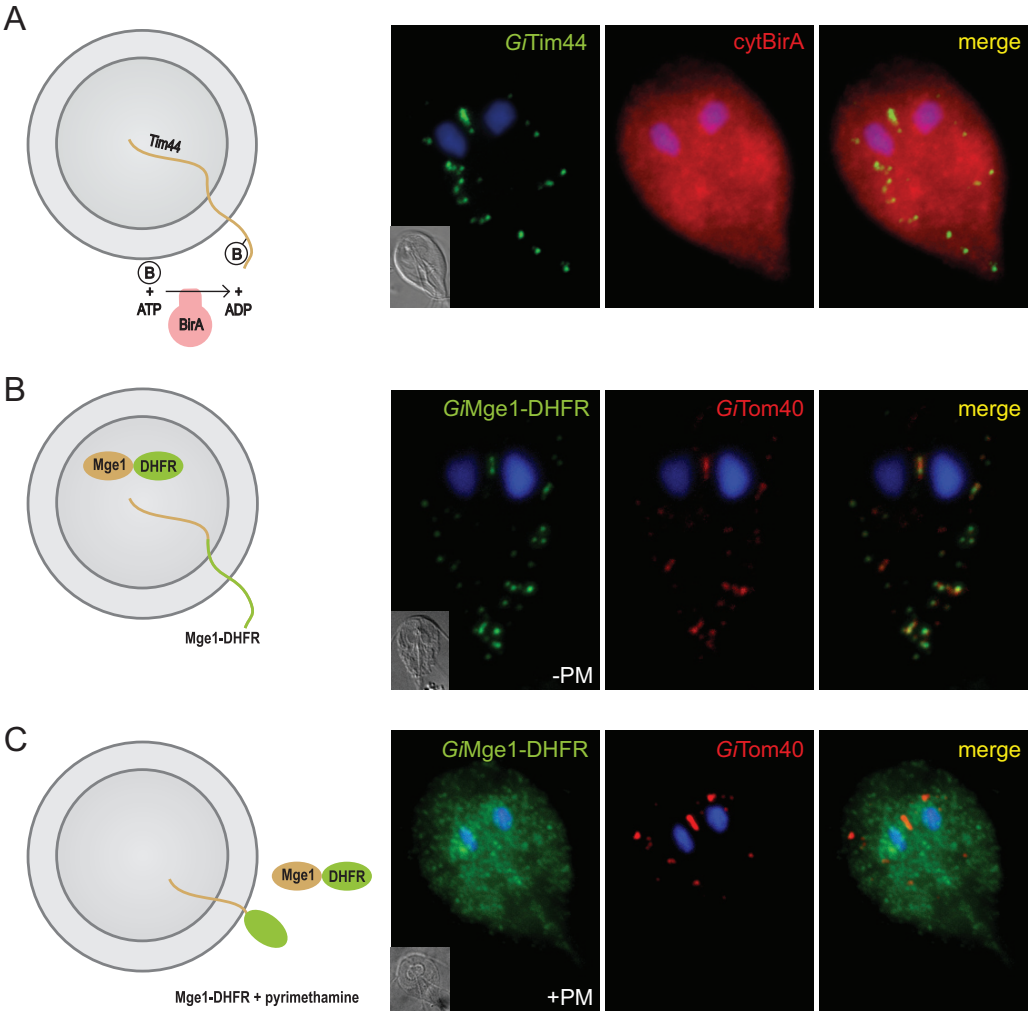

FIG 5 Mitosomal proteins are transported posttranslationally and in an unfolded state. BAP-tagged *Gi*Tim44 was coexpressed with cytosolic BirA (cytBirA), and the biotinylation of the tag was observed using fluorescence microscopy. Cells were stained with an anti-HA tag antibody (red) to detect cytBirA and with streptavidin-conjugated Alexa Fluor 488 (green) to detect the biotinylation of the BAP tag. Nuclei were stained with DAPI (blue). (A) A fusion protein of mouse DHFR, mitosomal *Gi*Mge1, and a C-terminal HA tag was expressed in *Giardia*. (B and C) The localization of the chimeric construct was assessed in the absence (B) or presence (C) of 100 μM pyrimethamine (+PM), which induces the folding of the DHFR domain. The cells were stained with anti-HA (green) and anti-*Gi*Tom40 antibodies (red). Nuclei were stained with DAPI (blue).

The only known outer mitosomal membrane protein has been *Gi*Tom40. This eukaryotic porin is a hallmark of all mitochondria (49), in which it constitutes the general import pore (18, 50) and interacts with the components of the SAM and ERMES complexes (51). The purification of *Gi*Tom40 led to the identification of *Gi*MOMP35. The protein had already been identified in giardial mitosomes, but neither its localization within the mitosome nor its topology had been determined (7). According to our results, the *Gi*MOMP35 protein is anchored in the outer mitosomal membrane with its C-terminal domain exposed to the cytosol. The phenotype of mitochondrial aggregation triggered by the overexpression of *Gi*MOMP35 is reminiscent of the overexpression of some of the outer membrane proteins involved in protein import (52) or mitochondrial dynamics (53). However, without further characterization of its C-terminal domain, the exact function of *Gi*MOMP35 in mitosome biology will remain unknown. This protein is exclusive to *Giardia*; no related sequences have been found in *S. salmonicida* or in other parasitic or free-living metamonads.

Due to the presence of Tom40 in the outer mitosomal membrane, the occurrence of Sam50 was expected (54). Sam50 is an essential component of the SAM complex, the β-barrel protein folding machine (55) that is considered an important evolutionary feature linking mitochondria to Gram-negative bacteria (56). Despite the omnipresence of Sam50 in eukaryotes, no ortholog has been identified in the *Giardia* genome (18) or among the proteins that copurified with *Gi*Tom40 or *Gi*MOMP35 in the present work. Surprisingly, while missing in the *G. intestinalis* and *S. salmonicida* genomes, Sam50 orthologs are present in the expressed sequence tag (EST) data of *C. membranifera* and *E. cyprinoides* (M. Kolísko and A. J. Roger, unpublished results). This strongly suggests that the unique loss of Sam50 in the evolution of eukaryotes occurred in the common ancestor of diplomonads.

However, 5 of the 13 novel mitosomal proteins seem to be

specific to the outer mitosomal membrane, as these were exclusive to *Gi*Tom40- and *Gi*MOMP35-derived data sets. Further investigation of these proteins may bring more information on the biogenesis of the outer mitosomal membrane as well as on the interaction between the mitosomes and other cellular organelles.

In general, the identification of novel mitosomal proteins, the vast majority of which are specific to *Giardia*, demonstrates that metabolic processes other than the formation of iron-sulfur clusters occur in mitosomes. The presence of a rhodanese ortholog indicates the existence of additional sulfur metabolism at a minimum. In addition, the striking presence of an Mlf1IP ortholog in mitosomes may shed light on the exact function of the protein, for which a precise role has not been assigned in the Metazoa.

In addition to the identification of new proteins, the techniques used in this study enabled us to demonstrate that proteins maintain an unfolded state while traveling to mitosomes post-translationally. However, no sign of mixing of the ER and mitosome lumina was detected. The reported mitosomal localization of *Giardia* Sec20 ortholog indicated that a vesicular transport may play a role in mitosomal protein import (39). Our data on the localization of the endogenous Sec20 (not shown in this work) using specific polyclonal antibody indicate that its mitosomal localization is a result of experimental artifact, a phenomenon often observed for the overexpression of tail-anchored proteins. These results provide new evidence that mitosomal biogenesis follows the same rules as mitochondrial biogenesis despite the absence of some of the core components.

Taken together, the data presented here demonstrate that techniques such as *in vivo* enzymatic tagging are extremely valuable tools to investigate the biology of organelles as small as *Giardia* mitosomes. The identification of *Giardia*-specific proteins also demonstrates that our current concept of mitosomes as highly simplified mitochondria may not entirely reflect the true biology of these organelles. Future studies will likely reveal yet-unknown mitosomal functions.

ACKNOWLEDGMENTS

We thank Veronika Klápštová, Vladimíra Najdrová, and Zuzana Drašnarová for valuable technical assistance.

This work was funded by a grant from the Czech Science Foundation (P305-10-0651), by the European Regional Development Fund to the Biomedicine Center of the Academy of Sciences and Charles University (CZ.1.05/1.1.00/02.0109), and by a grant from Charles University Grant Agency (98214).

REFERENCES

1. **Adam RD.** 2001. Biology of Giardia lamblia. Clin Microbiol Rev **14:**447–475. http://dx.doi.org/10.1128/CMR.14.3.447-475.2001.
2. **Ankarklev J, Jerlström-Hultqvist J, Ringqvist E, Troell K, Svärd SG.** 2010. Behind the smile: cell biology and disease mechanisms of Giardia species. Nat Rev Microbiol **8:**413–422. http://dx.doi.org/10.1038/nrmicro2317.
3. **Hehl AB, Marti M.** 2004. Secretory protein trafficking in Giardia intestinalis. Mol Microbiol **53:**19–28. http://dx.doi.org/10.1111/j.1365-2958.2004.04115.x.
4. **Lanfredi-Rangel A, Attias M, de Carvalho TM, Kattenbach WM, De Souza W.** 1998. The peripheral vesicles of trophozoites of the primitive protozoan Giardia lamblia may correspond to early and late endosomes and to lysosomes. J Struct Biol **123:**225–235. http://dx.doi.org/10.1006/jsbi.1998.4035.
5. **Konrad C, Spycher C, Hehl AB.** 2010. Selective condensation drives partitioning and sequential secretion of cyst wall proteins in differentiating Giardia lamblia. PLoS Pathog **6:**e1000835. http://dx.doi.org/10.1371/journal.ppat.1000835.
6. **Dolezal P, Smíd O, Rada P, Zubácová Z, Bursać D, Suták R, Nebesárová J, Lithgow T, Tachezy J.** 2005. Giardia mitosomes and trichomonad hydrogenosomes share a common mode of protein targeting. Proc Natl Acad Sci U S A **102:**10924–10929. http://dx.doi.org/10.1073/pnas.0500349102.
7. **Jedelský PL, Doležal P, Rada P, Pyrih J, Smíd O, Hrdý I, Sedinová M, Marcinčiková M, Voleman L, Perry AJ, Beltrán NC, Lithgow T, Tachezy J.** 2011. The minimal proteome in the reduced mitochondrion of the parasitic protist Giardia intestinalis. PLoS One **6:**e17285. http://dx.doi.org/10.1371/journal.pone.0017285.
8. **Regoes A, Zourmpanou D, León-Avila G, van der Giezen M, Tovar J, Hehl AB.** 2005. Protein import, replication, and inheritance of a vestigial mitochondrion. J Biol Chem **280:**30557–30563. http://dx.doi.org/10.1074/jbc.M500787200.
9. **Roger AJ, Svärd SG, Tovar J, Clark CG, Smith MW, Gillin FD, Sogin ML.** 1998. A mitochondrial-like chaperonin 60 gene in Giardia lamblia: evidence that diplomonads once harbored an endosymbiont related to the progenitor of mitochondria. Proc Natl Acad Sci U S A **95:**229–234. http://dx.doi.org/10.1073/pnas.95.1.229.
10. **Tachezy J, Sánchez LB, Müller M.** 2001. Mitochondrial type iron-sulfur cluster assembly in the amitochondriate eukaryotes Trichomonas vaginalis and Giardia intestinalis, as indicated by the phylogeny of IscS. Mol Biol Evol **18:**1919–1928. http://dx.doi.org/10.1093/oxfordjournals.molbev.a003732.
11. **Likic VA, Dolezal P, Celik N, Dagley M, Lithgow T.** 2010. Using hidden markov models to discover new protein transport machines. Methods Mol Biol **619:**271–284. http://dx.doi.org/10.1007/978-1-60327-412-8_16.
12. **Sickmann A, Reinders J, Wagner Y, Joppich C, Zahedi R, Meyer HE, Schönfisch B, Perschil I, Chacinska A, Guiard B, Rehling P, Pfanner N, Meisinger C.** 2003. The proteome of Saccharomyces cerevisiae mitochondria. Proc Natl Acad Sci U S A **100:**13207–13212. http://dx.doi.org/10.1073/pnas.2135385100.
13. **Schneider RE, Brown MT, Shiflett AM, Dyall SD, Hayes RD, Xie Y, Loo JA, Johnson PJ.** 2011. The Trichomonas vaginalis hydrogenosome proteome is highly reduced relative to mitochondria, yet complex compared with mitosomes. Int J Parasitol **41:**1421–1434. http://dx.doi.org/10.1016/j.ijpara.2011.10.001.
14. **Panigrahi AK, Ogata Y, Zíková A, Anupama A, Dalley RA, Acestor N, Myler PJ, Stuart KD.** 2009. A comprehensive analysis of Trypanosoma brucei mitochondrial proteome. Proteomics **9:**434–450. http://dx.doi.org/10.1002/pmic.200800477.
15. **Wampfler PB, Tosevski V, Nanni P, Spycher C, Hehl AB.** 2014. Proteomics of secretory and endocytic organelles in Giardia lamblia. PLoS One **9:**e94089. http://dx.doi.org/10.1371/journal.pone.0094089.
16. **Keister DB.** 1983. Axenic culture of Giardia lamblia in TYI-S-33 medium supplemented with bile. Trans R Soc Trop Med Hyg **77:**487–488. http://dx.doi.org/10.1016/0035-9203(83)90120-7.
17. **Martincová E, Voleman L, Najdrová V, De Napoli M, Eshar S, Gualdron M, Hopp CS, Sanin DE, Tembo DL, Van Tyne D, Walker D, Marcinčiková M, Tachezy J, Doležal P.** 2012. Live imaging of mitosomes and hydrogenosomes by HaloTag technology. PLoS One **7:**e36314. http://dx.doi.org/10.1371/journal.pone.0036314.
18. **Dagley MJ, Dolezal P, Likic VA, Smid O, Purcell AW, Buchanan SK, Tachezy J, Lithgow T.** 2009. The protein import channel in the outer mitosomal membrane of Giardia intestinalis. Mol Biol Evol **26:**1941–1947. http://dx.doi.org/10.1093/molbev/msp117.
19. **Howarth M, Takao K, Hayashi Y, Ting AY.** 2005. Targeting quantum dots to surface proteins in living cells with biotin ligase. Proc Natl Acad Sci U S A **102:**7583–7588. http://dx.doi.org/10.1073/pnas.0503125102.
20. **Gehde N, Hinrichs C, Montilla I, Charpian S, Lingelbach K, Przyborski JM.** 2009. Protein unfolding is an essential requirement for transport across the parasitophorous vacuolar membrane of Plasmodium falciparum. Mol Microbiol **71:**613–628. http://dx.doi.org/10.1111/j.1365-2958.2008.06552.x.
21. **Rada P, Doležal P, Jedelský PL, Bursac D, Perry AJ, Šedinová M, Smíšková K, Novotný M, Beltrán NC, Hrdý I, Lithgow T, Tachezy J.** 2011. The core components of organelle biogenesis and membrane transport in the hydrogenosomes of Trichomonas vaginalis. PLoS One **6:**e24428. http://dx.doi.org/10.1371/journal.pone.0024428.
22. **Söding J, Biegert A, Lupas AN.** 2005. The HHpred interactive server for protein homology detection and structure prediction. Nucleic Acids Res **33:**W244–W248. http://dx.doi.org/10.1093/nar/gki408.
23. **Eddy SR.** 2011. Accelerated profile HMM searches. PLoS Comput Biol **7:**e1002195. http://dx.doi.org/10.1371/journal.pcbi.1002195.

24. **Zhang Y.** 2008. I-TASSER server for protein 3D structure prediction. BMC Bioinformatics **9:**40. http://dx.doi.org/10.1186/1471-2105-9-40.
25. **Krogh A, Larsson B, von Heijne G, Sonnhammer EL.** 2001. Predicting transmembrane protein topology with a hidden Markov model: application to complete genomes. J Mol Biol **305:**567–580. http://dx.doi.org/10.1006/jmbi.2000.4315.
26. **Käll L, Krogh A, Sonnhammer ELL.** 2007. Advantages of combined transmembrane topology and signal peptide prediction—the Phobius web server. Nucleic Acids Res **35:**W429–W432. http://dx.doi.org/10.1093/nar/gkm256.
27. **Howarth M, Ting AY.** 2008. Imaging proteins in live mammalian cells with biotin ligase and monovalent streptavidin. Nat Protoc **3:**534–545. http://dx.doi.org/10.1038/nprot.2008.20.
28. **Chacinska A, van der Laan M, Mehnert CS, Guiard B, Mick DU, Hutu DP, Truscott KN, Wiedemann N, Meisinger C, Pfanner N, Rehling P.** 2010. Distinct forms of mitochondrial TOM-TIM supercomplexes define signal-dependent states of preprotein sorting. Mol Cell Biol **30:**307–318. http://dx.doi.org/10.1128/MCB.00749-09.
29. **Tieu Q, Okreglak V, Naylor K, Nunnari J.** 2002. The WD repeat protein, Mdv1p, functions as a molecular adaptor by interacting with Dnm1p and Fis1p during mitochondrial fission. J Cell Biol **158:**445–452. http://dx.doi.org/10.1083/jcb.200205031.
30. **Yoon Y, Krueger EW, Oswald BJ, McNiven MA.** 2003. The mitochondrial protein hFis1 regulates mitochondrial fission in mammalian cells through an interaction with the dynamin-like protein DLP1. Mol Cell Biol **23:**5409–5420. http://dx.doi.org/10.1128/MCB.23.15.5409-5420.2003.
31. **Merlin A, Voos W, Maarse AC, Meijer M, Pfanner N, Rassow J.** 1999. The J-related segment of tim44 is essential for cell viability: a mutant Tim44 remains in the mitochondrial import site, but inefficiently recruits mtHsp70 and impairs protein translocation. J Cell Biol **145:**961–972. http://dx.doi.org/10.1083/jcb.145.5.961.
32. **Ting S-Y, Schilke BA, Hayashi M, Craig EA.** 2014. Architecture of the TIM23 inner mitochondrial translocon and interactions with the matrix import motor. J Biol Chem **289:**28689–28696. http://dx.doi.org/10.1074/jbc.M114.588152.
33. **Brown A, Amunts A, Bai X-C, Sugimoto Y, Edwards PC, Murshudov G, Scheres SHW, Ramakrishnan V.** 2014. Structure of the large ribosomal subunit from human mitochondria. Science **346:**718–722. http://dx.doi.org/10.1126/science.1258026.
34. **Ott M, Prestele M, Bauerschmitt H, Funes S, Bonnefoy N, Herrmann JM.** 2006. Mba1, a membrane-associated ribosome receptor in mitochondria. EMBO J **25:**1603–1610. http://dx.doi.org/10.1038/sj.emboj.7601070.
35. **Lauwaet T, Davids BJ, Torres-Escobar A, Birkeland SR, Cipriano MJ, Preheim SP, Palm D, Svärd SG, McArthur AG, Gillin FD.** 2007. Protein phosphatase 2A plays a crucial role in Giardia lamblia differentiation. Mol Biochem Parasitol **152:**80–89. http://dx.doi.org/10.1016/j.molbiopara.2006.12.001.
36. **Cipollone R, Ascenzi P, Visca P.** 2007. Common themes and variations in the rhodanese superfamily. IUBMB Life **59:**51–59. http://dx.doi.org/10.1080/15216540701206859.
37. **Bonomi F, Pagani S, Cerletti P, Cannella C.** 1977. Rhodanese-mediated sulfur transfer to succinate dehydrogenase. Eur J Biochem **72:**17–24. http://dx.doi.org/10.1111/j.1432-1033.1977.tb11219.x.
38. **Ohno K, Takahashi Y, Hirose F, Inoue YH, Taguchi O, Nishida Y, Matsukage A, Yamaguchi M.** 2000. Characterization of a Drosophila homologue of the human myelodysplasia/myeloid leukemia factor (MLF). Gene **260:**133–143. http://dx.doi.org/10.1016/S0378-1119(00)00447-9.
39. **Elias EV, Quiroga R, Gottig N, Nakanishi H, Nash TE, Neiman A, Lujan HD.** 2008. Characterization of SNAREs determines the absence of a typical Golgi apparatus in the ancient eukaryote Giardia lamblia. J Biol Chem **283:**35996–36010. http://dx.doi.org/10.1074/jbc.M806545200.
40. **Eilers M, Schatz G.** 1986. Binding of a specific ligand inhibits import of a purified precursor protein into mitochondria. Nature **322:**228–232.
41. **Wang CC, Aldritt S.** 1983. Purine salvage networks in Giardia lamblia. J Exp Med **158:**1703–1712. http://dx.doi.org/10.1084/jem.158.5.1703.
42. **van der Giezen M, Tovar J.** 2005. Degenerate mitochondria. EMBO Rep **6:**525–530. http://dx.doi.org/10.1038/sj.embor.7400440.
43. **Clements A, Bursac D, Gatsos X, Perry AJ, Civciristov S, Celik N, Likic VA, Poggio S, Jacobs-Wagner C, Strugnell RA, Lithgow T.** 2009. The reducible complexity of a mitochondrial molecular machine. Proc Natl Acad Sci U S A **106:**15791–15795. http://dx.doi.org/10.1073/pnas.0908264106.
44. **Schey KL, Grey AC, Nicklay JJ.** 2013. Mass spectrometry of membrane proteins: a focus on aquaporins. Biochemistry **52:**3807–3817. http://dx.doi.org/10.1021/bi301604j.
45. **Xu F, Jerlström-Hultqvist J, Einarsson E, Astvaldsson A, Svärd SG, Andersson JO.** 2014. The genome of Spironucleus salmonicida highlights a fish pathogen adapted to fluctuating environments. PLoS Genet **10:**e1004053. http://dx.doi.org/10.1371/journal.pgen.1004053.
46. **Dolezal P, Dagley MJ, Kono M, Wolynec P, Likić VA, Foo JH, Sedinová M, Tachezy J, Bachmann A, Bruchhaus I, Lithgow T.** 2010. The essentials of protein import in the degenerate mitochondrion of Entamoeba histolytica. PLoS Pathog **6:**e1000812. http://dx.doi.org/10.1371/journal.ppat.1000812.
47. **Waller RF, Jabbour C, Chan NC, Celik N, Likic VA, Mulhern TD, Lithgow T.** 2009. Evidence of a reduced and modified mitochondrial protein import apparatus in microsporidian mitosomes. Eukaryot Cell **8:**19–26. http://dx.doi.org/10.1128/EC.00313-08.
48. **Handa N, Kishishita S, Morita S, Akasaka R, Jin Z, Chrzas J, Chen L, Liu Z-J, Wang B-C, Sugano S, Tanaka A, Terada T, Shirouzu M, Yokoyama S.** 2007. Structure of the human Tim44 C-terminal domain in complex with pentaethylene glycol: ligand-bound form. Acta Crystallogr D Biol Crystallogr **63:**1225–1234. http://dx.doi.org/10.1107/S0907444907051463.
49. **Zarsky V, Tachezy J, Dolezal P.** 2012. Tom40 is likely common to all mitochondria. Curr Biol **22:**R479–R481; author reply, R481–R482. http://dx.doi.org/10.1016/j.cub.2012.03.057.
50. **Baker KP, Schaniel A, Vestweber D, Schatz G.** 1990. A yeast mitochondrial outer membrane protein essential for protein import and cell viability. Nature **348:**605–609. http://dx.doi.org/10.1038/348605a0.
51. **Yamano K, Tanaka-Yamano S, Endo T.** 2010. Mdm10 as a dynamic constituent of the TOB/SAM complex directs coordinated assembly of Tom40. EMBO Rep **11:**187–193. http://dx.doi.org/10.1038/embor.2009.283.
52. **Yano M, Kanazawa M, Terada K, Namchai C, Yamaizumi M, Hanson B, Hoogenraad N, Mori M.** 1997. Visualization of mitochondrial protein import in cultured mammalian cells with green fluorescent protein and effects of overexpression of the human import receptor Tom20. J Biol Chem **272:**8459–8465. http://dx.doi.org/10.1074/jbc.272.13.8459.
53. **Rojo M, Legros F, Chateau D, Lombès A.** 2002. Membrane topology and mitochondrial targeting of mitofusins, ubiquitous mammalian homologs of the transmembrane GTPase Fzo. J Cell Sci **115:**1663–1674.
54. **Dolezal P, Likic V, Tachezy J, Lithgow T.** 2006. Evolution of the molecular machines for protein import into mitochondria. Science **313:**314–318. http://dx.doi.org/10.1126/science.1127895.
55. **Kozjak V, Wiedemann N, Milenkovic D, Lohaus C, Meyer HE, Guiard B, Meisinger C, Pfanner N.** 2003. An essential role of Sam50 in the protein sorting and assembly machinery of the mitochondrial outer membrane. J Biol Chem **278:**48520–48523. http://dx.doi.org/10.1074/jbc.C300442200.
56. **Gentle I, Gabriel K, Beech P, Waller R, Lithgow T.** 2004. The Omp85 family of proteins is essential for outer membrane biogenesis in mitochondria and bacteria. J Cell Biol **164:**19–24. http://dx.doi.org/10.1083/jcb.200310092.
57. **Josyula R, Jin Z, Fu Z, Sha B.** 2006. Crystal structure of yeast mitochondrial peripheral membrane protein Tim44p C-terminal domain. J Mol Biol **359:**798–804. http://dx.doi.org/10.1016/j.jmb.2006.04.020.
58. **Biasini M, Bienert S, Waterhouse A, Arnold K, Studer G, Schmidt T, Kiefer F, Cassarino TG, Bertoni M, Bordoli L, Schwede T.** 2014. SWISS-MODEL: modelling protein tertiary and quaternary structure using evolutionary information. Nucleic Acids Res **42:**W252–W258. http://dx.doi.org/10.1093/nar/gku340.

EC
Journals.ASM.org

Giardia intestinalis Incorporates Heme into Cytosolic Cytochrome b_5

Jan Pyrih,[a] Karel Harant,[b] Eva Martincová,[a] Robert Sutak,[a] Emmanuel Lesuisse,[c] Ivan Hrdý,[a] Jan Tachezy[a]

Department of Parasitology, Faculty of Science, Charles University in Prague, Prague, Czech Republic[a]; Department of Genetics and Microbiology, Faculty of Science, Charles University in Prague, Prague, Czech Republic[b]; Laboratoire Mitochondries, Métaux et Stress Oxydant, Institut Jacques Monod, UMR 7592 CNRS-Université Paris-Diderot, Paris, France[c]

The anaerobic intestinal pathogen *Giardia intestinalis* does not possess enzymes for heme synthesis, and it also lacks the typical set of hemoproteins that are involved in mitochondrial respiration and cellular oxygen stress management. Nevertheless, *G. intestinalis* may require heme for the function of particular hemoproteins, such as cytochrome b_5 (cytb_5). We have analyzed the sequences of eukaryotic cytb_5 proteins and identified three distinct cytb_5 groups: group I, which consists of C-tail membrane-anchored cytb_5 proteins; group II, which includes soluble cytb_5 proteins; and group III, which comprises the fungal cytb_5 proteins. The majority of eukaryotes possess both group I and II cytb_5 proteins, whereas three *Giardia* paralogs belong to group II. We have identified a fourth *Giardia* cytb_5 paralog (gCYTb5-IV) that is rather divergent and possesses an unusual 134-residue N-terminal extension. Recombinant *Giardia* cytb_5 proteins, including gCYTb5-IV, were expressed in *Escherichia coli* and exhibited characteristic UV-visible spectra that corresponded to heme-loaded cytb_5 proteins. The expression of the recombinant gCYTb5-IV in *G. intestinalis* resulted in the increased import of extracellular heme and its incorporation into the protein, whereas this effect was not observed when gCYTb5-IV containing a mutated heme-binding site was expressed. The electrons for *Giardia* cytb_5 proteins may be provided by the NADPH-dependent Tah18-like oxidoreductase GiOR-1. Therefore, GiOR-1 and cytb_5 may constitute a novel redox system in *G. intestinalis*. To our knowledge, *G. intestinalis* is the first anaerobic eukaryote in which the presence of heme has been directly demonstrated.

Heme, an iron-coordinating porphyrin, serves as a prosthetic group for hemoproteins that are involved in a number of vital functions, such as carrying diatomic gases, participating in electron transport in the mitochondrial respiratory chain, and providing defense against oxidative and nitrosative stress (1, 2). To fulfill their heme requirements, a vast majority of organisms possess a heme biosynthetic pathway that converts δ-aminolevulinic acid to heme in seven consecutive steps, which are conserved in all domains of life. Eukaryotes partially inherited this pathway from the bacterial predecessor of mitochondria and partially retained the original preeukaryotic system (3). The loss of the pathway in some organisms is typically associated with the evolution of a mechanism to acquire heme from exogenous sources, such as feeding on bacteria by *Caenorhabditis elegans* or free-living bodonids (4, 5) or parasitic lifestyles for blood-sucking ticks and trypanosomes (4, 6). An additional group of organisms devoid of heme synthesis is parasitic protists that are adapted for life in anaerobic or oxygen-poor environments. These organisms include intestinal parasites, such as *Giardia*, *Entamoeba*, *Cryptosporidium*, and *Blastocystis*, and urogenital tract parasites, such as *Trichomonas*. They all possess highly reduced forms of mitochondria, such as mitosomes or hydrogenosomes, that have lost the majority of their mitochondrial functions, including heme-dependent respiratory complexes (7, 8). In addition, common hemoproteins (oxidases, catalases, and hydrolases) that are involved in oxidative-stress management in aerobes are replaced by different protective enzymes that were likely acquired by the anaerobic protists through lateral gene transfer from anaerobic bacteria. These enzymes include flavodiiron protein, hydroperoxide reductase, rubrerythrin, and NADH oxidase (9–11). The anaerobic protists were previously hypothesized to live entirely without heme (12), which may be true for *Entamoeba histolytica*, because no gene encoding any hemoprotein has been identified in the *Entamoeba* genome. However, genome analyses of all other anaerobic parasites have revealed that they retain several genes encoding hemoproteins, which are most frequently members of the cytochrome b_5 (cytb_5) family (13).

The archetypal cytb_5 is a small acidic membrane protein consisting of two domains, an amino-terminal hydrophilic heme-binding domain and a carboxy-terminal domain consisting of hydrophobic residues (transmembrane segment) that is followed by positively charged residues at the carboxy terminus. The carboxy-terminal domain, which is a C-tail anchor, facilitates post-translational targeting and integration of cytb_5 into the membranes of various organelles, such as the endoplasmic reticulum and the outer membrane of mitochondria. The charged C terminus is typically present in the organellar matrix or intermembrane space of mitochondria, whereas the heme-binding domain faces the cytosol. The heme is inserted into the hydrophobic pocket of the N-terminal cytb_5 domain, which contains two invariable histidines, H44 and H68 (numbered according to the human cytb_5 [accession number P00167]), that coordinate the heme iron (14). H44 lies within the highly conserved HPGG motif, which is surrounded by several acidic residues. These residues have been implicated in the redox potential of cytb_5 (15). cytb_5 is a multifunctional protein that acts as an electron carrier in several oxidative reactions between reductases, such as NADH-cytochrome b_5 reductase and NADPH-cytochrome P450 reductase, and various

Received 29 August 2013 **Accepted** 22 November 2013
Published ahead of print 2 December 2013
Address correspondence to Jan Tachezy, tachezy@natur.cuni.cz.
Supplemental material for this article may be found at http://dx.doi.org/10.1128/EC.00200-13.

doi:10.1128/EC.00200-13

oxidases and fatty acid desaturases that are involved in lipid and cholesterol biosynthesis (16, 17). Additionally, cytb_5 is a component of various fusion enzymes (18, 19). However, the function of cytb_5 in anaerobic protists and its possible partners for electron transfer are unknown.

Giardia intestinalis, one of the most important intestinal pathogens, possesses two types of heme-binding proteins, a flavohemoglobin (gFLHb) (20) and cytb_5 (15). Recombinant gFLHb binds heme and flavin and exhibits NADH and NADPH oxidase activity. This activity is stimulated *in vitro* by the addition of the nitric oxide donor diethylammonium (Z)-1-(*N*,*N*-diethylamino) diazen-1-ium-1,2-diolate (diethylamine NONOate), which suggests that gFLHb may play a role in protecting *Giardia* against oxygen and nitric oxide (20). cytb_5 is encoded in *Giardia* by three paralogous genes, *gCYTb5-I*, *gCYTb5-II*, and *gCYTb5-III*. Recombinant gCYTb5-I that was expressed in *Escherichia coli* exhibited spectroscopic and electrochemical properties of heme-loaded cytb_5. Interestingly, the conserved heme-binding domains of all three gCYTb5 proteins are flanked by unconventional, highly charged N- and C-terminal sequences. Although these sequences are decisive for protein targeting to subcellular compartments, the localization of gCYTb5 in *Giardia* remains unclear. The ability of recombinant gCYTb5-I and gFLHb to bind heme in *E. coli* strongly suggests that functional heme-binding proteins may also exist in *Giardia*. However, direct evidence for the incorporation of heme into target proteins in an anaerobic protist has not yet been demonstrated.

Here, we investigated the cytb_5 proteins in *G. intestinalis* to determine (i) whether the unusual structure of gCYTb5 proteins is unique to *Giardia* or whether these proteins represent a distinct branch of the cytb_5 family of proteins, (ii) the cellular localization of these cytb_5 proteins, (iii) whether the parasite can incorporate exogenous heme into hemoproteins *in situ*, and (iv) whether *Giardia* possesses suitable redox partners that can reduce the cytb_5 proteins. We found that, in addition to the known gCYTb5 proteins, *Giardia* possesses an additional cytb_5-like protein that contains a long C-terminal extension (gCYTb5-IV) and a heme-binding domain. We demonstrate that this protein efficiently binds heme when *Giardia* cells are cultured in the presence of hemin and that functional gCYTb5-IV can be reduced by electrons that are provided by the recently identified diflavin oxidoreductase GiOR-1 (7). All *Giardia* cytb_5 paralogs appear to belong to a novel group of soluble cytosolic cytb_5 proteins that are ubiquitous in eukaryotes.

MATERIALS AND METHODS

Cell cultivation:. *G. intestinalis* cells (strain WB; ATCC 30975) were grown in TYI-S-33 medium supplemented with 10% heat-inactivated bovine serum (PAA Laboratories GmbH, Austria) and 0.1% bovine bile (Sigma) (21). For the determination of the heme content of *G. intestinalis*, the cells were cultured in TYI-S-33 medium supplemented with 4 μM hemin (Fluka).

Selectable transformation of *G. intestinalis*. The genes encoding the *Giardia* cytb_5 proteins (GiardiaDB accession numbers GL50803_9089, GL50803_27747, GL50803_33870, and GL50803_2972) were amplified using PCR and inserted into the plasmid pTG3039 (a kind gift from Frances D. Gillin, San Diego, CA) (22), which was modified for the expression of proteins that contain N-terminal hemagglutinin (HA) tags. The cells were transformed and selected as previously described (23).

Immunofluorescence microscopy. *G. intestinalis* cells were fixed with 1% formaldehyde as previously described (24) and stained for immunofluorescence microscopy using a rat monoclonal anti-HA antibody (Roche), a rabbit polyclonal TOM40 antibody (25), and an anti-PDI-2 (protein disulfide isomerase 2) antibody (a kind gift from Adrian B. Hehl) (26). Alexa Fluor 488 (green) donkey anti-mouse and anti-rabbit antibodies and Alexa Fluor 594 (red) donkey anti-rat antibody (all from Invitrogen) were used as the secondary antibodies. The slides were examined using an Olympus IX81 microscope equipped with an MT20 illumination system. The images were processed using ImageJ 1.41e software (NIH).

Preparation of subcellular fractions and immunoblot analysis. *Giardia* trophozoites were harvested, washed twice in phosphate-buffered saline (PBS), pH 7.4, and resuspended in SM buffer (250 mM sucrose and 20 mM MOPS [morpholinepropanesulfonic acid], pH 7.2) containing protease inhibitors (Complete EDTA-free Protease Inhibitor Cocktail; Roche). The cells were disrupted by sonication using approximately 15 1-s pulses at an amplitude of 40 (Bioblock Scientific Vibra-Cell 72405) and centrifuged twice at 1,000 × *g* for 10 min each time to remove any undisrupted cells. The supernatant was centrifuged at 50,000 × *g* for 30 min to obtain the organellar fraction (sediment). The high-speed supernatant that was obtained after an additional centrifugation at 200,000 × *g* for 30 min was used as the cytosolic fraction.

The cell fractionation samples were separated by SDS-13.5% PAGE and transferred to a nitrocellulose membrane. The HA-tagged proteins were detected using a rat monoclonal anti-HA antibody (Roche). Enolase, which is a cytosolic marker protein, was detected using a rabbit polyclonal antibody against *Trypanosoma brucei* enolase (a kind gift from Julius Lukes, Ceske Budejovice, Czech Republic) (27).

Protein expression and purification. The genes encoding gCYTb5-I to -IV and the mutant gCYTb5-IVH_{178}L, in which histidine 178 was replaced with leucine, were inserted into the pET42b (Qiagen) vector for the expression of the recombinant proteins containing a C-terminal hexahistidine tag in *E. coli*. Protein purification was performed under native conditions using Ni-nitrilotriacetic acid affinity chromatography according to the manufacturer's instructions (Qiagen GmbH, Hilden, Germany). The PCR fragment corresponding to gCYTb5-IVH_{178}L was amplified using two-step PCR and primers described in Table S1 in the supplemental material.

Determination of the heme content of *G. intestinalis*. The heme content of *G. intestinalis* was determined in wild-type (wt) cells and cells expressing gCYTb5-IV and gCYTb5-IVH_{178}L. The cells were cultured for 72 h in medium in the presence or absence of 4 μM hemin. Subsequently, approximately 4 × 10^8 cells were harvested and washed twice with sterile cold PBS. The high-speed cellular fraction (cytosol) was obtained as previously described and concentrated using Amicon Ultra Centrifugal Filters with Ultracel 30-kDa membrane filters (Millipore) to a final protein concentration of approximately 25 μg/μl. Heme extraction was performed as described previously (28). Briefly, 200 μl of 1% HCl in acetone was added to 50 μl of each sample, rigorously mixed, and centrifuged at 4,000 × *g* for 10 min at room temperature. The supernatant was collected, and the sediment was reextracted in 30 μl of HCl-acetone. The concentrations of heme were immediately determined by high-performance liquid chromatography (HPLC) (UltiMate 3000 RSLC; Dionex; DAD diode array detector) using a C_{18} (Acclaim 120 C_{18}; 3 μm; 120 Å; 4.6 by 150 mm; Dionex) reverse-phase column and absorbance detection at 400 nm, as previously described (28, 29). The linear gradient from 60% to 40% (vol/vol) solvent A-solvent B to 100% solvent B was run for 11 min using solvents A (56 mM ammonium phosphate in 40% methanol) and B (methanol) at a flow rate of 1.2 ml/min. Then, 100% solvent B was maintained for another 6.5 min. The column was restored to the original conditions over 2 min and maintained under these conditions for another 6 min.

UV-visible spectroscopy. The UV-visible spectra of the freshly purified gCYTb5 proteins in 50 mM NaH_2PO_4 and 300 mM NaCl, pH 8.0, were recorded at room temperature between 260 and 700 nm using a Shimadzu UV-1601 spectrophotometer. The low-temperature visible

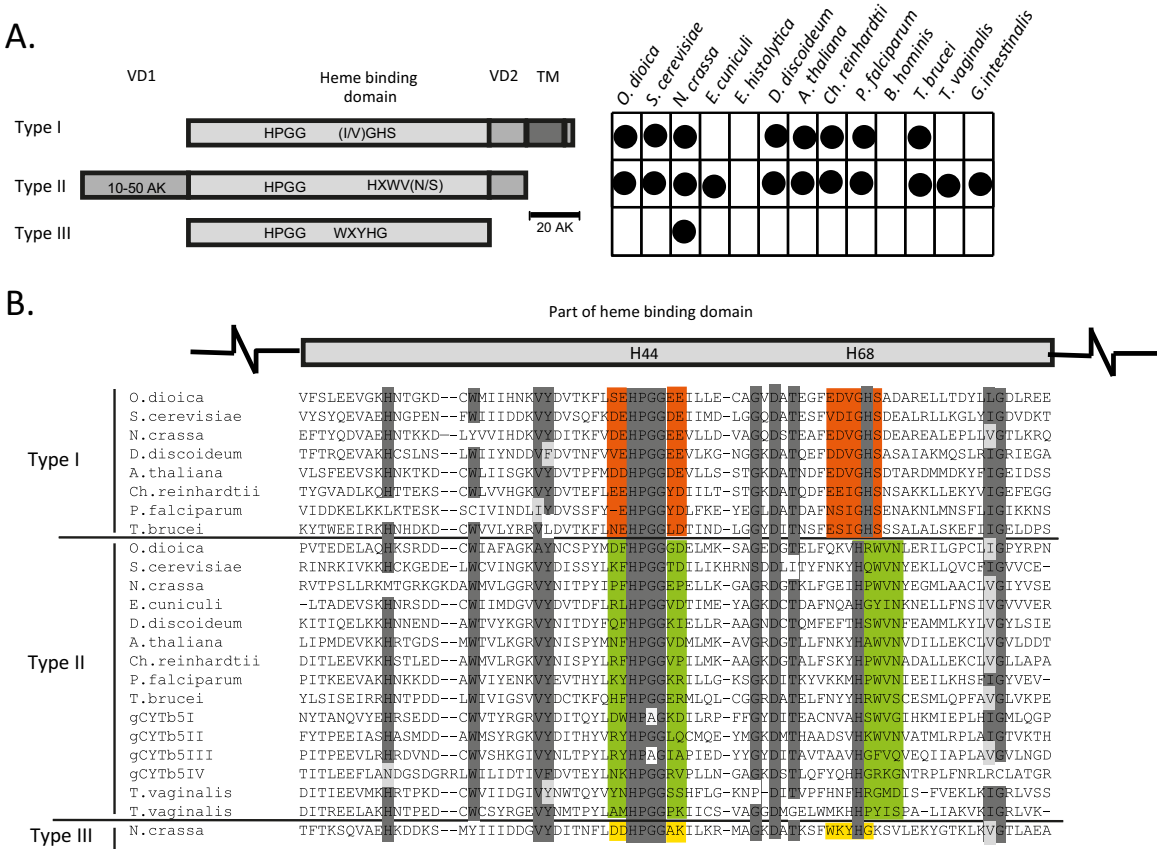

FIG 1 The three groups of cytb_5 proteins. (A) Schematic representation of the structural differences between the canonical group I cytb_5, group II soluble cytb_5, and fungal group III cytb_5 proteins. The chart indicates the distribution of cytochromes in representative eukaryotes. VD, variable domain; TM, transmembrane domain. *O. dioica*, *Oikopleura dioica*; *S. cerevisiae*, *Saccharomyces cerevisiae*; *N. crassa*, *Neurospora crassa*; *E. cuniculi*, *Encephalitozoon cuniculi*; *D. discoideum*, *Dictyostelium discoideum*; *A. thaliana*, *Arabidopsis thaliana*; *Ch. reinhardtii*, *Chlamydomonas reinhardtii*; *P. falciparum*, *Plasmodium falciparum*. (B) Alignment of partial heme-binding domains. The two histidine residues that are critical for heme iron coordination are highlighted in the schematic above the alignment. Highly conserved regions are shaded in dark gray, and similar amino acids in conserved regions are shaded in light gray. Red, green, and yellow highlight typical motifs for each type of cytb_5.

spectrum of whole cells was measured as previously described (30) using a Varian Cary 4000 spectrophotometer.

GiOR-1-dependent reduction of the gCYTb5 proteins. Recombinant GiOR-1 was prepared as previously described (7). The cytochrome reductase activity of GiOR-1 was spectrophotometrically assayed at 550 nm. The reaction mixture consisted of the gCYTb5 protein, GiOR-1, and NADPH (0.25 mM) in phosphate buffer (100 mM KH_2PO_4-KOH and 150 mM NaCl, pH 7.4). The reaction proceeded in anaerobic cuvettes under a nitrogen atmosphere at 25°C. The spectra were recorded using a Shimadzu UV-1601 spectrophotometer. The protein concentration was determined according to the Bradford method.

Bioinformatics analysis. The cytb_5 protein sequences were retrieved using protein BLAST searches (31) against a nonredundant GenBank protein database. The sequences were aligned using the ClustalX program (32). Columns with more than 25% gaps were stripped out. The final alignment retained 102 taxa and 68 sites. Phylogenetic analysis was performed using the WAG model with PhyML 3.0 (33). Support values are shown next to the branches as the maximum-likelihood bootstrap support (WAG model; PhyML).

RESULTS

Cytochrome b_5-like proteins in *Giardia*. *Giardia* cytb_5 gCYTb5-I (GL50803_9089) was used for BLAST searches in the GiardiaDB database to identify paralogous genes. The searches identified two other cytb_5-encoding genes that were previously reported as gCYTb5-II (GL50803_27747) and gCYTb5-III (GL50803_33870). In addition, we identified two cytb_5-like proteins named gCYTb5-IV (GL50803_2972) and GiTax (GL50803_17116).

An alignment of the *Giardia* proteins with eukaryotic orthologs revealed that cytb_5 forms three groups based on the primary structure of the heme-binding domain (Fig. 1; see Fig. S1 in the supplemental material). This domain includes the N-terminal (H44) and C-terminal (H68) histidines, which are two heme iron ligands. In all of the cytb_5 proteins, H44 is highly conserved within the HPGG motif. Group I represents canonical cytb_5 proteins that possess a HPGG motif that is surrounded by acidic residues (E and D), and H68 is flanked by the small amino acids glycine and serine (GHS). The group I cytb_5 proteins typically contain a C-terminal hydrophobic tail sequence (30 to 40 residues) that allows cytb_5 to attach to the cytosolic face of the endoplasmic reticulum or mitochondria (34). The C-tail anchor is connected to the heme-binding domain by a short variable domain of approximately 15 to 20 residues. In the group II cytb_5 proteins, the HPGG motif is not surrounded by acidic residues, and H68 lies within the distinct HXWV(N/S) motif. These proteins lack a C-tail anchor; however, they possess an N-terminal variable extension of approximately 10

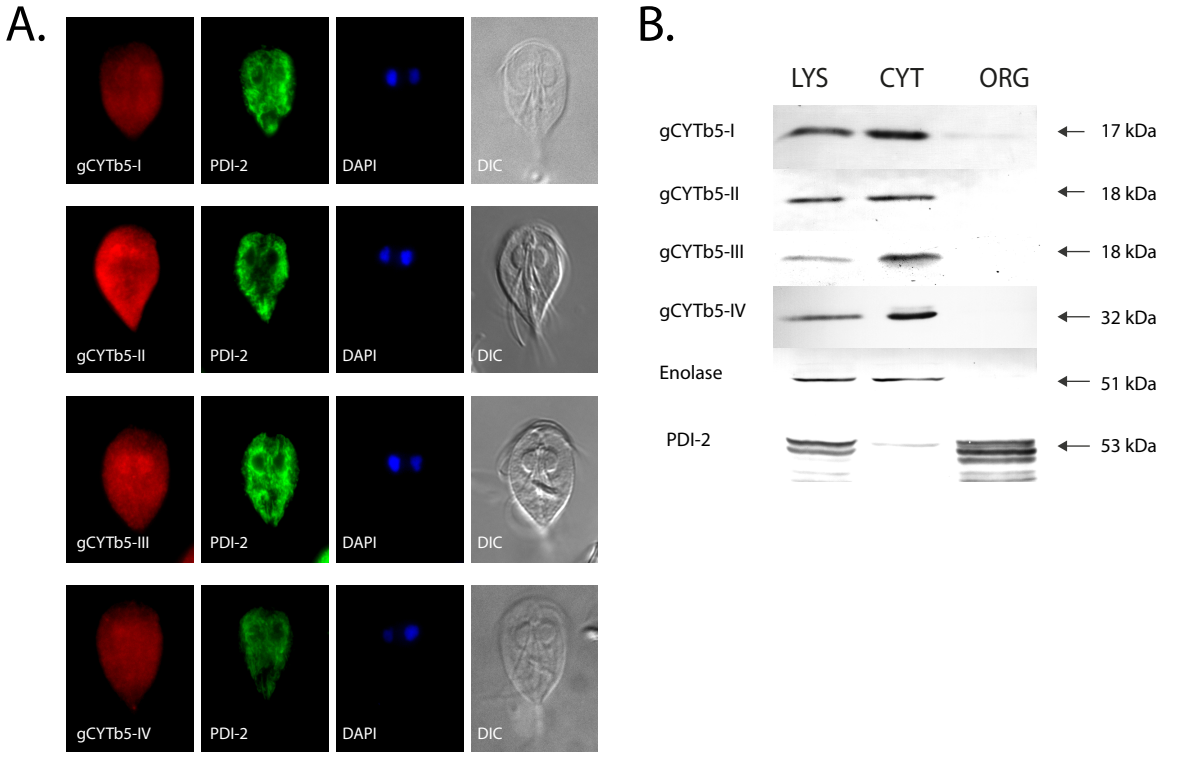

FIG 2 Localization of gCYTb5 proteins in *Giardia*. (A) The cytosolic localization of gCYTb5-I to -IV visualized using immunofluorescence microscopy. The gCYTb5 proteins were visualized using rat anti-HA tag and anti-rat Alexa Fluor 594 (red) antibodies. PDI-2 was detected using mouse anti-PDI-2 and anti-mouse Alexa Fluor 488 (green) antibodies. The nuclei were stained with DAPI (4′,6-diamidino-2-phenylindole) (blue). DIC, differential interference contrast. (B) Localization of gCYTb5 in subcellular fractions of *Giardia* using immunoblot analysis. LYS, cell lysate; CYT, cytoplasm; ORG, organellar fraction; Enolase, a cytosolic marker protein; PDI-2, an endoplasmic reticulum marker protein.

to 50 residues (Fig. 1). The group III cytb_5 proteins are short and lack both C- and N-terminal extensions. These proteins possess a unique conserved motif flanking H68 (WXYHG), and the HPGG motif is surrounded by acidic and basic residues at the N- and C-terminal sites, respectively (Fig. 1). The vast majority of eukaryotes appear to possess members of both group I and group II cytb_5 proteins, whereas group III cytb_5 proteins are present only in certain fungi (Fig. 1). Interestingly, *G. intestinalis* and *Trichomonas vaginalis* lack the canonical C-tail-anchored cytb_5, and cytb_5 proteins were not found in the parasitic protists *E. histolytica* and *Blastocystis hominis*.

The three *Giardia* cytochromes gCYTb5-I, -II, and -III exhibit characteristics of group II cytb_5 proteins, although gCYTb5-I and -III contain an alanine instead of a glycine at position 67. However, gCYTb5-IV appears to differ from the other *Giardia* cytb_5 proteins in several respects. Although gCYTb5-IV lacks acidic residues surrounding the HPGG motif, which is characteristic of group II cytb_5 proteins, two histidines are present at positions 67 and 68, and the protein lacks the conserved WV(N/S) residues. This double-histidine motif has been observed only in the cytb_5 of *T. vaginalis*. Additionally, gCYTb5-IV possesses a long N-terminal extension of 134 residues. However, an analysis of this extension using motif/domain search tools in the Pfam 27.0 and PROSITE 20.91 databases did not identify any known structure. Based on a phylogenetic reconstruction and according to the similarity of the key residues in proximity to both histidine binding motifs, gCYTb5-IV may represent a highly divergent member of group II cytb_5 proteins (Fig. 1; see Fig. S1 in the supplemental material). The cytb_5-like protein GiTax appears to be an ortholog of the *T. brucei* axonemal protein TAX-2, which is important for flagellar function (35). This protein represents a highly divergent cytb_5 protein that has lost both its conserved heme iron-coordinating histidine ligands. Therefore, we excluded the protein from further analysis.

Giardia gCYTb5 proteins are soluble cytosolic proteins. To determine the cellular localization of the *Giardia* cytb_5 proteins, all of the gCYTb5 genes were subcloned into expression vectors that were used for *G. intestinalis* transformation. To avoid any possible interference from the membrane-targeting signal that is located in the C-terminal portion of the membrane-associated cytb_5 (35, 36), we overexpressed these proteins in *Giardia* using a hemagglutinin tag located at the N terminus. Immunofluorescence microscopy of the HA-tagged gCYTb5-I to -IV revealed that all of the proteins are present in the cytosol, in addition to minor localization in the nuclei (Fig. 2A). All of the cells were additionally stained with the anti-PDI-2 antibody to confirm that the fluorescence of cytb_5 is distinct from that of the endoplasmic reticulum. The cytosolic localization of gCYTb5-I to -IV was confirmed by immunoblot analysis of the subcellular fractions (Fig. 2B) using enolase as a cytosolic marker protein. Because the PSORT II program (http://psort.hgc.jp/form2.html) identified a putative N-terminal cleavable mitochondrial targeting sequence in the gCYTb5-II and -III proteins, we additionally expressed these proteins with a C-terminal hemagglutinin tag in *G. intestinalis*. However, the two C-terminally tagged proteins demonstrated cytosolic

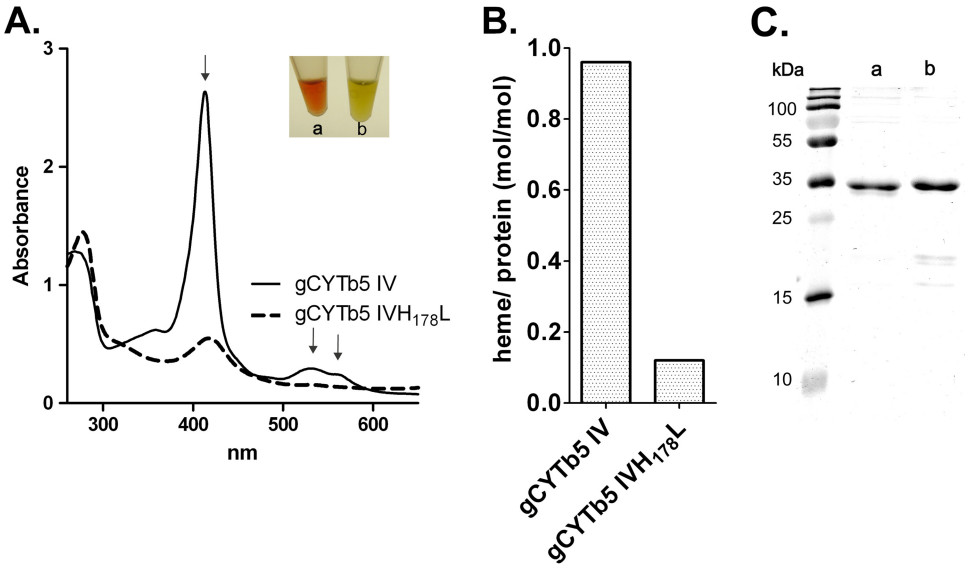

FIG 3 gCYTb5-IV coordinates heme. (A) UV-visible spectrum of recombinant gCYTb5-IV compared with that of the gCYTb5-IVH$_{178}$L mutant. The arrows indicate characteristic absorption maxima of oxidized gCYTb5-IV. The inset shows the colors of the purified proteins gCYTb5-IV (a) and gCYTb5-IVH$_{178}$L (b). The 280-nm peaks show that comparable amounts of proteins were used. (B) Determination of the heme contents in gCYTb5-IV and gCYTb5-IVH$_{178}$L using HPLC. (C) Purity of recombinant gCYTb5-IV (a) and gCYTb5-IVH$_{178}$L (b) tested by SDS-PAGE analysis using 13.5% gel. The proteins were stained with Coomassie brilliant blue.

localizations identical to those of the N-terminally tagged proteins (see Fig. S2 in the supplemental material). The cytosolic localization of the group II gCYTb5-I to -IV proteins is consistent with the absence of a C-tail hydrophobic anchor in these proteins.

Recombinant gCYTb5 proteins bind heme. The unorthodox structure of gCYTb5-IV, including the unusual motif surrounding H68, prompted us to determine whether gCYTb5-IV coordinates heme. As a positive control, we included gCYTb5-I, which was previously shown to bind heme, and we additionally characterized the paralogs gCYTb5-II and gCYTb5-III. All of the proteins were expressed with a C-terminal polyhistidine tag in *E. coli*, using the pET42b vector, and were isolated under native conditions. The presence of a heme cofactor was determined using UV-visible spectroscopy and HPLC analysis. All of the isolated proteins displayed the characteristic strong absorption at 413 nm and two absorption peaks at 529 and 563 nm. A typical spectrum for gCYTb5-IV is shown in Fig. 3A. Additionally, we expressed a mutant of gCYTb5-IV in which the histidine residue in the HPGG motif was replaced by leucine (gCYTb5-IVH$_{178}$L) (Fig. 3A). As expected, we observed a dramatic decrease (8-fold) in the heme-binding ability of the mutant (Fig. 3B; see Fig. S3 in the supplemental material).

gCYTb5 is reduced by the NADPH-dependent oxidoreductase GiOR-1. *G. intestinalis* does not contain genes encoding the typical cytb_5 partners, such as cytb_5 reductase or cytochrome P450 reductase, which deliver electrons for cytb_5 reduction (13). However, *G. intestinalis* does possess the oxidoreductase GiOR-1, which contains a flavodoxin-like flavin mononucleotide (FMN)-binding domain that is connected to a cytochrome P450 reductase-like domain, including a flavin adenine dinucleotide (FAD)-binding pocket and an NADP(H)-binding site (7). Therefore, we determined whether GiOR-1 is able to reduce the gCYTb5 proteins. Indeed, GiOR-1 reduced the *Giardia* cytochrome b_5 I, III, and IV proteins (gCYTb5-II was not evaluated) in the presence of NADPH, which was observed as a shift of the electronic absorption band from 413 to 426 nm and the appearance of sharp α and β bands at 559 and 529 nm. A representative spectrum of GiOR-1 reduction of gCYTb5 is shown for gCYTb5-IV in Fig. 4.

Heme is present in *G. intestinalis*. To provide direct evidence that *G. intestinalis* contains the heme cofactor, we initially attempted to detect the presence of heme in the cytosolic fraction that was isolated from wild-type cells grown in standard culture

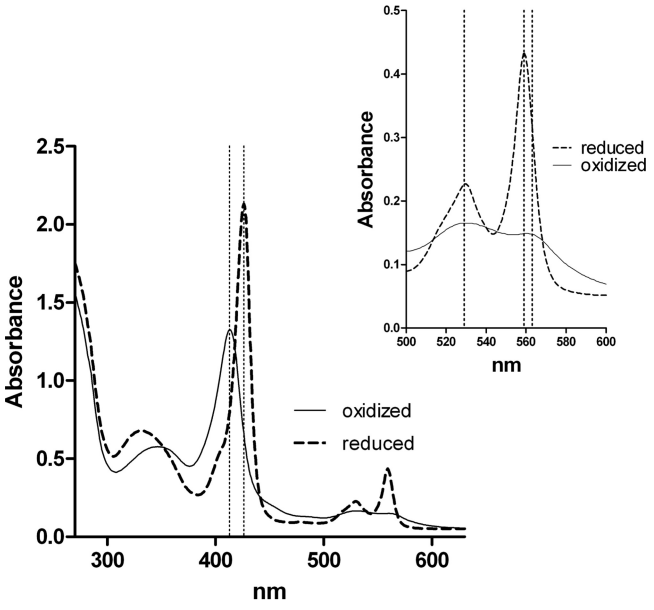

FIG 4 Reduction of gCYTb5-IV by GiOR-1. UV-visible spectra of reduced gCYTb5-IV (dashed lines) were recorded after incubation of oxidized gCYTb5-IV (solid lines) in the presence of NADPH and GiOR-1 for 10 min at 25°C in an anaerobic cuvette. The region between 500 and 600 nm is enlarged in the inset. The wavelengths 413, 426, 529, 559, and 563 nm are indicated by dotted lines.

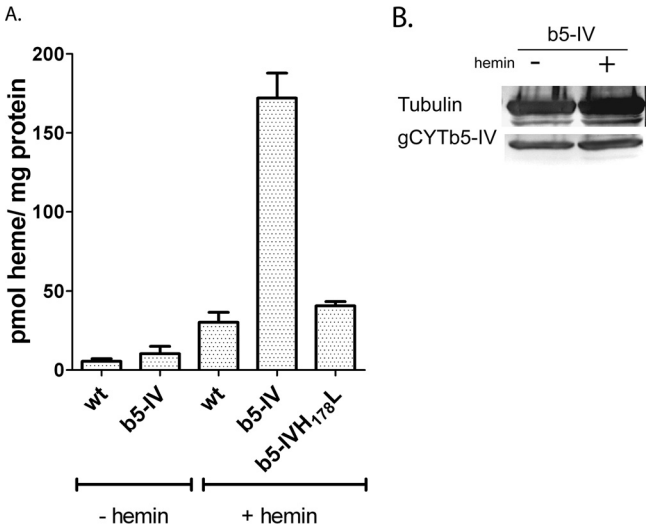

FIG 5 Detection of heme in *G. intestinalis*. (A) The concentration of heme was determined in *Giardia* cytosol using HPLC. The highest heme concentration was found in cells that expressed recombinant gCYTb5-IV (b5-IV) when the cells were cultured in TYI-S-33 medium supplemented with 4 μM hemin (+ hemin). The heme content was significantly lower in the strain harboring the gCYTb5-IVH_{178}L mutant. (B) Western blot analysis indicated comparable levels of recombinant gCYTb5-IV in the lysates of cells cultured in the presence and absence of hemin. An anti-tubulin antibody (TAT-1; Sigma-Aldrich) was used as a loading control. The error bars indicate standard deviations.

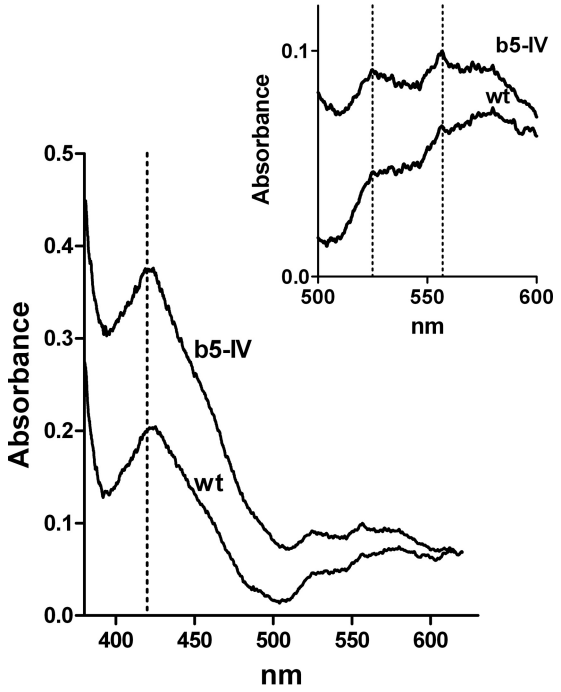

FIG 6 Detection of heme in *G. intestinalis*. A low-temperature visible spectrum of whole-cell lysates was obtained for wild-type cells (wt) and cells expressing the recombinant gCYTb5-IV (b5-IV). The region containing the characteristic absorption maxima for heme-loaded cytb_5 (420, 525, and 557 nm) is enlarged in the inset.

medium. Under these conditions, the amount of detected heme was at the detection limit of our HPLC system (approximately 1 pmol of heme per mg of protein), and we were unable to determine whether the low heme signal was intrinsic to the *Giardia* cells or was due to contamination from the complex culture medium, in which we detected heme at a concentration of 8 nM. Therefore, we compared the amount of endogenous heme in wild-type cells to that found in cells expressing recombinant gCYTb5-IV. The results indicated that the cells expressing gCYTb5-IV contained an approximately 2-fold-larger amount of heme than wild-type cells (Fig. 5A; see Fig. S4 in the supplemental material). Subsequently, we cultured *Giardia* in a medium that was supplemented with 4 μM hemin to increase the availability of heme in the cellular environment. The addition of hemin had no effect on cell growth (see Fig. S6 in the supplemental material), but the amount of heme in the wild-type cells increased to 32 pmol heme/mg protein, and a 6-fold-larger amount of heme was observed in the gCYTb5-IV-expressing cells. To determine whether the observed increase was specifically associated with heme incorporation into gCYTb5-IV, we also prepared a cell line that expressed a gCYTb5-IVH_{178}L mutant. As the expression of a gene with a negative mutation may be deleterious, we compared the growth of the wild-type strain and the strains expressing gCYTb5-IV and its mutated version. Only a subtle decrease in cell growth was observed in the gCYTb5-IVH_{178}L mutant (see Fig. S7 in the supplemental material). The amount of heme in this cell line was only slightly greater than that of the wild-type cells. We also determined whether the addition of exogenous heme affected the expression of recombinant gCYTb5-IV (Fig. 5B). Immunoblot analysis revealed comparable levels of gCYTb5-IV in the cytosol of cells that were grown in standard medium and in that of cells grown in medium containing hemin. Therefore, the observed changes in heme content within *Giardia* cells are related to the levels of heme incorporated into gCYTb5-IV, while the expression of the protein remained unaffected.

We further analyzed the presence of heme in *Giardia* cells using low-temperature spectroscopy. This complementary approach allows us to determine whether heme is incorporated by specific ligands. The analysis of homogenates of wild-type cells and gCYTb5-IV transformants that were cultured for 72 h in medium that contained hemin revealed a significantly higher Soret band at 420 nm in the transformed cells (Fig. 6). To determine whether the heme was bound to cytb_5, we determined the visible spectrum in the region between 500 and 600 nm, which is characteristic of distinct types of cytochromes (37, 38). The observed spectrum displayed maxima at 525 and 557 nm, which are typical for cytb_5 (Fig. 6) (39, 40). As a control, we determined the visible spectrum of *E. coli* cells expressing gCYTb5-IV, which exhibited characteristic absorption maxima identical to those observed for the *Giardia* cells (see Fig. S5 in the supplemental material). Altogether, these results demonstrate that *Giardia* cells are able to utilize an exogenous heme source and can incorporate heme into cytochrome b_5 proteins.

DISCUSSION

In this study, we demonstrated that the anaerobic protist *G. intestinalis*, despite lacking a heme synthesis pathway and the typical set of hemoproteins, is able to utilize extracellular heme and incorporate it into cytosolic group II cytb_5 proteins. To our knowledge, this is the first report that provides direct evidence for the presence of heme in an anaerobic eukaryote.

cytb_5 proteins form a large protein family with many biological

roles that appeared very early in evolution (16). They are known as typical C-tail-anchored proteins and are incorporated into organellar membranes. However, our analysis of *Giardia* CYTb5-I to -IV revealed the absence of the C-terminal transmembrane domain in these proteins. Surprisingly, searches for orthologs of *Giardia* cytb_5 proteins revealed that the vast majority of eukaryotes possess a soluble cytb_5 that does not contain the C-tail anchor (group II), in addition to the archetypal membrane-bound cytb_5 (group I). Moreover, fungi have evolved another cytb_5, which is most likely a soluble group III cytb_5. These three cytb_5 groups can be distinguished based on the characteristic vicinity of the highly conserved iron-coordinating histidines of the heme-binding pocket, and members of the groups form distinct branches in phylogenetic reconstructions. Interestingly, anaerobic protists, including *G. intestinalis*, exclusively possess members of the group II cytb_5 proteins. The lack of group I cytb_5 proteins in *Giardia* and other anaerobes suggests that these proteins preferentially provide electrons to oxygen-dependent acceptors, such as monooxygenases, that are not present in anaerobes. Importantly, the group II cytb_5 proteins are distinct from the well-known soluble cytb_5 proteins in erythrocytes that function in the reduction of methemoglobin (41). The erythrocyte cytb_5, which lacks a C-tail anchor, is a splice variant of a gene that additionally encodes a group I cytb_5 that is anchored in the membrane of the endoplasmic reticulum (42). An identical type of soluble cytb_5 is also involved in the activation of mammalian methionine synthase (43). However, despite the ubiquitous distribution of the group II cytb_5 proteins, the pathway in which these soluble cytb_5 proteins serve as electron transport proteins remains unknown.

In *G. intestinalis* and other anaerobic protists, electron transport is primarily dependent on ferredoxins that mediate single electron transfers. These FeS proteins are involved in energy metabolism that occurs in the *Giardia* cytosol and in the formation of FeS clusters in mitosomes. Recently, a novel *Giardia* oxidoreductase, GiOR-1, has been described (7). This enzyme efficiently transfers electrons from NADPH to artificial electron acceptors, such as dichlorophenolindophenol. However, it is unable to reduce [2Fe-2S] ferredoxin (7). The architecture of GiOR-1 corresponds to that of the multifunctional protein Tah18. Tah18 has been shown to form a complex with the FeS protein Dre2 and participates in the cytosolic assembly of FeS clusters (44). Under oxidative stress, Tah18 translocates to the mitochondria, where it interacts with cytochrome *c* and acts as a proapoptotic protein (45). In addition, yeast Tah18 is involved in NO synthesis (46). Human Tah18 (NR1) has been shown to act as a methionine synthase reductase that uses cytb_5 as a proximal electron donor for methionine synthase (43). Therefore, we determined whether GiOR-1 is able to reduce *Giardia* CYTb5 proteins. We found that CYTb5-I, -III, and -IV are efficiently reduced by GiOR-1 in the presence of NADPH as a source of reducing equivalents. However, the proximal partner of reduced CYTb5 remains unknown. Genes encoding Dre2 or methionine synthase have not been identified in the *G. intestinalis* genome thus far (47). Moreover, differences in the *Giardia* CYTb5 paralogs, particularly the presence of the unusual N-terminal extension of CYTb5-IV, suggest that they likely interact with different proximal partners. We further hypothesize that the function of the CYTb5 proteins may be related to the function of mitosomes, because GiOR-1 has been shown to be associated with these organelles (7). Moreover, *G. intestinalis* contains a paralogous gene encoding GiOR-2 that is associated with distinct vesicles, the characteristics of which remain to be clarified (7). Altogether, our results indicate that, in addition to ferredoxin-dependent electron transport, *G. intestinalis* contains a functional redox system that consists of an NADPH-dependent Tah18-like oxidoreductase and soluble group II CYTb5 proteins.

In anaerobic protists, there are several reasons for the absence of the heme synthesis pathway, which was likely lost during ancestral adaptations to anaerobic niches: (i) the organisms lost mitochondrial heme-dependent respiration and its high demand for heme, which was replaced by FeS protein-dependent energy metabolism; (ii) they replaced common hemoproteins that are involved in the defense against oxidative stress with heme-independent bacterial protective enzymes (9, 10); and (iii) two steps of the heme synthetic pathway that are catalyzed by the mitochondrial enzymes coproporphyrinogen III oxidase and protoporphyrinogen IX oxidase depend on molecular oxygen, which is not available in anaerobic niches (48, 49). Consequently, anaerobic protists retained a very limited set of hemoproteins, such as *G. intestinalis* cytb_5 and flavohemoglobin (15, 20). Not surprisingly, our results indicated a rather low level of heme in the cytosol of *G. intestinalis* when the parasite was grown in standard culture medium (<2.5 pmol per mg of protein) compared with 25 pmol heme/mg protein in macrophages (50). However, the amount of cytosolic heme increased upon the addition of hemin to the medium as an exogenous heme source. In particular, an increased level of heme was found in the strain expressing recombinant CYTb5-IV. This effect primarily reflects the incorporation of acquired heme into CYTb5-IV, because such an increase was not observed in the strain that expressed the mutant containing an impaired heme-binding site. The presence of heme-loaded CYTb5-IV in transformed *Giardia* was confirmed using low-temperature visible spectroscopy. These results indicated that *G. intestinalis* is able to compensate for the apparent lack of a heme synthesis pathway by utilizing an exogenous source of heme for its heme requirements. We cannot completely rule out the possibility that *Giardia* synthesizes heme via an undiscovered novel pathway, given that the functions of a large number of genes in the *Giardia* genome are unknown (46). Nevertheless, the heme-synthetic pathway is highly conserved in eukaryotes (13), and no alternative mechanisms for heme synthesis have been found in any organisms.

It is noteworthy that overexpression of CYTb5-IV caused the increase in cellular heme content. This observation suggests that import of heme in *Giardia* is a regulated process. We can speculate that overexpression of CYTb5-IV results in increased demand for cellular heme, which may provide a signal to increase the import of heme from the environment. Heme regulatory motifs were identified in a transcription factor in yeast (51), δ-aminolevulinate synthase (52), and several other diverse proteins (53). Moreover, iron regulates components of heme import machinery in enterocytes (54). Further studies are required to clarify whether heme transport is indeed a regulated process in *G. intestinalis* and to identify the molecular mechanism.

Parasites that lack genes for heme synthesis pathways but may require exogenous heme sources are not uncommon (13, 55). For example, bloodstream forms of trypanosomes satisfy their heme requirements via the uptake of hemoglobin (56). Intestinal parasites such as *G. intestinalis* may utilize dietary heme that is present in the small intestine (54). It is tempting to speculate that *G. intestinalis* may compete for heme with enterocytes that are able to take up intact

heme as a source of iron (54). However, the utilization of exogenous heme by parasitic protists has been experimentally assessed only in certain trypanosomatids (56–59). Moreover, the mechanisms for heme acquisition and its transport in trypanosomatids are poorly understood and are virtually unknown in other parasitic protists. In *Trypanosoma cruzi*, the uptake of heme analogs was shown to be reduced in the presence of ABC transporter inhibitors, which suggests a role for heme scavenging (57). ABC transporters were also suggested to be involved in the heme scavenging of *Leishmania* (60), a range of bacteria, and mammals (61, 62). More recently, the *Leishmania* heme response 1 (LHR1) protein was proposed to be the major heme importer in the parasite and other kinetoplastids (58). In the *G. intestinalis* genome, we did not find an LHR1 ortholog; however, the genome contains at least 27 ABC domain-containing proteins that are heme transporter candidates, although there is currently no information regarding the functions of these proteins.

It is unknown whether heme is essential for *G. intestinalis*, and the lack of a defined medium for the parasite did not allow us to address this question (13). However, the heme concentration in standard medium is rather low (8 nM), and the addition of 4 μM hemin showed no effect on cell growth. Therefore, either the heme requirements of *Giardia* fall below a concentration of 8 nM or heme may not be essential for parasite growth *in vitro*. Thus far, the kinetoplastid *Phytomonas serpens* is the only eukaryote that has been found to be able to survive entirely without heme (59). Similar to *Giardia* and other anaerobes, *P. serpens* lacks most of the known hemoproteins, although it is a protist with aerobic metabolism. However, *P. serpens* possesses unique metabolic adaptations that allow it to bypass the functions of proteins that are dependent on heme (59). Interestingly, group II cytb_5 appears to be the only heme-binding protein that is encoded in the *P. serpens* genome. This finding, together with the conservation of cytb_5 proteins in the majority of anaerobes, suggests that although cytb_5 proteins are potentially not essential for cell growth *in vitro*, they may play a role important for cells in their native environments.

In conclusion, we defined three groups of cytb_5 proteins in eukaryotes and determined that *G. intestinalis* exclusively possesses group II soluble cytb_5 proteins. We demonstrated that *Giardia* can utilize hemin as an exogenous heme source and incorporates it into the heme-binding site of gCYTb5-IV. The NADPH-dependent oxidoreductase GiOR-1 reduces CYTb5 proteins *in vitro*, which constitutes a novel redox system in *Giardia*. However, there is much to learn about the mechanisms by which *G. intestinalis*, which lacks a heme synthesis pathway, acquires and transports exogenous heme, in addition to the functions of group II cytb_5 proteins in *Giardia* and other eukaryotes.

ACKNOWLEDGMENTS

This work was supported by the Czech Ministry of Education (MSM 0021620858), Charles University in Prague (UNCE 204017 and GAUK 153010), and the project BIOCEV—Biotechnology and Biomedicine Centre of the Academy of Sciences and Charles University (CZ.1.05/1.1.00/02.0109) from the European Regional Development Fund.

REFERENCES

1. **Green J, Crack JC, Thomson AJ, Lebrun NE.** 2009. Bacterial sensors of oxygen. Curr. Opin. Microbiol. **12:**145–151. http://dx.doi.org/10.1016/j.mib.2009.01.008.
2. **Poole RK, Hughes MN.** 2000. New functions for the ancient globin family: bacterial responses to nitric oxide and nitrosative stress. Mol. Microbiol. **36:**775–783. http://dx.doi.org/10.1046/j.1365-2958.2000.01889.x.
3. **Koreny L, Sobotka R, Janouskovec J, Keeling PJ, Obornik M.** 2011. Tetrapyrrole synthesis of photosynthetic chromerids is likely homologous to the unusual pathway of apicomplexan parasites. Plant Cell **23:**3454–3462. http://dx.doi.org/10.1105/tpc.111.089102.
4. **Koreny L, Lukeš J, Obornik M.** 2010. Evolution of the haem synthetic pathway in kinetoplastid flagellates: an essential pathway that is not essential after all? Int. J. Parasitol. **40:**149–156. http://dx.doi.org/10.1016/j.ijpara.2009.11.007.
5. **Rao AU, Carta LK, Lesuisse E, Hamza I.** 2005. Lack of heme synthesis in a free-living eukaryote. Proc. Natl. Acad. Sci. U. S. A. **102:**4270–4275. http://dx.doi.org/10.1073/pnas.0500877102.
6. **Lara FA, Lins U, Bechara GH, Oliveira PL.** 2005. Tracing heme in a living cell: hemoglobin degradation and heme traffic in digest cells of the cattle tick *Boophilus microplus*. J. Exp. Biol. **208:**3093–3101. http://dx.doi.org/10.1242/jeb.01749.
7. **Jedelsky PL, Dolezal P, Rada P, Pyrih J, Smid O, Hrdy I, Sedinova M, Marcincikova M, Voleman L, Perry AJ, Beltran NC, Lithgow T, Tachezy J.** 2011. The minimal proteome in the reduced mitochondrion of the parasitic protist *Giardia intestinalis*. PLoS One **6:**e17285. http://dx.doi.org/10.1371/journal.pone.0017285.
8. **Rada P, Dolezal P, Jedelsky PL, Bursac D, Perry AJ, Sedinova M, Smiskova K, Novotny M, Beltran NC, Hrdy I, Lithgow T, Tachezy J.** 2011. The core components of organelle biogenesis and membrane transport in the hydrogenosomes of *Trichomonas vaginalis*. PLoS One **6:**e24428. http://dx.doi.org/10.1371/journal.pone.0024428.
9. **Coombs GH, Westrop GD, Suchan P, Puzova G, Hirt RP, Embley TM, Mottram JC, Müller S.** 2004. The amitochondriate eukaryote *Trichomonas vaginalis* contains a divergent thioredoxin-linked peroxiredoxin antioxidant system. J. Biol. Chem. **279:**5249–5256. http://dx.doi.org/10.1074/jbc.M304359200.
10. **Nixon JEJ, Wang A, Field J, Morrison HG, McArthur AG, Sogin ML, Loftus BJ, Samuelson J.** 2002. Evidence for lateral transfer of genes encoding ferredoxins, nitroreductases, NADH oxidase, and alcohol dehydrogenase 3 from anaerobic prokaryotes to *Giardia lamblia* and *Entamoeba histolytica*. Eukaryot. Cell **1:**181–190. http://dx.doi.org/10.1128/EC.1.2.181-190.2002.
11. **Smutna T, Goncalves VL, Saraiva LM, Tachezy J, Teixeira M, Hrdy I.** 2009. Flavodiiron protein from *Trichomonas vaginalis* hydrogenosomes: the terminal oxygen reductase. Eukaryot. Cell **8:**47–55. http://dx.doi.org/10.1128/EC.00276-08.
12. **Lindmark DG.** 1980. Energy metabolism of the anaerobic protozoon *Giardia lamblia*. Mol. Biochem. Parasitol. **1:**1–12.
13. **Koreny L, Obornik M, Lukeš J.** 2013. Make it, take it, or leave it: heme metabolism of parasites. PLoS Pathog. **9:**e1003088. http://dx.doi.org/10.1371/journal.ppat.1003088.
14. **Nakanishi N, Takeuchi F, Okamoto H, Tamura A, Hori H, Tsubaki M.** 2006. Characterization of heme-coordinating histidyl residues of cytochrome b5 based on the reactivity with diethylpyrocarbonate: a mechanism for the opening of axial imidazole rings. J. Biochem. **140:**561–571. http://dx.doi.org/10.1093/jb/mvj189.
15. **Alam S, Yee J, Couture M, Takayama SJ, Tseng WH, Mauk AG, Rafferty S.** 2012. Cytochrome b(5) from *Giardia lamblia*. Metallomics **4:**1255–1261. http://dx.doi.org/10.1039/c2mt20152f.
16. **Schenkman JB, Jansson I.** 2003. The many roles of cytochrome b(5). Pharmacol. Ther. **97:**139–152. http://dx.doi.org/10.1016/S0163-7258(02)00327-3.
17. **Vergeres G, Waskell L.** 1995. Cytochrome B(5), its functions, structure and membrane topology. Biochimie **77:**604–620.
18. **Guiard B, Lederer F.** 1977. The "b5-like" domain from chicken-liver sulfite oxidase: a new case of common ancestral origin with liver cytochrome b5 and bakers' yeast cytochrome b2 core. Eur. J. Biochem. **74:**181–190.
19. **Napier JA, Sayanova O, Stobart AK, Shewry PR.** 1997. A new class of cytochrome b5 fusion proteins. Biochem. J. **328:**717–718.
20. **Rafferty S, Luu B, March RE, Yee J.** 2010. *Giardia lamblia* encodes a functional flavohemoglobin. Biochem. Biophys. Res. Commun. **399:**347–351. http://dx.doi.org/10.1016/j.bbrc.2010.07.073.
21. **Keister DB.** 1983. Axenic culture of *Giardia lamblia* in Tyi-S-33 medium supplemented with bile. Trans. R. Soc. Trop. Med. Hyg. **77:**487–488.
22. **Lauwaet T, Davids BJ, Torres-Escobar A, Birkeland SR, Cipriano MJ, Preheim SP, Palm D, Svard SG, McArthur AG, Gillin FD.** 2007. Protein phosphatase 2A plays a crucial role in *Giardia lamblia* differentiation. Mol. Biochem. Parasitol. **152:**80–89. http://dx.doi.org/10.1016/j.molbiopara.2006.12.001.
23. **Sun CH, Chou CF, Tai JH.** 1998. Stable DNA transfection of the primitive

protozoan pathogen *Giardia lamblia*. Mol. Biochem. Parasitol. **92:**123–132.
24. **Dawson SC, Sagolla MS, Mancuso JJ, Woessner DJ, House SA, Fritz-Laylin L, Cande WZ.** 2007. Kinesin-13 regulates flagellar, interphase, and mitotic microtubule dynamics in *Giardia intestinalis*. Eukaryot. Cell **6:**2354–2364. http://dx.doi.org/10.1128/EC.00128-07.
25. **Dagley MJ, Dolezal P, Likic VA, Smid O, Purcell AW, Buchanan SK, Tachezy J, Lithgow T.** 2009. The protein import channel in the outer mitosomal membrane of *Giardia intestinalis*. Mol. Biol. Evol. **26:**1941–1947. http://dx.doi.org/10.1093/molbev/msp117.
26. **Sonda S, Stefanic S, Hehl AB.** 2008. A sphingolipid inhibitor induces a cytokinesis arrest and blocks stage differentiation in *Giardia lamblia*. Antimicrob. Agents Chemother. **52:**563–569. http://dx.doi.org/10.1128/AAC.01105-07.
27. **Long SJ, Changmai P, Tsaousis AD, Skalicky T, Verner Z, Wen YZ, Roger AJ, Lukeš J.** 2011. Stage-specific requirement for Isa1 and Isa2 proteins in the mitochondrion of *Trypanosoma brucei* and heterologous rescue by human and Blastocystis orthologues. Mol. Microbiol. **81:**1403–1418. http://dx.doi.org/10.1111/j.1365-2958.2011.07769.x.
28. **Sinclair PR, Gorman N, Jacobs JM.** 2001. Measurement of heme concentration. Curr. Protoc. Toxicol. Chapter 8: Unit 8.3. http://dx.doi.org/10.1002/0471140856.tx0803s00.
29. **Tzagoloff A, Nobrega M, Gorman N, Sinclair P.** 1993. On the functions of the yeast COX10 and COX11 gene products. Biochem. Mol. Biol. Int. **31:**593–598.
30. **Labbe P, Chaix P.** 1971. Inexpensive device for recording difference absorption spectra at low temperature (-196 degrees). Anal. Biochem. **39:**322.
31. **Altschul SF, Madden TL, Schaffer AA, Zhang JH, Zhang Z, Miller W, Lipman DJ.** 1997. Gapped BLAST and PSI-BLAST: a new generation of protein database search programs. Nucleic Acids Res. **25:**3389–3402.
32. **Jeanmougin F, Thompson JD, Gouy M, Higgins DG, Gibson TJ.** 1998. Multiple sequence alignment with Clustal X. Trends Biochem. Sci. **23:**403–405.
33. **Guindon S, Dufayard JF, Lefort V, Anisimova M, Hordijk W, Gascuel O.** 2010. New algorithms and methods to estimate maximum-likelihood phylogenies: assessing the performance of PhyML 3.0. Syst. Biol. **59:**307–321. http://dx.doi.org/10.1093/sysbio/syq010.
34. **Hwang YT, Pelitire SM, Henderson MP, Andrews DW, Dyer JM, Mullen RT.** 2004. Novel targeting signals mediate the sorting of different isoforms of the tail-anchored membrane protein cytochrome b5 to either endoplasmic reticulum or mitochondria. Plant Cell **16:**3002–3019. http://dx.doi.org/10.1105/tpc.104.026039.
35. **Farr H, Gull K.** 2009. Functional studies of an evolutionarily conserved, cytochrome b5 domain protein reveal a specific role in axonemal organisation and the general phenomenon of post-division axonemal growth in Trypanosomes. Cell Motil. Cytoskeleton **66:**24–35. http://dx.doi.org/10.1002/cm.20322.
36. **D'Arrigo A, Manera E, Longhi R, Borgese N.** 1993. The specific subcellular-localization of 2 isoforms of cytochrome-B5 suggests novel targeting pathways. J. Biol. Chem. **268:**2802–2808.
37. **Seguin A, Sutak R, Bulteau AL, Garcia-Serres R, Oddou JL, Lefevre S, Santos R, Dancis A, Camadro JM, Latour JM, Lesuisse E.** 2010. Evidence that yeast frataxin is not an iron storage protein in vivo. Biochim. Biophys. Acta **1802:**531–538. http://dx.doi.org/10.1016/j.bbadis.2010.03.008.
38. **Falk JE.** 1964. Porphyrins and metalloporphyrins. Elsevier Publishing Co. New York, NY.
39. **Bonnerot C, Galle AM, Jolliot A, Kader JC.** 1985. Purification and properties of plant cytochrome-B5. Biochem. J. **226:**331–334.
40. **Smith MA, Napier JA, Stymne S, Tatham AS, Shewry PR, Stobart AK.** 1994. Expression of a biologically-active plant cytochrome b(5) in *Escherichia coli*. Biochem. J. **303:**73–79.
41. **Hultquist DE, Passon PG.** 1971. Catalysis of methaemoglobin reduction by erythrocyte cytochrome B5 and cytochrome B5 reductase. Nat. New Biol. **229:**252–254.
42. **Giordano SJ, Steggles AW.** 1991. The human liver and reticulocyte cytochrome b5 mRNAs are products from a single gene. Biochem. Biophys. Res. Commun. **178:**38–44.
43. **Olteanu H, Banerjee R.** 2003. Redundancy in the pathway for redox regulation of mammalian methionine synthase: reductive activation by the dual flavoprotein, novel reductase 1. J. Biol. Chem. **278:**38310–38314. http://dx.doi.org/10.1074/jbc.M306282200.
44. **Netz DJ, Stumpfig M, Dore C, Muhlenhoff U, Pierik AJ, Lill R.** 2010. Tah18 transfers electrons to Dre2 in cytosolic iron-sulfur protein biogenesis. Nat. Chem. Biol. **6:**758–765. http://dx.doi.org/10.1038/nchembio.432.
45. **Vernis L, Facca C, Delagoutte E, Soler N, Chanet R, Guiard B, Faye G, Baldacci G.** 2009. A newly identified essential complex, Dre2-Tah18, controls mitochondria integrity and cell death after oxidative stress in yeast. PLoS One **4:**e4376. http://dx.doi.org/10.1371/journal.pone.0004376.
46. **Nishimura A, Kawahara N, Takagi H.** 2013. The flavoprotein Tah18-dependent NO synthesis confers high-temperature stress tolerance on yeast cells. Biochem. Biophys. Res. Commun. **430:**137–143. http://dx.doi.org/10.1016/j.bbrc.2012.11.023.
47. **Morrison HG, McArthur AG, Gillin FD, Aley SB, Adam RD, Olsen GJ, Best AA, Cande WZ, Chen F, Cipriano MJ, Davids BJ, Dawson SC, Elmendorf HG, Hehl AB, Holder ME, Huse SM, Kim UU, Lasek-Nesselquist E, Manning G, Nigam A, Nixon JE, Palm D, Passamaneck NE, Prabhu A, Reich CI, Reiner DS, Samuelson J, Svard SG, Sogin ML.** 2007. Genomic minimalism in the early diverging intestinal parasite *Giardia lamblia*. Science **317:**1921–1926. http://dx.doi.org/10.1126/science.1143837.
48. **Xu K, Elliott T.** 1993. An oxygen-dependent coproporphyrinogen oxidase encoded by the hemF gene of *Salmonella typhimurium*. J. Bacteriol. **175:**4990–4999.
49. **Dailey TA, Dailey HA.** 1996. Human protoporphyrinogen oxidase: expression, purification, and characterization of the cloned enzyme. Protein Sci. **5:**98–105.
50. **Chang CS, Chang KP.** 1985. Heme requirement and acquisition by extracellular and intracellular stages of *Leishmania mexicana amazonensis*. Mol. Biochem. Parasitol. **16:**267–276.
51. **Pfeifer K, Kim KS, Kogan S, Guarente L.** 1989. Functional dissection and sequence of yeast HapI activator. Cell **56:**291–301.
52. **Munakata H, Sun JY, Yoshida K, Nakatani T, Honda E, Hayakawa S, Furuyama K, Hayashi N.** 2004. Role of the heme regulatory motif in the heme-mediated inhibition of mitochondrial import of 5-aminolevulinate synthase. J. Biochem. **136:**233–238. http://dx.doi.org/10.1093/jb/mvh112.
53. **Zhang L, Guarente L.** 1995. Heme binds to a short sequence that serves a regulatory function in diverse proteins. EMBO J. **14:**313–320.
54. **West AR, Thomas C, Sadlier J, Oates PS.** 2006. Haemochromatosis protein is expressed on the terminal web of enterocytes in proximal small intestine of the rat. Histochem. Cell Biol. **125:**283–292. http://dx.doi.org/10.1007/s00418-005-0060-6.
55. **van Dooren GG, Kennedy AT, McFadden GI.** 2012. The use and abuse of heme in apicomplexan parasites. Antioxid. Redox Signal. **17:**634–656. http://dx.doi.org/10.1089/ars.2012.4539.
56. **Vanhollebeke B, De Muylder G, Nielsen MJ, Pays A, Tebabi P, Dieu M, Raes M, Moestrup SK, Pays E.** 2008. A haptoglobin-hemoglobin receptor conveys innate immunity to *Trypanosoma brucei* in humans. Science **320:**677–681. http://dx.doi.org/10.1126/science.1156296.
57. **Lara FA, Sant'anna C, Lemos D, Laranja GA, Coelho MG, Reis S, Michel IA, Oliveira PL, Cunha-E-Silva Salmon D, Paes MC.** 2007. Heme requirement and intracellular trafficking in *Trypanosoma cruzi* epimastigotes. Biochem. Biophys. Res. Commun. **355:**16–22. http://dx.doi.org/10.1016/j.bbrc.2006.12.238.
58. **Huynh C, Yuan X, Miguel DC, Renberg RL, Protchenko O, Philpott CC, Hamza I, Andrews NW.** 2012. Heme uptake by *Leishmania amazonensis* is mediated by the transmembrane protein LHR1. PLoS Pathog. **8:**e1002795. http://dx.doi.org/10.1371/journal.ppat.1002795.
59. **Koreny L, Sobotka R, Kovarova J, Gnipova A, Flegontov P, Horvath A, Obornik M, Ayala FJ, Lukes J.** 2012. Aerobic kinetoplastid flagellate Phytomonas does not require heme for viability. Proc. Natl. Acad. Sci. U. S. A. **109:**3808–3813. http://dx.doi.org/10.1073/pnas.1201089109.
60. **Campos-Salinas J, Cabello-Donayre M, Garcia-Hernandez R, Perez-Victoria I, Castanys S, Gamarro F, Perez-Victoria JM.** 2011. A new ATP-binding cassette protein is involved in intracellular haem trafficking in Leishmania. Mol. Microbiol. **79:**1430–1444. http://dx.doi.org/10.1111/j.1365-2958.2010.07531.x.
61. **Koster W.** 2001. ABC transporter-mediated uptake of iron, siderophores, heme and vitamin B12. Res. Microbiol. **152:**291–301. http://dx.doi.org/10.1016/S0923-2508(01)01200-1.
62. **Krishnamurthy PC, Du G, Fukuda Y, Sun D, Sampath J, Mercer KE, Wang J, Sosa-Pineda B, Murti KG, Schuetz JD.** 2006. Identification of a mammalian mitochondrial porphyrin transporter. Nature **443:**586–589. http://dx.doi.org/10.1038/nature05125.

OPEN ACCESS Freely available online

PLoS one

The Minimal Proteome in the Reduced Mitochondrion of the Parasitic Protist *Giardia intestinalis*

Petr L. Jedelský[1,2], Pavel Doležal[1], Petr Rada[1], Jan Pyrih[1], Ondřej Šmíd[1], Ivan Hrdý[1], Miroslava Šedinová[1], Michaela Marcinčiková[1], Lubomír Voleman[1], Andrew J. Perry[3], Neritza Campo Beltrán[1], Trevor Lithgow[3], Jan Tachezy[1]*

1 Department of Parasitology, Faculty of Science, Charles University in Prague, Prague, Czech Republic, **2** Laboratory of Mass Spectrometry, Faculty of Science, Charles University in Prague, Prague, Czech Republic, **3** Department of Biochemistry & Molecular Biology, Monash University, Clayton Campus, Melbourne, Australia

Abstract

The mitosomes of *Giardia intestinalis* are thought to be mitochondria highly-reduced in response to the oxygen-poor niche. We performed a quantitative proteomic assessment of *Giardia* mitosomes to increase understanding of the function and evolutionary origin of these enigmatic organelles. Mitosome-enriched fractions were obtained from cell homogenate using Optiprep gradient centrifugation. To distinguish mitosomal proteins from contamination, we used a quantitative shot-gun strategy based on isobaric tagging of peptides with iTRAQ and tandem mass spectrometry. Altogether, 638 proteins were identified in mitosome-enriched fractions. Of these, 139 proteins had iTRAQ ratio similar to that of the six known mitosomal markers. Proteins were selected for expression in *Giardia* to verify their cellular localizations and the mitosomal localization of 20 proteins was confirmed. These proteins include nine components of the FeS cluster assembly machinery, a novel diflavo-protein with NADPH reductase activity, a novel VAMP-associated protein, and a key component of the outer membrane protein translocase. None of the novel mitosomal proteins was predicted by previous genome analyses. The small proteome of the *Giardia* mitosome reflects the reduction in mitochondrial metabolism, which is limited to the FeS cluster assembly pathway, and a simplicity in the protein import pathway required for organelle biogenesis.

Citation: Jedelský PL, Doležal P, Rada P, Pyrih J, Šmíd O, et al. (2011) The Minimal Proteome in the Reduced Mitochondrion of the Parasitic Protist *Giardia intestinalis*. PLoS ONE 6(2): e17285. doi:10.1371/journal.pone.0017285

Editor: Bob Lightowlers, Newcastle University, United Kingdom

Received November 8, 2010; **Accepted** January 26, 2011; **Published** February 24, 2011

Funding: This work was supported by the Czech Ministry of Education (MSM0021620858, LC07032) and the Czech Science Foundation grants 204/05/H023 (P.J.) and 204/06/0947 (J.T.) and the Australian Research Council (T.L.). The funders had no role in study design, data collection and analysis, decision to publish, or preparation of the manuscript.

Competing Interests: The authors have declared that no competing interests exist.

* E-mail: tachezy@gmail.com

Introduction

Mitochondria are eukaryotic organelles that are thought to have evolved from an alpha-proteobacterial endosymbiont about two billion years ago. The loss of bacterial autonomy and transition of the endosymbiont to a "protomitochondrion" were associated with a reduction in the number of genes in the endosymbiont genome; these genes were either transferred to the nuclear genome or lost. While the genome of the extant alpha-proteobacterium *Rickettsia prowazekii* contains 834 protein-coding genes [1], the largest number of genes (67 protein-coding genes) in a mitochondrial genome is found in *Reclinomonas americana* [2], with only three protein-coding genes present in the *Plasmodium falciparum* mitochondrial genome [3]. Paradoxically, the reduction of the mitochondrial genome did not lead to a reduction of the organellar proteome [4]. The acquisition of a mechanism for mitochondrial import at the earliest stage of the endosymbiont-to-protomitochondrion transition allowed the recruitment of the proteins of endosymbiotic origin that were now encoded in the nucleus, and the import of proteins of other origins [5]. Contemporary mitochondrial proteomes contain hundreds of proteins, up to 1100 proteins in the mouse [6].

Mitosomes are the most highly reduced forms of mitochondria, having completely lost their genomes and dramatically reduced their proteomes. Mitosomes have also lost many of the typical mitochondrial functions, such as respiration, the citric acid cycle, and ATP synthesis. Biosynthesis of FeS clusters is the only mitochondrial function seen to be retained by at least some mitosomes [7]. Mitosomes have become established independently in diverse groups of unicellular eukaryotes (protists); many of them once considered to be amitochondrial because they lack organelles with the expected mitochondrial morphology [8].

Organisms with mitosomes live under oxygen-limiting conditions, like the human intestinal parasites *Giardia intestinalis* [9] and *Entamoeba histolytica* [10], or are intracellular parasites like the microsporidians *Encephalitozoon cuniculi* and *Trachipleistophora hominis* [11,12] and the apicomplexan *Cryptosporidium parvum* [13]. Mitosomes are tiny ovoid organelles enclosed by two membranes. Unlike mitochondria, the inner membrane of mitosomes does not form cristae. The morphology of the mitosome is reminiscent of the hydrogenosome, another form of mitochondrion that is present in some anaerobic protists, such as *Trichomonas vaginalis*. Unlike mitosomes, however, hydrogenosomes are metabolically active organelles that produce ATP by substrate level phosphorylation [14].

The limited knowledge of mitosomal proteomes has been gained mainly from analyses of genome sequences and localization studies of a few model mitosomal proteins [9,11,15–21]. The only published proteomics study that focused on mitosomes was that

recently reported for the amoeba *E. histolytica*, identifying a unique sulfate activation pathway [22]. To increase our understanding of the function and origin of these enigmatic organelles, we established a large-scale proteomic approach to analyze the mitosomes of *Giardia intestinalis*. This organism was selected because *Giardia intestinalis* is a common human intestinal pathogen, its genome sequence has been published [23,24], and it is considered to be among the most basal eukaryotes [25]. Moreover, previous analysis of the *G. intestinalis* genome provided little new information pertaining to the putative mitosomal proteome [24], so there are substantial gaps in our knowledge of the structure and function of this essential organelle. Here, we quantitatively analyzed the presence of isobarically-tagged proteins in mitosome enriched fractions. This technique allowed us to discriminate the mitosomal proteins from those of contaminating cellular structures. Combined with an exhaustive bioinformatics analysis, this strategy identified 139 putative mitosomal proteins; 20 of which were experimentally confirmed to be localized in mitosomes. Our results revealed that the proteome of the *G. intestinalis* mitosome is selectively reduced and houses a single metabolic pathway for FeS cluster assembly, a novel diflavin protein with NADPH reductase activity, a minimal protein import machinery and proteins that may be important for the interaction of mitosomes with other cellular compartments.

Results and Discussion

Identification of putative mitosomal proteins by isobaric tagging

Mitosome-enriched fractions were separated from a *Giardia* homogenate by preparative centrifugation using a discontinuous Optiprep (iodixanol) gradient [26]. This method produced five dense organellar fractions (Fig. 1A). The mitosomal marker protein IscU was particularly enriched in fraction #4 and to a lesser extent in fraction #3 (Fig. 1B). Electron microscopy confirmed the presence of mitosomes in both fractions; however, co-fractionating vesicles of similar densities were also found (data not shown).To discriminate between putative mitosomal proteins and those of contaminating cellular structures, we compared the relative distribution of each protein in fractions #3 and #4. Because the mitosomal proteins necessarily co-fractionate (i.e. being contained within mitosomes) during gradient centrifugation, each of the *bona fide* mitosomal protein should display similar distribution ratios [27]. To this end, the proteins of fractions #3 and #4 were digested in parallel with trypsin and each peptide population was labeled with a distinct iTRAQ reagent and then combined. The isobaric mass characteristics of the iTRAQ reagents means the differentially-labeled peptides from fractions #3 and #4 form a single peak in the MS scan for protein identification. MS/MS analysis of the iTRAQ-labelled peptides liberates the isotope-encoded reporter ions, the ratio of which can reflects the distribution of the protein across the two fractions. In our analysis, the pooled peptides were analyzed by tandem mass spectrometry after subsequent separation with isoelectric focusing and nano-liquid chromatography (nano-LC MS/MS). The iTRAQ ratio was then calculated for each protein, and the proteins were sorted according to the relative distributions in the fractions (Fig. 2).

Validating the methodology, mitosomal markers (IscS, IscU, [2Fe2S] ferredoxin, Cpn60, Hsp70 and glutaredoxin 5) [28] clustered together with similar iTRAQ ratios (Fig. 2). Proteins with ratios between the lowest and highest values for the markers were considered to be candidate mitosomal proteins. We also extended this window on both sides by half of the distance between the limiting markers and included all proteins in this extended window (Fig. 2). In total, we identified 638 proteins (Table S1), with 139 of these proteins meeting the defined criteria for mitosomal proteins (Tables 1–7). Each of the 139 mitosomal candidates was assigned to a probable function based on current annotations in the GiardiaDB, PSI BLAST searches in the NCBI nr database, and motif and domain searches in the Pfam database. Three additional bioinformatics tools were used to predict cellular localization (PsortII, TargetP 1.1 and SignalP 3.0), and two web-based programs were used to predict alpha-helical transmembrane region segments (TMHMM and Memsat3) (Tables S2–S4, summary is given in Tables 1–7). The candidate proteins were clustered into 13 groups according to their predicted functions (Tables 1–7, Fig. 3). The proteomic data confirmed the validity of 250 hypothetical genes predicted from the complete genome sequence of *Giardia* [24]; 40 of these formed the largest group of candidate mitosomal proteins.

Evolution-inspired orthology phylogenetic profiling

Previous phylogenetic analyses of known mitosomal proteins have generally confirmed their alpha-proteobacterial origin [28–30]. On this premise, we compared the genomes of *G. intestinalis* and *Rickettsia typhi* using the orthology phylogenetic profile tool at GiardiaDB (http://www.orthomcl.org/cgi-bin/OrthoMclWeb.cgi) to identify proteins of alpha-proteobacterial ancestry in the *G. intestinalis* genome. The phylogenetic profiling yielded 106 candidate genes that were analyzed with the topology prediction algorithms described above (Table S5). Based on these analyses, six additional proteins: acetyl CoA acetyl transferase, CDP-diacylglycerol-glycerol-3-phosphate 3-phosphatidyltransferase, guanylate kinase, J-protein HesB, thioredoxin reductase, and thymidylate kinase were added to the set of candidate mitosomal proteins identified by our proteomics approach (Tables 1–7).

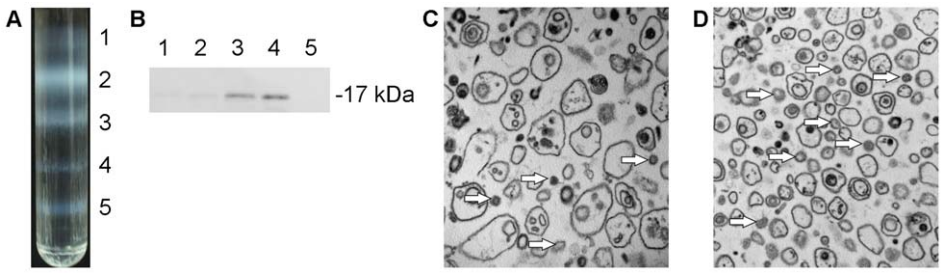

Figure 1. Isolation of mitosome-rich fractions. (A) Trophozoites were disrupted and centrifuged to remove unbroken cells, nuclei and cytoskeletal residue. The high-speed pellet was resuspended in sucrose buffer, layered onto an Optiprep density gradient, and centrifuged overnight. Five distinct fractions were obtained. (B) Fractions were collected and analyzed by SDS-PAGE and Western blot. The mitosomal marker GiIscU was detected in fractions #3 and #4 using a polyclonal rabbit antibody. (C–D) Electron microscopy of subcellular fractions. Fraction #3 (C) contains numerous vesicles of variable sizes, while fraction #4 (D) contains vesicles of more homogeneous sizes. Arrows indicate mitosomes.
doi:10.1371/journal.pone.0017285.g001

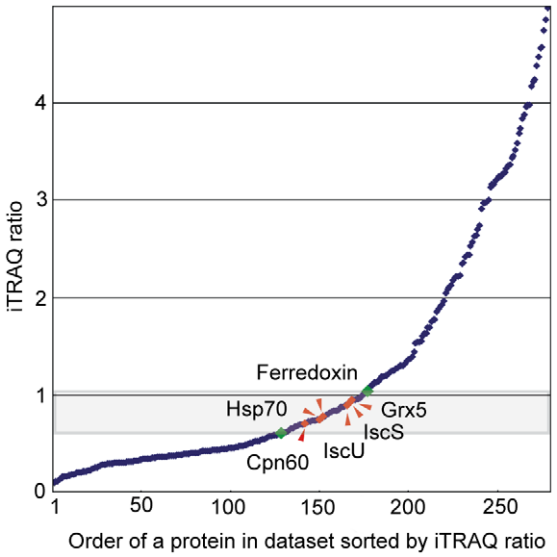

Figure 2. iTRAQ ratios define protein subcellular localization. Proteins in fractions #3 and #4 isolated on the Optiprep gradient were labeled with the iTRAQ-114 and iTRAQ-115 reagents, respectively, analyzed by LC MS/MS, and sorted according to the iTRAQ ratios. Mitosomal marker proteins (red diamonds) fall into a narrow range of iTRAQ ratios. Green diamondsdindicate the zone of proteins considered as mitosomal candidates (mitosomal distribution, MiD).
doi:10.1371/journal.pone.0017285.g002

Experimental validation of protein subcellular localization

The cellular localization of the selected candidate proteins was observed by stable episomal expression in *Giardia*. To establish the morphology of subcellular localizations by this approach, we first observed the localization of five marker proteins: cytosolic enolase, two proteins from the endoplasmic reticulum (Hsp70 and protein disulfide isomerase 5), mitosomal Hsp70 and glutaredoxin (Fig. 4A). We added to these markers of known location, three proteins of untested location with iTRAQ ratios outside that of the mitosomal range: glutamate dehydrogenase, copine and peroxiredoxin. Glutamate dehydrogenase and copine were associated with cytoskeletal structures, while peroxiredoxin localizes to the endoplasmic reticulum network. This strategy was used to test the sub-cellular localization of 44 selected proteins. Of these 20 expressed fluorescent fusions that were found in the mitosomes (Tables 1–7). By way of example, four of these: VAP, Pam16, Cpn10 and unknown proteins GL50803_9296 and GL50803_ 14939 are shown in Fig. 4B.

Iron-sulfur cluster assembly

Proteins involved in FeS cluster assembly formed the most prominent functional group within the predicted mitosomal proteins. These included components required for the formation of transient FeS clusters on the molecular scaffold (IscS, IscU, Nfu) (Fig. S1) and components that have been proposed to transfer the transient FeS clusters to target apoproteins, including IscA (Fig. S2), the monothiol glutaredoxin 5, chaperone Hsp70 and its co-chaperones the J-protein HscB (Fig. S3) and nucleotide exchange factor GrpE (Fig. S4). The identification of the FeS cluster assembly machinery in the mitosomal proteome is consistent with the ability of the mitosome-enriched fraction to catalyze the formation of FeS clusters on a ferredoxin apoprotein [9]. However, when we compared the FeS cluster machinery of *Giardia* mitosomes to that of *S. cerevisiae* and *Trypanosoma brucei* mitochondria, we found that several mitochondrial components were absent from the mitosomes (Table 8).

A striking deviation from other eukaryotes is the absence of frataxin in *Giardia* mitosomes. Frataxin is invariably present in eukaryotes that contain the ISC-type FeS cluster assembly machinery. The presence of frataxin in mitosomes was found in *E. cuniculi* [17], and genes encoding frataxin are present in the genomes of *C. parvum* and the diplomonad *Spironucleus vortens*, a close relative of *Giardia*. We failed to identify frataxin in the genomes of three *G. intestinalis* strains in the GiardiaDB, using either BLAST searches or the motif search tool.

Two IscA-like proteins, IscA1 (Isa1) and IscA2 (Isa2) are present in virtually all mitochondria [31] and are thought to act as scaffold proteins for transient FeS clusters [32–34] and/or serve as iron donors [35]. Interestingly, the *Giardia* mitosome contains only a single IscA-2 type protein (Fig. S2), while IscA-1 is absent. The same situation was found in hydrogenosomes of *Trichomonas vaginalis* (Table 8). No genes encoding IscA were found in the genomes of other organisms with mitosomes. The observed distributions of IscA therefore suggest that IscA-1 was lost in mitosomes and hydrogenosomes together with a specific set of mitochondrial FeS proteins, while IscA-2 was retained in *Giardia* mitosomes to function either in the maturation of specific FeS protein(s) or as an iron transporter [35].

The mitosomes did not contain Ind1 or Iba57. In mitochondria, these proteins are required for the formation of FeS clusters on specific substrates. Ind1 is a P-loop NTPase that is required for the maturation of FeS proteins of the multi-subunit respiratory complex I [36,37]. Homologues of Ind1 are also present in the hydrogenosomes of *T. vaginalis* (Table 8), which contain a highly reduced form of complex I with only two FeS catalytic subunits [38]. The selective absence of Ind1 in the mitosomes of *Giardia* (Table 8) is thus consistent with the absence of complex I and highlights the specific role of Ind1 in the biogenesis of this respiratory complex. Iba57 forms a complex with the scaffold protein IscA (Isa1p and Isa2p in yeast), which plays a specific role in [4Fe4S] cluster assembly of aconitase-type proteins and the functional activation of mitochondrial radical-SAM FeS proteins [39]. As in the case of Ind1, the absence of Iba57 likely reflects the absence of the respective substrate proteins in mitosomes.

Pyridine nucleotide-driven electron transport in mitosomes

The formation of FeS clusters requires reducing equivalents, which are provided by a short electron chain consisting of the [2Fe2S] ferredoxin and ferredoxin:$NADP^+$ reductase (FNR) [40]. The presence of this chain has been predicted in the mitosomes of *C. parvum* and *E. cuniculi*; however, [2Fe2S] ferredoxin, but not FNR, was found in *Giardia* mitosomes (Table 1). We identified a distinct protein with a possible redox activity named GiOR-1 (GL50803_91252), which is currently annotated in the GiardiaDB as an inducible nitric oxide synthase. This protein consists of a flavodoxin-like FMN-binding domain that is connected to a cytochrome p450 reductase-like domain, including a FAD binding pocket and an NADP(H) binding site (Fig. S5). These two domains are present in the C-termini of various oxidoreductases, such as cytochrome p450 reductase and nitric oxide synthase, and serve as electron donors (Fig. S5). GiOR-1 does not contain an N-terminal domain that determines the specific functions of known oxidoreductases.

The architecture of GiOR-1 resembles that of the recently identified protein Tah18 in *Saccharomyces cerevisiae* [41,42]. Tah18 was shown to form a complex with Dre2 in the cytosol, where it participates in cytosolic FeS cluster assembly [43]. Under oxidative stress, the Dre2-Tag18 complex was destabilized, and Tah18 relocalized from the cytosol to the mitochondria. This behavior has been shown to be associated with apoptotic events.

Table 1. Putative mitosomal proteins classified by predicted function: Iron-sulfur cluster assembly, chaperones, redox mechanism and protein translocation and processing.

Accession number	Annotation	Identification		Localization					Structure		
		MASCOT	Coverage	MiD	SignalP	Target P	Psort II	Exp Ver.	MEMSAT3	SGP	TMHMM
		score	peptides				% mito		TM No.		TM No.
Iron-sulfur cluster assembly											
GL50803_14519	IscS, cysteine desulfurase	296	4	Y	N	O		M	0	#	0
GL50803_15196	IscU	243	5	Y	N	M	17%	M	0	#	0
EAA38809	Nfu	60	2	Y	N	M	39%	M	1		0
GL50803_14821	IscA	198	3	Y	N	O	35%	M	0	#	0
GL50803_2013	Glutaredoxin 5	249	3	Y	N	O	13%	M	0	#	0
Molecular chaperones											
GL50803_14581	mitochondrial type HSP70	404	7	Y	N	O	13%	M	0	#	0
GL50803_1376	GrpE	29	1	Y	N	M	39%	M	0	#	0
GL50803_17030	DnaJ protein, Jac1	*	*	*	N	O	35%	M	0	#	0
GL50803_9751	DnaJ protein, Type III	34	1	Y	N	O	13%	M	1		1
GL50803_103891	Cpn60	336	6	Y	N	O		M	0	#	0
GL50803_29500	Cpn10	68	1	Y	Y	O	9%	M	0	#	0
Redox mechanism											
GL50803_27266	[2Fe-2S] ferredoxin	182	2	Y	N	M	48%	M	0	#	0
GL50803_91252	GiOR-1, oxidoreductase	40	1	N	N	O	13%	M	0	#	0
GL50803_15897	GiOR-2, oxidoreductase	*	*	*	N	O	21%	O	0	#	0
GL50803_9827	Thioredoxin reductase	*	*	*	N	M	13%	O	0	#	0
GL50803_9719	NADH oxidase	271	5	Y	N	O	9%	**	0	#	0
GL50803_16076	Peroxiredoxin 1	293	5	Y	N	O	9%		0	#	0
Protein translocation and processing											
GL50803_17161	Tom40	208	2	Y	N	O	13%	M	0	#	0
XP_002364144	Pam18	68	1	Y	N	M	30%	M	0	#	0
GL50803_19230	Pam16	35	1	Y	N	O	13%	M	0	#	0
GL50803_9478	GPP, processing peptidase	30	1	Y	N	O	4%	M	0	#	0

Mascot score, Mascot total ion score for the identified protein. Coverage, number of unique peptides per identified protein. MiD, mitosomal distribution. Proteins are marked "Y" if their distributions in fractions #3 and #4 of the Optiprep gradient (measured by the iTRAQ ratio) were within the range between Cpn10 and IscU and the window that extended in both directions by half of the distance between these markers. Proteins with ratios outside of this range are indicated with "N". TargetP and PsortII were used to predict the subcellular location of *Giardia* proteins. S, secretory; N, non-secretory; M, mitochondrial; O, other. Exp. ver., experimental verification of protein localization using the pONDRA expression vector. The recombinant tagged proteins were localized by fluorescence microscopy. M, mitosome; ER, endoplasmic reticulum; O, other; ? inconclusive. MEMSAT3 and TMHMM were used to predict transmembrane domains. SGP, predicted soluble proteins are marked with number sign (#). Asterisk (*) is used where no data were available. (**) transformed *Giardia* did not express the recombinant tagged protein.
doi:10.1371/journal.pone.0017285.t001

Searches for a Dre2 homologue in *Giardia* were unsuccessful. However, we identified a second paralogue of Tah18 named GiOR-2 (GL50803_15897, Fig. S5). The expression of tagged GiOR-1 and GiOR-2 in *G. intestinalis* confirmed that the GiOR-1 is localized to the mitosome, but GiOR-2 was found in numerous vesicles that did not correspond to mitosomes (Fig. 4C). To assess the oxidoreductase activity of GiOR-1, recombinant GiOR-1 was produced in *Escherichia coli* and isolated as a yellow protein, which is expected for diflavin oxidoreductases. GiOR-1 efficiently transferred electrons from NADPH to dichlorophenolindolphenol, whereas an about 30 fold lower activity was measured using NADH as the electron donor (Table 9). Low specific activities were observed also with methyl viologen and oxygen as electron acceptors (Table 9). No activity was observed when GiOR-1 was assayed with *G. intestinalis* mitosomal ferredoxin as a possible native electron acceptor. These results suggest that GiOR-1 does not act directly as a ferredoxin reductase in mitosomes, however, its ability to utilize NADPH as an electron donor indicates that pyridine nucleotides are involved in mitosomal electron transport.

Molecular chaperones in the mitosomal matrix: protein folding and assembly

A single mitosomal Hsp70, three J-protein co-chaperones and the nucleotide exchange factor GrpE were identified in the mitosomes. The J-proteins included HscB, an orthologue of yeast Jac1 (Fig. S3)that has a predicted role in FeS cluster biogenesis [44], and Pam18/Tim14, which is required for translocation of proteins across the mitochondrial inner membrane [45]. The third J-protein also contains an N-terminal DnaJ domain (type III family); however, its function cannot be inferred from domain structure or phylogenetic profiling. We also identified the chaperonins Cpn60 and Cpn10 (Fig. S6), that function in folding and assembly of newly-imported proteins [46,47] (Table 1).

Table 2. Putative mitosomal proteins classified by predicted function: transporters and proteins known to operate in endoplasmic reticulum and tramsport vesicles.

Accession number	Annotation	Identification		Localization					Structure		
		MASCOT	Coverage	MiD	SignalP	Target P	Psort II	Exp Ver.	MEMSAT3	SGP	TMHMM
		score	peptides				% mito		TM No.		TM No.
Transporters											
GL50803_114777	major facilitator superfamily mfs_1	658	8	N	N	M	4%	ER	10		12
GL50803_17296	major facilitator superfamily mfs_1	32	1	Y	N	M		**	7		10
GL50803_17342	major facilitator superfamily mfs_1	151	3	Y	N	M		**	10		12
GL50803_87446	ABC transporter, A family, putative	554	7	Y	N	O		**	4		7
GL50803_3470	ABC transporter, A family, putative	95	2	Y	N	M		**	6		7
GL50803_17165	ABC transporter, A family, putative	113	2	Y	N	O	4%		8		7
GL50803_21411	ABC transporter, A family, putative	429	10	Y	N	S			0		14
ER, vesicle transport											
GL50803_5744	Sec61-alpha	175	3	Y	N	M	22%	ER	10		9
GL50803_16906	Phosphatidate cytidylyltransferase	48	2	Y	N	M	9%	ER	7		8
GL50803_14200	Molybdenum cofactor sulfurase	56	1	Y	N	O	22%	ER	2		1
GL50803_14670	Protein disulfide isomerase PDI3	69	1	Y	Y	S	22%		1		0
GL50803_8064	Protein disulfide isomerase PDI5	58	1	Y	Y	S	13%	ER	1		1
GL50803_17121	ER Hsp70 (Bip)	1626	24	Y	Y	S	11%	ER	0	#	1
GL50803_15204	Endosomal cargo receptor 3	95	2	Y	Y	S			1		1
GL50803_14469	R-SNARE 3	45	1	Y	N	O			1		2
GL50803_8559	Vacuolar ATP synthase 16 kDa proteolipid subunit	90	1	Y	N	O	11%		4		4
GL50803_7532	Vacuolar ATP synthase catalytic subunit A	146	2	Y	N	O	17%		1		0
GL50803_13000	Vacuolar ATP synthase subunit d	342	5	Y	N	O	13%		1		0
GL50803_23833	Vacuolar protein sorting 35	26	1	Y	N	O	11%		1		0
GL50803_18470	Vacuolar proton-ATPase subunit, putative	608	8	Y	N	O	4%		6		6
GL50803_96670	Potassium-transporting ATPase alpha chain 1	473	9	Y	N	O	4%		10		8

Mascot score, Mascot total ion score for the identified protein. Coverage, number of unique peptides per identified protein. MiD, mitosomal distribution. Proteins are marked "Y" if their distributions in fractions #3 and #4 of the Optiprep gradient (measured by the iTRAQ ratio) were within the range between Cpn10 and IscU and the window that extended in both directions by half of the distance between these markers. Proteins with ratios outside of this range are indicated with "N". TargetP and PsortII were used to predict the subcellular location of *Giardia* proteins. S, secretory; N, non-secretory; M, mitochondrial; O, other. Exp. ver., experimental verification of protein localization using the pONDRA expression vector. The recombinant tagged proteins were localized by fluorescence microscopy. M, mitosome; ER, endoplasmic reticulum; O, other; ? inconclusive. MEMSAT3 and TMHMM were used to predict transmembrane domains. SGP, predicted soluble proteins are marked with number sign (#). Asterisk (*) is used where no data were available. (**) transformed *Giardia* did not express the recombinant tagged protein.
doi:10.1371/journal.pone.0017285.t002

Protein import

We identified four components that are potentially involved in transporting proteins across the mitosomal membranes: a homologue of a mitochondrial Tom40, which would form a general import pore in the outer mitosomal membrane, and the three essential components of the PAM (presequence translocase-associated motor) complex: Pam18, Pam16 (Fig. S7) and mHsp70. Pam18 and Pam16 form an intimate complex that anchors a population of the matrix Hsp70 to the inner membrane and regulates its activity to drive protein translocation across the inner

Table 3. Putative mitosomal proteins classified by predicted function: protein modification, cztosceletal and motor proteins.

Accession number	Annotation	Identification		Localization				Structure		
		MASCOT	Coverage	MiD	SignalP	Target P	Psort II	MEMSAT3	SGP	TMHMM
		score	peptides				% mito	TM No.		TM No.
Protein modification										
GL50803_8587	Kinase, AGC NDR	22	1	Y	N	O	4%	0	#	0
GL50803_14223	Kinase, NEK	124	2	Y	N	O	13%	0	#	0
GL50803_16824	Kinase, NEK	87	2	Y	N	O		0	#	0
GL50803_17510	Kinase, NEK	25	1	Y	N	O	17%	0	#	0
GL50803_5375	Kinase, NEK	46	1	Y	N	O	17%	0	#	0
GL50803_11775	Kinase, NEK-frag	50	2	Y	N	O	17%	0	#	0
GL50803_7183	Kinase, NEK-frag	22	1	Y	N	O	13%	0	#	0
GL50803_8805	Kinase, SCY1	159	2	Y	N	O	11%	1		0
GL50803_7110	Ubiquitin	360	5	Y	N	O	17%	0	#	0
Cytoskeletal and motor proteins										
GL50803_11654	Alpha-1 giardin	934	17	Y	N	O	13%	1		0
GL50803_7796	Alpha-2 giardin	478	8	Y	N	O	17%	1		0
GL50803_5649	Alpha-10 giardin	294	5	Y	N	O	9%	1		0
GL50803_15097	Alpha-14 giardin	643	9	Y	N	O	4%	0	#	0
GL50803_112079	Alpha-tubulin	394	7	Y	N	O		0	#	0
GL50803_136020	Beta tubulin	841	13	Y	N	O		0	#	0
GL50803_42285	Ciliary dynein heavy chain 11	23	1	Y	N			1		0
GL50803_93736	Dynein heavy chain	29	1	Y	N		13%	0		0
GL50803_16993	FtsJ cell division protein, putative	24	1	Y	N	O	17%	0	#	0
GL50803_102101	Kinesin-3	85	1	Y	N	O	26%	0	#	0
GL50803_21444	Spindle pole protein, putative	63	2	Y	N	O	22%	0	#	0
GL50803_8589	Suppressor of actin 1	81	2	Y	N	O	11%	3		2

Mascot score, Mascot total ion score for the identified protein. Coverage, number of unique peptides per identified protein. MiD, mitosomal distribution. Proteins are marked "Y" if their distributions in fractions #3 and #4 of the Optiprep gradient (measured by the iTRAQ ratio) were within the range between Cpn10 and IscU and the window that extended in both directions by half of the distance between these markers. Proteins with ratios outside of this range are indicated with "N". TargetP and PsortII were used to predict the subcellular location of *Giardia* proteins. S, secretory; N, non-secretory; M, mitochondrial; O, other. Exp. ver., experimental verification of protein localization using the pONDRA expression vector. The recombinant tagged proteins were localized by fluorescence microscopy. M, mitosome; ER, endoplasmic reticulum; O, other; ? inconclusive. MEMSAT3 and TMHMM were used to predict transmembrane domains. SGP, predicted soluble proteins are marked with number sign (#). Asterisk (*) is used where no data were available. (**) transformed *Giardia* did not express the recombinant tagged protein.

doi:10.1371/journal.pone.0017285.t003

membrane [48]. Typically, it functions together with a TIM complex that forms the translocation pore for protein passage across the membrane. In representative organisms from all lineages of eukaryotes, the TIM complex is built from one or two proteins of the Tim17/22/23 family [49]. Surprisingly, we find no evidence for a member of this protein in our proteomics data, and sensitive hidden Markov model searches detected no related sequences in the *Giardia* genome (unpublished, see Methods). In eukaryotes, the Sec61 channel catalyzes protein transport across the endoplasmic reticulum [2], while a highly-related protein called SecY is the translocation channel in the inner membrane of bacteria, including the alpha-proteobacteria from which mitochondria are derived. Interestingly, *Reclinomonas americana* encodes a bacterial-type SecY protein translocation channel in its mitochondrial genome [50], and our proteomics analysis detected what appeared to be contamination of the mitosomal membranes with GiSecY/Sec61. We expressed a tagged version of this protein in *Giardia* but it localized to the endoplasmic reticulum, as expected for a cognate Sec61, rather than to the mitosomes. The nature of the mitosomal inner membrane protein translocation channel remains unknown, and yet must exist given that at least 17 of the proteins detected in the mitosomal proteome are likely to reside in the matrix.

We suggest that Tim23/17/22 protein(s) have been secondarily lost from *Giardia*, given that the these proteins appear to be derived from components of the ancestral endosymbiont [48] and are present in all other groups of eukaryotes including other members of the Excavata [51], particularly *T. vaginalis* (TrichDB, http://trichdb.org/trichdb; our unpublished data). Because there is evidence to suggest that *T. vaginalis* and *G. intestinalis* share a common ancestor [44,52], the absence of a Tim23 homologue in *Giardia* likely reflects the overall simplification of the organelle than a primitive trait. Why has the TIM complex been replaced? In addition to a reliance on ATP hydrolysis mediated by the PAM motor, the TIM complex is powered by the membrane potential through its physical association with the respiratory complexes III and IV [53,54]. *Giardia* mitosomes do not generate a large membrane potential, as shown by their inability to accumulate the routinely used mitochondrial probes that are sensitive to the membrane potential (e.g., mitotrackers, JC-1, our observations). Perhaps any membrane potential that is present, is insufficient to support the function of a TIM23 translocase.

Table 4. Putative mitosomal proteins classified by predicted function: various metabolic processes, lipid metabolism.

Accession number	Annotation	Identification		Localization					Structure		
		MASCOT	Coverage	MiD	SignalP	Target P	Psort II	Exp Ver.	MEMSAT3	SGP	TMHMM
		score	peptides				% mito		TM No.		TM No.
Various metabolic processes											
GL50803_7203	Guanylate kinase	*	*	*	N	M	65%	O	0	#	0
GL50803_3287	Acetyl-CoA acetyltransferase	*	*	*	N	M	22%	O	0	#	0
GL50803_8163	Manganese-dependent inorganic pyrophosphatase, putative	25	1	Y	N	O	22%		0	#	0
GL50803_6497	Metal-dependent hydrolase	30	1	Y	N	O	13%		1		0
GL50803_10311	Ornithine carbamoyltransferase	665	8	Y	N	O	9%		1		0
GL50803_14993	Pyrophosphate-fructose 6-phosphate 1-phosphotransferase alpha subunit	56	1	Y	N	M	35%		1		0
GL50803_15380	CDC8 Thymidylate kinase	*	*	*	N	O	35%	O	0	#	0
Lipid metabolism											
GL50803_9062	Long chain fatty acid CoA ligase 5	279	3	Y	N	O	22%	**	0	#	0
GL50803_21118	Long chain fatty acid CoA ligase 5	25	1	Y	N	O	26%		0	#	0
GL50803_113892	Long chain fatty acid CoA ligase, putative	224	4	Y	N	O	26%		0	#	0
GL50803_7259	CDP-diacylglycerol-glycerol-3-phosphate 3-phosphatidyltransferase	43	1	N	N	M	22%		6		2

Mascot score, Mascot total ion score for the identified protein. Coverage, number of unique peptides per identified protein. MiD, mitosomal distribution. Proteins are marked "Y" if their distributions in fractions #3 and #4 of the Optiprep gradient (measured by the iTRAQ ratio) were within the range between Cpn10 and IscU and the window that extended in both directions by half of the distance between these markers. Proteins with ratios outside of this range are indicated with "N". TargetP and PsortII were used to predict the subcellular location of *Giardia* proteins. S, secretory; N, non-secretory; M, mitochondrial; O, other. Exp. ver., experimental verification of protein localization using the pONDRA expression vector. The recombinant tagged proteins were localized by fluorescence microscopy. M, mitosome; ER, endoplasmic reticulum; O, other; ? inconclusive. MEMSAT3 and TMHMM were used to predict transmembrane domains. SGP, predicted soluble proteins are marked with number sign (#). Asterisk (*) is used where no data were available. (**) transformed *Giardia* did not express the recombinant tagged protein.
doi:10.1371/journal.pone.0017285.t004

Interaction of mitosomes with other cellular compartments

In the *Giardia* mitosomes, we identified a VAMP (vesicle-associated membrane protein)-associated protein, VAP (Table 6). VAPs are involved mainly in membrane trafficking and lipid metabolism. They provide membrane anchors for various lipid binding proteins on the surfaces of the endoplasmic reticulum and Golgi complex [53] and physically interact with SNARE proteins, with FFAT-motif containing lipid transport proteins and microtubules. Like other VAPs, the *Giardia* VAP protein contains an N-terminal domain that includes the VAP consensus sequence [55], a central coiled-coil domain and a C-terminal transmembrane domain with the putative dimerization motif GxxxG (Fig. S8). The presence of a VAP protein has not been reported in mitochondria or other mitosomes so far. In *Giardia*, GiVAP was found within the set of hypothetical proteins with distribution value corresponding to mitosomal proteins (Table 6) and its mitosomal localization was experimentally confirmed (Fig. 4B).

Hypothetical proteins

The set of mitosomal candidates contains 40 proteins annotated as hypothetical proteins. We selected six proteins with high mitochondrial score (Tables 6–7) for the verification of their subcellular localization. Three proteins were confirmed to reside in mitosomes (Table 6, Fig 4): (i) putative VAP (GL50803_15985) that is discussed above, (ii) hypothetical protein GL50803_14939 that contains two predicted transmembrane domains (residues 13–35 and 102–124), and (iii) a putative soluble globular protein GL50803_9296. The latter two proteins seem to be unique for giardia as no orthologues were identified in available databases. Two other hypothetical proteins (GL50803_16596 and GL50803_4768) were observed in the cytosol and in association with kinetosomes, respectively (Table 6, data not shown). The cellular localization of hypothetical protein GL50803_12999 remains inconclusive. Although the protein co-localized with IscU in some vesicles, it was not observed in typical rod-like structure between nuclei (data not shown).

Origin of mitosomes and perspectives

Mitosomes are thought to have evolved several times in different eukaryotic lineages through the reduction of ancestral mitochondria. For example, microsporidians are intracellular parasites allied with Fungi; whereas Fungi typically possess fully equipped mitochondria with large proteomes (>850 proteins) [11,56], only twenty to thirty proteins have been identified from genome analysis of *E. cuniculi* as having similarity to *bona fide* mitochondrial proteins of *Saccharomyces cerevisiae* [15,18,21]. Apicomplexan parasites related to *Plasmodium* also include

Table 5. Putative mitosomal proteins classified by predicted function: miscellaneous.

Accession number	Annotation	Identification		Localization					Structure		
		MASCOT	Coverage	MiD	SignalP	Target P	Psort II	Exp Ver.	MEMSAT3	SGP	TMHMM
		score	peptides				% mito		TM No.		TM No.
Miscellaneous											
GL50803_11953	Coatomer alpha subunit (WD40)	31	1	Y	N	O			0	#	0
GL50803_88765	Cytosolic HSP70	22	1	Y	N	O	4%		1		0
GL50803_112312	Elongation factor 1-alpha	424	10	Y	N	O	4%		1		0
GL50803_12102	Elongation factor 1-gamma	158	3	Y	N	M	13%		1		0
GL50803_28379	Multidrug resistance-associated protein 1	210	4	Y	N	O			0		10
GL50803_16313	Pescadillo (ribosome biogenesis)	52	1	Y	N	M	17%	**	0	#	0
GL50803_15380	CDC8 Thymidylate kinase	*	*	*	N	O	35%	O	0	#	0
GL50803_16354	Protein 21.1	25	1	Y	N	O	4%		0	#	0
GL50803_17288	Protein 21.1	54	2	Y	N	O	4%		0		0
GL50803_23492	Protein 21.1	130	1	Y	N	O	30%		1		0
GL50803_86855	Protein 21.1	22	1	Y	N	O	9%		0	#	0
GL50803_88245	Protein 21.1	23	1	Y	N	O	17%		0	#	0
GL50803_21662	Coiled-coil protein	31	1	N	N	M		**	0	#	0
GL50803_16152	Coiled-coil protein	57	2	Y	N	O			0	#	0
GL50803_8564	Coiled-coil protein	74	3	Y	N	O			0		0
GL50803_9515	Coiled-coil protein	61	2	Y	N	O			0	#	0
GL50803_40244	P24, putative	53	1	Y	N	O	13%		1		1
GL50803_6430	14-3-3 protein	78	2	Y	N	O	13%		1		0
GL50803_8903	Copine I	190	4	Y	N	O	44%	O	0	#	0
GL50803_14225	CXC-rich protein	494	8	Y	Y	S			0		1
GL50803_17476	CXC-rich protein	255	7	Y	Y	S	4%		0		1
GL50803_113656	Cysteine protease	73	2	Y	Y	S			1		1
GL50803_103454	High cysteine membrane protein Group 1	1038	14	Y	Y	S			1		1
GL50803_17328	High cysteine membrane protein Group 2	113	3	Y	Y	S			0		1
GL50803_91099	High cysteine membrane protein Group 2	65	1	Y	Y	S	13%		0	#	1
GL50803_114042	High cysteine membrane protein Group 4	330	5	Y	Y	S			1		1
GL50803_11359	Ribosomal protein S4	31	1	Y	N	O	17%		1		0
GL50803_17411	TCP-1 chaperonin subunit gamma	24	1	Y	N	O			1		0

Mascot score, Mascot total ion score for the identified protein. Coverage, number of unique peptides per identified protein. MiD, mitosomal distribution. Proteins are marked "Y" if their distributions in fractions #3 and #4 of the Optiprep gradient (measured by the iTRAQ ratio) were within the range between Cpn10 and IscU and the window that extended in both directions by half of the distance between these markers. Proteins with ratios outside of this range are indicated with "N". TargetP and PsortII were used to predict the subcellular location of *Giardia* proteins. S, secretory; N, non-secretory; M, mitochondrial; O, other. Exp. ver., experimental verification of protein localization using the pONDRA expression vector. The recombinant tagged proteins were localized by fluorescence microscopy. M, mitosome; ER, endoplasmic reticulum; O, other; ? inconclusive. MEMSAT3 and TMHMM were used to predict transmembrane domains. SGP, predicted soluble proteins are marked with number sign (#). Asterisk (*) is used where no data were available. (**) transformed *Giardia* did not express the recombinant tagged protein.

doi:10.1371/journal.pone.0017285.t005

organisms with mitosomes, such as *Cryptosporidium parvum* and *Cryptosporidium hominis*. Based on genomic analyses, 37–54 proteins have been predicted to reside in these mitosomes [19], of which 18 were detected by mass spectrometry in whole *C. parvum* sporozoites [25].

An intriguing question concerns the nature of the mitochondrial progenitor from which mitosomes of *G. intestinalis* have evolved. *Giardia* is a member of the Excavate group, which has recently been re-considered to belong to the basal groups of eukaryotes based on its mechanism of cytochrome c and c1 biogenesis

Table 6. Putative mitosomal proteins classified by predicted function: miscellaneous - continued; hypothetical proteins.

Accession number	Annotation	Identification		Localization					Structure		
		MASCOT	Coverage	MiD	SignalP	Target P	Psort II	Exp Ver.	MEMSAT3	SGP	TMHMM
		score	peptides				% mito		TM No.		TM No.
GL50803_10330	Tenascin precursor	330	4	Y	Y	S	11%		0	#	0
GL50803_16477	Tenascin-37	178	4	Y	Y	S	17%		1		0
GL50803_16833	Tenascin-like	96	2	Y	Y	S			0	#	0
GL50803_13561	Translation elongation factor	36	1	Y	N	O	13%		1		0
GL50803_15889	UDP-N-acetylglucosamine-dolichyl-phosphateN-acetylglucosamine-phosphotransferase	36	1	Y	Y	S	4%		10		7
GL50803_11521	VSP	198	3	Y	Y	S			1		1
GL50803_137618	VSP	530	9	Y	N	O	4%		2		1
GL50803_11470	VSP with INR	220	3	Y	N	O			2		1
GL50803_6733	Zinc finger domain	55	1	Y	N	S	22%		4		4
Hypothetical proteins											
GL50803_12999	Hypothetical protein	414	5	Y	Y	M		?	2		2
GL50803_14939	Hypothetical protein	133	2	Y	Y	M	30%	M	1		2
GL50803_15985	Hypothetical protein (VAP, VAMP associated protein)	35	1	Y	N	M	13%	M	1		1
GL50803_16596	Hypothetical protein	177	3	N	N	M	30%	O	0	#	0
GL50803_4768	Hypothetical protein	21	1	Y	N	M	57%	O	0	#	0
GL50803_9296	Hypothetical protein	178	4	Y	Y	M	57%	M	0	#	0
GL50803_11237	Hypothetical protein	24	1	Y	N	O	9%		1		0
GL50803_11557	Hypothetical protein	41	1	Y	N	O	17%		1		0
GL50803_11866	Hypothetical protein	25	1	Y	N	O	22%		0	#	0
GL50803_13288	Hypothetical protein	35	1	Y	N	O	9%		1		0
GL50803_13413	Hypothetical protein	95	2	Y	N	O	11%		2		2
GL50803_137685	Hypothetical protein	200	4	Y	N	S			13		9
GL50803_137746	Hypothetical protein	25	1	Y	N	O			0	#	0
GL50803_13922	Hypothetical protein	1121	14	Y	Y	S			1		1
GL50803_14164	Hypothetical protein	23	1	Y	N	O	13%		0	#	0
GL50803_14278	Hypothetical protein	31	1	Y	N	O	13%		0	#	0
GL50803_14660	Hypothetical protein	105	2	Y	N	O	35%		1		0

Mascot score, Mascot total ion score for the identified protein. Coverage, number of unique peptides per identified protein. MiD, mitosomal distribution. Proteins are marked "Y" if their distributions in fractions #3 and #4 of the Optiprep gradient (measured by the iTRAQ ratio) were within the range between Cpn10 and IscU and the window that extended in both directions by half of the distance between these markers. Proteins with ratios outside of this range are indicated with "N". TargetP and PsortII were used to predict the subcellular location of *Giardia* proteins. S, secretory; N, non-secretory; M, mitochondrial; O, other. Exp. ver., experimental verification of protein localization using the pONDRA expression vector. The recombinant tagged proteins were localized by fluorescence microscopy. M, mitosome; ER, endoplasmic reticulum; O, other; ? inconclusive. MEMSAT3 and TMHMM were used to predict transmembrane domains. SGP, predicted soluble proteins are marked with number sign (#). Asterisk (*) is used where no data were available. (**) transformed *Giardia* did not express the recombinant tagged protein.
doi:10.1371/journal.pone.0017285.t006

[25,57]. These and other data have placed the root of eukaryotes between Excavata and Euglenozoa, a group of protists that includes trypanosomatids [58]. In this respect, there is an apparent simplicity in the protein import machinery of the *Giardia* mitosomes that deserves attention (Fig. 5). The proteomics analysis detected in mitosomes a protein recently shown to be Tom40, the protein translocation channel across the outer membrane [25,59]. The current model for the evolution of the TOM complex posits that Tom40 was derived from a beta-barrel protein in the endosymbiont's outer membrane, perhaps of an usher or autotransporter type protein translocase [60]. Because two other proteins: Tom7 and Tom22, have been found in representative species of all other eukaryotic groups [58], the model further suggests that the first TOM complex was composed of Tom40, Tom22 and Tom7. Our proteomics finds no evidence of Tom7 or Tom22 in mitosomes, and sensitive hidden Markov model searches likewise fail to find any proteins encoded in the *Giardia* genome with similarity to Tom7 or Tom22 [25,57]. Whether reflecting a secondary gene loss or the ancestral condition, GiTom40 would appear to be a selectively simple protein translocase. In addition to Tom40, mitochondria contain one other member of the mitochondrial porin family, the voltage-

Table 7. Putative mitosomal proteins classified by predicted function: hypothetical proteins – continued.

Accession number	Annotation	Identification		Localization				Structure		
		MASCOT	Coverage	MiD	SignalP	Target P	Psort II	MEMSAT3	SGP	TMHMM
		score	peptides				% mito	TM No.		TM No.
GL50803_14845	Hypothetical protein	69	2	Y	N	O	4%	0	#	0
GL50803_15084	Hypothetical protein	22	1	Y	N	O		0	#	0
GL50803_16424	Hypothetical protein	117	3	Y	N	O	26.1%	0	#	0
GL50803_16430	Hypothetical protein	32	1	Y	N	O	9%	1		0
GL50803_16998	Hypothetical protein	24	1	Y	N	O	17%	0	#	0
GL50803_17236	Hypothetical protein	69	1	Y	N	M		10		10
GL50803_1937	Hypothetical protein	75	2	Y	N	S		2		2
GL50803_23389	Hypothetical protein	33	1	Y	N	O		4		6
GL50803_28962	Hypothetical protein	39	1	Y	Y	S	4%	1		1
GL50803_29327	Hypothetical protein	111	2	Y	N	O	17%	1		0
GL50803_3021	Hypothetical protein	21	1	Y	N	O	13%	0	#	0
GL50803_32999	Hypothetical protein	98	3	Y	N	O	13%	0	#	0
GL50803_3491	Hypothetical protein	25	1	Y	N	O	30%	1		0
GL50803_6617	Hypothetical protein	350	5	Y	Y	S		1		1
GL50803_7188	Hypothetical protein	926	11	Y	Y	S	13%	3		1
GL50803_7242	Hypothetical protein	69	1	Y	N	O	22%	3		3
GL50803_7244	Hypothetical protein	144	3	Y	N	O	11%	4		3
GL50803_94658	Hypothetical protein	27	1	Y	N	O	13%	0	#	0
GL50803_9503	Hypothetical protein	206	3	Y	N	O	9%	0	#	0
GL50803_9780	Hypothetical protein	333	5	Y	Y	S	11%	0	#	0
GL50803_9861	Hypothetical protein	137	2	Y	N	O	4%	0	#	0
GL50803_10016	Hypothetical protein	265	5	Y	Y	S	22%	1		0
GL50803_111809	Hypothetical protein	34	1	Y	N	O		0	#	0

Mascot score, Mascot total ion score for the identified protein. Coverage, number of unique peptides per identified protein. MiD, mitosomal distribution. Proteins are marked "Y" if their distributions in fractions #3 and #4 of the Optiprep gradient (measured by the iTRAQ ratio) were within the range between Cpn10 and IscU and the window that extended in both directions by half of the distance between these markers. Proteins with ratios outside of this range are indicated with "N". TargetP and PsortII were used to predict the subcellular location of *Giardia* proteins. S, secretory; N, non-secretory; M, mitochondrial; O, other. Exp. ver., experimental verification of protein localization using the pONDRA expression vector. The recombinant tagged proteins were localized by fluorescence microscopy. M, mitosome; ER, endoplasmic reticulum; O, other; ? inconclusive. MEMSAT3 and TMHMM were used to predict transmembrane domains. SGP, predicted soluble proteins are marked with number sign (#). Asterisk (*) is used where no data were available. (**) transformed *Giardia* did not express the recombinant tagged protein.
doi:10.1371/journal.pone.0017285.t007

dependent anion channels (VDAC), which serve to exchange metabolites [61]. The absence of VDAC in *Giardia* mitosomes might reflect the disappearance of many of the metabolic pathways, and the concomitant decrease in metabolite flux across the outer membrane. It is likely that the *Giardia* Tom40, in addition to importing proteins, exchanges ions and small metabolites across the outer mitosomal membrane as has been demonstrated for the yeast Tom40 in mutants lacking VDAC [44,62–64].

Another surprising result, one that can only be explained by a secondary gene loss, is the absence of the outer membrane protein Sam50 in *Giardia*. Sam50 is a component of the SAM (sorting and assembly machinery) complex, which is required for the assembly of both Tom40 and VDAC [48,65]. The apparent absence of Sam50 from the *Giardia* genome and from our proteomics data is unique among eukaryotes. A putative Sam50 homologue has been predicted in the genomes of all eukaryotes, including trypanosomatids [58,65] and mitosome- and hydrogenosome-containing protists (*C. parvum*, *E. cuniculi*, *E. histolytica* and *T. vaginalis*) [66]. Numerous phylogenetic and functional analyses indicate that Sam50 was derived from the Omp85/BamA protein present in the outer membrane of the ancestral, alpha-proteobacterial endosymbiont and it must, therefore, have been present in the earliest mitochondria [44]. It is not clear how *Giardia* Tom40 is assembled within the outer membrane without the assistance of the SAM complex. It is known that even in yeast Tom40 mediates the import of new molecules of Tom40 into mitochondria [67] and it is tempting to speculate that the *Giardia* Tom40 is capable of mediating its own import and membrane insertion, given the highly simplified nature of the TOM complex in mitosomes.

Our proteomics data support the hypothesis that ISC assembly is an important and possibly the only biosynthetic function of *Giardia* mitosomes. Previous phylogenic analyses have indicated that the ISC assembly machinery was obtained from the alpha-proteobacterial endosymbiont; nearly complete ISC assembly machinery is present from trypanosomatids to higher eukaryotes. Therefore, the absence of certain components, such as IscA-1, Iba57, and Ind, in the mitosomal machines (Table 8) is apparently due to a secondary loss of specific target proteins. Noteworthy, we did not identify any proteins that would carry FeS clusters in *Giardia* mitosomes, except for components of the FeS cluster assembly machinery itself. It seems likely then that the main role of

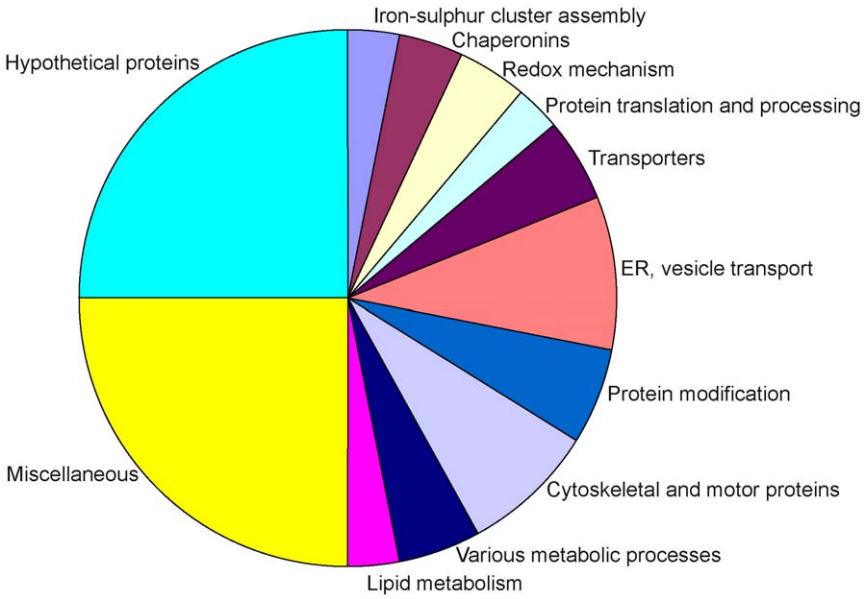

Figure 3. Classification of the identified proteins according to function. Functions were assigned based upon *Giardia*DB annotations, PSI-BLAST analysis and searches of the Pfam database (Tables 1, 2, 3, 4, 5, 6 and 7, Tables S2–S3).
doi:10.1371/journal.pone.0017285.g003

mitosomes could be to export preassembled FeS clusters, or other compounds that are essential for the biogenesis of FeS proteins, to other cellular compartments. In mitochondria, the export of these enigmatic compounds is dependent on the membrane ABC "half-transporter" Atm1 [68] and sulfhydryl oxidase Erv1 [69]. In the mitosome-enriched fraction, we identified four ABC half-transporters by mass spectrometry, and another candidate was predicted based on phyletic profiling of the *G. intestinalis* genome (Table 2). However, compared to other Atm1 homologues, these candidates lack the x-loop with the conserved arginine, which is essential for known Atm1 transporters (Fig. S9). No protein with homology to Erv1 was found by proteomics or by analysis of the *Giardia* genome.

Another remaining question pertains to the source of ATP that is required for the multiple processes identified in mitosomes including FeS cluster assembly and export, organelle division, protein import and protein folding. In *E. histolytica*, it has been shown that a mitochondrial carrier family (MCF) protein localizes to mitosomes and exchanges ATP and ADP across the inner membrane, effecting the import ATP into mitosomes [20]. *E. cuniculi* mitosomes contain a distinct bacterial nucleotide transporter that may fulfill the same function [23,24]. However, our proteomic analysis did not revealed a candidate nucleotide transporter in the mitosomes of *Giardia* leaving open the question of ATP acquisition.

In conclusion, using iTRAQ-based mass spectrometry and bioinformatics we identified 139 candidate mitosomal proteins. Mitosomal localization was confirmed experimentally for 20 of 44 proteins tested, suggesting the complete mitosomal proteome of *Giardia* to be of the order of 50-100 proteins. Previous genome analyses failed to predict any of the novel mitosomal proteins identified here [70]; only by combining quantitative mass spectrometry and bioinformatics were these novel proteins identified. The small proteome of the *G. intestinalis* mitosome indicates a marked reduction in mitochondrial metabolic activity and reduced requirements for organelle biogenesis. These do not mirror the reductions seen in the mitosomal proteome of *Cryptosporidium*, supporting the view that lineage-specific reductions produce organelles with distinct metabolic pathways and specific "short-cut" pathways for biogenesis. Our findings provide new insight into aspects of mitochondrial evolution and the basis from which to begin reconstructing the details of precisely how these organelles are built and replicated to support *Giardia* growth and division.

Methods

Cell culture and fractionation

G. intestinalis strain WB (American Type Culture Collection) was grown in TYI-S-33 medium supplemented with 10% heat-inactivated bovine serum and 0.1% bovine bile [9]. Trophozoites were freeze-detached, washed in PBS and collected by centrifugation. Cells were then resuspended in hypotonic buffer (12 mM MOPS, pH 7.4) and incubated for 15 minutes. The cells were then pelleted at 680× g for 15 minutes, resuspended in the same buffer with DNase I (40 µg/mL) and homogenized by 10 passages through a 25G needle. After homogenization, the isotonicity was immediately restored with the addition of an equal volume of 500 mM sucrose in MOPS buffer. The homogenate was then treated with trypsin (200 µg/mL) for 10 minutes at 37°C to release the organelles from the cytoskeleton. Proteases inhibitors were then added (5 mg/mL of soybean trypsin inhibitor, leupeptin and TLCK), and the homogenate was diluted and centrifuged for 20 minutes at 2760× g to remove cellular debris. The collected supernatant was centrifuged using a Beckman rotor Ti 50 at 20,000 rpm for 30 minutes. After centrifugation, the pellet was collected and washed in SM buffer (250 mM sucrose and 12 mM MOPS, pH 7.4). Next, the pellet was resuspended in 0.5 mL of SM buffer and layered onto a discontinuous density OptiPrep (Axis-Shield PoC AS, Oslo, Norway) gradient, which consisted of 1 ml each of 15%, 20%, 25%, 30% and 50% OptiPrep diluted in 12 mM MOPS buffer. The gradient was centrifuged for 24 h in a Beckman SW 40 rotor at 120,000× g at 4°C. Fractions (1 mL each) were collected, washed and analyzed by immunoblot using a polyclonal rabbit anti-IscU antibody [71,72].

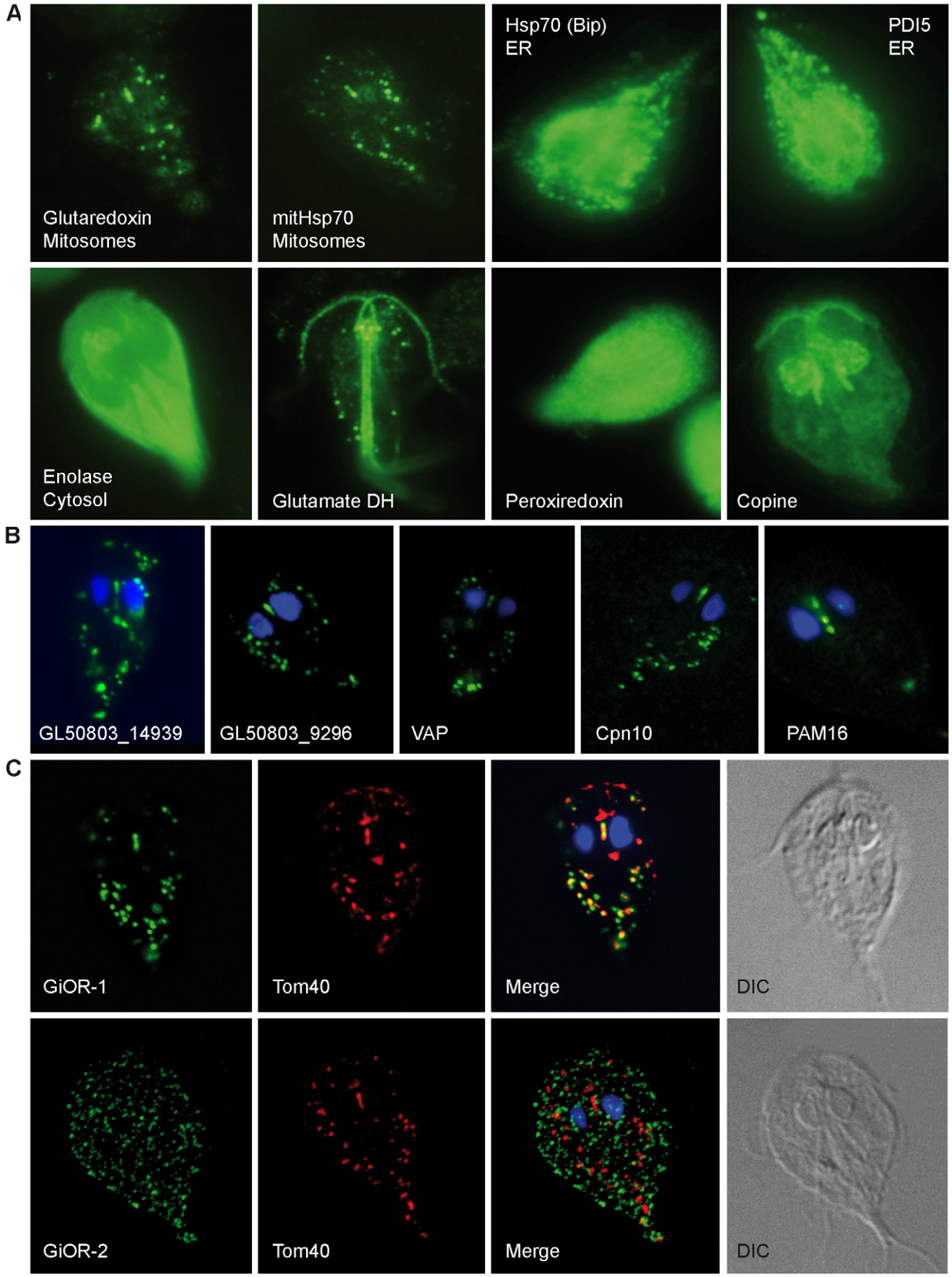
A
Glutaredoxin
Mitosomes
mitHsp70
Mitosomes
Hsp70 (Bip)
ER
PDI5
ER
Enolase
Cytosol
Glutamate DH
Peroxiredoxin
Copine
B
GL50803_14939
GL50803_9296
VAP
Cpn10
PAM16
C
GiOR-1
Tom40
Merge
DIC
GiOR-2
Tom40
Merge
DIC

Figure 4. Sub-cellular localization of selected proteins in *Giardia*. Transformed *G. intestinalis* cells with episomally-expressed HA-tagged proteins. (A) Marker proteins were stained using a mouse anti-HA antibody (green). Grx5, glutaredoxin 5; ER, endoplasmic reticulum; glutamate DH, glutamate dehydrogenase. (B) Predicted mitosomal proteins (GL50803_14939, GL50803_9296, VAP, Cpn10, Pam16) were stained using a mouse anti-HA antibody (green). (C) Cellular localization of tagged diflavin proteins GiOR-1 and GiOR-2 stained with mouse anti HA antibody (green). Tom40 was detected by polyclonal rabbit anti-Tom40 antibody (red).
doi:10.1371/journal.pone.0017285.g004

Mass spectrometry analysis

Samples of two selected fractions (100 µg of total protein each) were precipitated with acetone at −20°C for 2 hours and then pelleted at 13,000× g for 15 min. The proteins were trypsin digested and labeled with sample-specific iTRAQ reagents according to the manufacturer's protocol (Applied Biosystems). Labeled samples were mixed and precipitated with acetone. The pellet was dissolved in 2 M urea in HPLC grade water, and the solution was subjected to IEF using 7 cm immobilized pH 3–10 gradient strips (Bio-Rad) for 20,000 VHrs. The strips were cut into 2-mm wide slices, and peptides were extracted using 50% ACN with 1% TFA. Extracted peptides were then separated using an Ultimate 3000 HPLC system (Dionex) coupled to a Probot micro-fraction collector (Dionex). The samples were loaded onto a PepMap 100 C18 RP column (3 µm particle size, 15 cm long, 75 µm internal diameter; Dionex) and separated with a gradient of 5% (v/v) ACN and 0.1% (v/v) TFA to 80% (v/v) ACN and 0.1% (v/v) TFA over 60 min at a flow rate of 300 nl/min. The eluate was mixed 1:3 with matrix solution (20 mg/mL α-cyano-4-hydroxycinnamic acid in 80% ACN) prior to spotting onto a MALDI target. Spectra were acquired using a 4800 Plus MALDI TOF/TOF analyzer (Applied Biosystems/MDS Sciex) equipped with a Nd:YAG laser (355 nm, 200 Hz firing rate). All spots were measured in MS mode; up to 10 of the strongest precursors were selected for MS/MS analysis, which was performed using collision energy of 1 kV and operating pressure of the collision cell of 10^{-6} Torr. Peak lists from the MS/MS spectra were generated using GPS Explorer v. 3.6 (Applied Biosystems/MDS Sciex) subtraction of baseline enabled with peak width 50, smoothing with Savitsky-Golay algorithm of polynomial order of four and three points across peak, minimum signal to noise (S/N) 3, local noise window 250 m/z, cluster area S/N optimization enabled with S/N threshold 5. Spectra were searched with locally installed Mascot v. 2.1 (Matrix Science) against the *Giardia*DB release 1.3 annotated protein database (4892 sequences, 2663813 residues) and *GiardiaDB* release 1.2 Open Reading Frame translations greater than 50 amino acids (85612 sequences, 9633221 residues). The database search criteria were as follows: trypsin; one missed cleavage site allowed; fixed modifications iTRAQ 4-plex on *N*-terminal- and lysine ε-amino group, methylthiolation of cysteine; variable modification methionine oxidation; peptide mass tolerance of 100 ppm; MS/MS tolerance of 0.2 Da; maximum peptide rank of 1, minimum ion score C.I. (peptide) of 95%.

Table 8. Comparison of iron-sulfur cluster assembly machineries in organisms with mitosomes (*Giardia intestinalis*, *Cryptosporidium parvum*, and *Encephalitozoon cuniculi*), hydrogenosomes (*Trichomonas vaginalis*), and mitochondria (*Trypanosoma brucei*, *Saccharomyces cerevisiae*).

Name	*G. intestinalis*	*C. parvum*	*E. cuniculi*	*T. vaginalis*	*T. brucei*	*S. cerevisiae*
IscS (Nfs)	•	•	•	••	•	•
Isd11	○	○	•	••	•••	•
Nfu	•	○	○	•••	•••	•
IscU (Isu)	•	•	•	•	•	••
IscA1(Isa1)	○	○	○	○	•	•
IscA2 (Isa2)	•	○	○	••••	•	•
Iba57	○	○	○	○	•	•
Ind	○	○	○	•••	•	•
Grx5	•	○	•	○	•	•
Ferredoxin (Yah1)	•	•	•	•••••••	••	•
FOR (Arh1)	○	•	•	○	•	•
Frataxin (Yfh1)	○	•	•	••	•	•
HSP70	•	•	•	•••	••	•♦♦
Dna-J (Jac1)	•	•	•	••	•	•
GrpE	•	•	•	••	•	•
Atm1	○	•	•	○	•	•
Erv1	○	○	•	○	•	•

Filled circles indicate the presence of protein exhibiting homology to the known component of mitochondrial iron-sulfur cluster assembly machinery identified by BLAST searches. Empty circles indicates absence of homologous protein. Mitochondria of *S. cerevisiae* possess three distinct Hsp70 of which Ssq1 is devoted for FeS cluster assembly (filled circle), while Ssc1, and Ecm10 have other fuctions (diamonds). Other eukaryotes possess multifunctional Hsp70. IscS, cysteine desulfurase; Isd11, IscS binding protein; Nfu, IscU, IscA, a scafold proteins; Iba57, IscA binding protein required for [4Fe4S] cluster assembly; Ind, P-loop NTPaseb required for assembly of respiratory complex I; Grx5, glutaredoxin 5; ferredoxin, [2Fe2S] ferredoxin that transport electrons; FOR, ferredoxin oxidoreductase; frataxin, iron binding protein; Hsp70, chaperone; DnaJ, GrpE, co-chaperones; Atm1, ABC half trasnporter; Erv1, sulfhydryl oxidase. Names of proteins used for *S. cerevisiae* orthologs are in brackets.
doi:10.1371/journal.pone.0017285.t008

Table 9. Activity of mitosomal diflavin oxidoreductase GiOR-1.

Substrate	Specific activity [$\mu g.min^{-1}.mg^{-1}$]	Standard deviation
NADPH	0	
NADPH+DCIP	9,053	0,111
NADH + DCIP	0,269	0,034
NADPH + MV	0,450	0,205
NADPH + O_2	0,144	0,042
NADPH+ferredoxin	0	

Electron donors: NADPH, NADH.
Electron acceptors: DCIP, dichlorophenol-indolephenol; MV, methyl viologen; O_2, aerobic conditions; ferredoxin, recombinant *G. intestinalis* [2Fe2S]ferredoxin.
doi:10.1371/journal.pone.0017285.t009

Bioinformatics

Bioinformatics searches based on simple pair-wise alignment Psi-BLAST and hidden Markov models (HMMs) were applied to verify the automatic protein annotations and estimate their functions. Protein sequences (<1000 residues) were submitted (*i*) against a 90% redundancy reduced NCBI nr database for 8 iterations at an e-value cutoff of 10^{-3} and (*ii*) against Pfam 23.0 A+B database of families represented by multiple sequence alignments and hidden Markov models at an e-value of 0.044 (http://pfam.sanger.ac.uk/search). Where noted in the text, tailored HMM libraries were used to search for components of the protein import machinery [16].

Programs based on a combination of artificial neural networks (TargetP) and hidden Markov models (SignalP, both http://www.cbs.dtu.dk/services/) together with PsortII (http://psort.ims.u-tokyo.ac.jp/) were used to predict the subcellular localizations of the proteins. The secondary structures and topologies of alpha-helical integral membrane proteins were predicted using two bioinformatics tools: TMHMM, a program based on hidden Markov models (http://www.cbs.dtu.dk/services/), and Memsat3 (http://bioinf.cs.ucl.ac.uk/memsat/).

Transformation of *G. intestinalis* and immunofluorescence

Selected genes were amplified by PCR from genomic *Giardia* DNA and inserted into the pONDRA plasmid [73]. Table S6 contains a list of primers that were used for subcloning of genes into expression vector. Cells were transformed and selected as described previously [16]. *G. intestinalis* cells expressing the recombinant proteins fused to a hemagglutinin tag (HA) at the C-terminus were fixed and stained for immunofluorescence microscopy with a mouse monoclonal anti-HA antibody. A secondary AlexaFluor-488 (green) donkey anti-mouse antibody was used.

Preparation of recombinant proteins and enzyme assay

The coding region of GiOR-1 and [2Fe2S]ferredoxin was subcloned into pET42b and pET3a (Invitrogen), respectively and

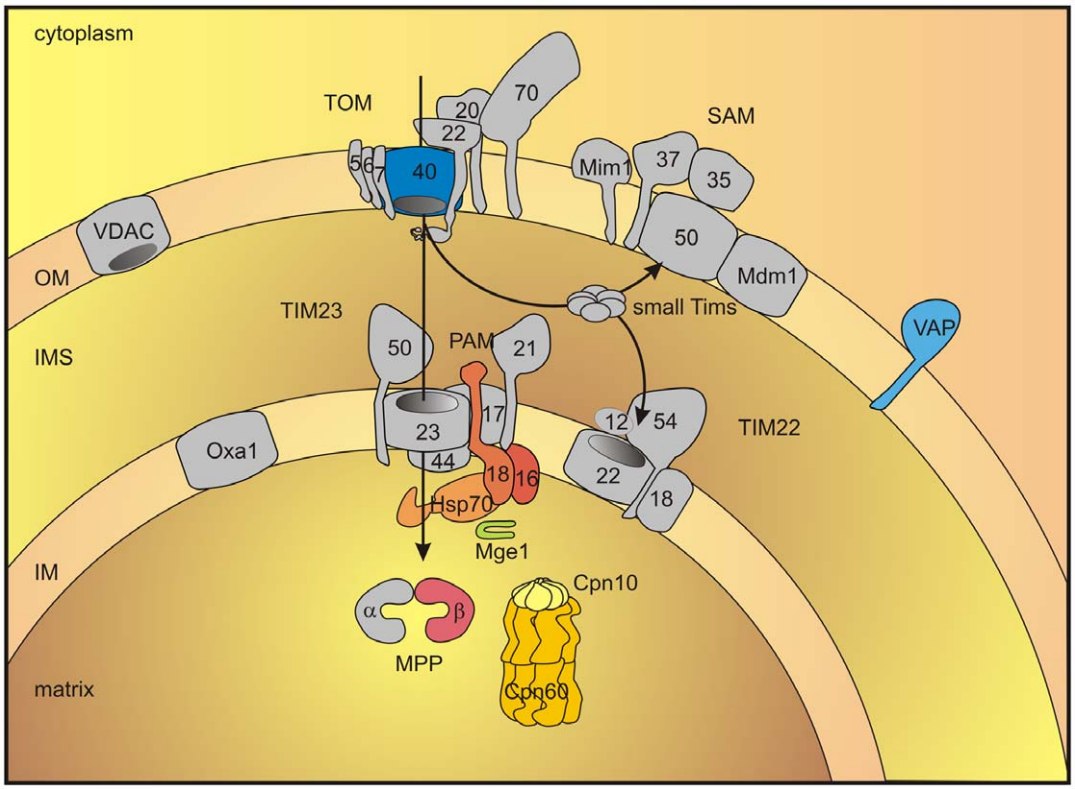

Figure 5. Schematic representation of protein import pathway in the mitosome of *G. intestinalis*. Components identified in mitosome are highlighted by color. Components that are known to participate in the protein import into mitochondria of animals and fungi are shown in grey colour. OM, outer membrane; IMS, intermembrane space; IM, inner membrane; TOM, translocase of outer membrane; SAM, sorting and assembly machinery; TIM, translocase of inner membrane; PAM, presequence translocase-associated motor; VAP, VAMP (vesicle-associated membrane protein)-associated protein; VDAC, voltage-dependent anion channel; MPP, mitochondrial processing peptidase.
doi:10.1371/journal.pone.0017285.g005

expressed in *Escherichia coli* BL21. The bacteria were induced with 0,5 mM IPTG (isopropyl-β-D-thiogalactopyranoside) and grown at 37°C in LB medium. For expression of GiOR-1, the LB medium was supplemented with 250 μM flavin adenine dinucleotide (FAD) and 250 μM flavin mononucleotide (FMN), whereas the LB medium supplemented with 400 μM ferric ammonium citrate was used for expression of ferredoxin. After induction, the cells were incubated overnight at 4°C. The harvested cells were homogenized, and soluble fraction was obtained by centrifugation at 250,000× g, 1 h, 4°C. The his-tagged GiOR-1was affinity purified under native conditions using a Ni-NTA column (Qiagen) according to manufacture's protocol. Ferredoxin was isolated by gel filtration chromatography using a BioLogic HR system (BioRad).

Enzyme activity of GiOR-1 was assayed spectrophotometrically at 25°C in anaerobic cuvettes under nitrogen atmosphere. The activity was monitored as a rate of NADPH or NADH (0,25 mM) oxidation in the presence of dichlorophenol-indolephenol (0,1 mM) or ferredoxin at 340 nm, or as a rate of methyl viologen (2 mM) reduction at 600 nm. NADPH oxidase activity was measured under aerobic conditions at 340 nm. The enzymatic activity was determined in phosphate buffer (100 mM KH_2PO_4/KOH, 150 mM NaCl, pH 7,4). Protein concentration was determined according to Lowry method.

Supporting Information

Figure S1 Sequence alignment of Giardia Nfu against ekaryotic and prokaryotic orthologues. Conserved thioredoxin-like CXXC motif is shown in green. Giardia, *Giardia intestinalis* EAA38809; Trichomonas, *Trichomonas vaginalis*, TVAG_146780; Trypanosoma, *Trypanosoma brucei*, XP_845796; Leishmania, *Leishmania infantum*, XP_001470367; Toxoplasma, *Toxoplasma gondii*, XP_002371042; Plasmodium, *Plasmodium falciparum*, CAX64255; Saccharomyces, *Saccharomyces cerevisiae*, NP_012884; Homo, *Homo sapiens*, AAI13695; Rickettsia, *Rickettsia prowazekii*, NP_221029; Stigmatella, *Stigmatella aurantiaca*, ZP_01463912.
(PDF)

Figure S2 Sequence alignment of *Giardia* IscA against eukaryotic and bacterial orthologs. The conserved cysteine residues are highlited in yellow. Organism names and accession numbers: Giardia, *Giardia intestinalis* GL50803_14821; Trichomonas, *Trichomonas vaginalis* TVAG_055320; Trypanosoma, *Trypanosoma cruzi* XP_806610; Saccharomyces, *Saccharomyces cerevisiae* Q12425; Homo, *Homo sapiens* NP_919255; Arabidopsis, *Arabidopsis thaliana* NP_179262; Chlamydomonas, *Chlamydomonas reinhardtii* XP_001697636; Rickettsia, *Rickettsia conorii* NP_360365; Escherichia, Escherichia coli CAQ32901; Mycobacterium, *Mycobacterium leprae* NP_301657.
(PDF)

Figure S3 Sequence alignment of *Giardia* Jac1 against eukaryotic and bacterial orthologs. The conserved HSP70 interactin site is highlited in green. Organism names and accession numbers: Giardia, *Giardia intestinalis*, GL50803_17030; Trichomonas, *Trichomonas vaginalis*, TVAG_422630; Trypanosoma, *Trypanosoma brucei*, XP_843770; Leishmania, *Leishmania infantum*, XP_001466207; Plasmodium, *Plasmodium falciparum*, CAX64223; Toxoplasma, *Toxoplasma gondii*, XP_002368309; Naegleria, *Naegleria gruberi*, EFC47366; Saccharomyces, *Saccharomyces cerevisiae*, NP_011497; Homo, *Homo sapiens*, AAN85282; Escherichia, *Escherichia* coli, YP_002408666.
(PDF)

Figure S4 Sequence alignment of *Giardia* Mge1 against eukaryotic (Mge1) and bacterial (GrpE) orthologs. The residues in yellow indicate a GrpE dimer interface. HSP70 binding sites are shown in green (Harrison CJ, Hayer-Hartl M, Di Liberto M, Hartl F, Kuriyan J, Crystal structure of the nucleotide exchange factor GrpE bound to the ATPase domain of the molecular chaperone DnaK, Science 1999, 276:431–435. *Giardia intestinalis*, GL50803_1376; *Homo sapiens*, NP_079472; *Saccharomyces cerevisae*, NP_014875; *Escherichia coli*, NP_417104; *Arabidopsis thaliana*, NP_567757; *Trichomonas vaginalis*, XP_001329309; *Trypanosoma brucei*, XP_845338; *Dictyostelium discoideum*, XP_638912; *Bacillus subtilis*, NP_390426; *Halobacterium sp.*, NP_279548.
(PDF)

Figure S5 Sequence alignment of *G. intestinalis* mitosomal oxidoreductase OR-1 (GL50803_91252), against *G. intestinalis* non-mitosomal paralogue OR-2 (GL50803_15897) and structurally related proteins containing flavodoxin-like FMN-binding domain (conserved residua in blue), FAD binding pocket (residua involved in FAD binding in green) and NADP(H) binding site (residua involved in NADP(H) in red). *Saccharomyces cerevisiae* Tah18, DAA11472; *Homo sapiens* NDOR, NADPH dependent diflavin oxidoreductase, AAH15735; *Rattus norvegicus* NOS, nitric oxide synthase, AAC13747; *Rattus norvegicus* CPR, cytochrome P450 reductase, NP_113764; *Escherichia coli* SiR, sulfite reductase, YP_002330508; *Homo sapiens* MSR, methionine synthase reductase, NP_076915; *Trichomonas vaginalis* Hyd, hydrogenase, TVAG_136330; *Leptospira interrogans* FNR, ferredoxin reductase, YP_003372.
(PDF)

Figure S6 Conserved glycine which is present in all GroES and Cpn10 homologues is shown in green. Hsp60 binding site is shown in yellow (van der Giezen M, León-Avila G, Tovar J. (2005) Characterization of chaperonin 10 (Cpn10) from the intestinal human pathogen *Entamoeba histolytica*. Microbiology 151:3107-15). *Giardia intestinalis* GL50803_29500; *Trichomonas vaginalis* TVAG_191660; *Saccharomyces cerevisiae* NP_014663.1; *Homo sapiens* XP_001118014.1; *Leishmania infantum* XP_001470405.1; *Plasmodium falciparum* PFL0740c; Arabidopsis thaliana NP_563961.1; *Dictyostelium discoideum* XP_636819.1; *Mycobacterium tuberculosis* NP_217935.1; *Escherichia coli* NP_290775.1.
(PDF)

Figure S7 Sequence alignment of *Giardia* Pam16 against eukaryotic Pam 16 orthologues and giardial Pam 18 paralogue. Conserved leucin in an interacting hydrofobic pocket is shown in green (D'Silva PR, Schilke B, Hayashi M, Craig EA (2008) Interaction of the J-protein heterodimer Pam18/Pam16 of the mitochondrial import motor with the translocon of the inner membrane. Mol Biol Cell 19:424-32). The typical HPD motif (in blue) present in Pam18 is degenerated in Pam16, in yellow (Mokranjac D, Bourenkov G, Hell K, Neupert W, Groll M (2006) Structure and function of Tim14 and Tim16, the J and J-like components of the mitochondrial protein import motor. EMBO J 25:4675-85). *Giardia intestinalis* Pam 16 GL50803_19230; *Trichomonas vaginalis* TVAG_470110; *Toxoplasma gondii* XP_002367323.1; *Saccharomyces cerevisiae* NP_012431.1; *Neurospora crassa* XP_960477.1; *Pediculus humanus* XP_002428010.1; *Schistosoma japonicum* CAX74438.1; *Homo sapiens* NP_057153.8; *Mus musculus* NP_079847.1; *Xenopus laevis* NP_001084733.1; *Giardia intestinalis* Pam 18 XP_002364144.
(PDF)

Figure S8 Protein sequence alignment of VAP (VAMP-associated protein) homologues. Domain structure is depicted for each represented sequence according to HHPRED (http://toolkit.tuebingen.mpg.de/). Major sperm protein domain, yellow. Coiled-coil domain in green and dimerization motif GXXXG in red. The *G. intestinalis* VAP contains all protein characteristics as described for human homologue.
(PDF)

Figure S9 Sequence alignment of *Giardia* AbcB transporter against mitochondrial and bacterial orthologs. *Giardia intestinalis* AbcB, GL50803_17315; *Saccharomyces cerevisiae* Atm1, NP_014030; *Saccharomyces cerevisae* Mdl1, NP_013289; *Homo sapiens* AbcB7, NP_004290; *Homo sapiens* AbcB10, NP_036221; *Arabidopsis thaliana* Atm3, NP_200635; *Naegleria gruberi* Atm1,XP_002683195; *Rhodobacter sphaeroides* AbcB, YP_001168064; *Halobacterium sp*. AbcB, NP_279266. Walker A part of a conserved ATP-binding motif in yellow; Q-loop part of a conserved ATP-binding motif in green; ABC signature, a conserved sequence specific for ABC proteins in pink; Walker B part of a conserved ATP-binding motif in blue; D-loop part of a conserved ATP-binding motif in red; H-loop part of a conserved ATP-binding motif in purple; X-loop contains a conserved arginine in AbcB transporters (•), which is not present in Giardia sequence, in cyan (Dawson RJ, Locher KP (2006) Structure of a bacterial multidrug ABC transporter. Nature 443:180-185; Bernard DG, Cheng Y, Zhao Y, Balk J (2009) An allelic mutant series of ATM3 reveals its key role in the biogenesis of cytosolic iron-sulfur proteins in Arabidopsis. Plant Physiol 151: 590-602).
(PDF)

Table S1 Complete list of proteins identified by LC MS/MS in mitosomal fractions labelled by iTRAQ reagents.
(PDF)

Table S2 List of *Giardia* proteins within the mitosomal distribution range (MiD) identified by LC MS/MS.
(PDF)

Table S3 Identification of protein families using PfamA+B databases.
(PDF)

Table S4 Predictions of cellular localization.
(PDF)

Table S5 Orthology phylogenetic profililng. Genomes of *G. intestinalis* and *Rickettsia typhi* were compared using orthology phylogenetic profile tool at GiardiaDB.
(PDF)

Table S6 List of primers that were used for subcloning of genes into expression vector pONDRA to investigate subcellular localization of corresponding gene products in *G. intestinalis*.
(PDF)

Author Contributions

Conceived and designed the experiments: JT PLJ PD IH PR. Performed the experiments: PLJ PD PR JP OŠ MŠ MM LV NCB. Analyzed the data: PLJ PD PR JP AJP JT TL. Wrote the paper: JT PLJ.

References

1. Andersson SG, Zomorodipour A, Andersson JO, Sicheritz-Ponten T, Alsmark UC, et al. (1998) The genome sequence of *Rickettsia prowazekii* and the origin of mitochondria. Nature 396: 133–140.
2. Lang BF, Burger G, O'Kelly CJ, Cedergren R, Golding GB, et al. (1997) An ancestral mitochondrial DNA resembling a eubacterial genome in miniature. Nature 387: 493–497.
3. Vaidya AB, Mather MW (2009) Mitochondrial evolution and functions in malaria parasites. Annu Rev Microbiol 63: 249–267. 10.1146/annurev.micro.091208.073424 [doi].
4. Gabaldon T, Huynen MA (2004) Shaping the mitochondrial proteome. Biochim Biophys Acta 1659: 212–220.
5. Gabaldon T, Huynen MA (2007) From endosymbiont to host-controlled organelle: the hijacking of mitochondrial protein synthesis and metabolism. PLoS Comput Biol 3: e219.
6. Pagliarini DJ, Calvo SE, Chang B, Sheth SA, Vafai SB, et al. (2008) A mitochondrial protein compendium elucidates complex I disease biology. Cell 134: 112–123.
7. Tachezy J, Smid O (2008) Mitosomes in parasitic protists. In: Tachezy J, ed. Hydrogenosomes and Mitosomes: Mitochondria of Anaerobic Eukaryotes. Berlin, Heidelberg: Springer-Verlag. pp 201–230.
8. Cavalier-Smith T (1987) The origin of eukaryotic and archaebacterial cells. Ann N Y Acad Sci 503: 17–54:17–54.
9. Tovar J, Leon-Avila G, Sanchez LB, Sutak R, Tachezy J, et al. (2003) Mitochondrial remnant organelles of *Giardia* function in iron-sulphur protein maturation. Nature 426: 172–176.
10. Tovar J, Fischer A, Clark CG (1999) The mitosome, a novel organelle related to mitochondria in the amitochondrial parasite *Entamoeba histolytica*. Mol Microbiol 32: 1013–1021.
11. Katinka MD, Duprat S, Cornillot E, Metenier G, Thomarat F, et al. (2001) Genome sequence and gene compaction of the eukaryote parasite *Encephalitozoon cuniculi*. Nature 414: 450–453.
12. Williams BAP, Hirt RP, Lucocq JM, Embley TM (2002) A mitochondrial remnant in the microsporidian *Trachipleistophora hominis*. Nature 418: 865–869.
13. Riordan CE, Langreth SG, Sanchez LB, Kayser O, Keithly JS (1999) Preliminary evidence for a mitochondrion in *Cryptosporidium parvum*: Phylogenetic and therapeutic implications. Journal of Eukaryotic Microbiology 46: 52S–55S.
14. Hrdy I, Tachezy J, Müller M (2008) Metabolism of trichomonad hydrogenosomes. In: Tachezy J, ed. Hydrogenosomes and Mitosomes:Mitochondria of Anaerobic Euakryotes. Berlin, Heidelberg: Springer-Verlag. pp 114–145.
15. Abrahamsen MS, Templeton TJ, Enomoto S, Abrahante JE, Zhu G, et al. (2004) Complete genome sequence of the apicomplexan, *Cryptosporidium parvum*. Science 304: 441–445. 10.1126/science.1094786 [doi];1094786 [pii].
16. Dolezal P, Smid O, Rada P, Zubacova Z, Bursac D, et al. (2005) *Giardia* mitosomes and trichomonad hydrogenosomes share a common mode of protein targeting. Proc Natl Acad Sci U S A 102: 10924–10929.
17. Goldberg AV, Molik S, Tsaousis AD, Neumann K, Kuhnke G, et al. (2008) Localization and functionality of microsporidian iron-sulphur cluster assembly proteins. Nature 452: 624–628.
18. Putignani L, Tait A, Smith HV, Horner D, Tovar J, et al. (2004) Characterization of a mitochondrion-like organelle in *Cryptosporidium parvum*. Parasitology 129: 1–18.
19. Sanderson SJ, Xia D, Prieto H, Yates J, Heiges M, et al. (2008) Determining the protein repertoire of *Cryptosporidium parvum* sporozoites. Proteomics 8: 1398–1414.
20. Tsaousis AD, Kunji ER, Goldberg AV, Lucocq JM, Hirt RP, et al. (2008) A novel route for ATP acquisition by the remnant mitochondria of *Encephalitozoon cuniculi*. Nature 453: 553–556. nature06903 [pii];10.1038/nature06903 [doi].
21. Xu P, Widmer G, Wang Y, Ozaki LS, Alves JM, et al. (2004) The genome of *Cryptosporidium hominis*. Nature 431: 1107–1112.
22. Mi-ichi F, Abu YM, Nakada-Tsukui K, Nozaki T (2009) Mitosomes in *Entamoeba histolytica* contain a sulfate activation pathway. Proc Natl Acad Sci U S A 106: 21731–21736. 0907106106 [pii];10.1073/pnas.0907106106 [doi].
23. Franzen O, Jerlstrom-Hultqvist J, Castro E, Sherwood E, Ankarklev J, et al. (2009) Draft genome sequencing of *Giardia intestinalis* assemblage B isolate GS: is human giardiasis caused by two different species? PLoS Pathog 5: e1000560. 10.1371/journal.ppat.1000560 [doi].
24. Morrison HG, McArthur AG, Gillin FD, Aley SB, Adam RD, et al. (2007) Genomic minimalism in the early diverging intestinal parasite *Giardia lamblia*. Science 317: 1921–1926.
25. Cavalier-Smith T (2010) Kingdoms Protozoa and Chromista and the eozoan root of the eukaryotic tree. Biol Lett 6: 342–345.
26. Billington D, Maltby PJ, Jackson AP, Graham JM (1998) Dissection of hepatic receptor-mediated endocytic pathways using self-generated gradients of iodixanol (Optiprep). Anal Biochem 258: 251–258. S0003-2697(98)92561-1 [pii];10.1006/abio.1998.2561 [doi].
27. Dunkley TP, Watson R, Griffin JL, Dupree P, Lilley KS (2004) Localization of organelle proteins by isotope tagging (LOPIT). Mol Cell Proteomics 3: 1128–1134. 10.1074/mcp.T400009-MCP200 [doi];T400009-MCP200 [pii].

28. Smid O, Matuskova A, Harris SR, Kucera T, Novotny M, et al. (2008) Reductive evolution of the mitochondrial processing peptidases of the unicellular parasites *Trichomonas vaginalis* and *Giardia intestinalis*. PLoS Pathog 4: e1000243.
29. Rada P, Smid O, Sutak R, Dolezal P, Pyrih J, et al. (2009) The monothiol single-domain glutaredoxin is conserved in the highly reduced mitochondria of *Giardia intestinalis*. Eukaryot Cell 8: 1584–1591. EC.00181-09 [pii];10.1128/EC.00181-09 [doi].
30. Tachezy J, Sanchez LB, Müller M (2001) Mitochondrial type iron-sulfur cluster assembly in the amitochondriate eukaryotes *Trichomonas vaginalis* and *Giardia intestinalis*, as indicated by the phylogeny of IscS. Molecular Biology and Evolution 18: 1919–1928.
31. Vinella D, Brochier-Armanet C, Loiseau L, Talla E, Barras F (2009) Iron-sulfur (Fe/S) protein biogenesis: phylogenomic and genetic studies of A-type carriers. PLoS Genet 5: e1000497. 10.1371/journal.pgen.1000497 [doi].
32. Krebs C, Agar JN, Smith AD, Frazzon J, Dean DR, et al. (2001) IscA, an alternate scaffold for Fe-S cluster biosynthesis. Biochemistry 40: 14069–14080. bi015656z [pii].
33. Pelzer W, Muhlenhoff U, Diekert K, Siegmund K, Kispal G, et al. (2000) Mitochondrial Isa2p plays a crucial role in the maturation of cellular iron-sulfur proteins. FEBS Lett 476: 134–139. S0014-5793(00)01711-7 [pii].
34. Song D, Tu Z, Lee FS (2009) Human ISCA1 interacts with IOP1/NARFL and functions in both cytosolic and mitochondrial iron-sulfur protein biogenesis. J Biol Chem 284: 35297–35307. M109.040014 [pii];10.1074/jbc.M109.040014 [doi].
35. Ding H, Clark RJ, Ding B (2004) IscA mediates iron delivery for assembly of iron-sulfur clusters in IscU under the limited accessible free iron conditions. J Biol Chem 279: 37499–37504. 10.1074/jbc.M404533200 [doi];M404533200 [pii].
36. Bych K, Kerscher S, Netz DJ, Pierik AJ, Zwicker K, et al. (2008) The iron-sulphur protein Ind1 is required for effective complex I assembly. EMBO J 27: 1736–1746. emboj200898 [pii];10.1038/emboj.2008.98 [doi].
37. Sheftel AD, Stehling O, Pierik AJ, Netz DJ, Kerscher S, et al. (2009) Human ind1, an iron-sulfur cluster assembly factor for respiratory complex I. Mol Cell Biol 29: 6059–6073. MCB.00817-09 [pii];10.1128/MCB.00817-09 [doi].
38. Hrdy I, Hirt RP, Dolezal P, Bardonova L, Foster PG, et al. (2004) *Trichomonas* hydrogenosomes contain the NADH dehydrogenase module of mitochondrial complex I. Nature 432: 618–622.
39. Gelling C, Dawes IW, Richhardt N, Lill R, Mühlenhoff U (2008) Mitochondrial Iba57p is required for Fe/S cluster formation on aconitase and activation of radical SAM enzymes. Mol Cell Biol 28: 1851–1861. MCB.01963-07 [pii];10.1128/MCB.01963-07 [doi].
40. Mühlenhoff U, Richhardt N, Gerber J, Lill R (2002) Characterization of iron-sulfur protein assembly in isolated mitochondria. A requirement for ATP, NADH, and reduced iron. J Biol Chem 277: 29810–29816. 10.1074/jbc.M204675200 [doi];M204675200 [pii].
41. Vernis L, Facca C, Delagoutte E, Soler N, Chanet R, et al. (2009) A newly identified essential complex, Dre2-Tah18, controls mitochondria integrity and cell death after oxidative stress in yeast. PLoS One 4: e4376. 10.1371/journal.pone.0004376 [doi].
42. Zhang Y, Lyver ER, Nakamaru-Ogiso E, Yoon H, Amutha B, et al. (2008) Dre2, a conserved eukaryotic Fe/S cluster protein, functions in cytosolic Fe/S protein biogenesis. Mol Cell Biol 28: 5569–5582. MCB.00642-08 [pii];10.1128/MCB.00642-08 [doi].
43. Walsh P, Bursac D, Law YC, Cyr D, Lithgow T (2004) The J-protein family: modulating protein assembly, disassembly and translocation. EMBO Rep 5: 567–571.
44. Chacinska A, Koehler CM, Milenkovic D, Lithgow T, Pfanner N (2009) Importing mitochondrial proteins: machineries and mechanisms. Cell 138: 628–644. S0092-8674(09)00967-2 [pii];10.1016/j.cell.2009.08.005 [doi].
45. Horwich AL, Fenton WA, Chapman E, Farr GW (2007) Two families of chaperonin: physiology and mechanism. Annu Rev Cell Dev Biol 23: 115–145. 10.1146/annurev.cellbio.23.090506.123555 [doi].
46. Elsner S, Simian D, Iosefson O, Marom M, Azem A (2009) The Mitochondrial Protein Translocation Motor: Structural Conservation between the Human and Yeast Tim14/Pam18-Tim16/Pam16 co-Chaperones. Int J Mol Sci 10: 2041–2053. 10.3390/ijms10052041 [doi].
47. Mokranjac D, Bourenkov G, Hell K, Neupert W, Groll M (2006) Structure and function of Tim14 and Tim16, the J and J-like components of the mitochondrial protein import motor. EMBO J 25: 4675–4685. 7601334 [pii];10.1038/sj.emboj.7601334 [doi].
48. Schneider A, Bursac D, Lithgow T (2008) The direct route: a simplified pathway for protein import into the mitochondrion of trypanosomes. Trends Cell Biol 18: 12–18. S0962-8924(07)00297-8 [pii];10.1016/j.tcb.2007.09.009 [doi].
49. Osborne AR, Rapoport TA, van den Berg B (2005) Protein translocation by the Sec61/SecY channel. Annu Rev Cell Dev Biol 21: 529–550. 10.1146/annurev.cellbio.21.012704.133214 [doi].
50. Clements A, Bursac D, Gatsos X, Perry AJ, Civciristov S, et al. (2009) The reducible complexity of a mitochondrial molecular machine. Proc Natl Acad Sci U S A 106: 15791–15795. 0908264106 [pii];10.1073/pnas.0908264106 [doi].
51. Simpson AG, Inagaki Y, Roger AJ (2006) Comprehensive multigene phylogenies of excavate protists reveal the evolutionary positions of "primitive" eukaryotes. Mol Biol Evol 23: 615–625. msj068 [pii];10.1093/molbev/msj068 [doi].
52. van der Laan M, Meinecke M, Dudek J, Hutu DP, Lind M, et al. (2007) Motor-free mitochondrial presequence translocase drives membrane integration of preproteins. Nat Cell Biol 9: 1152–1159. ncb1635 [pii];10.1038/ncb1635 [doi].
53. Lev S, Ben HD, Peretti D, Dahan N (2008) The VAP protein family: from cellular functions to motor neuron disease. Trends Cell Biol 18: 282–290. S0962-8924(08)00120-7 [pii];10.1016/j.tcb.2008.03.006 [doi].
54. Hanada K, Kumagai K, Yasuda S, Miura Y, Kawano M, et al. (2003) Molecular machinery for non-vesicular trafficking of ceramide. Nature 426: 803–809. 10.1038/nature02188 [doi];nature02188 [pii].
55. Reinders J, Zahedi RP, Pfanner N, Meisinger C, Sickmann A (2006) The complete yeast mitochondrial proteome: Multidimensional separation techniques for mitochondrial proteomics. Journal of Proteome Research 5: 1543–1554.
56. Waller RF, Jabbour C, Chan NC, Celik N, Likic VA, et al. (2009) Evidence of a reduced and modified mitochondrial protein import apparatus in microsporidian mitosomes. Eukaryot Cell 8: 19–26. EC.00313-08 [pii];10.1128/EC.00313-08 [doi].
57. Pusnik M, Charriere F, Maser P, Waller RF, Dagley MJ, et al. (2009) The single mitochondrial porin of *Trypanosoma brucei* is the main metabolite transporter in the outer mitochondrial membrane. Mol Biol Evol 26: 671–680. msn288 [pii];10.1093/molbev/msn288 [doi].
58. Dolezal P, Dagley MJ, Kono M, Wolynec P, Likic VA, et al. (2010) The essentials of protein import in the degenerate mitochondrion of *Entamoeba histolytica*. PLoS Pathog 6: e1000812. 10.1371/journal.ppat.1000812 [doi].
59. Alcock F, Clements A, Webb C, Lithgow T (2010) Evolution. Tinkering inside the organelle. Science 327: 649–650. 327/5966/649 [pii];10.1126/science.1182129 [doi].
60. Macasev D, Whelan J, Newbigin E, Silva-Filho MC, Mulhern TD, et al. (2004) Tom22′, an 8-kDa trans-site receptor in plants and protozoans, is a conserved feature of the TOM complex that appeared early in the evolution of eukaryotes. Mol Biol Evol 21: 1557–1564. 10.1093/molbev/msh166 [doi];msh166 [pii].
61. Kmita H, Budzinska M (2000) Involvement of the TOM complex in external NADH transport into yeast mitochondria depleted of mitochondrial porin1. Biochim Biophys Acta 1509: 86–94. S0005273600002844 [pii].
62. Gentle I, Gabriel K, Beech P, Waller R, Lithgow T (2004) The Omp85 family of proteins is essential for outer membrane biogenesis in mitochondria and bacteria. J Cell Biol 164: 19–24. 10.1083/jcb.200310092 [doi];jcb.200310092 [pii].
63. Kozjak V, Wiedemann N, Milenkovic D, Lohaus C, Meyer HE, et al. (2003) An essential role of Sam50 in the protein sorting and assembly machinery of the mitochondrial outer membrane. J Biol Chem 278: 48520–48523. 10.1074/jbc.C300442200 [doi];C300442200 [pii].
64. Paschen SA, Waizenegger T, Stan T, Preuss M, Cyrklaff M, et al. (2003) Evolutionary conservation of biogenesis of beta-barrel membrane proteins. Nature 426: 862–866. 10.1038/nature02208 [doi];nature02208 [pii].
65. Dolezal P, Likic V, Tachezy J, Lithgow T (2006) Evolution of the molecular machines for protein import into mitochondria. Science 313: 314–318.
66. Gatsos X, Perry AJ, Anwari K, Dolezal P, Wolynec PP, et al. (2008) Protein secretion and outer membrane assembly in Alphaproteobacteria. FEMS Microbiol Rev 32: 995–1009. FMR130 [pii];10.1111/j.1574-6976.2008.00130.x [doi].
67. Kispal G, Csere P, Guiard B, Lill R (1997) The ABC transporter Atm1p is required for mitochondrial iron homeostasis. Febs Letters 418: 346–350.
68. Lange H, Lisowsky T, Gerber J, Mühlenhoff U, Kispal G, et al. (2001) An essential function of the mitochondrial sulfhydryl oxidase Erv1p/ALR in the maturation of cytosolic Fe/S proteins. Embo Reports 2: 715–720.
69. Chan KW, Slotboom DJ, Cox S, Embley TM, Fabre O, et al. (2005) A novel ADP/ATP transporter in the mitosome of the microaerophilic human parasite *Entamoeba histolytica*. Current Biology 15: 737–742.
70. Keister DB (1983) Axenic Culture of Giardia-Lamblia in Tyi-S-33 Medium Supplemented with Bile. Transactions of the Royal Society of Tropical Medicine and Hygiene 77: 487–488.
71. Dagley MJ, Dolezal P, Likic VA, Smid O, Purcell AW, et al. (2009) The protein import channel in the outer mitosomal membrane of *Giardia intestinalis*. Mol Biol Evol 26: 1941–1947. msp117 [pii];10.1093/molbev/msp117 [doi].
72. Likic VA, Dolezal P, Celik N, Dagley M, Lithgow T (2010) Using hidden markov models to discover new protein transport machines. Methods Mol Biol 619: 271–284. 10.1007/978-1-60327-412-8_16 [doi].
73. Sun CH, Chou CF, Tai JH (1998) Stable DNA transfection of the primitive protozoan pathogen *Giardia lamblia*. Mol Biochem Parasitol 92: 123–132.

Iron Sulphur cluster assembly in cytoplasm of anaerobic protist *G. intestinalis* - manuscript in preparation

Jan Pyrih[1], Eva Martincová[1], Martin Kolísko[2], Darja Stojanovová[1], Somsuvro Basu[3], Alexander Haindrich[3], Julius Lukeš[3], Andrew Roger[2], Jan Tachezy[1]

1 Department of Parasitology, Charles University in Prague, Vinicna 7, Prague 2, 128 44, Czech Republic

2 Centre for Comparative Genomics and Evolutionary Bioinformatics, Department of Biochemistry and Molecular Biology, Dalhousie University, Sir Charles Tupper Medical Building, 5850 College St., PO Box 15000, Halifax, NS, Canada, B3H 4R2

3 Biology Centre, Institute of Parasitology, 37005, České Budějovice (Budweis), Czech Republic; Faculty of Sciences, University of South Bohemia, 37005, České Budějovice (Budweis), Czech Republic

Abstract

Eukaryotes combined several pathways for Iron/Sulphur (FeS) cluster synthesis for effective delivery of clusters to apoproteins in various cellular compartments. The Cytosolic Iron/Sulphur cluster Assembly (CIA) pathway, which consist of at least eight proteins (Tah18, Dre2, Nbp35, Cfd1, Nar1, Cia1, Cia2, and MMS19), is ubiquitous in all eukaryotic cells.

In yeasts, FeS clusters formation via CIA pathway is fully dependent on mitochondrial FeS cluster assembly machinery (ISC). Atm1 transporter in the inner mitochondrial membrane and Erv1 protein in the intermembrane space of mitochondria were found to be involved in this connection.

Giardia intestinalis, a member of phyla Metamonada, is adapted for living in anaerobic conditions, which is reflected by reduction of its mitochondria to mitosomes. The only pathway conserved within this organelle is FeS clusters synthesis mediated by ISC machinery. Thus, the key function of this organelle is most likely to cooperate with CIA pathway in maturation of FeS proteins in the cytosol. Surprisingly Atm1, Erv1, Dre2, Cfd1 and MMS19 proteins are absent in Giardia genomic data, and only Tah18-like protein (GiOR1), Nbp35, Nar1,Cia1, and Cia2 were identified.

Here, we investigated (i) cellular localization of CIA components in *G. intestinalis*, (ii) distribution of CIA related components in Metamonada and (iii) the origin of Tah18-like proteins in Metamonada. Phylogenetic analysis revealed that two giardia Tah18-like proteins

are evolutionary closely related to Pyruvate: NADP oxidoreductase, and do not cluster with Tah18 orthologues. Moreover, we were unable to identify any orthologue of Tah18 and Dre2 protein in other Metamonada. All CIA machinery components possess exclusive cytoplasmic distribution with exception of Cia2 and two paralogues of Nbp35 protein, which are partially associated with mitosomes. We propose, that dual localization of Cia2 and Nbp35 proteins in Giardia might be important for ISC and CIA connection.

Introduction

Iron/sulphur (Fe-S) clusters are important cofactors found in variety of proteins in all organisms. Their ability of electron transfer is essential in processes such as respiration, photosynthesis, DNA metabolism and translation. ISC (Iron Sulfur Cluster) pathway is present in mitochondria, SUF (Sulfur Activation) pathway in plastids and CIA (Cytosolic Iron/Sulphur cluster Assembly) in cytoplasm enables cluster synthesis in several cellular compartments.

The CIA pathway is ubiquitous in all eukaryotic cells and eight proteins in this pathway have been identified thus far (Tah18, Dre2, Nbp35, Cfd1, Nar1, Cia1, Cia2 and MMS19).

Initially, transient 4Fe4S cluster is assembled on Cfd1-Nbp35 scaffold complex (1). The cluster is then transferred to various apoproteins with assistance of hydrogenase-like protein Nar1 (2) and CIA targeting complex formed by Cia1, Cia2 and Mms19 protein (3-6). In addition, Grx3/Grx4 proteins were reported to assist transfer of clusters from Cfd1-Nbp35 complex to apoproteins (7).

Furthermore, diflavin oxidoreductase Tah18 and FeS protein Dre2 were identified as early situated CIA members (8). It was demonstrated that FMN and FAD cofactors of Tah18 can maintain electron transfer from NADPH to Dre2. Additionally, it was proposed, that these electrons are then transferred to nbp35 protein. Nevertheless, experimental evidence is missing.

In yeasts, it has been shown that FeS cluster formation via CIA pathway is fully dependent on mitochondrial ISC machinery (9-11). Atm1 transporter in inner membrane and Erv1 protein in intermembrane space of mitochondria were found to be involved in this connection. Additionally, thiol containing compound glutathione was shown to stimulate the ATPase activity of ATM1 in yeast (12,13). Nevertheless, the mechanism of export of yet

unknown sulfur containing precursor of FeS cluster across the outer mitochondrial membrane remains unknown.

Although we have detailed information about CIA machinery in yeast, human and plants, some key question in FeS cluster maturation have not been solved yet. Current knowledge is nicely reviewed in (14). For example, molecular mechanism of ISC and CIA connection, the exact role of Tah18 and Dre2 proteins in CIA machinery as well as involvement of reactive cysteine in Cia2 in cluster delivery to apoproteins remains undescribed. Furthermore, only limited information is available about cluster assembly in other eukaryotes. Key components of CIA machinery are highly conserved in eukaryotes (15,16) , but interestingly, Dre2, Erv1 and typical tah18 protein are missing in anaerobes (16).

As an adaptation to anaerobic environment, *Giardia intestinalis*, a member of anaerobic phyla Metamonada, reduces its mitochondria to mitosomes (17,18). The only pathway identified within this organelle is FeS clusters synthesis mediated by ISC. Thus, the key function of this organelle is most likely the cooperation with CIA pathway to maturate FeS proteins in the cytosol and nuclei. Surprisingly Atm1, Erv1 and Dre2 proteins are absent in Giardia genomic data, and only Tah18-like protein GiOR, Nbp35, Nar1 and Cia1 and Cia2 were identified (15,16,19). GiOR protein was recently reported as possible reductases of cytoplasmic cytochromes b5 in Giardia (20).

Here we investigated (i) components of CIA machinery in Metamonada, (ii) localization of CIA proteins in *Giardia intestinalis*.

We have shown, that GiOR protein does not likely functioning as Tah18 and that in Giardia this protein has different cellular role. Moreover, based on EST sequences of various matamonads it is likely, that no Tah18, Dre2, Erv1, Atm1 and MMS19 protein is present in this lineage of excavates. Interestingly, Cfd1 protein is missing in Giardia and Spironucleus but it is present in some basal Metamonads, such as Carpediemonas and Trichomonas.

As expected, we identified Cia1, Nar1 and one paralogue of Nbp35 proteins in cytoplasm of Giardia. Surprisingly, two remaining paralogues of Nbp35 and Cia2 revealed dual mitosomal/cytoplasmic localization. Mitosomal portion of the Nbp35 proteins was identified on the surface of the organelle. On the other hand, Cia2 protein is inner mitosomal protein.

Considering findings that i) Giardia lacks typical ISC and CIA linking proteins and that ii) initial CIA pathway proteins Nbp35 involved in cluster transferring are present on the surface of mitosomes and iii) apparent need for Giardia to link these pathways, we propose that

Nbp35 on the surface of the mitosomes is the functional link between mitosomal ISC pathway and CIA pathway in cytoplasm.

Materials and methods

Cell culture and fractionation

Trophozoites of *G. intestinalis* strain WB (ATCC 30957) were grown in TY S 33 medium (21) supplemented with 10% heat-inactivated bovine serum (PAA Laboratories), 0.1% bovine bile and antibiotics.

Selectable transformation of G. intestinalis

The genes encoding the Giardia CIA proteins (GiardiaDB accession numbers GL50803_15324, GL50803_10969, GL50803_14604, GL50803_33030, GL50803_17550, GL50803_8819) were amplified using PCR and inserted into the plasmid pTG3039 for episomal expression (a kind gift from Frances D. Gillin, San Diego, CA) (22), which was modified for the expression of proteins that contain C-terminal hemagglutinin (HA) tags. The cells were transformed and selected as previously described (23). Genes for co-precipitation experiments (GL50803_8819 and GL50803_91252) were subcloned into pONDRA plasmid with C-terminal biotin acceptor peptide (24). These genes were coexpressed with BirA gene on pTG plasmid as was described previously (24).

Immunofluorescence microscopy

G. intestinalis cells were fixed with 1% formaldehyde as previously described (24). Proteins of interest were stained for immunofluorescence microscopy using a rat monoclonal anti-HA antibody (Roche), rabbit polyclonal GiOR-1 antibody or rat polyclonal Nbp35-1 antibody. Rabbit polyclonal TOM40 antibody (25) and rat Grx5 antibody (25) were used as mitosomal marker proteins. Alexa Fluor 488 (green) donkey anti-rat and anti-rabbit antibodies and Alexa Fluor 594 (red) donkey anti-rabbit and anti-rat antibody (all from Invitrogen) were used as the secondary antibodies. The slides were examined using an Olympus IX81 microscope equipped with an MT20 illumination system. The images were processed using ImageJ 1.41e software (NIH).

Preparation of subcellular fractions and immunoblot analysis

Giardia trophozoites were harvested, washed twice in phosphate-buffered saline (PBS), pH 7.4, and resuspended in SM buffer (250 mM sucrose and 20 mM MOPS [morpholinepropanesulfonic acid], pH 7.2) containing protease inhibitors (Complete EDTA-free Protease Inhibitor Cocktail; Roche). The cells were disrupted by sonication using approximately 15 1-s pulses at an amplitude of 40 (Bioblock Scientific Vibra-Cell 72405) and centrifuged twice at 1,000 × g for 10 min each time to remove any undisrupted cells. The supernatant was centrifuged at 50,000 × g for 30 min to obtain the organellar fraction (ORG). The cell fractionation samples were separated by SDS-13.5% PAGE and transferred to a nitrocellulose membrane. The proteins were detected using same sets of antibodies as was used for immunofluorescence. Anti rabbit IscU antibody was used as an inner mitosomal marker. To determine whether proteins were inserted in the outer mitosomal membrane, ORG fraction (2 mg/ml) in SM buffer supplemented with protease inhibitors was incubated with trypsin (200 μg/ml) for 10 min at 37°C.

Crosslinking, protein isolation and mass spectrometry

We used same strategy as was recently developed for study of proteins involved in mitosomal protein import (24). Same procedure was done with wild type cells and cells overexpressing BirA protein only (both strains used as a negative control). Briefly, the organelar fraction (~15 mg) was used for the crosslinking and protein isolation. The pellet was resuspended in PBS (pH 7.4) supplemented with protease inhibitors (Roche) at a final protein concentration of 1.5 mg/ml. Then, DSP crosslinker (dithiobis [succinimidyl propionate]) (Thermo Scientific) in 25 μM final concentration was added, followed by a 1 h incubation on ice. The sample was centrifuged at 30,000 x g for 10 min at 4°C, and the resulting pellet was resuspended in boiling buffer (50 mM Tris, 1 mM EDTA, 1% SDS, pH 7.4) supplemented with protease inhibitors at a final protein concentration of 1.5 mg/ml. The sample was incubated at 80°C for 10 min. The resulting supernatant was diluted 1:10 in incubation buffer (50 mM Tris, 150 mM NaCl, 5 mM EDTA, 1% Triton X 100, pH 7.4) supplemented with protease inhibitors. Then, 100 μl of streptavidin coupled magnetic beads (Dynabeads® MyOne™ Streptavidin C1, Invitrogen) was mixed with the sample and incubated overnight at 4°C with gentle rotation. The beads were then subjected to the following washes: 3 times for 5 min each in incubation buffer supplemented with 0.1% SDS, once for 5 min in boiling buffer, once for 5 min in washing buffer (60 mM Tris, 2% SDS, 10% glycerol) and twice for 5 min each in incubation buffer supplemented with 0.1% SDS. Finally, proteins were eluted

from the beads in SDS PAGE sample buffer supplemented with 20 mM biotin for 5 min at 95°C. The eluate was resolved by SDS PAGE and stained with Coomassie brilliant blue. The gel was cut, destained, trypsin digested and analyzed on a mass spectrometer.

Mass spectrometry and MS/MS analyses

Spectra were acquired using a 4800 Plus MALDI TOF/TOF analyzer (Applied Biosystems/MDS Sciex) equipped with an Nd:YAG laser (355 nm) with a firing rate of 200 Hz. The MS/MS analyses were performed as previously described (26). Data analysis were performed using Scaffold software version 4.4.6 (Proteome Software, Portland, OR, USA). Same filtering strategy for data analysis as was recently used in analysis of mitosomal import machinery was performed (24). We took advantage of the fact that in enriched fraction of mitosomes huge contamination mainly from endoplasmic reticulum is present. As those proteins are highly abundant in the fraction these are preferentially measured in negative control. Interestingly, no known mitosomal protein was measured in any negative control. Therefore, we extracted all proteins identified in negative controls.

Bioinformatic analyses

To identify the co-purified proteins, their amino acid sequences were analyzed by BLASTP against the NCBI nr database and using the following algorithm: HHpred at http://toolkit.tuebingen.mpg.de/hhpred# (27). For phylogenetic analysis of Tah18 and Nar1 like proteins in eukaryotes, protein sequences were retrieved using protein BLAST searches (28) against a nonredundant GenBank protein database or in sequence data of various metamonads (data from Andrew Roger lab). The sequences were aligned using the Mafft program (29). Columns were stripped out using BMGE software with default settings (30). Best substitional model (LG+G4+I) was calculated using IQ tree program (31). Phylogenetic analysis was performed using PhyML 3.0 (32) and MrBayes (33). Support values are shown next to the branches as the maximum-likelihood bootstrap support (PhyML) or posterior probabilities (Mr Bayes).

Trypanosome cell culture

Procyclic T. brucei 29-13 were cultured in SDM-79 medium (34) containing 10% fetal bovine serum, 15 μg ml−1 geneticin and 50 μg ml−1 hygromycin. The GiOR-1 and GiOR-2 genes were cloned into pABPURO (possessing HAx3 tag) vector. The generated GiOR-1-pABPURO and GiOR-2-pABPURO constructs were linearized using NotI and electroporated individually into the TbTah18-TbDre2 RNAi double knockdown PS cells (35) using BTX electroporator, as described elsewhere (36). Positive transfectants were selected by clonal dilution using puromycin as a marker. RNAi was induced by the addition of tetracycline (1 μg ml^{-1}) and with the presence of puromycin (1 μg ml^{-1}). The GiOR proteins were subsequently expressed. Cell densities were measured using a Beckman Coulter Z2 counter every 24 h over a period of 10 days after induction.

The cytosolic and mitochondrial fractions were obtained by the digitonin fractionation (37). Aconitase activity was measured, in both subcellular compartments, spectrophotometrically at 240 nm via the production of cis-aconitate from isocitrate (38).

Results

CIA components in Metamonads

We performed homology searches for the CIA components in metamonads. Genomic data are available for *G. intestinalis*, *T. vaginalis* and *Spironucleus salmonicida*. For other metamonads, only EST data are available. We were able to identifying majority of CIA components (Fig1). In all metamonads Dre2 and MMS19 is most likely missing (with exception of divergent MMS19 homologue in Trimastix). Grx3 or Grx4 homologues are not present as well. On the other hand, Nbp35, Nar1, Cia1 and Cia2 are present ubiquitously. Absence of some of these key components in Trimastix, *Spironucleus vortens*, Ergobibamus and Carpediemonas-like organism (CLO NY171) is most likely due to insufficient sequence data. Only one protein revealed different distribution in Metamonads. We identified Cfd1 homologue in *T. vaginalis*, *C. membranifera*, CLO NY171 and *Chilomastix cuspidate*, while in other metamonads, this protein is missing, including genomic database of Giardia and Spironucleus. As latter are more derived we propose that Cfd1 was present in ancestor of all metamonads and then secondarily lost. The presence of Tah18 is most challenging task due to

the presence of other highly similar groups of proteins in eukaryotes. Although classical Tah18 homologue is missing in Metamonads, we identified unknown proteins with similar domain organization. Interestingly, in some Metamonads, Tah18-like protein is C-terminally fused to hydrogenase like protein domain (Figure 1).

Furthermore, we searched for ISC and CIA linking proteins Erv1 and ATM1 and interestingly we were unable to identify any homologue of ERV1 or clear homologue of ATM1, although ABC transporters with such possible function are present. As Tah18, Dre2, MMS19, Erv1, ATM1 and Grx3/Grx4 proteins are present in other member of phylum Excavata, we assume that the absence of this component in metamonads is due to the secondary loss.

Tripeptide glutathione (GSH) was identified as a compound important for cytosolic FeS synthesis. In Giardia, glutaredoxin 5 protein was characterized and it was shown that GSH is important for the glutaredoxin 5 protein stability. GSH synthesis proteins, Glutathione synthase and Glutamate cysteine ligase are present in Giardia as well. Surprisingly, in *Trichomonas vaginalis* and *Spironucleus salmonicida* the GSH synthesis enzymes and glutaredoxins are missing.

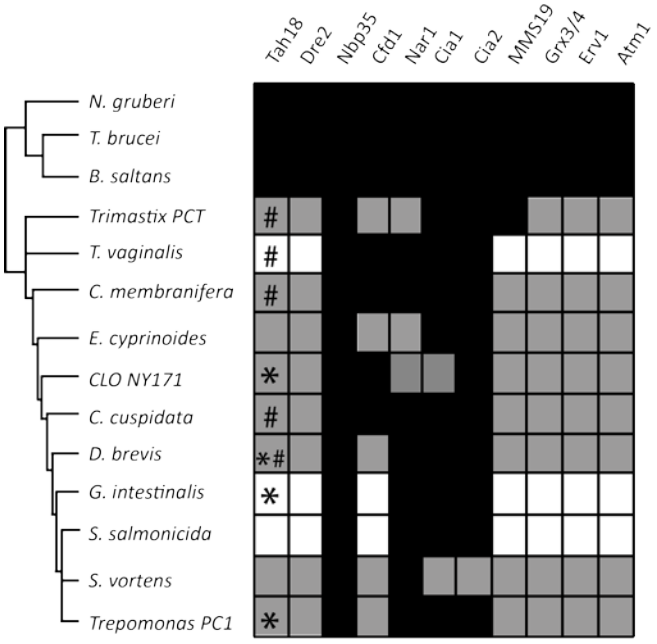

Fig. 1

Distribution of CIA machinery components in Metamonads

In other excavates, entire CIA pathway is present. However, in Metamonads, this pathway is reduced only to minimal set of proteins: Nbp35, Cfd1, Nar1, Cia1 a Cia2. Presence of ortholog is denoted by black shading. Absence is visualized by white color. Grey represents a

missing gene in given EST database. For Tah18-like orthologue, the presence of similarly organized protein alone or fused with hydrogenase-like domain is marked with asterix or # respectively. Relationships between different eukaryotic groups is consensus of current opinion (39). Grey mark in case of these ubiquitous CIA proteins is most likely caused by insufficient EST dataset.

Localization of CIA pathway components in Giardia

In Giardia we found one gene for Nar1, Cia1 and Cia2. Interestingly, we identified three genes for nbp35 (Nbp35-1,Nbp35-2 and Nbp35-3). We expressed all giardia CIA machinery components fused with C-terminal hemaglutinine (HA) tag to investigate their subcellular localization. As expected, we observed cytoplasmic localization for Nar1, Cia1 and for one nbp35 protein (Nbp35-3) (Fig. 2), which is in agreement with the distribution of these proteins in other eukaryotes. These data were then confirmed by sub-cellular fractionation (Fig 2B).

Surprisingly, two Nbp35 proteins (Nbp35-1 and Nbp35-2) possess dual cytoplasmic/ mitochondrial localization. We further explored localization of these proteins by sub-cellular fractionation followed by protease protection assay. In organellar fraction there is just faint band in case of Nbp35-1 (or band is nearly undetectable in case of Nbp35-2) and this band disappears after addition of trypsin (Figure 2B). This leads us to conclusion that these proteins are most likely partially in cytoplasm and partially associated with the outer mitosomal membrane. Faint or missing bands in ORG fraction is most probably due transient interaction between nbp35 and mitosomes, which was likely disrupted during fractionation procedure and washing steps. This dual localization was in case of nbp35-1 confirmed using polyclonal antibody (Fig 2A).

Most striking difference in CIA machinery of Giardia and other eukaryotes is partial mitosomal distribution of Cia2 protein. This proteins is usually localized in cytoplasm, where it is considered to cooperate with Cia1 and Nar1. This is most likely true for Cia2 present in cytoplasm of Giardia. However, based on protease protection assay, the fraction of Cia2 protein is additionally localized within the mitosome. (Fig 2B).

Localization of Tah18-like proteins in Giardia was already characterized. GiOR-2 protein was identified in surface associated vesicules and GiOR-1 displays mitosomal pattern, but its exact topology in mitosome was not described (19). Therefore, we investigated the localization of

GiOR-1 more in detail, due to its possible ability to interact with mitosome-associated CIA components. Based on protease protection assay, protein is situated within the mitosome (Fig 2B). Data was then strengthen by polyclonal antibody raised against GiOR-1 protein. Protease protection assay and immuno-fluorescence revealed that the localization of native GiOR-1 protein is identical to its HA-tagged version (Figure 2A,B).

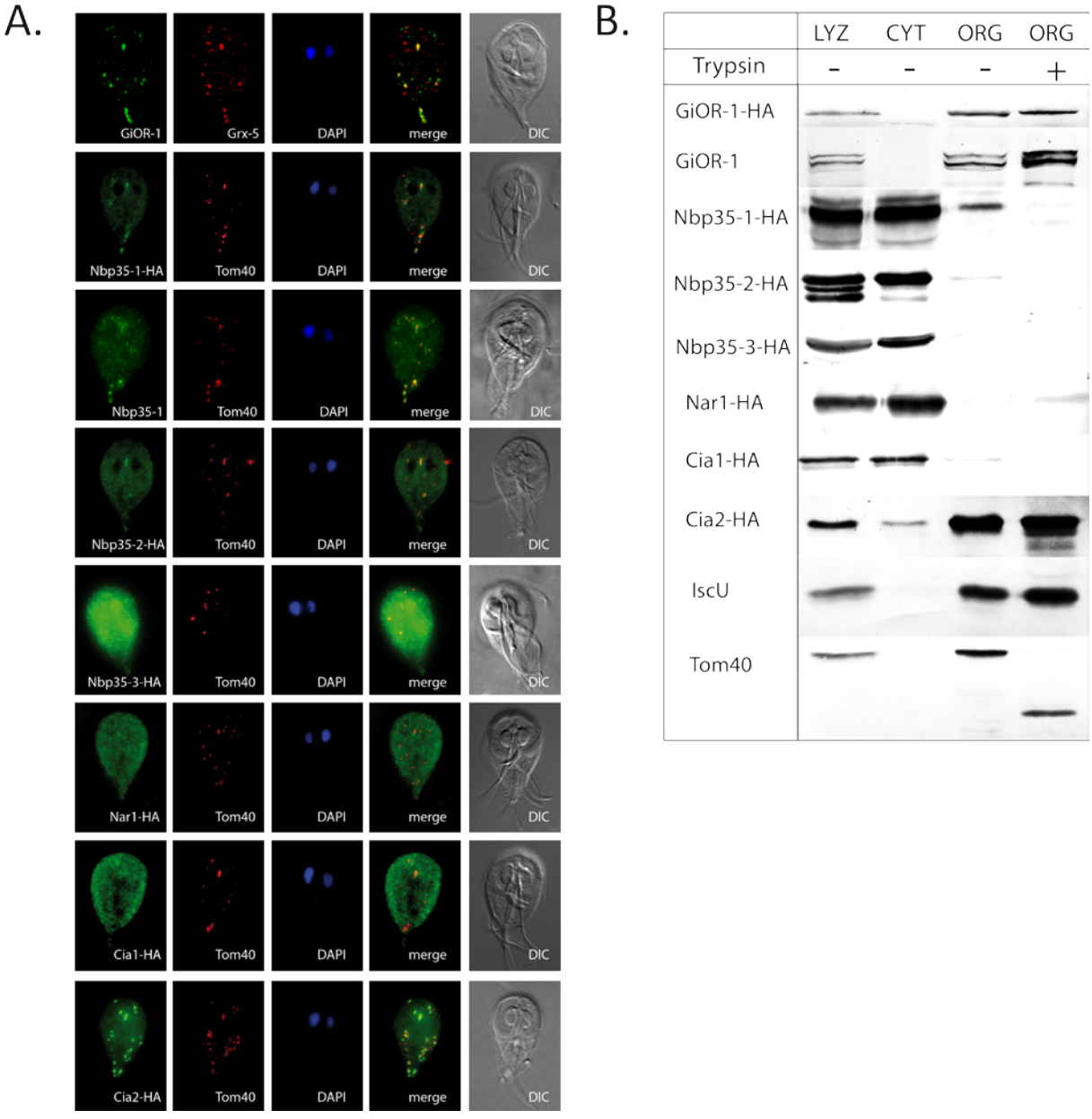

Fig 2 Subcellular distribution of CIA pathway proteins in Giardia

A. Localization of proteins of CIA pathway in Giardia. Anti HA rat antibody and anti-rat Alexa Fluor 488 (green) were used to detect HA-tagged proteins. GiOR-1 protein was detected using specific GiOR-1 rabbit antibody and anti-rabbit Alexa Fluor 488 (green). Anti

Nbp15324 rat antibody and anti-rat Alexa Fluor 488 (green) was used to inspect Nbp15324 distribution in wild type cells. Grx5, mitosomal marker protein detected by anti-Grx5 specific rat antibody and anti-rat Alexa Fluor 594 (red) antibodies. Tom40, mitosomal marker protein was detected by anti-Tom40 specific rabbit antibody and anti-rabbit Alexa Fluor 594 (red) antibodies. Nuclei were stained with DAPI (4=,6-diamidino-2-phenylindole) (blue). DIC, differential interference contrast.

B. Subcelullar fractionation followed by protease protection assay. Presence or absence of trypsin is symbolized by – or + mark. LYS, cell lysate; CYT, cytoplasm; ORG, organellar fraction. Rat anti-HA and Rabbit anti-GiOR-1, IscU and Tom40 antibody were used for detection. Wild type form of GiOR-1 protein has the same pattern as Ha-tagged version of the protein. IscU, misomal matrix marker protein. Tom40, an outer mitosomal membrane marker protein.

Intramitosomal distribution of Cia2 and GiOR-1 proteins

Technique for mitosome fractionation is currently unavailable and we failed to establish it. In order to better understand the topology of GiCia2 and GiOR-1 protein within the mitosome we performed the in vivo-biotynilation assay followed by precipitation of interaction proteins. This technique was recently established for Giardia (24). Briefly, protein of interest is fused with Biotin acceptor peptide and the desired construct is then tranfected in cell line of Giardia, where biotin ligase is co-expressed. Protein of interest is then biotinilated *in vivo* and interacting proteins are then crosslinked by membrane permeable DSP crosslink reagent and purified by streptavidin coupled magnetic beads. Due to the high affinity of streptavidin to biotin, beads can be washed up to 2% of SDS resulting in extremely pure final sample.

We identified typical mitochondrial matrix protein set when we purified interacting proteins of GiOR1 (Fig 3A). These proteins were previously precipitated with matrix mitosomal proteins (Tim44 and Pam18) as well (24). Therefore, we suppose that GiOR-1 protein is localized in the mitosomal matrix.

Interestingly, after co-precipitation of GiCia2 protein from mitosome containing fraction, we did not identify any known mitosomal matrix proteins (Fig 3B). However, from 11 proteins identified, 10 were previously identified by co-precipitation with mitosomal outer membrane proteins (Tom40 and GiMOMP35) (24). Both these proteins have transmembrane domains and they are facing both cytoplasm and IMS space. Sharing the interactome with the proteins

facing mitosomal inter-membrane space together with the fact that the Cia2 is present within the organelle suggest, that mitosomal fraction of Cia2 is present in inter-membrane space of the mitosome.

A.

Name of the protein	G.I. number	TM	UP	Pam 18	Tim 44	Hsp 70	Tom 40	Mom 35	Cia 2
GiOR-1	GL50803_91252	0	19			■			
Hsp70	GL50803_14581	0	13	■	■	■	■	■	
Tim44	GL50803_14845	0	7	■	■	■			
Hypothetical	GL50803_3491	0	6		■	■			
Glutaredoxin 5	GL50803_2013	0	2	■	■	■			
Nfu	GL50803_32838	0	4	■				■	
Ferredoxin	GL50803_27266	0	1		■	■		■	
GPP	GL50803_9478	0	3	■	■	■	■		
IscS	GL50803_14519	0	2		■	■	■		
Cpn60	GL50803_103891	0	2	■	■	■	■		
Hypothetical	GL50803_16506	0	1						
Hypothetical	GL50803_5908	0	2						
Thioredoxin Red	GL50803_9827	0	1						
S/T protein Kinase	GL50803_92741	0	1	■	■				
Hypothetical	GL50803_16471	0	1						

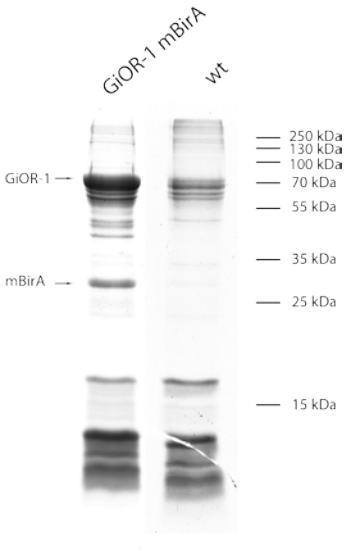

B.

Name of the protein	G.I. number	TM	UP	Pam 18	Tim 44	Hsp 70	Tom 40	Mom 35	GiOR 1
Cia2	GL50803_8819	0	10				■		
Hypothetical	GL50803_17249	0	15				■	■	
Hypothetical	GL50803_113603	0	9			■		■	
Carboxy peptidase (putative)	GL50803_10976	0	5			■	■	■	
Protein kinase	GL50803_16824	0	1			■	■	■	
Na/K transporting ATPase	GL50803_96670	8	3			■	■	■	
Hypothetical	GL50803_94542	1	3			■		■	
Hypothetical	GL50803_7723	0	3			■	■	■	
Multidrug MFS transporter	GL50803_8444	11	3			■	■	■	
Myeloid leukemia factor	GL50803_16424	0	2	■	■	■	■	■	
Hypothetical	GL50803_16648	0	2			■	■	■	
Hypothetical	GL50803_16273	0	1						

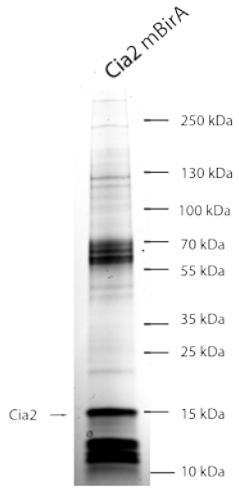

Fig 3 Coprecipitation of GiOR-1 and Cia2 interacting proteins in mitosome

A. List of proteins co-precipitated with biotynilated GiOR-1 and their distribution in previously published mitosomal proteins interactomes. GPP, Giardia processing peptidase; IscS, cysteine desulphurase; Red, reductase; S/T, Serine/Threonin; SDS-page gel used for Mass spectrometry analysis is dispayed, GiOR-1 protein and mBirA protein are highlighted by arrows. Molecular weight is indicated. GiOR-1 mBirA, sample of eluted proteins from Giardia cells expressing GiOR-1 protein with biotin accessory peptide and mBirA enzyme; wt, sample of eluted proteins from wild type cells.

B. List of proteins co-precipitated with mitosomal portion of biotynilated Cia2 protein and their distribution in previously published mitosomal protein interactomes. Na/K, Sodium/potassium. Cia2 protein is highlighted by arrow in SDS-page used for mass spectrometry analysis.

TM, number of transmembrane domains based on TMHMM transmembrane prediction software; UP, number of unique peptides identified for given protein. Pam18, Tim44, Hsp70, Tom40, Mom35, Cia2, GiOR-1 proteins detected in Pam18, Tim44, Hsp70, Tom40, GiMOMP35 and Cia2 interactomes. Presence of proteins precipitated with GiOR-1 in previously published interactomes is denoted by black color, absence by white. G.I. numbers represents gene ID in giardiadb.org database.

Functional and evolutional characterization of Tah18 protein in Metamonads

CPR domain (cytochrome p450 reductase) found in Tah18 homologues is a common domain of various eukaryotic proteins (8). It enables electron transfer to redox center of acceptor proteins. Methionine synthase reductase reduces Co^{2+} containing cofactor center in Methionine synthase, Cytochrome p450 reductase reduces heme in cytochrome p450 and Tah18 reduces FeS cluster in Dre2 protein. This domain is also part of several fusion proteins, such as Nitric oxide synthase in metazoans and Pyruvate : NADP+ oxidoreductase (PNO) enzyme in various anaerobes.

In Giardia, clear homologues of these enzymes are missing and only two CPR domain containing proteins GiOR-1 and GiOR-2 were found (19). Interestingly, no suitable redox partners for these proteins are present in genomic data so far. Previously, it was described that these proteins have cytochrome b5 reductase activity (20). However, at least for inner mitosomal GiOR-1 protein it is unlikely to interact with cytoplasmic cytochromes b5 in Giardia. Thus, measured activities can be just artificial due to the in vitro experiment conditions.

Therefore we tested the ability of GiOR proteins to rescue Tah18 dependent activity in CIA pathway of *Trypanosoma brucei*. When both TbTah18 a TbDre2 protein expressions were lowered, we observed just slight growth rescue phenotype when GiOR proteins were expressed (FigS1A). However, strong rescue phenotype was measured in activity of cluster dependent cytosolic enzyme aconitase (FigS1B). Therefore we propose that GiOR proteins can substitute Tah18 protein in *T. brucei*.

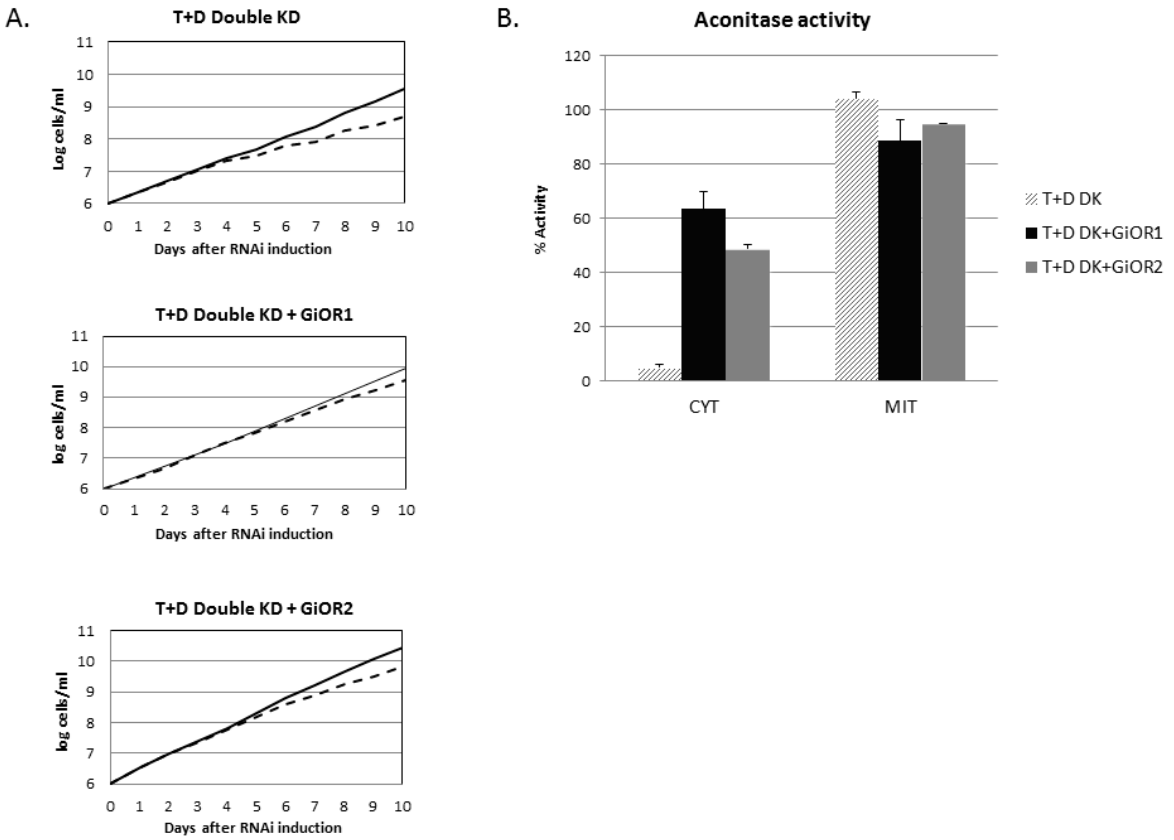

FigS1 GiOR rescue experiment in *Trypanosoma brucei*

Tah18 and Dre2 knockdown phenotype can be rescued by expressing of GiOR-1 and GiOR-2 proteins. A. Growth of *T. brucei* RNAi cell lines is partially rescued by expression GiOR proteins. Cumulative density of the cells is indicated by solid line (non-induced) or broken line (induced). T+D Double KD, TbTah18 and TbDre2 double RNAi inducible knockdown strain; + GiOR1(2), cells expressing GiOR1(2) protein;

B. Aconitase activity is restored in cytoplasm of *T.brucei* RNAi cell lines upon expression of GiOR proteins. Measurement was performed after 6 days of RNAi induction. Aconitase activity in mitochondria (negative control) is not affected due to CIA independent cluster insertion via ISC pathway. T+D DK, TbTah18 and TbDre2 double RNAi inducible knockdown strain; CYT, cytoplasmic fraction; MIT, mitochondrial fraction

However, in Giardia, suitable redox partner for Tah18 dependent activity is missing as Dre2 is not present in genomic data. Additionally, both GiOR proteins have non cytoplasmic distribution necessary for functioning as an electron donor for Nbp35 proteins. Accordingly, it

is thus likely that Tah18 dependent activity of GiOR proteins in *T. brucei* is artificial and that these proteins have different cellular role in Giardia.

Then we analyzed the evolution of GiOR-1 proteins to investigate the possible activity of the protein. *Giardia intestinalis* is an example of extreme reduction in number of coding proteins and is known to possess highly divergent protein sequences. As a consequence it is rather difficult to classify GiOR proteins to different diflavin reductase classes. Previous studies revealed similarity of GiOR proteins to C-terminal domain of PNO enzyme (15). Nevertheless, the bootstrap support was below 50. Hence, we performed similar analysis, but we added sequences from other metamonads to better support origin of GiOR proteins in *Giardia*.

First we searched for GiOR homologues in other metamonads. We identified similarly organized genes in Trepomonas and CLO NY171. Interestingly in Trichomonas, Carpediemonas, Trimastix and Chilomastix we were able to identify just fusion genes of CPR with hydrogenase domain. Surprisingly, in Dysnectes we identified both fusion and only CPR domain containing genes. The fusion protein structure was already identified in *T. vaginalis* by Basu et al. Authors suggested that it is a fusion of hydrogenase-like protein Nar1 and Tah18 gene (16). Nevertheless, this statement was not supported by any phylogenetic analysis.

Our phylogenetic analysis revealed that GiOR proteins in Giardia cluster with CPR-hydrogenase fusion proteins in other metamonads and that this protein lineage is indeed closely related to PNO enzyme (Figure 4). Same is true for fusion proteins in *Trichomonas vaginalis* and other metamonads, therefore hypothesis of Tah18 and Narf fusion is most likely not correct.

Moreover, when we searched for the phylogenetic origin of N-terminal hydrogenase-like domain in metamonads fusion proteins, we realized, that these proteins are derived from hydrogenases and not from Nar1 protein (Fig S2). Although motif for H cluster, which is essential for proper function of hydrogenase (TSCCP) is missing in Trichomonas fusion proteins, this motif is present in other metamonads and those hydrogenase domain are most likely active.

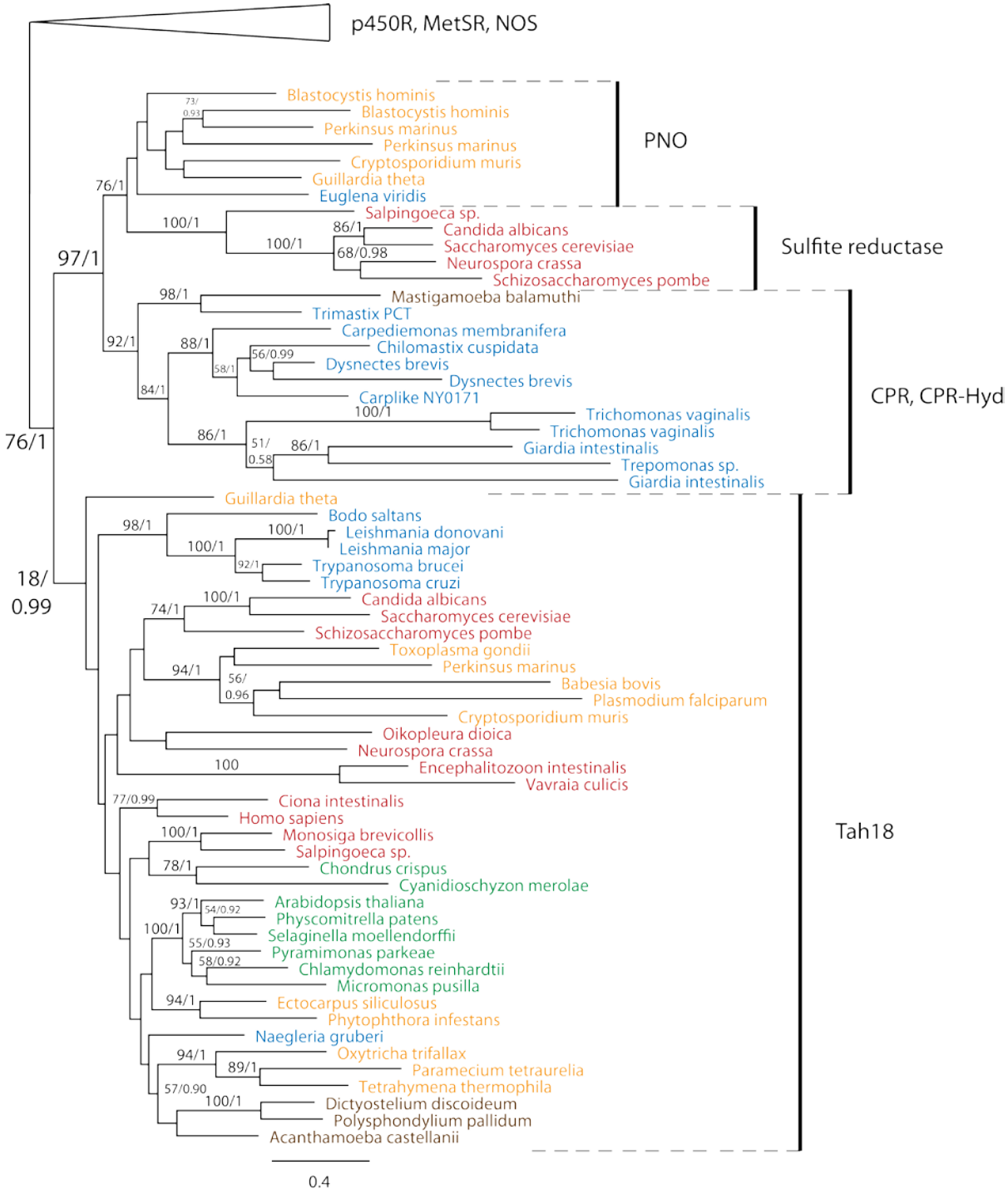

Fig 4. Gene tree of CPR domain containing proteins

Maximum likelihood phylogeny of CPR domain containing proteins in eukaryotes. Numerical values display statistical support in form of bootstrap or PP values. Scale bar represents estimated number of amino acid substitutions per site. Only bootstrap support and PP values greater than 50 and 0.5, respectively, are shown. p450 reductase (p450R), Methionine synthase reductase (MetSR) and Nitric oxide synthase (NOS) form distant branch of proteins.

Tah18 branch groups known Tah18 homologues in several eukaryotic clades. PNO homologues, Sulfite reductase alpha (SR) and CPR domain containing proteins in Metamonads form indiscrete cluster with bootstrap support of 97. Green color was used for visualization of Viridiplantae clade, red for Opisthokonta, yellow for SAR supergroup, brown for Amoebozoa, and blue for Excavata.

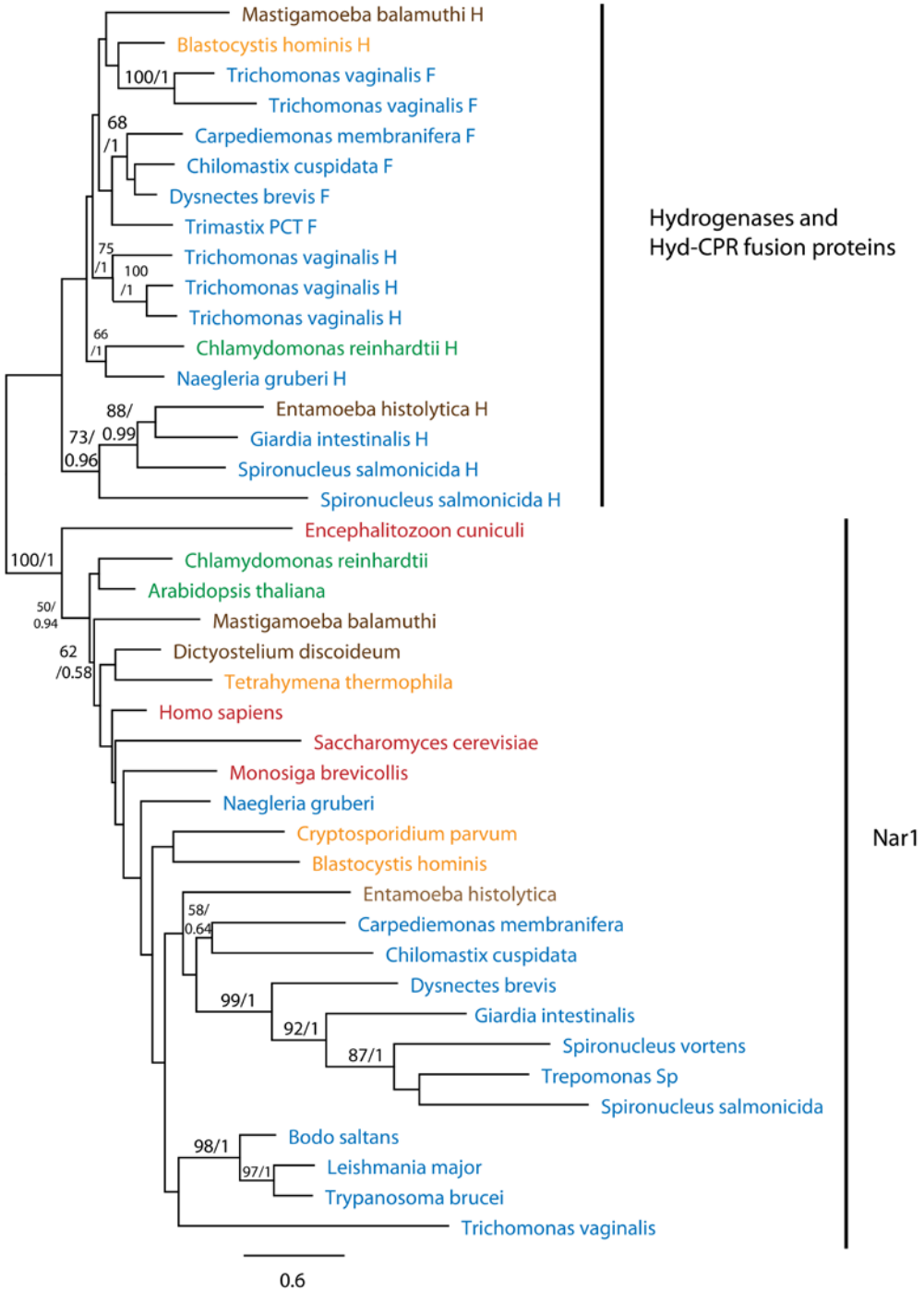

Fig S2. Phylogeny of hydrogenase domain containing proteins

A maximum likelihood phylogeny of Nar1 and hydrogenease domain containing proteins in eukaryotes. Numerical values display statistical support in form of bootstrap values or PP values, respectively. Scale bar represents estimated number of amino acid substitutions per site. Only bootstrap support values greater than 50 and PP values greater than 0.5 are shown. Green color was used for visualization of Viridiplantae clade, red for Opisthokonta, yellow for SAR supergroup, brown for Amoebozoa, and blue for Excavata. H, only hydrogenase domain containing protein; F, hydrogenase-CPR fusion protein. Hydrogenase like proteins cluster together with CPR-hydrogenase fusion proteins from metamonads.

Presence of Ribonucleotide reductase in anaerobes

The absence of Tah18 proteins in Metamonads and other anaerobes is striking, since this protein is essential in yeast, human and plants (40,41). Recently, it was shown that Tah18 and Dre2 are additionally involved in maturation of diferric-tyrosyl radical cofactor for RNR2 protein (Ribonucleotide reductase) (42). Therefore it is possible that essential role of Tah18 and Dre2 is not connected with their roles in CIA pathway. Hypothetical correlation between the distribution of Ribonucleotide reductase proteins and Tah18 a Dre2 proteins could serve as a supportive information for this assumption.

We searched if RNR proteins are indeed missing in organisms, where Tah18-Dre2 proteins are absent. Nevertheless, we failed to find any such correlation to support this hypothesis (FigS3).

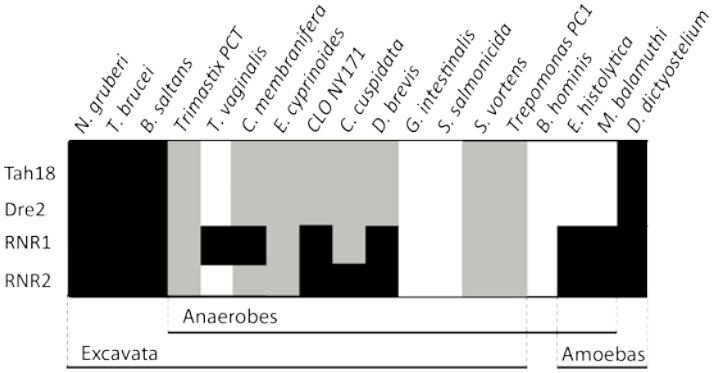

Fig S3. Distribution of Tah18, Dre2, RNR1 and RNR2 proteins in Metamonads and various anaerobes.

RNR1, Ribonucleotide reductase 1; RNR2, Ribonucleotide reductase 2

Disscussion

Distribution of Cia machinery components in Metamonads

Here we present the basic characteristics of CIA machinery pathway in *Giardia intestinalis* and other Metamonads. Tah18, Dre2, MMS19, Erv1 and ATM1 proteins are missing in Metamonada, although these homologues are present in other member of phyla Excavata. Absence of MMS19 is not as striking as this protein was lost independently in several groups of organisms (15) and is not essential in plants (4). All other missing proteins are essential in yeast and plants and their absence in Metamonads is therefore puzzling.

CIA machinery in Giardia was shown to be functional as activities of several FeS containing proteins were measured in cytoplasm of the cell (43,44). However, how Metamonads are assembling clusters on nbp35 without electron donor complex Tah18/Dre2 remains unknown and require further detailed studies.

The absence of Erv1 and ATM1 is surprising especially when considering that the proposed role for the mitosomes and hydrogenosomes in Metamonads is FeS cluster assembly of proteins in cytosol and nuclei. Since the presence of cysteine desulfurase was never reported in cytoplasm of any member of Metamonds, it is likely that CIA machinery in Metamonads is dependent on ISC pathway. However, how this connection is mantained without Erv1 and ATM1 remains unknown.

Interestingly, Giardia possesses 3 genes for Nbp35 protein. This is unusual, as in Trypanosoma, Bodo or Naegleria, only one copy of Nbp35 gene was identified. We suppose that Giardia might substituted for the loss of some key CIA proteins by gene duplication in case of Nbp35 and by dual cytoplasmic/mitosomal functions of cia2 and 2 Nbp35 paralogues.

The involvement of glutathione in CIA pathway in Metamonada is questionable, as not all members of the group Metamonada possess enzymes necessary for glutathione synthesis.

Localization of CIA components in Giardia

CIA machinery in Giardia consists only of 3 paralogues of Nbp35 protein, and single genes for cia1, nar1 and cia2. All these proteins are in the cytoplasm of Giardia. Interestingly, Nbp35-1, Nbp35-2 and Cia2 additionally possess mitosomal distribution. This dual

localization phenomenon is not exceptional in eukaryotes as it was recently reported for Dre2 in yeasts (45). Nevertheless, it was never shown for Nbp35 or Cia2.

While searching for the proper localization of nbp35-1 and nbp35-2 paralogues in Giardia, we obtained seemingly incompatible results from fractionation and immunofluorescence experiments. Based on IFA, proteins had dual cytoplasmic/mitosomal localization. On the other hand, based on fractionation, only small (in case of Nbp35-1) or almost undetectable (Nbp35-2) portion of the protein was found associated with the mitosomes. Those proteins lack any transmembrane domain or hydrophobic locus. Therefore they are most likely associated with the mitosome by protein-protein interaction. Consequently, during the fractionation majority of the protein is washed away. Similar behavior was already reported for another dual mitochondrial/cytoplasmic distributed protein Dre2 on the surface of the yeast mitochondria (46). Therefore, we claim that Nbp35-1 and Nbp35-2 are likely partially on the surface of the mitosome.

To discover exact localization of GiOR-1 and Cia2 within the mitosome, interacting proteins were precipitated and the list of the resulting proteins were then compared to already known interactomes of several mitosomal proteins (24). GiOR-1 interacting proteins are abundant in the proteomes of mitosomal matrix proteins Pam18 and Tim44 (Figure 3). In comparism, only slight overlap with outer mitochondrial proteins Tom40 and GiMomp35 interactomes is observed. Proteins from Tom40 and GiMOMP35 interactomes are instead abundant in Cia2 protein set. Interestingly, proteins precipitated with mitosomal matrix Hsp70 are abundant in both GiOR-1 and Cia2 proteins set. This could be explained by crucial poly-functional role of mHsp70, which is expected to interact with several mitosomal proteins during mitosomal protein transport and FeS cluster assembly (47-49). In consequence, this could result in crosslinking of whole mitosome through inner membrane proteins.

We could only hypothesize about the proper localization of the Cia2 protein. Based on protease protection assay and interacting proteins precipitation we conclude that portion of the protein is in the intermembrane space of the mitosome. In plants, it was recently shown that in Cia2 mutant cells, activity of mitochondrial aconitase was reduced in addition to expectedly decreased activities of several FeS proteins in cytoplasm (4). If there is any connection between the plant and giardia Cia2 protein we could however only speculate and further analysis is needed.

GioR proteins in Giardia

In previous work we have shown, that GiOR is able to reduce cytochromes b5 *in vitro*. And that these cytochromes are exclusively in cytoplasm (20). Here we show, that GiOR1 is present within the mitosome. This lead us to conclusion that GiOR-1 is not functioning as a cytochrome reductase *in vivo*. We performed additional experiment and interestingly we have found that GiOR proteins in Giardia are able to restore cluster assembly ability in cytoplasm of *T. brucei*, when Tah18 was knocked down (FigS1).
Previously it was shown, that for function of Tah18, Dre2 protein is necessary (40). However in Giardia, protein is absent, Therefore we suppose, that this common CPR domain in GiOR-1 protein is universal and promiscuously functioning as a reductase in different situations. It can reduce cytochromes in *in vitro* system, when electron donor NADPH is present. It can restore clustering activity in cytoplasm, when Dre2 is present in cytoplasm of Trypanosoma.
Based on (i) absence GiOR-1 in cytoplasm of Giardia, (ii) different evolution origin of the protein and (iii) missing Dre2 protein in all metamonads we assume that GiOR-1 protein have different cellular function than Tah18 in other eukaryotes.

Our findings are in agreement with the hypothesis that Tah18 and Dre2 proteins were lost in anaerobes (16). Interestingly, the exact role of Tah18 and Dre2 in CIA pathway in eukaryotes is unclear. First model raised in 2009 (8), which propose, that Tah18 and Dre2 are donors of electrons to Nbp35 has never been experimentally proven. However, recently it was shown that Tah18 and Dre2 are additionally involved in maturation of diferric-tyrosyl radical cofactor for RNR2 protein (Ribonucleotide reductase) (42). Therefore, it is possible that essential role of Tah18 and Dre2 protein is not due to the involvement in CIA pathway. RNR proteins are absent in Giardia, therefore Tah18 and Dre2 presence is not necessary for cofactor synthesis in *Giardia*. Nevertheless, we failed to find any correlation between the presence of Tah18, Dre2 and RNR genes in anaerobes to support this hypothesis (FigS3).

Origin of GiOR-1 related proteins in Metamonda

We searched for the origin of CPR domain containing proteins in Metamonada. Interestingly, we realized, that they all group together with PNO enzyme from various anaerobes and its close relative protein sulphite reductase alpha from Fungi (50). Our findings are in agreement

with Tsaousis et al. (15), where GiOR proteins in Giardia were identified as relatives of PNO proteins.

In more basal metamonads, CPR domain is fused to N-terminal hydrogenase-like domain. Basu et al., suggested, that N-terminal hydrogenase-like domain is actually derived from Nar1 protein, but this assumption was not supported by any phylogenetical analysis (16). However, our phylogenetical analysis revealed, that this N-terminal part is rather hydrogenase derived. The bootstrap support for this statement is 100. We assume, that this CPR-hydrogenase fusion protein was present in ancestor of all metamonads and was secondarily reduced only to CPR domain in common ancestor of Giardia and other more developed diplomonads (39) (Figure 1). Interestingly, in *Dysnectes brevis*, both CPR-Hydrogenase fusion and CPR-only gene are present which points out that gene duplication occurred prior the structural reduction of the gene. Fusion of hydrogenase and CPR domain is unique among the eukaryotes and so far there is no clue about its possible function.

Possible connection between ISC and CIA pathways in Giardia

It was shown, that CIA pathway in yeast is fully dependent on ISC pathway in mitochondria. However, no data are available about connection of those pathways in metamonds. ISC pathway is the only pathway which has been identified within Giardia mitosome so far. Furthermore, there is no known iron-sulphur protein in mitosome apart from components of ISC pathway itself. Therefore, it is likely that the function of the mitosome is to assist cluster assembly in cytoplasm. Presence of paralogues of scaffold proteins Nbp35 on the surface of the mitosome is strong support for this assumption. How Giardia is substituting the function of intermembrane space protein Erv1 and inner membrane internal protein ATM1 needs further investigation. Cia2 protein in intermembrane space of the mitosome might be used for this purpose.

Summary

This is the first detailed study which revealed unusually distributed components of CIA machinery proteins in eukaryotes. All-together, our data suggests that Giardia is the first eukaryote to be reported where CIA machinery is functioning without electron donor complex Tah18/Dre2. Additionally, this pathway is likely dependent on ISC pathway within the

mitosome, even when typical linking proteins ATM1 and Erv1 are absent. Uniquely localized scaffold proteins Nbp35-1 and Nbp35-2 on the surface and cluster delivery protein Cia2 in the inter-membrane space of the mitosome might be involved in this connection. Exact function of all components is yet to be discovered.

Reference List

1. **Netz, D. J. A., A. J. Pierik, M. Stuempfig, U. Muhlenhoff, and R. Lill**. 2007. The Cfd1-Nbp35 complex acts as a scaffold for iron-sulfur protein assembly in the yeast cytosol. Nature Chemical Biology **3**:278-286.

2. **Balk, J., A. J. Pierik, D. J. A. Netz, U. Muhlenhoff, and R. Lill**. 2004. The hydrogenase-like Nar1p is essential for maturation of cytosolic and nuclear iron-sulphur proteins. Embo Journal **23**:2105-2115.

3. **Balk, J., D. J. A. Netz, K. Tepper, A. J. Pierik, and R. Lill**. 2005. The essential WD40 protein Cia1 is involved in a late step of cytosolic and nuclear iron-sulfur protein assembly. Molecular and Cellular Biology **25**:10833-10841.

4. **Luo, D. X., D. G. Bernard, J. Balk, H. Hai, and X. F. Cui**. 2012. The DUF59 family gene AE7 acts in the cytosolic Iron-Sulfur cluster assembly pathway to maintain nuclear genome integrity in Arabidopsis. Plant Cell **24**:4135-4148.

5. **Gari, K., A. M. L. Ortiz, V. Borel, H. Flynn, J. M. Skehel, and S. J. Boulton**. 2012. MMS19 links cytoplasmic Iron-Sulfur cluster assembly to DNA metabolism. Science **337**:243-245.

6. **Stehling, O., A. A. Vashisht, J. Mascarenhas, Z. O. Jonsson, T. Sharma, D. J. A. Netz, A. J. Pierik, J. A. Wohlschlegel, and R. Lill**. 2012. MMS19 assembles Iron-Sulfur proteins required for DNA metabolism and genomic integrity. Science **337**:195-199.

7. **Muhlenhoff, U., S. Molik, J. R. Godoy, M. A. Uzarska, N. Richter, A. Seubert, Y. Zhang, J. Stubbe, F. Pierrel, E. Herrero, C. H. Lillig, and R. Lill**. 2010. Cytosolic monothiol glutaredoxins function in intracellular iron sensing and trafficking via their bound Iron-Sulfur cluster. Cell Metabolism **12**:373-385.

8. **Netz, D. J. A., M. Stumpfig, C. Dore, U. Muhlenhoff, A. J. Pierik, and R. Lill**. 2010. Tah18 transfers electrons to Dre2 in cytosolic iron-sulfur protein biogenesis. Nature Chemical Biology **6**:758-765.

9. **Kispal, G., P. Csere, C. Prohl, and R. Lill**. 1999. The mitochondrial proteins Atm1p and Nfs1p are essential for biogenesis of cytosolic Fe/S proteins. Embo Journal **18**:3981-3989.

10. **Muhlenhoff, U., J. Balk, N. Richhardt, J. T. Kaiser, K. Sipos, G. Kispal, and R. Lill**. 2004. Functional characterization of the eukaryotic cysteine desulfurase Nfs1p from *Saccharomyces cerevisiae*. Journal of Biological Chemistry **279**:36906-36915.

11. **Lange, H., T. Lisowsky, J. Gerber, U. Muhlenhoff, G. Kispal, and R. Lill**. 2001. An essential function of the mitochondrial sulfhydryl oxidase Erv1p/ALR in the maturation of cytosolic Fe/S proteins. Embo Reports **2**:715-720.

12. **Kuhnke, G., K. Neumann, U. Muehlenhoff, and R. Lill**. 2006. Stimulation of the ATPase activity of the yeast mitochondrial ABC transporter Atm1p by thiol compounds. Molecular Membrane Biology **23**:173-184.

13. **Srinivasan, V., A. J. Pierik, and R. Lill**. 2014. Crystal structures of nucleotide-free and glutathione-bound mitochondrial ABC transporter Atm1. Science **343**:1137-1140.

14. **Netz, D. J. A., J. Mascarenhas, O. Stehling, A. J. Pierik, and R. Lill**. 2014. Maturation of cytosolic and nuclear iron-sulfur proteins. Trends in Cell Biology **24**:303-312.

15. **Tsaousis, A. D., E. Gentekaki, L. Eme, D. Gaston, and A. J. Roger**. 2014. Evolution of the cytosolic Iron-Sulfur cluster assembly machinery in Blastocystis species and other microbial eukaryotes. Eukaryotic Cell **13**:143-153.

16. **Basu, S., J. C. Leonard, N. Desai, D. A. I. Mavridou, K. H. Tang, A. D. Goddard, M. L. Ginger, J. Lukes, and J. W. A. Allen**. 2013. Divergence of Erv1-associated mitochondrial import and export pathways in Trypanosomes and anaerobic protists. Eukaryotic Cell **12**:343-355.

17. **Tovar, J., G. Leon-Avila, L. B. Sanchez, R. Sutak, J. Tachezy, M. van der Giezen, M. Hernandez, M. Muller, and J. M. Lucocq**. 2003. Mitochondrial remnant organelles of Giardia function in iron-sulphur protein maturation. Nature **426**:172-176.

18. **Dolezal, P., O. Smid, P. Rada, Z. Zubacova, D. Bursac, R. Sutak, J. Nebesarova, T. Lithgow, and J. Tachezy**. 2005. Giardia mitosomes and trichomonad hydrogenosomes share a common mode of protein targeting. Proceedings of the National Academy of Sciences of the United States of America **102**:10924-10929.

19. **Jedelsky, P. L., P. Dolezal, P. Rada, J. Pyrih, O. Smid, I. Hrdy, M. Sedinova, M. Marcincikova, L. Voleman, A. J. Perry, N. C. Beltran, T. Lithgow, and J. Tachezy**. 2011. The minimal proteome in the reduced mitochondrion of the parasitic protist *Giardia intestinalis*. PLoS.One. **6**:e17285. doi:10.1371/journal.pone.0017285 [doi].

20. **Pyrih, J., K. Harant, E. Martincova, R. Sutak, E. Lesuisse, I. Hrdy, and J. Tachezy**. 2014. *Giardia intestinalis* incorporates heme into cytosolic cytochrome b(5). Eukaryotic Cell **13**:231-239.

21. **Keister, D. B.** 1983. Axenic culture of *Giardia lamblia* in Tyi-S-33 medium supplemented with bile. Transactions of the Royal Society of Tropical Medicine and Hygiene **77**:487-488.

22. **Lauwaet, T., B. J. Davids, A. Torres-Escobar, S. R. Birkeland, M. J. Cipriano, S. P. Preheim, D. Palm, S. G. Svard, A. G. McArthur, and F. D. Gillin**. 2007. Protein phosphatase 2A plays a crucial role in *Giardia lamblia* differentiation. Molecular and Biochemical Parasitology **152**:80-89.

23. **Singer, S. M., J. Yee, and T. E. Nash**. 1998. Episomal and integrated maintenance of foreign DNA in *Giardia lamblia*. Molecular and Biochemical Parasitology **92**:59-69.

24. **Martincova, E., L. Voleman, J. Pyrih, V. Zarsky, P. Vondrackova, M. Kolisko, J. Tachezy, and P. Dolezal**. 2015. Probing the biology of *Giardia intestinalis* mitosomes using in vivo enzymatic tagging. Molecular and Cellular Biology **35**:2864-2874.

25. **Rada, P., O. Smid, R. Sutak, P. Dolezal, J. Pyrih, V. Zarsky, J. J. Montagne, I. Hrdy, J. M. Camadro, and J. Tachezy**. 2009. The monothiol single-domain glutaredoxin is conserved in the highly reduced mitochondria of *Giardia intestinalis*. Eukaryotic Cell **8**:1584-1591.

26. **Rada, P., P. Dolezal, P. L. Jedelsky, D. Bursac, A. J. Perry, M. Sedinova, K. Smiskova, M. Novotny, N. C. Beltran, I. Hrdy, T. Lithgow, and J. Tachezy**. 2011. The core components of organelle biogenesis and membrane transport in the hydrogenosomes of *Trichomonas vaginalis*. Plos One **6**.

27. **Soding, J., A. Biegert, and A. N. Lupas**. 2005. The HHpred interactive server for protein homology detection and structure prediction. Nucleic Acids Research **33**:W244-W248.

28. **Altschul, S. F., T. L. Madden, A. A. Schaffer, J. H. Zhang, Z. Zhang, W. Miller, and D. J. Lipman**. 1997. Gapped BLAST and PSI-BLAST: a new generation of protein database search programs. Nucleic Acids Research **25**:3389-3402.

29. **Katoh, K., K. Misawa, K. Kuma, and T. Miyata**. 2002. MAFFT: a novel method for rapid multiple sequence alignment based on fast Fourier transform. Nucleic Acids Research **30**:3059-3066.

30. **Criscuolo, A. and S. Gribaldo**. 2010. BMGE (Block Mapping and Gathering with Entropy): a new software for selection of phylogenetic informative regions from multiple sequence alignments. Bmc Evolutionary Biology **10**.

31. **Nguyen, L. T., H. A. Schmidt, A. von Haeseler, and B. Q. Minh**. 2015. IQ-TREE: a fast and effective stochastic algorithm for estimating maximum-likelihood phylogenies. Molecular Biology and Evolution **32**:268-274.

32. **Guindon, S. and O. Gascuel**. 2003. A simple, fast, and accurate algorithm to estimate large phylogenies by maximum likelihood. Systematic Biology **52**:696-704.

33. **Huelsenbeck, J. P. and F. Ronquist**. 2001. MRBAYES: Bayesian inference of phylogenetic trees. Bioinformatics **17**:754-755.

34. **Carruthers, V. B. and G. A. M. Cross**. 1992. High efficiency clonal growth of blood stream form and insect form *Trypanosoma brucei* on agarose plates. Proceedings of the National Academy of Sciences of the United States of America **89**:8818-8821.

35. **Basu, S., D. J. Netz, A. C. Haindrich, N. Herlerth, T. J. Lagny, A. J. Pierik, R. Lill, and J. Lukes**. 2014. Cytosolic iron-sulphur protein assembly is functionally conserved and essential in procyclic and bloodstream *Trypanosoma brucei*. Molecular Microbiology **93**:897-910.

36. **Vondruskova, E., J. van den Burg, A. Zikova, N. L. Ernst, K. Stuart, R. Benne, and J. Lukes**. 2005. RNA interference analyses suggest a transcript-specific regulatory role for mitochondrial RNA-binding proteins MRP1 and MRP2 in RNA editing and other RNA processing in Trypanosoma brucei. Journal of Biological Chemistry **280**:2429-2438.

37. **Smid, O., E. Horakova, V. Vilimova, I. Hrdy, R. Cammack, A. Horvath, J. Lukes, and J. Tachezy**. 2006. Knock-downs of iron-sulfur cluster assembly proteins IscS and IscU down-regulate the active mitochondrion of procyclic *Trypanosoma brucei*. Journal of Biological Chemistry **281**:28679-28686.

38. **Long, S. J., P. Changmai, A. D. Tsaousis, T. Skalicky, Z. Verner, Y. Z. Wen, A. J. Roger, and J. Lukes**. 2011. Stage-specific requirement for Isa1 and Isa2 proteins in the mitochondrion of *Trypanosoma brucei* and heterologous rescue by human and *Blastocystis* orthologues. Molecular Microbiology **81**:1403-1418.

39. **Takishita, K., M. Kolisko, H. Komatsuzaki, A. Yabuki, Y. Inagaki, I. Cepicka, P. Smejkalova, J. D. Silberman, T. Hashimoto, A. J. Roger, and A. G. B. Simpson**. 2012. Multigene phylogenies of diverse Carpediemonas-like organisms identify the closest relatives of 'Amitochondriate' Diplomonads and Retortamonads. Protist **163**:344-355.

40. **Bernard, D. G., D. J. A. Netz, T. J. Lagny, A. J. Pierik, and J. Balk**. 2013. Requirements of the cytosolic iron-sulfur cluster assembly pathway in Arabidopsis. Philosophical Transactions of the Royal Society B-Biological Sciences **368**.

41. **Vernis, L., C. Facca, E. Delagoutte, N. Soler, R. Chanet, B. Guiard, G. Faye, and G. Baldacci**. 2009. A newly identified essential complex, Dre2-Tah18, controls mitochondria integrity and cell death after oxidative stress in yeast. Plos One **4**.

42. **Zhang, Y., H. R. Li, C. G. Zhang, X. X. An, L. L. Liu, J. Stubbe, and M. X. Huang**. 2014. Conserved electron donor complex Dre2-Tah18 is required for ribonucleotide reductase metallocofactor assembly and DNA synthesis. Proceedings of the National Academy of Sciences of the United States of America **111**:E1695-E1704.

43. **Emelyanov, V. V. and A. V. Goldberg**. 2011. Fermentation enzymes of *Giardia intestinalis*, pyruvate:ferredoxin oxidoreductase and hydrogenase, do not localize to its mitosomes. Microbiology-Sgm **157**:1602-1611.

44. **Townson, S. M., J. A. Upcroft, and P. Upcroft**. 1996. Characterisation and purification of pyruvate:ferredoxin oxidoreductase from *Giardia duodenalis*. Molecular and Biochemical Parasitology **79**:183-193.

45. **Banci, L., I. Bertini, S. Ciofi-Baffoni, F. Boscaro, A. Chatzi, M. Mikolajczyk, K. Tokatlidis, and J. Winkelmann**. 2011. Anamorsin is a [2Fe-2S] cluster-containing substrate of the Mia40-dependent mitochondrial protein trapping machinery. Chemistry & Biology **18**:794-804.

46. **Peleh, V., J. Riemer, A. Dancis, and Herrmann J.M.** 2014. Protein oxidation in the intermembrane space of mitochondria is substrate-specific rather than general. Microbial Cell **1**:81-93. doi:10.15698/mic2014.01.130 [doi].

47. **Uzarska, M. A., R. Dutkiewicz, S. A. Freibert, R. Lill, and U. Muehlenhoff**. 2013. The mitochondrial Hsp70 chaperone Ssq1 facilitates Fe/S cluster transfer from Isu1 to Grx5 by complex formation. Molecular Biology of the Cell **24**:1830-1841.

48. **Gambill, B. D., W. Voos, P. J. Kang, B. J. Miao, T. Langer, E. A. Craig, and N. Pfanner**. 1993. A dual role for mitochondrial Heat-shock protein-70 in membrane translocation of preproteins. Journal of Cell Biology **123**:109-117.

49. **Krimmer, T., J. Rassow, W. H. Kunau, W. Voos, and N. Pfanner**. 2000. Mitochondrial protein import motor: the ATPase domain of matrix Hsp70 is crucial

for binding to Tim44, while the peptide binding domain and the carboxy-terminal segment play a stimulatory role. Molecular and Cellular Biology **20**:5879-5887.

50. **Rotte, C., F. Stejskal, G. Zhu, J. S. Keithly, and W. Martin**. 2001. Pyruvate : NADP(+) oxidoreductase from the mitochondrion of *Euglena gracilis* and from the apicomplexan *Cryptosporidium parvum*: A biochemical relic linking pyruvate metabolism in mitochondriate and amitochondriate protists. Molecular Biology and Evolution **18**:710-720.